PHOTOCHEMICAL FORMATION OF *TRANS*-CYCLOHEXENE AND *TRANS*-CYCLOHEPTENE

By

WINSTON (Cường) VI TRINH

Bachelor of Science in Chemistry

The University of Texas at Austin

Austin, Texas

2013

Submitted to the Faculty of the
Graduate College of the
Oklahoma State University
in partial fulfillment of
the requirements for
the Degree of
MASTER OF SCIENCE
December, 2016

PHOTOCHEMICAL FORMATION OF *TRANS*-

CYCLOHEXENE AND *TRANS*-CYCLOHEPTENE

Thesis Approved:

Dr Jimmie D. Weaver

(ThesisAdviser)

Dr Jeffery L. White

Dr Ronald Rahaim

ACKNOWLEDGEMENTS

- Advisor: Dr. Jimmie D. Weaver
- Professor Committee: Dr. Ronald Rahaim, Dr. Jeffery L. White
  The Weaver group: Amandeep, Sameera, Kamaljeet, Kip, Jon, Manjula, Sonal, Brayden, Mo, Erika, Cameron, Kabryn, and Morgan.
- Oklahoma State University Dept. of Chemistry faculty
  Funding: Oklahoma Center for the Advancement of Science and Technology. (OCAST)

Name: Winston (Cường) Vi Trinh

Date of Degree: DECEMBER, 2016.

Title of Study: PHOTOCHEMICAL FORMATION OF *TRANS*-CYCLOHEXENE AND *TRANS*-CYCLOHEPTENE

Major Field: Chemistry

Abstract: For nearly forty years, the transient existence of *trans*-cyclohexene has been postulated and believed to be accessible via UV-irradiation of *cis*-cyclohexene. Most text books suggest that *trans*-cyclooctene, which is the smallest *trans*-cycloalkene that has been prepared in pure form and is stable at room temperature,[1] is the smallest that can be formed. Herein, we provide stereochemical evidence which supports the existence of *trans*-cyclohexene as well as our efforts to directly observe it with low temperature NMR. Furthermore, we demonstrate a practical method for the generation of the *trans*-cyclohexene utilizing blue LEDs, which provides facile access to a class of oxobicyclic structures currently inaccessible via thermal methods.

In an example of uphill catalysis, a catalyzed reaction that is endergonic in nature, we synthesize the endergonic product, cyclohexanediol, via *trans*-cyclohexene which undergoes facile reversion to the cyclohexene when the light source is removed. These results suggest the possibility of a new class of chemical switch.

Because *trans*-cycloheptenеis a larger ring, it is less strained and has a longer life-time when compared to *trans*-cyclohexene. Consequently, *trans*-cycloheptene is more amenable to intermolecular chemical reactions. In the second project, we can generate *trans*-cycloheptene using blue LEDs, which provides facile access to a regio- and stereoselective access to a tricyclodiol which is a [2+2] dimer of the corresponding cycloheptenol.

TABLE OF CONTENTS

Chapter 1

ON THE EXISTENCE OF *TRANS*-CYCLOHEXENE AND ITS USE SYNTHESIS OF OXABICYCLO[2.2.1]HEPTANES

I.INTRODUCTION

Trans-cycloalkenes with less than 12 atoms within the ring have additional strain because of difficulty accommodating the ideal double bond geometry.[2] While *trans*-cyclooctene is an isolable substance,[3] *trans*-cycloheptenehas only been observed using low temperature ^{1}H NMR spectroscopy.[4] At 1 ^{o}C, the *trans*-cycloheptene reverts to the *cis*-isomer with a half-life of 10 min in methanol.[5] *Trans*-cyclohexene is more strained than other larger rings and has only been observed as a transient intermediate during laser flash photolysis.[3] In 1976, Bonneau carried out a laser photolysis of *cis*-1-phenylcyclohexene in methanol at room temperature. Upon photolysis, the transient UV-Vis spectrum peak at 380 nm was assigned to be *trans*-phenylcyclohexene.[6] The transient species has a lifetime 9 μs in methanol at room temperature.[6] The lifetime of *trans* species has an inverse dependence on temperature, increasing with decreasing temperature. At -70^{o}C, the lifetime of *trans*-phenylcyclohexene is 500 μs in methanol.[7] In 1979, by direct irradiation of *cis*-1-phenylcyclohexene, Bonneau and Dubien provided new chemical evidence to support the existence of *trans*-isomer of cyclohexene.[7] Direct irradiation with the wavelength of 300 nm of *cis*-1-phenylcyclohexene in neutral methanol at -75^{o}C yields a new dimer product (Figure I).[7]

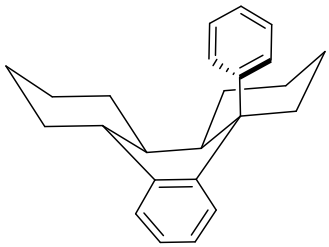

Figure 1: A computer-generated perspective of the material.[7]

The authors propose the dimer results from a [4+2] cycloaddition of *cis*-1-phenylcyclohexene with *trans*-alkene.[7] After formation of the *trans* species, the [4+2] reaction occurs, followed by 1,3-hydrogen shift to yield the dimer product (Scheme 1).[7] Transient deprotonation/reprotonation may be a better explanation than1,3-hydrogen shift, since this is not geometrically feasible.

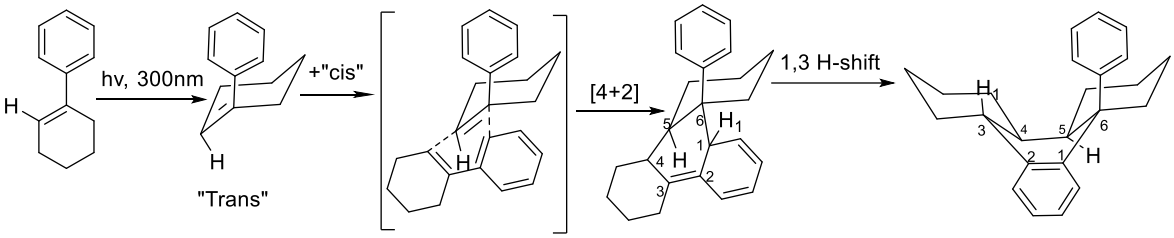

Scheme 1: Mechanism of dimer product.

In 1976, Bonneau carried out a flash laser photolysis experiment, he had seen a *trans*-phenylcyclohexene species at 380 nm in acidic methanol.[7] In scheme 2, *trans*-phenylcyclohexene is formed from *cis*-phenylcyclohexene as the initial species, then followed by protonation to form phenylcyclohexyl cation.[7] However, the 1-phenylcyclohexyl cation was not actually observed in the intermediate in Scheme 2. The authors propose that this is because methanol is a highly nucleophilic solvent and it reacts quickly with the cationic intermediate species.[8]

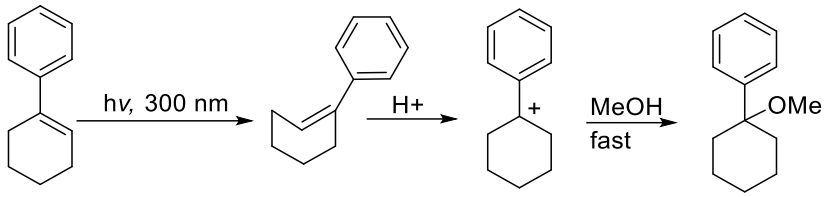

Scheme 2: Proposed mechanism showing *trans*-phenycyclohexene intermediate

In 1993, using weakly nucleophilic hexafluoroisopropanol as the solvent which slowed down the solvolysis, Steen Steenken observed the cation of *cis*-1-phenylcyclohexene generated with laser flash photolysis.[9] Flash photolysis can be used to measure the absorbance of transient species formed during photochemical reactions that are extremely short lived, i.e., in nanosecond time scale.[10] Steenken carried out several flash photolysis experiments and his observations were consistent with the mechanism in Scheme 3.[9] *Trans*-1-phenylcyclohexene is formed from *cis*-1-phenylcyclohexene as the initial species in this photochemical reaction and is assumed to be a twist-boat *trans*-conformer. This is followed by protonation to form the phenylcyclohexyl cation which is then subsequently trapped by the solvent.[9] Steenken detected the transient species at 335-400 nm in HFIP (1,1,1,3,3-hexafluoroisopropyl alcohol), which was attributed to 1-phenylcyclohexyl cation.[9]

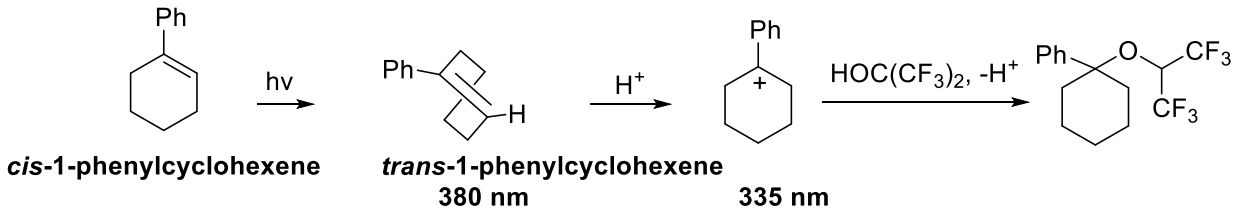

Scheme 3: Proposed mechanism showing the phenylcyclohexyl cation intermediate.

In addition to the evidence provided by laser flash photolysis, the existence of *trans*-phenylcyclohexene has been supported computationally.[11] In 1995, Richard and Kenneth

performed computational study on *trans*-cyclohexene. They found two distinct conformers which were local minima (**2** and **3**, Scheme 4) using TCSCF/6-31G* optimization, namely, the chair (**3**) and twist-boat (**2**) forms.[3] Scheme 4 provides a graphical summary of their work with all of relevant structures of *trans*-cyclohexene. Structure **1** is well known as half-chair conformation of *cis*-cyclohexene.[3] Next, two transition states **4TS** and **5TS** were found that lead to the twist-boat *trans*-cyclohexene (**2**, 59.3 kcal/mol) and chair *trans*-cyclohexene (**3**, 54.7 kcal/mol) respectively. A transition state between the two high energy *trans*-conformers (**2** and **3**) was found, (**6TS**, 61.1 kcal/mol).[3] The lowest energy unstable conformer is the *trans*-cyclohexene (**3**) and it is 54.7 kcal/mol above *cis*-cyclohexene (**1**).[3] The chair *trans*-conformer (**3**) has a barrier of 10.6 kcal/mol to reversion back to *cis*-cyclohexene (**1**) and 6.4 kcal/mol to twist-boat *trans*-cyclohexene (**2**).[3] The twist-boat conformer (**2**) has a barrier of 10.2 kcal/mol for π-bond rotation to return to *cis*-cyclohexene (**1**) and only a barrier of 1.8 kcal/mol to interconvert to the other *trans*-form (**3**).[3] The chair conformer (**3**) is 4.6 kcal/mol lower in energy than twist-boat conformer (**2**) and has higher barrier to reversion back to *cis*-cyclohexene when compared to (**2**). Thus it is likely, that the chair conformer (**3**) has a longer life-time and plays a more dominant role in the chemical reactions of the strained species.

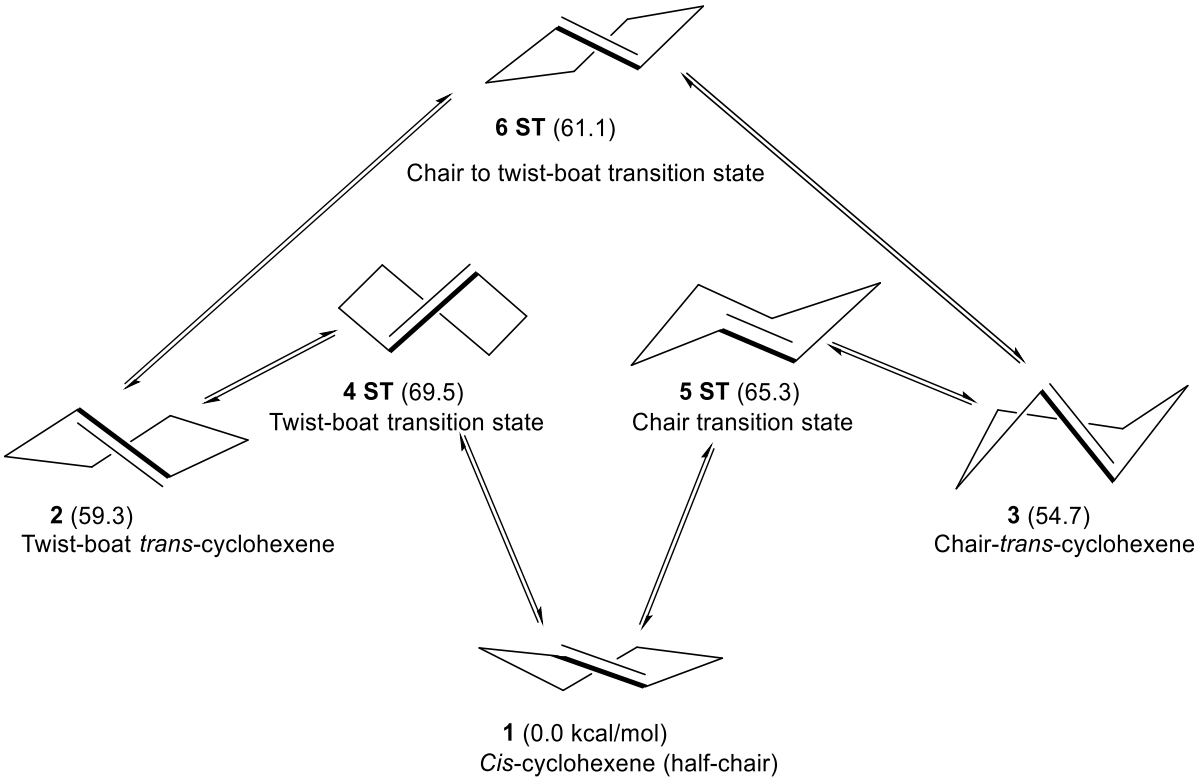

Scheme 4: Structures and Relative Energies (kcal/mol) for *trans*-Cyclohexene Conformers and Transition States.[3]

Table 1: Select Structural Data from TCSCF/6-31G* Optimiztion.[3]

	Structure	Double bond length, A	dihedral angle H−C=C−H, deg	dihedral angle C−C=C−C, deg
1	Cis-cyclohexene (half-chair)	1.341	1.7	-0.316
2	Twist-boat trans-cyclohexene	1.381	174.6	88.1
3	Chair trans-cyclohexene	1.382	176.6	84.0
4TS	Twist-boat transition state	1.478	132.6	60.7
5TS	Chair transition state	1.482	129.3	55.2
6TS	Chair to twist-boat transition state	1.376	173.5	91.2

In previous work from the Weaver group, a method was developed to access the less stable *Z*-alkene via photocatalyzed isomerization of the thermodynamically more stable *E*-alkene.[13] The strategy utilized a photocatalyst which absorbs light in the visible region and can provide the high amount of energy necessary for excitation and isomerization of the *E*-alkene to the *Z*-alkene (Figure 3).[13]

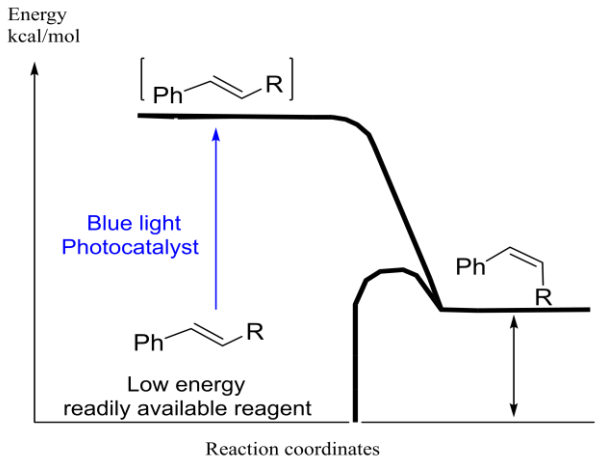

Figure 3: Energy vs. Reaction coordinate.

An attractive feature of photocatalysis is the potential ability to overcome the normal thermodynamic constraints of a reaction. Namely, thermal catalysis requires that reactions be exergonic in their totality, because catalysis lowers energy barriers in both the forward and backward directions. Photocatalysis, on the other hand, may react selectively with the starting material in an effectively uni-directional manner, and thus, it may be possible to drive a reaction in a single direction, even an endergonic direction.[13] Inline with this strategy, we hoped that we could form *trans*-cyclohexene directly from *cis*-cyclohexene by the use of photocatalysis. Rather than building up a large amount of the highly strained molecule, we hoped that the strain energy could be used to induce chemical reactions from the unstable *trans*-cyclohexene species, that would not otherwise take place.

Allinger and Sprague predicted that the *trans*-cyclohexene is 42 kcal/mol less stable than *cis*-cyclohexene,[14] and the barrier from thermal isomerization from *cis*- to *trans*-isomer is 54.7 kcal/mol.[3] While the absolute numbers are significantly lower from that predicted by Richard and Kenneth, the trends are similar. Since it is expected that the transition state structure will be

similar regardless how it is achieved, it was clear that it would be necessary to find a catalyst that can provide at least 55 kcal/mol energy in order for *cis*-phenylcyclohexene to pass above the barrier. Herein, we report that we can generate *trans*-cyclohexene using a photocatalyst, blue LEDs, at temperatures near ambient. However, given the relatively small reversion barrier 10-15 kcal/mol, the half-life of *trans*-isomer is short, and is never actually observed by NMR. Nonetheless, the life-time is sufficiently long to participate in an intramolecular hydroalkoxylation reaction to yield the bridged ether product in Scheme 5. Even though oxabicyclic structures play a significant role in biological functions,[19] andoxabicyclo [2.2.1]heptene is also a useful intermediate for synthesis of complex molecules in the areas of material science, natural products, and polymers.[19] This particular motif with benzylic ethers has never been observed. We postulate that this is a result that it cannot be made by via Brønsted-acid mediated hydroalkoxylation. We have found that in the presence of strong acids the alcohol simply undergoeselimination. Not only does photocatalysis provide a practical synthesis to this motif that is not currently feasible via thermal methods, but it also provides strong stereochemical evidence of the existence of *trans*-cyclohexene.

Our current understanding is outlined in Scheme 5. In the presence of visible light and photocatalyst, *cis*-1-phenylcyclohexenol (**1**) undergoes excitation to a biradical which upon intersystem crossing allows facile formation of the strained chair *tran*-isomer (**2**). Because of the great amount of strain associated with a six-membered cyclic *trans*-alkene, protonation of the alkene is expected to be facilitated as it converts an sp^2 center to an sp^3 center which is more accommodating of the strain induced deformation from ideal geometry. This leads to chair phenylcyclohexenyl cation species (**3**), after conversion to the boat phenylcyclohexenyl cation (**4**), the oxygen traps the cation to produce the oxygen bridging ether after deprotonation(**5**).

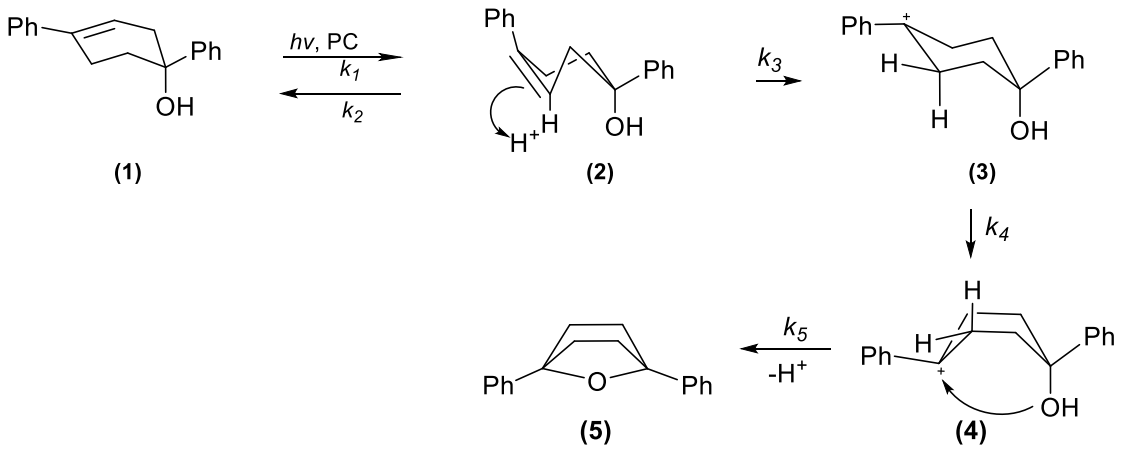

Scheme 5: Proposed mechanism.

Scheme 6 demonstrates the differential stereochemical outcomes of hydroalkoxylation from both the *cis*- and *trans*-cyclohexenes. First, while it is not expected to occur, and there is no evidence that protonation of the relaxed cyclohexene does occur (**1a**), if protonation of (**1a)** did occur either by formation of a photo-acid with special ability to protonate the *cis*-alkene or by protonation of the *cis*-triplet biradical prior to intersystem crossing, protonation would likely lead to the low energy chair (**1b)**, (addition of bromine to cyclohexene is one of the example of proton protonation to the axial position because only at axial positions on adjation atoms of a cyclohexane ring are coplanar)[20] which would then need to convert to boat form (**1c)** to undergo C–O bond formation. Careful examination of the label (deuterium) shows that it is in the equatorial position in the product (**1d)**. In contrast, protonation of lowest energy *trans*-cyclohexene conformer according to Richard and Kenneth (Scheme 4),[3] chair *trans*-cyclohexene **2a**, from the exo-face gives the carbenium ion with equatorial deuteration (**2b**), which upon the necessary conversion to the boat conformer (**2c**) prior to cyclization, places the label (deuterium) in the axial position in the product(**2d**).

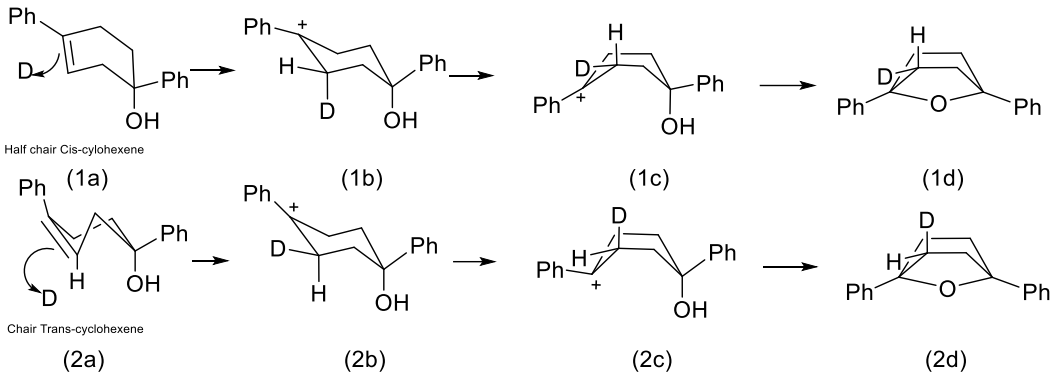

Scheme 6: Stereochemical Assessment.

Our hope was that in addition to providing stereochemical evidence of a *trans*-cyclohexene, we might also provide a convenient method for the generation of *trans*-cyclohexene. The ability to avoid the use of UV-light would make the method more convenient and functional group compatible. We also attempted to directly observe the *trans*-cyclohexene via ^{1}H NMR experiments at low temperature. However, limitations of the instrumentation and experimental setup prevented us from obtaining evidence at temperatures below -87 ^{o}C thus, precluding fully conclusive direct NMR observation of *trans*-cyclohexene.

II. RESULTS AND DISCUSSION

Section 1: Optimization of reaction conditions.

In the development of the synthesis of the ether product (**1a)**, we found that the conditions in the reaction scheme within Table 1 were optimal. Entry 1, the reaction takes place in the presence of *fac*-Ir(4'-F-ppy)$_3$, acid, and blue LEDs. However, when acid (Entry 2), catalyst (Entry 5), or light is left out (Entry 4) no reaction occurs. Furthermore, attempts to use a stronger Brønsted acid (HCl) (Entry 3) to facilitate the cyclization, led to elimination.

Table 1: The impact of the deviations to the optimal conditions

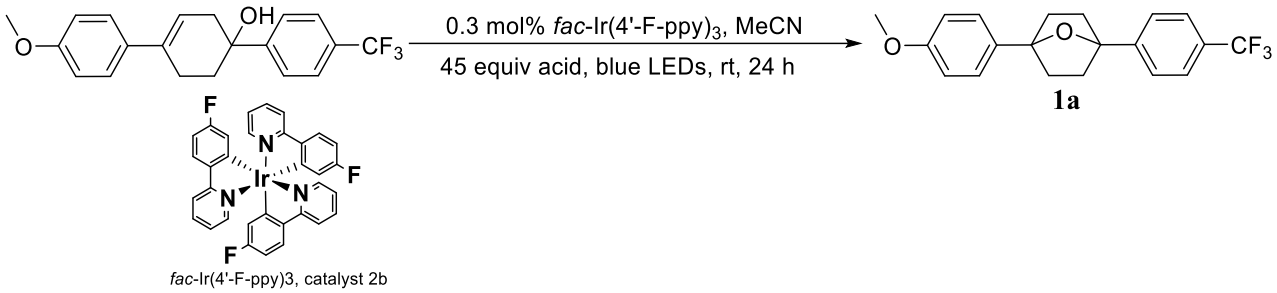

Entry	Catalyst	Acid	Product
1.	*fac*-Ir(4'-F-ppy)$_3$[a]	HCO_2H	78 % Yield
2.	*fac*-Ir(4'-F-ppy)$_3$	None	No reaction
3.	None	HCl	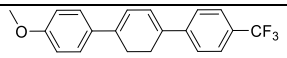
4.	*fac*-Ir(4'-F-ppy)$_3$	HCO_2H	No reaction
5.	None	HCO_2H	No reaction

Reaction were checked by NMR.[a] is the reaction with the presence of blue LEDs.

To investigate the importance of the solvent in the reaction, a screen of various solvents was conducted (Table 2). In toluene, no conversion was observed after 3 hours (Entry 1). Whereas, in acetonitrilethe reaction went to completion within3 hours, and the reaction rate was

faster in acetonitrile compared to THF, DMF, or DCM (Entries 3, 4, and 5). Thus, while the reaction was amenable to many solvents, MeCN was used for further studies.

Table 2: Optimization of the Different Solvents

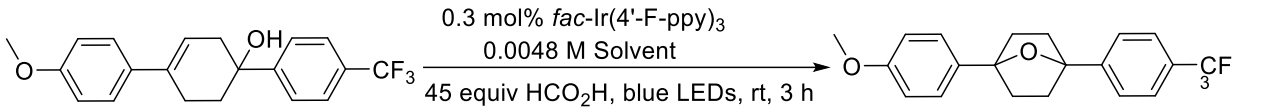

Entry	Solvent	Conversion in 3 h
1.	MeCN	100 %
2.	Toluene	0 %
3.	DMF	32 %
4.	DCM	59 %
5.	THF	24 %

Reactions were run with 0.0144 mmol of substrate, and theconversion was determined by NMR.

We had seen in table 1, there was no reaction in the absence of formic acid. While it was clear that an acid was an important component of the reaction mixture, it was not clear that we were using the optimal acid. Thus, we optimized different type of acids with pK_a (H_2O) range from 0.2 to 4.7. With trifloroacetic acid (Entry 1, Table 3) there was no reaction. We believe this was a result of deactivation of the catalyst which was evidenced by the loss of the characteristic yellow solution. There was no reaction in the presence of terephthalic acid (Entry 4). Formic acid gave 98 % conversion after 8 hours, and was faster when compared to trichloroacetic and acetic acid (Entries 2, 3, Table 3).

The previous study revealed weaker acids were generally effective; therefore, we wanted to study the acid loading on the reaction. Figure 4 shows conversion of the reaction as a function of formic acid loading, as it was varied from 1 to 45 equivalents of formic acid. At 3 h, the conversion increased steeply at low acid loadings, then more gradually up to 45 equivalents, and

finally began to slowly decrease up to 80 equivalents. Thus, 45 equivalents of formic acid were used as the optimal loading thereafter.

Table 3: Optimization of the Different Acids

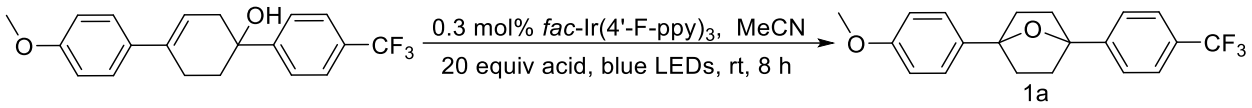

Entry	Acid	1a	Conversion in 8h	pK_a
1.	Trifluoroacetic acid	None	0 %	0.2
2.	Acetic acid	Yes	60 %	4.7
3.	Trichloroacetic acid	Yes	7.4 %	0.7
4.	Terephthalic acid	None	0 %	3.5
5.	Formic	Yes	98 %	3.8

Reactions were run with 0.0144 mmol of substrate, and the conversion was determined by ^{1}H NMR.

Figure 4: Optimization of the Different Equivalent of Acids

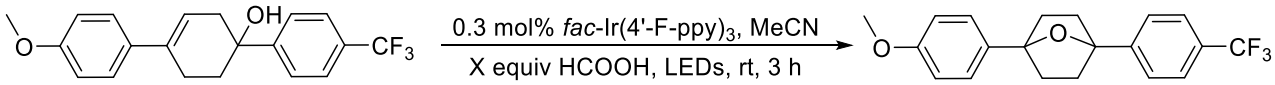

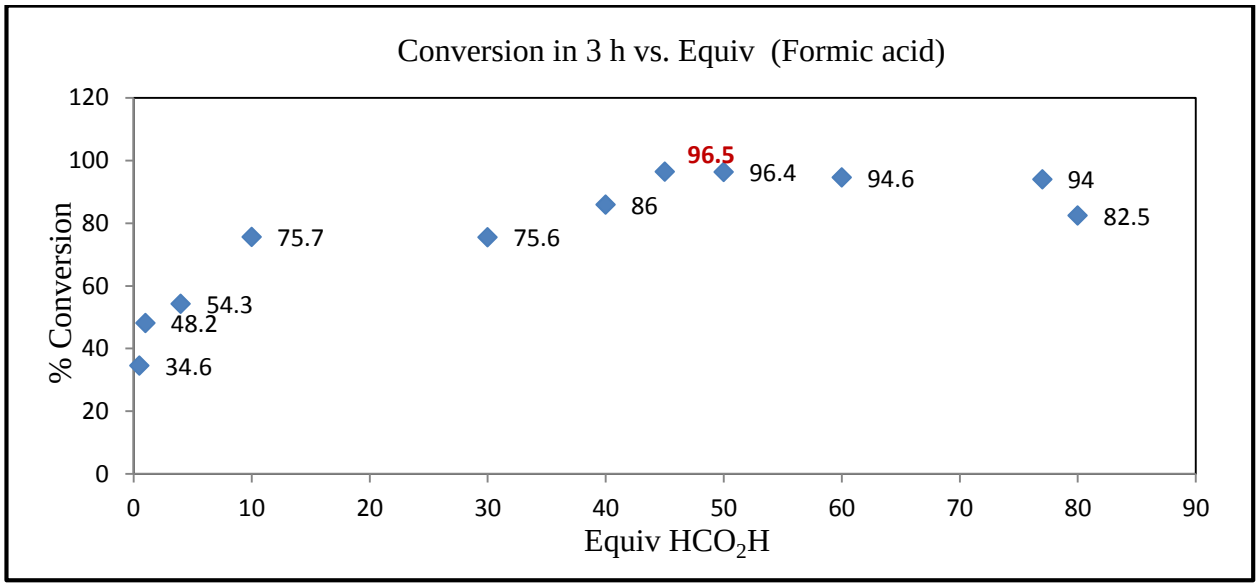

Figure 4: Conversion vs. Equivalence of formic acid

Reactions were run with 0.0144 mmol of substrate, and the conversion was determined by NMR.

The photocatalyst was expected to have a significant impact on the rate of the reaction for two reasons. The emissive energy of the catalyst must match the energy levels of the substrate inorder for the isomerization to take place. If the energy of the biradicalis much greater than the emissive energy of the energy donor (excited photocatalyst), then energy transfer will be a very unlikely event. In addition to energy considerations, the sterics of the catalyst are known to be important and were similarly expected to be important for this reaction.[18] While holding other conditions constant, the catalyst structure was varied (Figure 5 and 6). Catalyst*fac*-Ir(4'-F-ppy)$_3$ **2b** gave the greatest conversion while **2a** gave the lowest. This finding is consistent with earlier findings in the group,[18] which suggested that the rate of alkene isomerization depended heavily on the catalyst volume, with smaller and high energy catalysts being the best at isomerization.[18]

Table 5: Optimization of the Different Catalyst

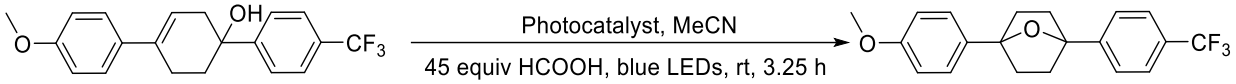

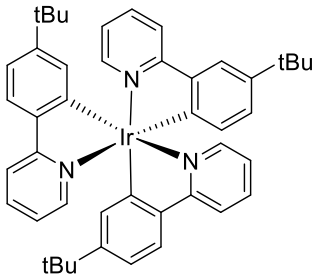

2a

Emission: 54.5 kcal/mol
Radius: 5.00 Å

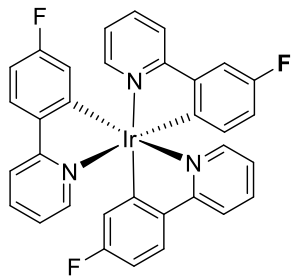

2b

Emission: 58.6 kcal/mol
Radius: 4.57 Å

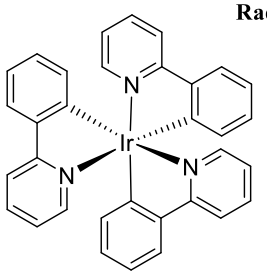

2c

Emission: 55.2 kcal/mol
Radius: 4.40 Å

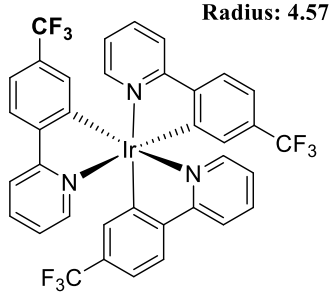

2d

Emission: 56.4 kcal/mol
Radius: 4.80 Å

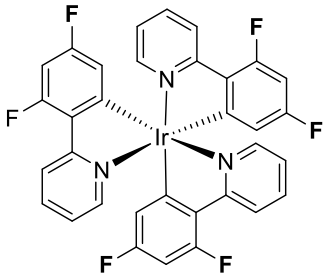

2e

Emission: 60.1 kcal/mol
Radius: 4.62 Å

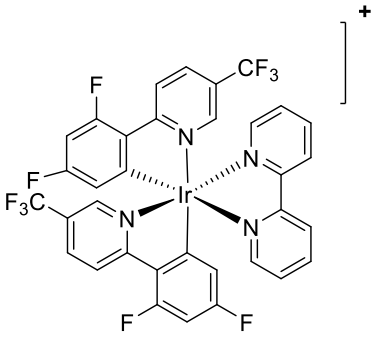

3a

Emission: 60.4 kcal/mol
Radius: n/a Å

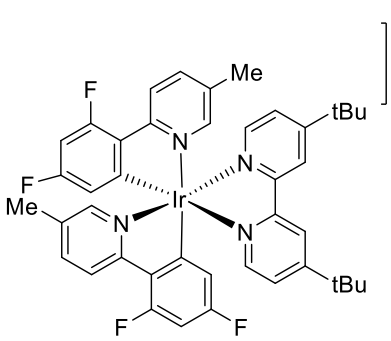

3b

Emission: 60.2 kcal/mol
Radius: n/a Å

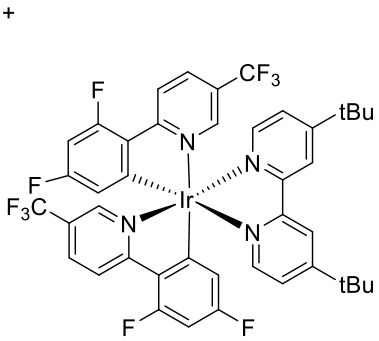

3c

Emission: 60.1 kcal/mol
Radius: 5.02 Å

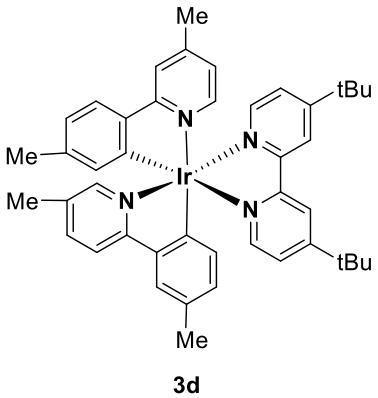

3d

Emission: 47.89 kcal/mol
Radius: n/a Å

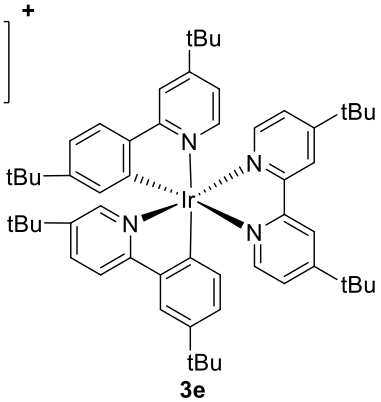

3e

Emission: 49.04 kcal/mol
Radius: n/a Å

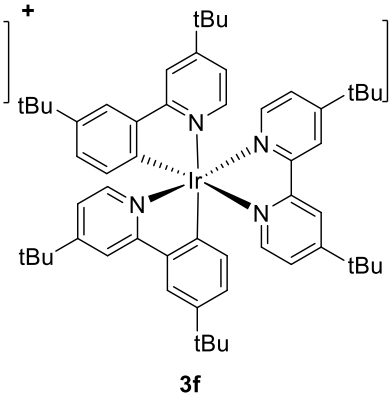

3f

Emission: 46.56 kcal/mol
Radius: n/a Å

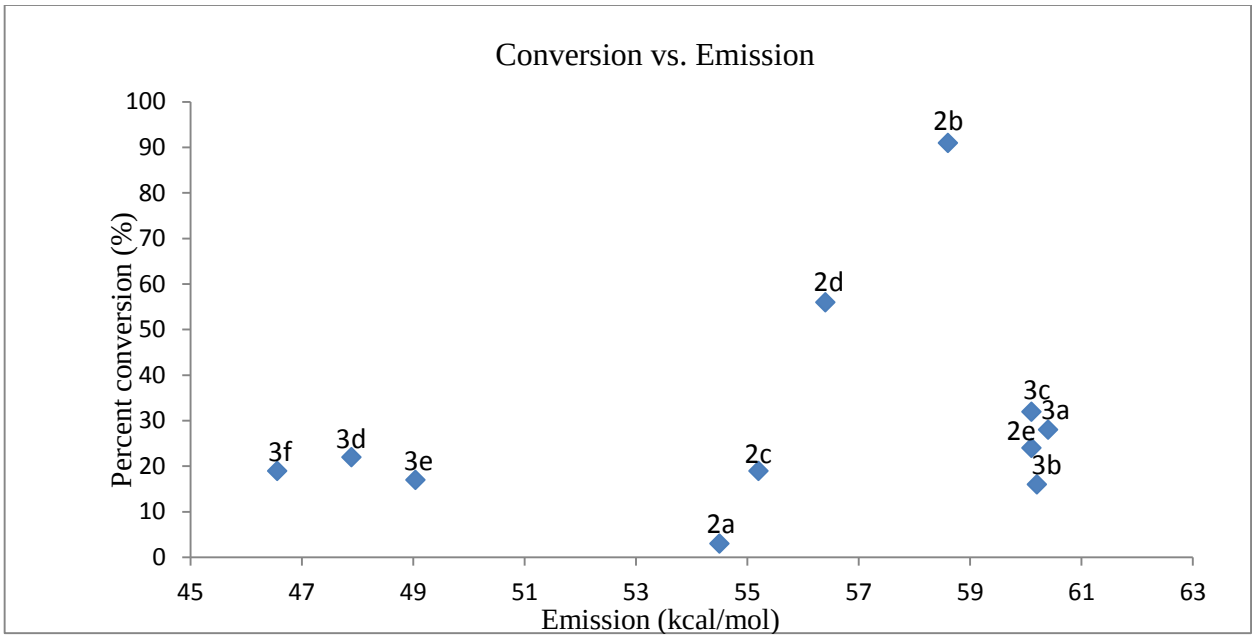

Figure 5: Conversion vs. Emissive Energy

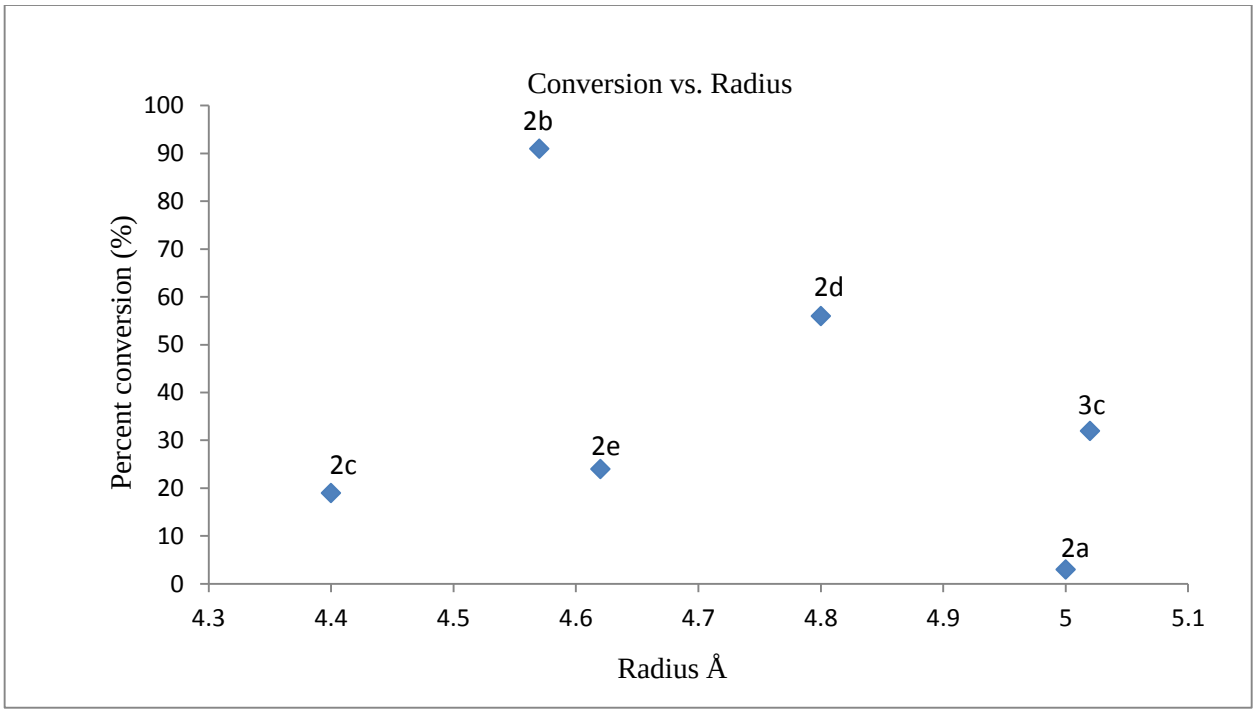

Figure 6: Conversion vs. Radius

Reactions were run with 0.0144 mmol of substrate, and the conversion was determined by NMR after 3.25 hour.

Table 6: Optimization of the Different Temperature.

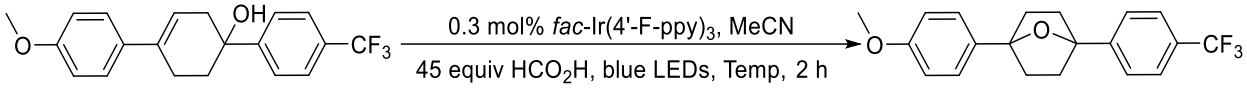

Trial	Temperature (^{o}C)	Conversion
1.	-20	41 %
2.	-10	48 %
3.	0	17 %
4.	30	29 %
5.	45	61 %
6.	60	59 %

Reactions were run with 0.0144 mmol of substrate, and the conversion was determined by NMR after 2 h.

Next, we examined the reaction as a function of temperature (Table 6). The reaction was particularly interesting in that temperature profile was bifurcated. Maxima were observed at both -10 ^{o}C and 45 ^{o}C. This can be rationalized in the following way. At lower temperature, the life-time of *trans*-phenylcyclohexeneincreases and leads to a greater concentration of the reactive species, leading to higher reaction rates. While, at higher temperature the extra energy led to more intermolecular collisions which also may have factored into the rate equation. Intermolecular collisions are expected to be important for both protonation and energy transfer.

While exploring the scope of the reaction, we noticed that with some substrates upon addition of formic acid, the reactions changed from the typical yellow solution to a pink solution and that in every case like this, a low yield was obtained. In addition to the expected ether, an undesired product **3b** was formed and confirmed by isolation. A control study without the catalyst suggest that this product is formed in the absence of the photocatalyst. In order to investigate if it is possible for the formate product to reenter the catalytic cycle, the isolated product was resubjected to reaction conditions, the reaction did not turn to pink and after 24 h, there was no reaction (Scheme 7).

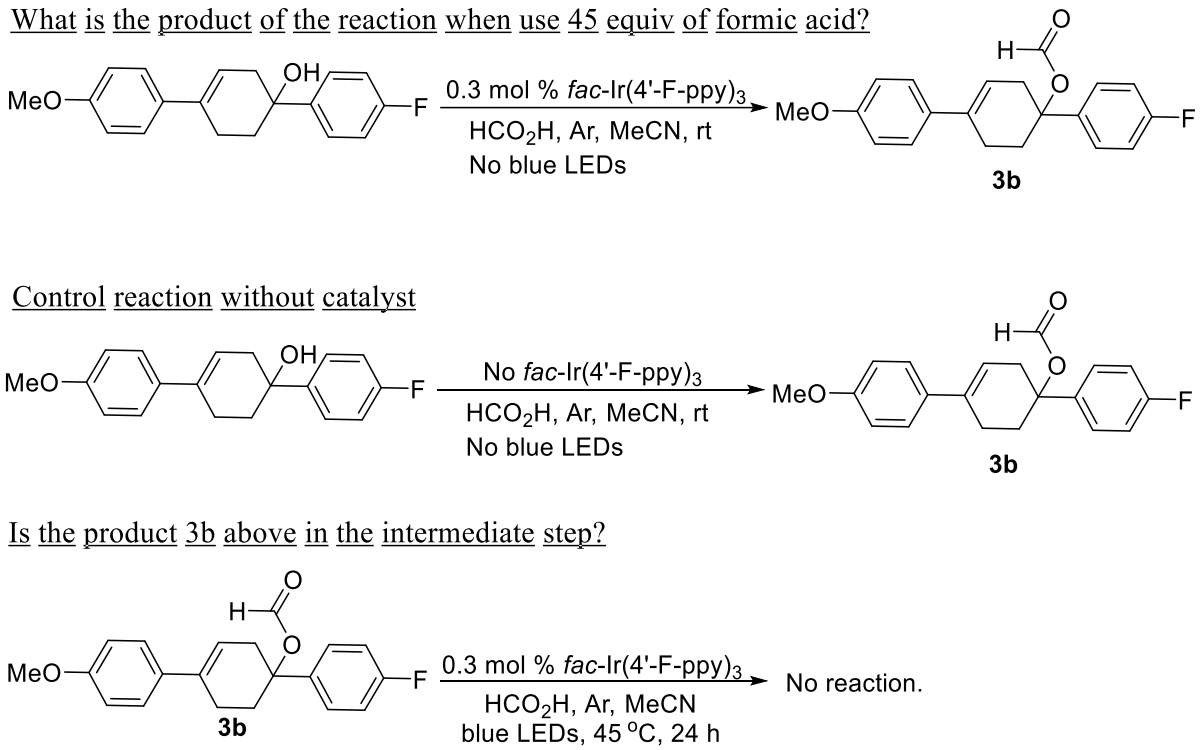

Scheme 7: Testing the viability of the undesired product**3b** under catalytic conditions.

We found it was possible to facilitate the reaction as long as the addition of acid stopped prior to the formation of the pink color. However, the amount of acid which led to the pink solution, varied from substrate to substrate. Thus, we added the formic acid into the reaction for each substrate, stopping just before the color of the solution changed to pink (We had to discard one sample, which used to check how much of formic acid should added to the reaction before the reaction changed to pink). Table 7 shows the actual amount of formic acid needed for each substrate to form the pink solution.

Table 7: The equivalents of formic acid added the reaction with different R functional group before the reaction turn to pink.

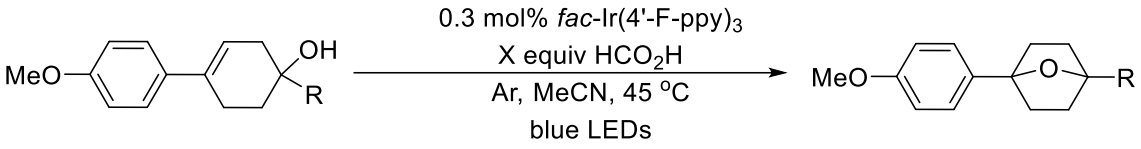

Substrates	Number of equivalent (equiv)
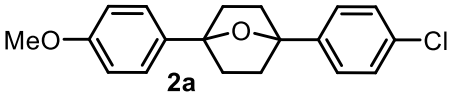 **2a**	6.7
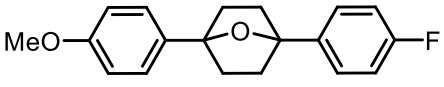 **3a**	9.6
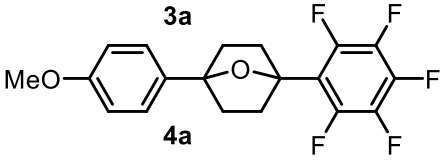 **4a**	23.0
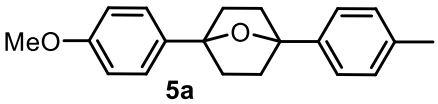 **5a**	15.6
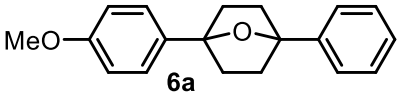 **6a**	8.2
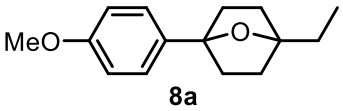 **8a**	29.0

The final optimized conditions are 0.3 mol% of catalyst *fac*-Ir(4'-F-ppy)$_3$(**2b**), 45 equivalents of formic acid, in [0.05 M] in MeCN, at 45^{o}C, the reaction mixture was degased with argon bubbling, and was irradiated with blue LEDs.

Next, the scope of the reaction was evaluated, (Table 8). First, we evaluated substrates with electron rich 4-methoxy-phenylcyclohexenes. The reaction worked well regardless of whether the R substituentwas a strong electron withdrawing group (**1a, 4a)**, weak electron withdrawing group (**2a**, **3a**), and neutral functional group (**5a, 6a, 7a, 8a**). All gave high yield

from 75 to 90 %. Next, we evaluated the reaction with different functional groups at the aryl position. We found that substrates with the electro-neutral groups gave good yields (**10a,** 85 %). While weak electron withdrawing groups (**11a** and **12a**) gave reasonable isolated yields of 56% to 85 %, respectively. However, the substrate with the strong electron withdrawing group (**13a**) did not react. This last class may have failed as a result of difficult protonation or because the carbenium ion underwent rapid elimination to reform the starting material.

Table 8: Final products and percent yield.

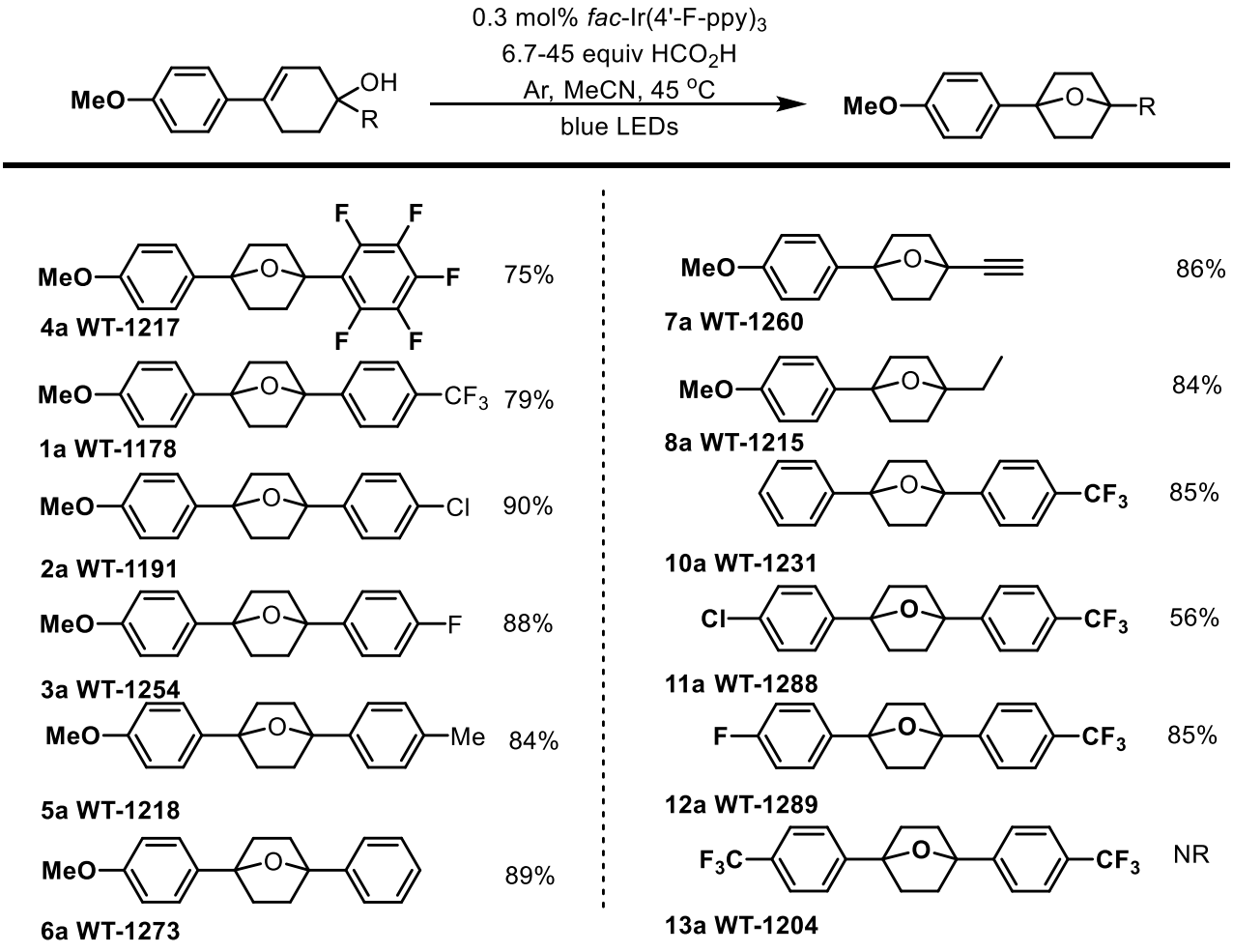

Section 2: Stereochemical Evidence:

As previously discussed (Scheme 6), we believe that the etherification reaction is taking place via the photocatalytic isomerization to the *trans*-cyclohexene which then undergoes acid catalyzed hydroalkoxylation. To confirm the stereochemical outcome of the reaction, we carried out a labeling experiment twhich provides stereochemical evidence of the existence of *trans*-cyclohexene. The isolated products**1b**are shown in the spectra below (Fig. 7). Spectrum A shows the product obtained from normal reaction conditions, the spectrum shows all 4 protons at axial position and 4 protons at the equatorial position at 2.25 and 2.00 ppm, respectively. Whereas, spectrum B is the product obtained when the reaction was run with 450 equiv of D_2O added to it prior to photolysis. Due to the large excess of D_2O and rapid exchange of acidic protons, it was expected that this would ensure that effectively all acidic protons were replaced with deuterium, and thus, should lead to deuteration of the double bond. Indeed, there was 25% deuterium incorporation according to H integration of methylene region of spectrum B. This represents 100% incorporation because it is only possible for one of four positions to be deuterated. At 2.25 ppm, the peak integrates to 3protons (Spectra B) instead of 4 protons (Spectra A). The deuterium is incorporated in downfield peak which indicates it is in the axial position. To confirm the assignment of the deuterium in the axial position, energy minimization and ^{1}H NMR structure calculations were performed using of B3LYP/6-31G method for the diphenyl analog (The Cartesian coordinates, energy minimization RAM1 Energy 0.034524252166 Hartree, and NMR chemical shift data are in the Supporting Information). In the figure 8, the protons at axial positions (19, 21, 35, and 36) have chemical shift downfield at 2.67 ppm while the protons at equatorial positions (18, 20, 34, and 37) have the chemical shift upfield at 2.53ppm.While the absolute values of the shift are different, the relative position is as expected. The calculations

areconsistent with protonation of a chair *trans*-cyclohexene which leads to the chair conformer, followed by interconversion to the boat and cyclization as outlined in Scheme 5.

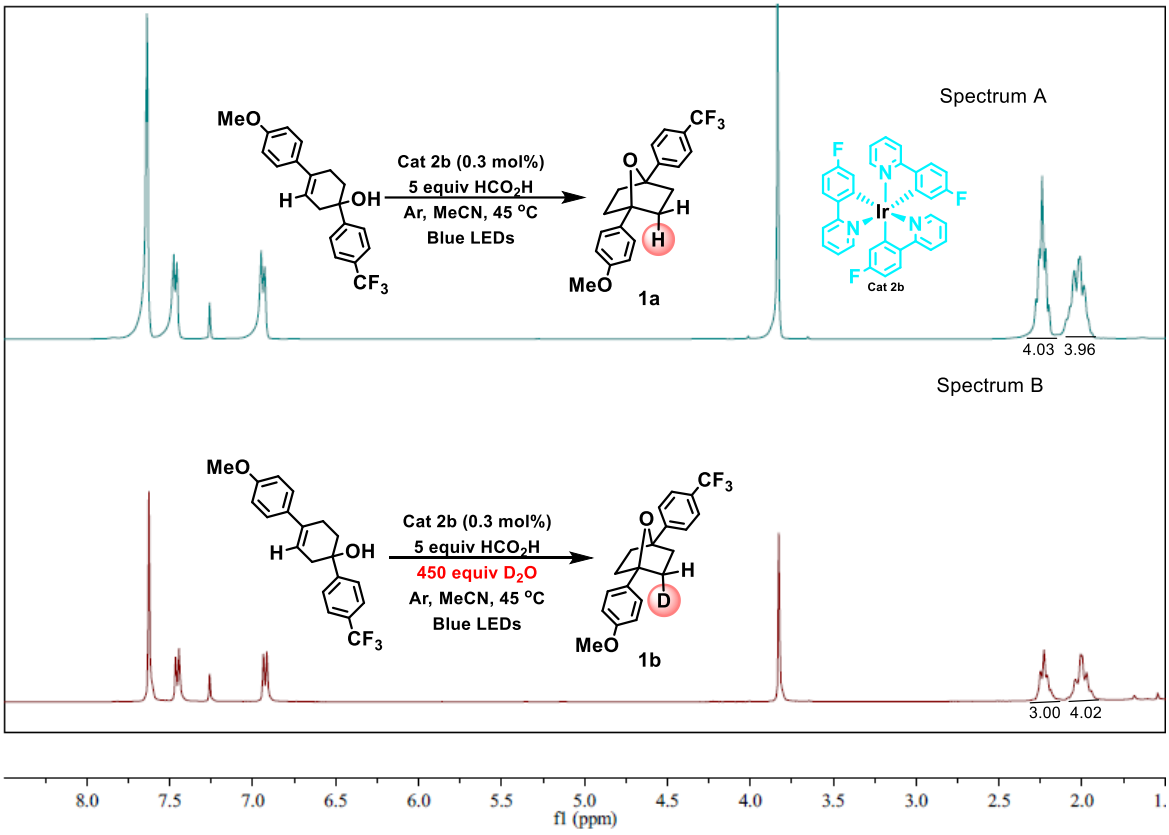

Figure 7: ^{1}H NMRs of ether product from the standard reaction condition and from the reaction in the presence of excess D_2O.

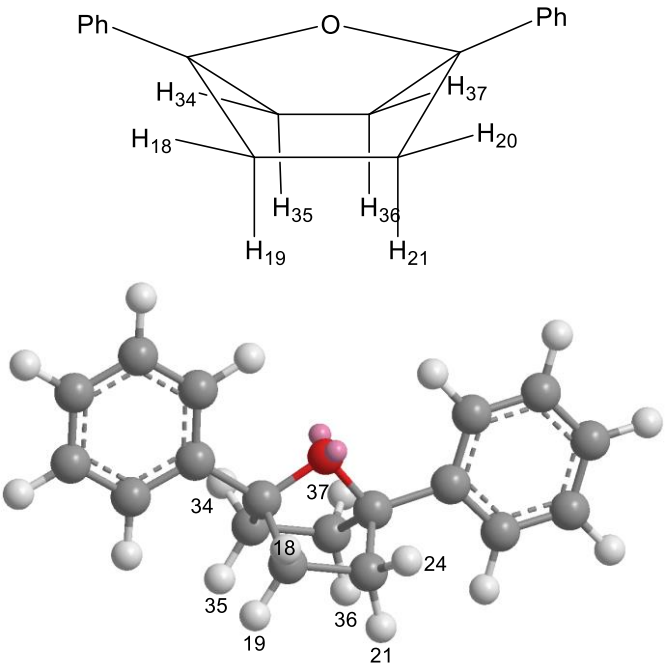

Figure 8: The structure was used for calculation by using B3LYP/6-31G

Section 3: ^{1}H NMR evidence

In order to provide additional evidence of the existence of *trans*-cyclohexene, we conducted low temperature NMR experiments in hopes of observing the transient species. From the beginning, we assumed that we would not be able to have the alcohol moiety present on the molecule or even acid present. Consequently, we utilized reaction **I** in our NMR experiments in which the des-alcohol substrate was used and the reaction was devoid of acid.

Reaction **I** was observed by ^{1}H NMR at -70 ^{o}C, there was a new peak that appeared at 4.15 ppm in spectrum A (Figure 9). To rule this out as a peak related to *trans*-cyclohexene, or a conformer of *cis*-cyclohexene peak, we warmed the NMR tube to the room temperature. The ^{1}H NMR at 25 ^{o}C, the peak at 4.15 ppm disappeared (Spectrum B). However, when we ran the ^{1}H NMR of the control reaction without catalyst at -70 ^{o}C, the peak started to appear again (Spectrum C). This proved the peak at 4.15 ppm was not *trans*-cyclohexene, though it seemed conceivable that it could be a conformer of *cis*-cyclohexene which was freezing out at low temperature (Scheme 8). To test this hypothesis, we also ran ^{1}H NMR of only THF. Indeed, there was a new peak appeared (Spectra D) which has a peak very near the signal. The slight difference is likely due to the absence of DMF as a cosolvent, which was necessary to depress the freezing point and maintain solubility. This suggests the new peak in spectra B and C was not a conformer of *cis*- or *trans*-cyclohexene, but rather, that it was most likely a conformer of THF which becomes observable at low temperature (Scheme 9).

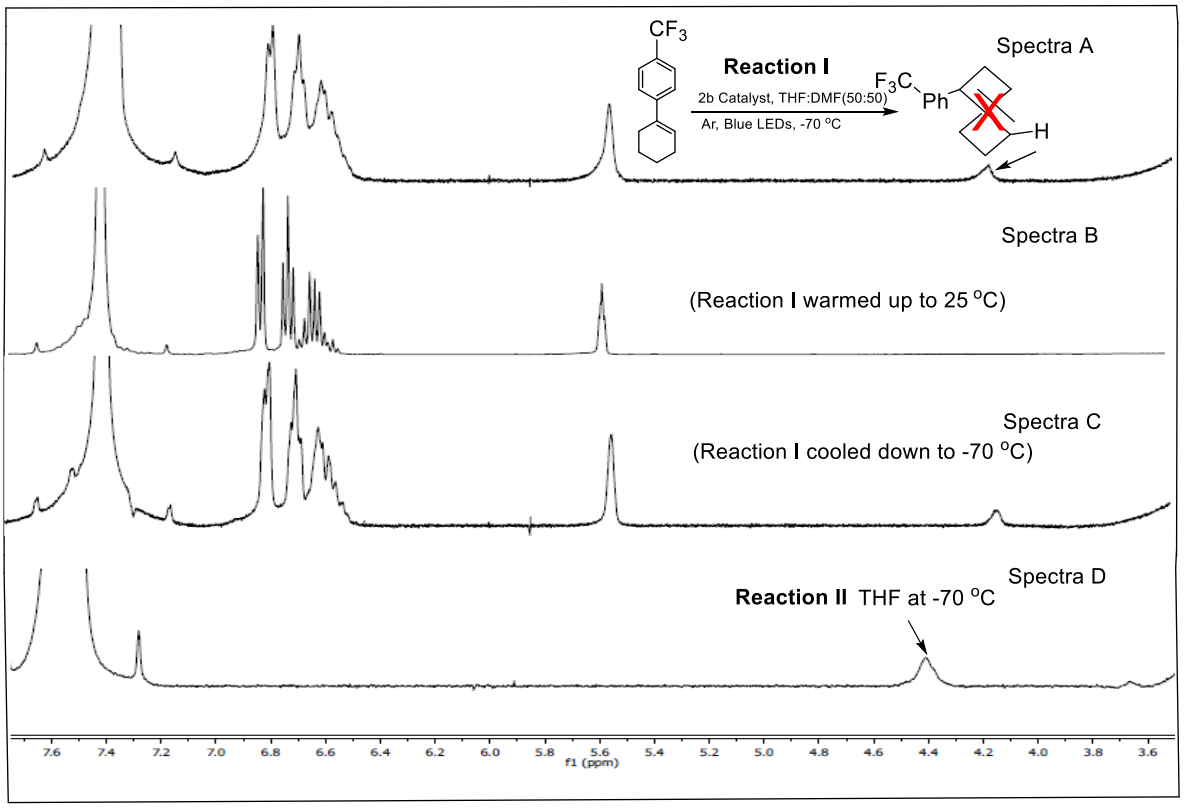

Figure 9: Spectrum A is ^{1}H NMR of the reaction with blue LEDs at -70 ^{o}C. Spectrum B is ^{1}H NMR of the reaction warm up to 25 ^{o}C. Spectrum C is ^{1}H NMR of the reaction cool down to -70 ^{o}C after warm up. Spectrum D is the ^{1}H NMR of THF solvent. Reaction I When the photocatalytic isomerization of phenyl-cyclooctenewas attempted using was DMF (in an unpublished result) it cleanly and rapidly established a photo-stationary state with the *trans*-phenylcyclooctene and thus seemed ideal for estabilishing a significant population of *trans*-phenylcyclohexene. However, DMF has melting point at -60.5 ^{o}C which precluded its exclusive use as the solvent. Thus, we added THF as a cosolvent to make sure the reaction wouldn't freeze at least at -87 ^{o}C.

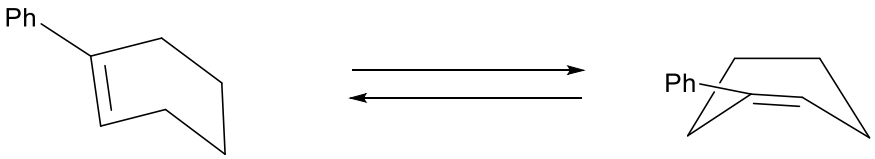

Room temperature (25 ^{o}C) (-87 ^{o}C to 50 ^{o}C)

Scheme 8: Potential conformers of phenylcyclohexene

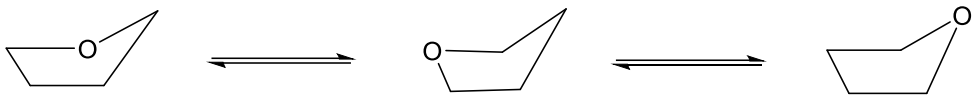

Scheme 9: Potential conformers of THF

At -70 ^{o}C, we were not able to see *trans*-phenylcyclohexene. To further investigate, we set up the reaction at -87 ^{o}C, in hopes that the life-time of the *trans*-cyclohexene species might increase enough for us to run an ^{1}H NMR. Indeed a new peak that appeared at 5.85 ppm (Spectrum A, Figure 10). We believe this peak could be *trans*-cyclohexene, to confirm the new peak is a *trans*-phenylcylohexene peak, a similar set of control experiments were performed. Namely, we warmed the NMR tube to the room temperature, and ran the ^{1}H NMR, and the peak at 5.75 ppm disappeared (Spectra B, Figure 10). However, after warming to room temperature and cooling to -87 ^{o}C, the peak at 5.75 ppm had disappeared (Spectra C, Figure 10), suggesting that this was really a transient species that was formed only at low temperature which was not stable at elevated temperatures.

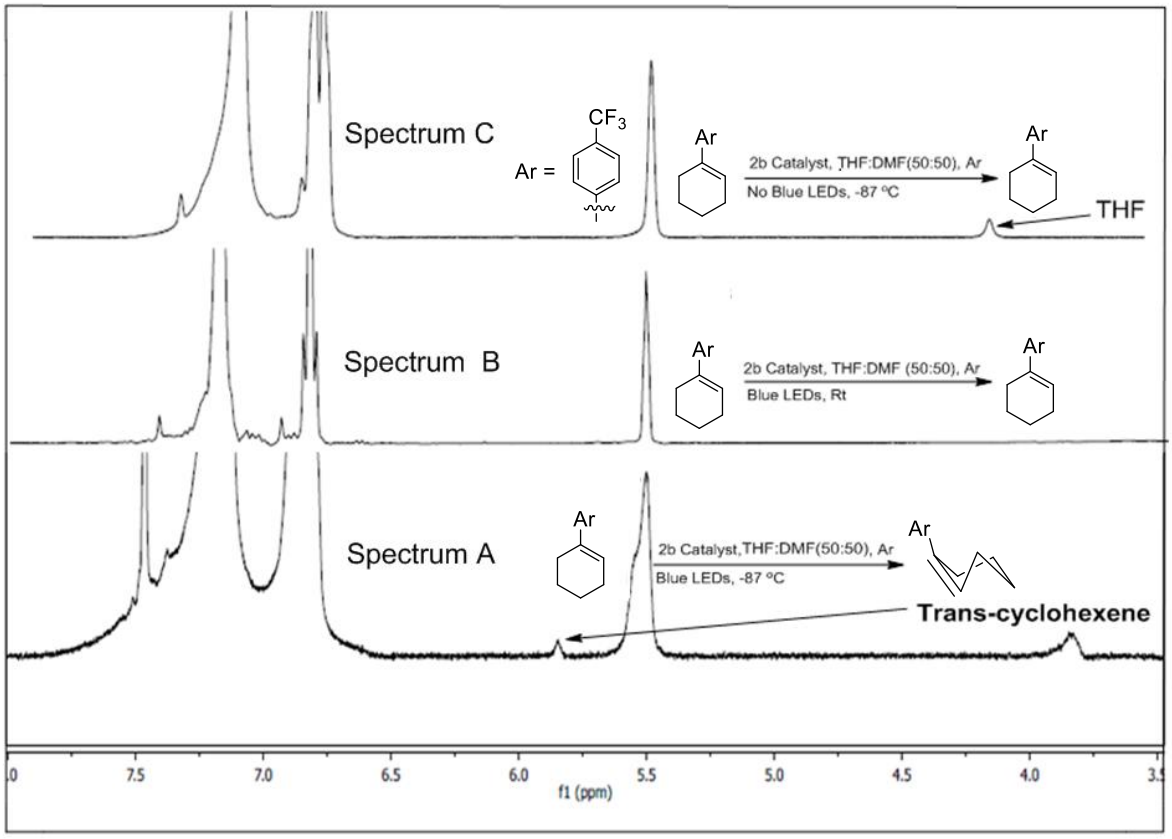

Figure 10: Spectrum A is ^{1}H NMR of the reaction one with blue LEDs at -87 ^{o}C, spectrum B is ^{1}H NMR of the reaction one with blue LEDs at 25 ^{o}C, spectrum C is ^{1}H NMR of the reaction one without blue LEDs at -87 ^{o}C.

Experimentally, these reactions were accomplished by setting the reaction up in an NMR tube and placing within a spinner, and then we placed the spinner with the NMR tube in a very thin plastic bag. Carefully, we placed the plastic bag which had the NMR tube in the blue LEDs bath which was made out of a mirrored dewar which was cooled with a thermostated cold finger and held at -99 ^{o}C. After 24 h of irradiation, the NMR tube was removed. However, before removing the NMR tube from the chilled bath, we added liquid nitrogen into the plastic bag which led to the rapid freezing of the solution within the NMR tube. After freezing, we

transferred NMR tube into a portable nitrogen bath and transported the sample to the NMR. By flash freezing the NMR sample we were able to ensure that the reaction in the NMR tube was still frozen by the time it was inserted into the NMR machine, which was precooled to -87 ^{o}C (the lower limit of the instrument). We discovered several limitations that had to be addressed associated with the low temperature ^{1}H NMR. The first was that we had to find a solvent which has lower melting point than -87 ^{o}C, less the reaction mixture would still be frozen. Secondly, the starting material should not precipitate at -87 ^{o}C in the solvent. Additionally, the NMR instrument had difficulty locking and shimming at low temperature. Finally, sample locking was time consuming which was expected to be a problem given the expected very finite lifetime of *trans*-isomer (recall we could not detect it at -70 ^{o}C). The addition of DMF, in which the photocatalytic etherification also works (see table 2), was added as a cosolvent. We determined the freezing point of a 1:1 mixture to be around 90-100 ^{o}C and we ensured the solubility of the starting material and photocatalyst at the necessarily low temperature. However, the one problem we were not able to solve was the lower temperature limit of the NMR instrument and the time it took to lock the instrument. Therefore, while we have observed a new ^{1}H signal consistent with a vinyl signal of a transiently formed species, the project is on hold until some of these practical limitations are overcome. At which time, we will conduct more NMR experiments which will allow us to more fully characterize the complex.

Section 4: Chemical switch reaction

As discussed, the etherification worked well regardless of the hybridization of the carbon attached to the alcoholic carbon. However, when the carbinol substituent was replaced with a hydrogen, the expected ether did not form, but rather the diol product (**9b**, Scheme 10). As shown in Scheme 9, 1-(4-methoxyphenyl)cyclohexane-1,4-diol (**9b**) was made via the photocatalytic hydration of 4'-methoxy-2,3,4,5-tetrahydro-[1,1'-biphenyl]-4-ol (**9a**)in the presence of catalyst*fac*-Ir(4'-F-ppy)$_3$(**2b**), 45 equivalents of formic acid, acetonitrile, at 25 ^{o}C. It is interesting that a different type of product that was formed when this substrate was used when compared to substrates containing a tertiary alcohol. This may be a result of the fact that the alcohol functional group, having a larger A-value than hydrogen, adopts the equatorial position. Nonetheless, at slightly higher temperatures, 45 ^{o}C, the diol product was found to revert to the thermodynamically favored starting material (**9a**). Resubjecting **9b** to reaction conditions, less the photocatalyst, show that the photocatalyst was not necessary for the elimination reaction. Thus, the hydration reaction was photocatalyzed, while the dehydration was a thermal process. This is an interesting scenario which allows the possibility to easily toggle between two states simply by changing one stimuli, namely light or dark. So when the reaction vessel was irradiated the diol (**9b**) is formed, and after turning the lights off, the product undergoes clean dehydration to form the starting material (**9a**). It is conceivable that, with further development, this reaction might be able to serve as a chemical switch.

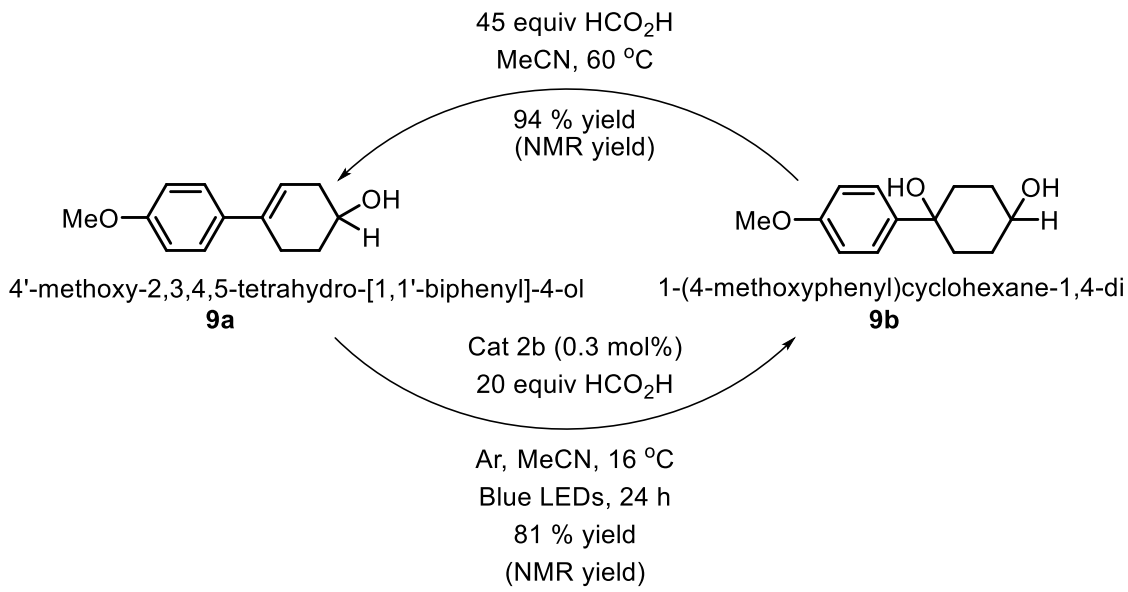

Scheme 10: Chemical switch reaction

III. CONCLUSION

First and foremost, we have developed a convenient method for generation of *trans*-cyclohexene which utilizes blue LEDs rather than UV-light. It is expected that the oxabicyclic products will have some bioactivity, given that related molecules are active. Given that it does not seem possible to synthesize this class of motif via a Brønsted acid, this should be a useful transformation. Additionally, we also provided convincing stereochemical evidence of a *trans*-cyclohexene. We have shown it may be possible to directly observe a *trans*-cyclohexne via NMR at temperatures below -87 ^{o}C. Finally, we have also demonstrated a proof of concept in a new type of photocatalytic chemical switch.

IV. REFERENCES

(1) Brown, W.H; Foote, C.S; Inversion, B.L; Anslyn, E.V; Novak, B.M. Organic Chemistry. 6th Ed.

(2) http://chemistry.stackexchange.com/questions/30940/*cis-trans*-stability-of-cycloalkenes

(3) Richard P.J; Kenneth, J. D. J. Org. Chem. 1995, 60, 1074-1076.

(4) Wallraff, G. M; Michl, J. J. Org. Chem. 1986, 51, 1794.

(5) Inoue, Y; Ueoka, T; Kuroda, T; Hakushi, T. J. Chem. Soc. Perkin *Trans*, 2 1983, 983.

(6) Bonneau. R; Dubien, J. J; Salem.L; Yarwood, J. A.J. Am. Chem. Soc., 1976, 98 (14), pp 4329–4330.

(7) Dauben, W. G; Riel, H. C. H. A; Hauw, C; Leroy, F; Dubien, J. J; Bonneau, R. J. Am. Chem. Soc, 1979, 101 (7), 1901-1903.

(8) Richard, J;Rothenberg, M.E;Jencks,W.P. J. Am. Chem. Soc.1984,106, 1361-1372.

(9) Frances L. Cozens; Robert A. Clelland; Steen Steenken. J. Am. Chem. Soc. 1993, 115, 5050-5055.

(10) http://chemwiki.ucdavis.edu/Core/Physical_Chemistry/Kinetics/Reaction_Rates/Experimental_Determination_of_Kinetcs/Relaxation_Methods/Flash_Photolysis

(11) Verbeek, J; Lenthe, J. H; Timmermans, P. J. J. A; Mackor, A. Budzelaar, P. H. M. J. Org. Chem, 1989, 52 (13), 2955-2957.

(12) Strickland, A. D; Caldwell, R. A. J. Phys. Chem. 1993, 97, 13394.

(13) Singh, K; Staig, S. J; Weaver, J. D. J. Am. Chem. Soc. 2014, 136, 5275-5278.

(14) Allinger, N. L.; Sprague, J. T. J .Am. Chem. SOC 1972,94,5734.

(15) Abraham, R. J; Warne, M. A; Gri, L. J. Chem. Soc. Perkin *Trans*. 2, 1998, 1751

(16) Singh, A.; Teegardin, K.; Kelly, M.; Prasad, K. S.; Krishnan, S.; Weaver, J. D. J. Org. Chem. 2015, 776, 51.

(17) Friese, A.; Hell-Momeni, K.; Zündorf, I.; Winckler, T.; Dingermann, T.; Dannhardt, G. J. Med. Chem. 2002, 45, 1535.

(18) Singh, A; Fennell, C. J; Weaver, J. D. Chem. Sci. 2016

(19) Joaquin, P; Silcia, R. Heterocycles. 2015, 90, 2

(20) Brown, W.H; Foote, C.S; Inversion, B.L; Anslyn, E.V; Novak, B.M. Organic Chemistry. 6th Edition.

V.SUPPORTIVE INFORMATION

All reagents were obtained from commercial suppliers (Aldrich, Oakwood chemicals, and VWR) and used without further purification unless otherwise noted. Acetonitrile (CH_3CN) was dried using molecular sieves. Photocatalyst was synthesized by using our previous method.[16] Reactions were monitored by thin layer chromatography (TLC), obtained from sorbent technology Silica XHL TLC Plates, w/UV254, glass backed, 250 μm, and were visualized with ultraviolet light, potassium permanganate stain. Reaction progress was occasionally monitored GC-MS (QP 2010S, Shimadzu equipped with auto sampler).

Photo catalytic reactions were set up in a light bath which is described below. Strips of blue LEDs,(18 LED's/ft) were purchased from Solid Apollo and were wrapped around on the walls of glass crystallization dish and secured with masking tape and then wrapped with aluminum foil. A lid which rest on the top was fashioned from cardboard and holes were made such that reaction tubes (12 X 75 mm cultural borosilicate tube) were held firmly in the cardboard lid which was placed on the top of bath. Water was added to the bath such that the tubes were submerged in the water which was maintained at 45^{o}C with the aid of a sand bath connected to a thermostat.

Flash chromatography was carried out with Merck 60 Å, mesh 230-400 silica gel. NMR spectra were obtained on 400 MHz Bruker Avance III spectrometer. ^{1}H and ^{13}C NMR chemical shifts are reported in ppm relative to the residual protio solvent peak (^{1}H, ^{13}C). IR spectra were recorded on Perkin Elmer 2000 FT-IR..Melting points were determined on Mel-Temp apparatus and reported uncorrected. Molecular weight of the molecules was carried out by Agilent 6850 Series GC-MS system.

Section 2: Synthesize substrates

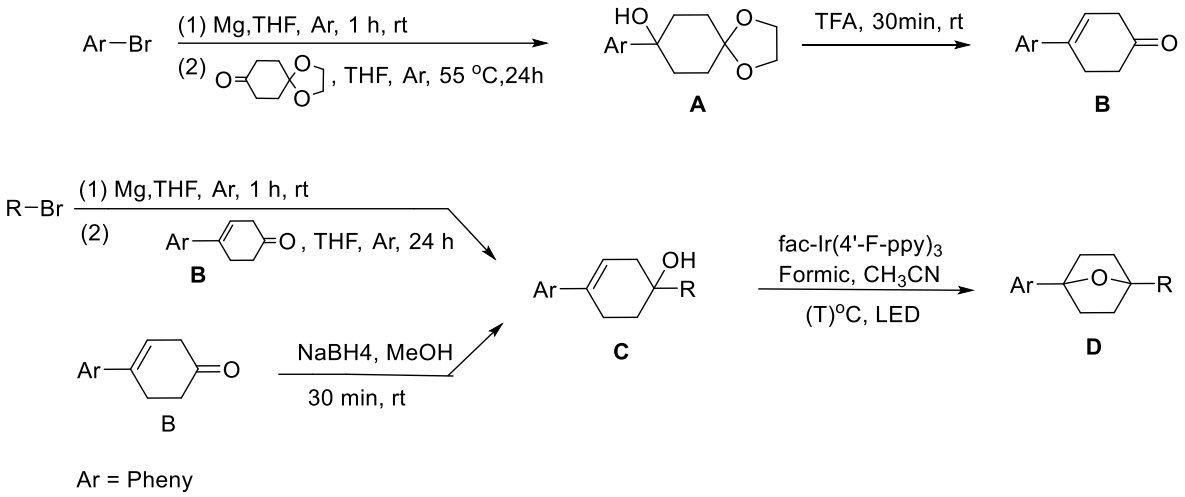

Table 1: Summary of various substrates A and B with percent yields.

S.No	Ar	% Yield of A	% Yield of B
1	4-Methoxyphenyl	46	62
2	Phenyl	41	92
3	4-Fluorophenyl	33	45
4	4-Chlorophenyl	40	96
5	4-Trifluoromethylphenyl	30	35

Table 3: Summary of various substrates C with percent yields.

S.No	Ar	R	% Yield
1a	4-Methoxyphenyl	4-Trifluoromethylphenyl	12
2a	4-Methoxyphenyl	4-Chlorophenyl	13
3a	4-Methoxyphenyl	4-Florophenyl	35
4a	4-Methoxyphenyl	Pentaflourophenyl	5
5a	4-Methoxyphenyl	Toluene	35
6a	4-Methoxyphenyl	Phenyl	42
7a	4-Methoxyphenyl	Ethyne	45
8a	4-Methoxyphenyl	Ethyl	25
9a	4-Methoxyphenyl	H	90
10a	Phenyl	4-Trifluoromethylphenyl	42
11a	4-Chlorophenyl	4-Trifluoromethylphenyl	18
12a	4-Fluorophenyl	4-Trifluoromethylphenyl	14
13a	4-Trifluoromethylphenyl	4-Trifluoromethylphenyl	4

General Procedure A[17].

To an oven dried round bottom flash equipped with magnetic stir bar was added magnesium metal (56.09 mmol, 2.5 equiv), a pinch of I_2, THF (20 equiv) then 1-bromo-4-methoxybenzene (44.87 mmol, 2.0 equiv) was added portion-wise. The mixture was stirred at room temperature for 1 hour. After the complete consumption of 1-bromo-4-methoxybenzene, the reaction mixture was cooled to 0^{o}C, and 1,4cyclohexanedionemonothyleneacetal (22.44 mmol, 1 equiv) in (10-20 eqv) THF was added drop-wise to the mixture. The reaction mixture heated at

55°C until goes to completion in between 16-24h. After the completion, the mixture was quenched by NH_4Cl (50 mL) and extracted with EtOAc (3x50 mL). The combined organic layer was washed with 0.1M NaOH (40 mL). The organic layer was separated and dried with $MgSO_4$, and concentrated to obtain the crude product that was purified by normal phase chromatography. Normal phase chromatography was performed with Teledyne ISCO automated chromatography system using Hexane: Ethyl acetate over 0-70 column volumes using flow rated from 35-80 mL/min on Redisep column of 40-80 g with product detection at 254 and 288 nm. The product is dilute from 15-20% of ethyl acetate.

General Procedure B[17].

To an oven dried round bottom flash equipped with magnetic stir bar was added A (1 equiv), THF (13 equiv). The mixture was stirred at room temperature for 30 min. After the completion, the mixture was quenched by saturated $NaHCO_3$ (1 mL) and extract with DCM (2x10 mL). The combined organic layer was washed with distilled water (10mL). The organic layer was separated and dried with $MgSO_4$, and concentrated to obtain the crude product that was purified by normal phase chromatography. Normal phase chromatography was performed using Hexane: Ethyl acetate over 0-70 volume columns using flow rated from 35-80 mL/min on Redisep column of 40-80 g with product detection at 254 and 288 nm. The product is dilute in 100 % hexane.

General Procedure C

Same as procedure A and if X = H to an oven dried round bottom flash equipped with magnetic stir bar was added compound B (1 equiv), MeOH (55 equiv), then added $NaBH_4$ (3 equiv) portion-wise. The mixture was stirred at room temperature for 30 min. After the completion, the mixture was quenched with HCl (1M, 10 mL) and extract with CH_2Cl_2 (2x10

mL). The organic layer was separated and dried with $MgSO_4$, and concentrated to obtain the crude product that was purified by normal phase chromatography. Normal phase chromatography was performed using Hexane: Ethyl acetate over 0-70 volume columns using flow rated from 35-80 mL/min on Redisep column of 40-80 g with product detection at 254 and 288 nm. The product was dilute with 15-20% of ethyl acetate.

General procedure D (Photocatalytic reactions and characterization)

A 20 mL disposable scintillation vial was charged with compound D (x mmol,1 equiv), y mL of stock solution of 2b catalyst, *fac*-Ir(4'-F-ppy)$_3$(2 mg, 0.0028 mmol 2b catalyst, 20 mL CH_3CN). 45 equiv of formic acid added to the mixture.The mixture was divided equal amount into NMR tubes. A sealed glass capillary containing C_6D_6 was added to each NMR tube. The NMR tube was capped with a septum (Ace glass, part no. 9096-25) and secured with parafilm. The reaction was degassed via Ar bubbling for 10 min at room temperature, then placed in the light bath (*vide supra*) such that the filled portion of the tube was submerged under water. The reaction was monitored periodically by ^{1}H NMR. After the complete consumption of starting material, CH_3CN was removed via rotavap and then purified by normal phase chromatography.

1a (1-(4-methoxyphenyl)-4-(4-(trifluoromethyl)phenyl)-7-oxabicyclo[2.2.1]heptane)

General procedure D was followed using 4''-methoxy-4-(trifluoromethyl)-3',6'-dihydro-[1,1':4',1''-terphenyl]-1'(2'H)-ol (100.00 mg, 0.28 mmol, 1.0 equiv), 6.0 mL of stock solution of*fac*-Ir(4'-F-ppy)$_3$ (2 mg, 0.0028 mmol 2b catalyst, 20 mL CH_3CN), and formic acid (580 mg, 12.6 mmol, 475.39 μL, 45 equiv) was used to afford **1a** in 79% yield (79 mg, 0.226 mmol) as white solid. The crude material was purified by flash chromatography using hexane: ethyl acetate on a 4 g silica column with product

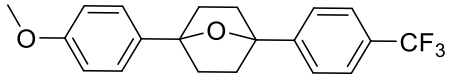

eluting at 5%. ^{1}H NMR (400 MHz, $CDCl_3$) δ 7.62 (dd, 4H), 7.45 (d, *J* = 8.7 Hz, 2H), 6.92 (d, *J* = 8.7 Hz, 2H), 3.83 (s, 3H), 2.30 – 2.17 (m, 4H), 2.09 – 1.92 (m, 4H).^{13}C NMR (101 MHz, $CDCl_3$) δ 158.8, 147.1, 134.7, 129.2 (q, *J* = 32.3 Hz), 126.5, 125.6, 125.2 (q, *J* = 3.6 Hz), 124.3 (q, *J* = 271.9 Hz), 113.7, 87.4, 86.9, 55.3, 38.7, 38.6. ^{19}F NMR (376 MHz, $CDCl_3$) δ -62.37. FT-IR cm^{-1} 2955, 1514, 1333, 1106. GC/MS (m/z, relative intensity) 348 (M^+, 15), 160 (30), 135 (100), 77 (38). Melting point 99-101°C.

1b 1-(4-methoxyphenyl)-4-(4-(trifluoromethyl)phenyl)-7-oxabicyclo[2.2.1]heptane-2-d

General procedure D was followed using 4''-methoxy-4-(trifluoromethyl)-3',6'-dihydro-

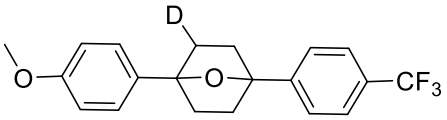

[1,1':4',1''-terphenyl]-1'(2'H)-ol (100.00 mg, 0.28 mmol, 1.0 equiv), 6.0 mL of stock solution of*fac*-Ir(4'-F-ppy)$_3$(2 mg, 0.0028 mmol 2b catalyst, 20 mL CH_3CN), formic acid (5 equiv), and D_2O (450 equiv) was used to afford **1b** in 57% yield (79 mg, 0.226 mmol) as white solid. The crude material was purified by flash chromatography using hexane: ethyl acetate on a 4 g silica column with product eluting at 5%.^{1}H NMR (400 MHz, $CDCl_3$) δ 7.54 (s, 4H), 7.36 (d, *J* = 8.7 Hz, 2H), 6.83 (d, *J* = 8.6 Hz, 2H), 3.73 (s, 3H), 2.19 – 2.07 (m, 3H), 2.01 – 1.80 (m, 4H). ^{13}C NMR (101 MHz, CDCl3) δ 158.80, 147.07, 134.64, 129.18 (q, *J* = 32.3 Hz), 126.52, 125.54, 125.18 (q, *J* = 3.8 Hz), 113.68, 87.32, 86.89, 55.30, 38.69, 38.61, 38.55, 38.23. ^{19}F NMR (376 MHz, $CDCl_3$) δ -62.37.

2a (1-(4-chlorophenyl)-4-(4-methoxyphenyl)-7-oxabicyclo[2.2.1]heptane)

General procedure D was followed using 4-chloro-4''-methoxy-3',6'-dihydro-[1,1':4',1''-

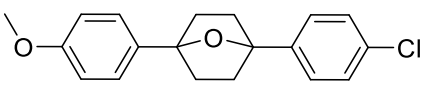

terphenyl]-1'(2'H)-ol (100.00 mg, 0.32 mmol, 1.0 equiv), 5.4 mL of stock solution of*fac*-Ir(4'-F-ppy)$_3$ (2 mg, 0.0028 mmol2bcatalyst, 20 mL CH_3CN), and formic acid (98.6 mg, 2.14 mmol, 80.8 μL, 6.7 equiv) was

used to afford **2a** in 90% yield (90 mg, 0.226 mmol) as white solid. The crude material was purified by flash chromatography using hexane : ethyl acetate on a 4 g silica column with product eluting at 10%.^{1}H NMR (400 MHz, $CDCl_3$) δ 7.51 – 7.44 (m, 4H), 7.36 (d, *J* = 8.4 Hz, 2H), 6.94 (d, *J* = 8.6 Hz, 2H), 3.85 (s, 3H), 2.22 (d, *J* = 7.4 Hz, 4H), 2.11 – 1.93 (m, 4H). ^{13}C NMR (101 MHz, $CDCl_3$) δ 158.7, 141.6, 134.8, 132.7, 128.3, 126.7, 126.5, 113.7, 87.3, 86.8, 55.3, 38.7, 38.6. FT-IR cm^{-1} 2953, 1515,1254, 1088. GC/MS (m/z, relative intensity) 314 (M^+, 20), 279 (10), 135 (100), 77 (45). Melting point 98-99^{o}C.

3a (1-(4-fluorophenyl)-4-(4-methoxyphenyl)-7-oxabicyclo[2.2.1]heptane)

General procedure D was followed using 4-fluoro-4"-methoxy-3',6'-dihydro-[1,1':4',1"-terphenyl]-

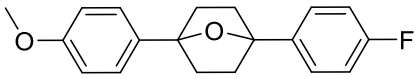

1'(2'H)-ol (100.00 mg, 0.34 mmol, 1.0 equiv), 7 mL of stock solution of*fac*-Ir(4'-F-ppy)$_3$(2 mg, 0.0028 mmol 2b catalyst, 20 mL CH_3CN), and formic acid (148.2 mg, 2.14 mmol, 121.5 μL, 9.6 equiv) was used to afford **2a** in 88% yield (90 mg, 0.30 mmol) as white solid. The crude material was purified by flash chromatography using hexane: ethyl acetate on a 4 g silica column with product eluting at 5%.^{1}H NMR (400 MHz, $CDCl_3$) δ 7.64 – 7.42 (m, 4H), 7.16 – 7.02 (m, 2H), 7.02 – 6.87 (m, 2H), 3.84 (s, 3H), 2.41 – 2.15 (m, 4H), 2.15 – 1.86 (m, 4H). ^{13}C NMR (101 MHz, $CDCl_3$) δ 162.33 (d, *J* = 244.7 Hz), 159.14, 139.22, 135.29, 127.38 (d, *J* = 7.9 Hz), 126.94, 115.40 (d, *J* = 21.3 Hz), 114.05,, 87.63, 87.29, 55.71, 39.20, 39.10. ^{19}F NMR (376 MHz, Chloroform-*d*) δ -115.87 (s, 1F). FT-IR cm^{-1} 2952, 1511, 1247, 1172. GC/MS (m/z, relative intensity) 298 (M^+, 100), 270 (30), 135 (100), 77 (50). Melting point 99-100^{o}C.

4a (1-(4-methoxyphenyl)-4-(perfluorophenyl)-7-oxabicyclo[2.2.1]heptane)

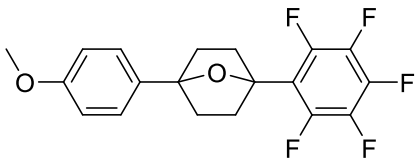

General procedure D was followed using 2,3,4,5,6-pentafluoro-4"-methoxy-3',6'-dihydro-[1,1':4',1"-terphenyl]-1'(2'H)-ol (60.00 mg, 0.16 mmol, 1.0 equiv), 3.4 mL of stock solution of *fac*-Ir(4'-F-ppy)$_3$ (2 mg, 0.0028 mmol2bcatalyst, 20 mL CH_3CN), and formic acid (171.4 mg, 3.73 mmol, 140 μL, 23 equiv) was used to afford **4a** in 75% yield (45 mg, 0.12 mmol) as white solid. The crude material was purified by flash chromatography using hexane : ethyl acetate on a 4 g silica column with product eluting at 5%.^{1}H NMR (400 MHz, $CDCl_3$) δ 7.42 (d, *J* = 8.8 Hz, 2H), 6.91 (d, *J* = 8.7 Hz, 2H), 3.86 – 3.78 (m, 3H), 2.37 (dqd, *J* = 11.2, 5.0, 3.3, 2.4 Hz, 2H), 2.24 – 2.07 (m, 4H), 2.04 – 1.92 (m, 2H). ^{13}C NMR (101 MHz, $CDCl_3$) δ 158.8, 144.7 (d, *J* = 255.9 Hz), 140.2 (d, *J* = 233.5 Hz), 137.7 (d, *J* = 231.8 Hz), 134.1, 126.4, 116.1 – 115.5 (m), 113.70, 87.1, 83.8, 55.3, 38.0 (t, *J* = 2.8 Hz), 37.6. ^{19}F NMR (376 MHz, $CDCl_3$) δ -138.30 (dd, *J* = 22.5, 7.2 Hz, 2F), -156.24 (td, *J* = 21.3, 4.2 Hz, 1F), -162.31 – -162.63 (m, 2F). FT-IR cm^{-1} 2920, 1488, 1248, 1179. GC/MS (m/z, relative intensity) 370 (M^+, 20), 342 (80), 135 (50), 77 (20). Melting point 133-134^{o}C.

5a (1-(4-methoxyphenyl)-4-(p-tolyl)-7-oxabicyclo[2.2.1]heptane)

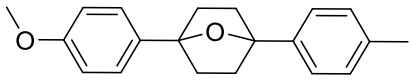

General procedure D was followed using 4"-methoxy-4-methyl-3',6'-dihydro-[1,1':4',1"-terphenyl]-1'(2'H)-ol (100.00 mg, 0.34 mmol, 1.0 equiv), 7.1 mL of stock solution of *fac*-Ir(4'-F-ppy)$_3$ (2 mg, 0.0028 mmol2bcatalyst, 20 mL CH_3CN), CH_3CN (7.1 mL), and formic acid (244 mg, 5.30 mmol, 200 μL, 15.6 equiv) was used to afford **5a** in 84% yield (84 mg, 0.29 mmol) as white solid. The crude material was purified by flash chromatography using hexane: ethyl acetate on a 4 g silica column with product eluting at 5%.^{1}H NMR (400 MHz, $CDCl_3$) δ 7.50 – 7.43 (m, 2H), 7.43 – 7.38 (m,

2H), 7.18 (d, *J*= 7.9 Hz, 2H), 6.96 – 6.87 (m, 2H), 3.82 (s, 3H), 2.35 (s, 3H), 2.19 (d, *J* = 8.3 Hz, 4H), 2.00 (d, *J* = 6.7 Hz, 4H). ^{13}C NMR (101 MHz, $CDCl_3$) δ 158.7, 140.0, 136.6, 135.2, 128.9, 126.6, 125.2, 113.6, 87.2, 87.1, 55.3, 38.8, 38.7, 21.2. FT-IR cm^{-1} 2956, 1514, 1247, 1174. GC/MS (m/z, relative intensity) 294 (M+, 30), 150 (40), 135(100), 91 (45). Melting point 101-102ºC.

6a (1-(4-methoxyphenyl)-4-phenyl-7-oxabicyclo[2.2.1]heptane)

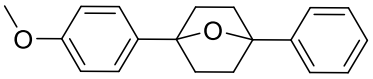

General procedure D was followed using 4"-methoxy-3',6'-dihydro-[1,1':4',1"-terphenyl]-1'(2'H)-ol (100 mg, 0.36 mmol, 1.0 equiv), 7.5 mL of stock solution of *fac*-Ir(4'-F-ppy)$_3$(2.00 mg, 0.0028 mmol2bcatalyst, 20 mL CH_3CN), CH_3CN (7.5 mL), and formic acid (135.5 mg, 2.944 mmol, 111 μL, 8.18 equiv) was used to afford **6a** in 89% yield (89 mg, 0.32 mmol) as white solid. The crude material was purified by flash chromatography using hexane: ethyl acetate on a 4 g silica column with product eluting at 10%.^{1}H NMR (400 MHz, $CDCl_3$) δ 7.63 – 7.50 (m, 2H), 7.50 – 7.43 (m, 2H), 7.37 (d, *J* = 7.6 Hz, 2H), 7.33 – 7.27 (m, 1H), 7.03 – 6.85 (m, 2H), 3.82 (s, 3H), 2.32 – 2.12 (m, 4H), 2.12 – 1.92 (m, 4H). ^{13}C NMR (101 MHz, $CDCl_3$) δ 158.7, 143.1, 135.1, 128.3, 127.0, 126.6, 125.3, 113.7, 87.3, 87.1, 55.3, 38.8, 38.7. FT-IR cm^{-1}2950, 1515, 1248, 1174. GC/MS (m/z, relative intensity) 280 (M^+, 20), 150 (40), 135 (100), 77 (100). Melting point 58-60ºC.

7a (1-ethynyl-4-(4-methoxyphenyl)-7-oxabicyclo[2.2.1]heptane)

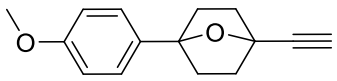

General procedure D was followed using 4"-methoxy-3',6'-dihydro-[1,1':4',1"-terphenyl]-1'(2'H)-ol (100.00 mg, 0.44 mmol, 1.0 equiv), 9.0 mL of stock solution of *fac*-Ir(4'-F-ppy)$_3$ (2 mg, 0.0028 mmol2bcatalyst, 20 mL CH_3CN), and formic acid (907 mg, 19.7 mmol, 744 μL, 45 equiv) was used to afford **7a** in 86% yield (86 mg, 0.38 mmol) as white solid. The crude material was purified by flash chromatography using

hexane: ethyl acetate on a 4 g silica column with product eluting at 5%.^{1}H NMR (400 MHz, $CDCl_3$) δ 7.36 (d, *J* = 8.8 Hz, 2H), 6.87 (d, *J* = 8.8 Hz,2H), 3.80 (s, 3H), 2.64 (s, 1H), 2.20 – 2.11 (m, 2H), 2.11 – 2.01 (m, 4H), 2.00 – 1.87 (m, 2H). ^{13}C NMR (101 MHz, $CDCl_3$) δ 158.77, 133.83, 126.46, 113.58, 87.69, 82.67, 77.23, 74.40, 55.27, 38.48, 37.81. FT-IR cm^{-1} 3238, 2922, 1513, 1255. GC/MS (m/z, relative intensity) 228 (M^+, 15), 135 (100), 77 (70), 39 (65). Melting point 130-131^{o}C.

8a (1-ethyl-4-(4-methoxyphenyl)-7-oxabicyclo[2.2.1]heptane)

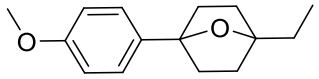

General procedure D was followed using 4-ethyl-4'-methoxy-2,3,4,5-tetrahydro-[1,1'-biphenyl]-4-ol (90.00 mg, 0.39 mmol, 1.0 equiv), 8.1 mL of stock solution of *fac*-Ir(4'-F-ppy)$_3$ (2 mg, 0.0028 mmol2bcatalyst, 20 mL CH_3CN), and formic acid (516 mg, 12.2 mmol, 423 μL, 29 equiv) was used to afford **8a** in 84% yield (75.6 mg, 0.33 mmol) as clear oil. The crude material was purified by flash chromatography using hexane: ethyl acetate on a 4 g silica column with product eluting at 5%.^{1}H NMR (400 MHz, $CDCl_3$) δ 7.37 (d, *J* = 8.7 Hz, 2H), 6.88 (d, *J* = 8.7 Hz, 2H), 3.80 (s, 3H), 2.10 – 2.01 (m, 2H), 1.96 – 1.82 (m, 4H), 1.82 – 1.64 (m, 4H), 1.04 (t, *J* = 7.6 Hz, 3H). ^{13}C NMR (101 MHz, $CDCl_3$) δ 158.9, 135.8, 126.9, 113.9, 87.7, 86.9, 55.7, 38.8, 35.7, 28.9, 9.9. FT-IR cm^{-1} 2964, 1515, 1245, 1175. GC/MS (m/z, relative intensity) 232 (M^+, 20), 189 (20), 150 (30), 135 (100).

9a 1-(4-methoxyphenyl)cyclohexane-1,4-diol

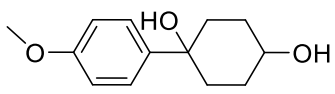

General procedure D was followed by using 4'-methoxy-2,3,4,5-tetrahydro-[1,1'-biphenyl]-4-ol (100.00 mg, 0.49 mmol, 1.0 equiv), 10.5 mL of stock solution of *fac*-Ir(4'-F-ppy)$_3$ (2 mg, 0.0028 mmol2bcatalyst, 20 mL CH_3CN), and formic acid (932.6 mg, 22.05 mmol, 656 μL, 45equiv) was used to afford **9a** in 45% yield (45. mg, 0.22 mmol) as white solid. The crude material was purified by flash chromatography

using hexane : ethyl acetate on a 4 g silica column with product eluting at 5%.^{1}H NMR (400 MHz, $CDCl_3$)^{1}δ 7.46 (d, *J* = 8.6 Hz, 1H), 6.89 (d, *J* = 8.6 Hz, 1H), 4.11 (s, 0H), 3.81 (s, 1H), 2.45 – 2.16 (m, 1H), 2.13 – 1.93 (m, 0H), 1.81 – 1.58 (m, 2H).^{13}C NMR (101 MHz, $CDCl_3$) δ 158.5, 140.9, 126.0, 113.6, 72.6, 66.1, 55.3, 33.1, 29.3. FT-IR cm^{-1} 3315, 2922, 812. GC/MS (m/z, relative intensity).

10a (1-phenyl-4-(4-(trifluoromethyl)phenyl)-7-oxabicyclo[2.2.1]heptane)

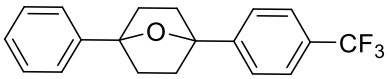

General procedure D was followed using 4-(trifluoromethyl)-3',6'-dihydro-[1,1':4',1''-terphenyl]-1'(2'H)-ol (100 mg, 0.31 mmol, 1.0 equiv), 6.6 mL of stock solution of *fac*-Ir(4'-F-ppy)$_3$ (2 mg, 0.0028 mmol2bcatalyst, 20 mL CH_3CN), and formic acid (641 mg, 13.95 mmol, 526 μL, 45 equiv) was used to afford **10a** in 85% yield (85 mg, 0.27 mmol) as white solid. The crude material was purified by flash chromatography using hexane : ethyl acetate on a 4 g silica column with product eluting at 5%.^{1}H NMR (400 MHz, $CDCl_3$) δ 7.56 (s, 4H), 7.46 (d, 2H), 7.31 (t, *J* = 7.5 Hz, 2H), 7.23 (d, *J* = 7.3 Hz, 1H), 2.28 – 2.07 (m, 4H), 2.04 – 1.85 (m, 4H). ^{13}C NMR (101 MHz, $CDCl_3$) δ 147.0, 142.5, 129.2 (q, *J* = 32.2 Hz), 128.3, 127.1, 125.5, 125.2, 125.2, 124.3 (q), 87.6, 86.9, 38.7, 38.6. ^{19}F NMR (376 MHz, $CDCl_3$) δ -62.39. FT-IR cm^{-1} 2953, 1323, 1154, 1109. GC/MS (m/z, relative intensity) 318 (M^+, 20), 145 (50), 105 (100), 77 (80). Melting point 72^{o}C.

11a (1-(4-chlorophenyl)-4-(4-(trifluoromethyl)phenyl)-7-oxabicyclo[2.2.1]heptane)

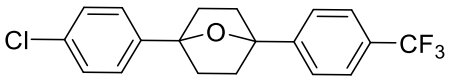

General procedure A was followed using 4''-chloro-4-(trifluoromethyl)-3',6'-dihydro-[1,1':4',1''-terphenyl]-1'(2'H)-ol (100 mg, 0.28 mmol, 1.0 equiv), 5.9 mL of stock solution of *fac*-Ir(4'-F-ppy)$_3$(2 mg, 0.0028 mmol2bcatalyst, 20 mL CH_3CN), CH_3CN (5.9 mL) and formic acid (588 mg, 12.78 mmol, 482 μL, 45 equiv) was used to afford **11a** in 56% yield (56 mg, 0.159 mmol) as white solid. The crude

material was purified by flash chromatography using hexane : ethyl acetate on a 4 g silica column with product eluting at 5%.^{1}H NMR (400 MHz, $CDCl_3$) δ 7.63 (s, 4H), 7.50 – 7.43 (m, 2H), 7.39 – 7.33 (m, 2H), 2.33 – 2.16 (m, 4H), 2.05 – 1.94 (m, 4H). ^{13}C NMR (101 MHz, $CDCl_3$) δ 146.69 (d, *J* = 1.5 Hz), 141.06, 132.92, 129.31 (q, *J* = 32.4 Hz), 128.43, 126.64, 125.48, 125.23 (q, *J* = 3.8 Hz), 124.24 (q, *J* = 271.9 Hz), 87.14, 87.08, 38.60, 38.57. ^{19}F NMR (376 MHz, $CDCl_3$) δ -62.40. FT-IR cm^{-1} 2922, 1321, 1124, 1067. GC/MS (m/z, relative intensity) 352 (M^+, 20), 173 (30), 139 (100), 115 (60). Melting point 102-104^{o}C.

12a (1-(4-fluorophenyl)-4-(4-(trifluoromethyl)phenyl)-7-oxabicyclo[2.2.1]heptane)

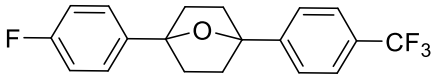

General procedure A was followed using 4''-fluoro-4-(trifluoromethyl)-3',6'-dihydro-[1,1':4',1''-terphenyl]-1'(2'H)-ol (100 mg, 0.30 mmol, 1.0 equiv), 6.2 mL of stock solution of *fac*-Ir(4'-F-ppy)$_3$(2 mg, 0.0028 mmol 2b catalyst, 20 mL CH_3CN), and formic acid (616 mg, 13.39 mmol, 504 μL, 45 equiv) was used to afford **12a** in 85% yield (85mg, 0.252 mmol) as white solid. The crude material was purified by flash chromatography using hexane: ethyl acetate on a 4 g silica column with product eluting at 5%.^{1}H NMR (400 MHz, $CDCl_3$) δ 7.54 (s, 4H), 7.37 (d, *J* = 8.0 Hz, 2H), 7.26 (d, *J* = 8.2 Hz, 2H), 2.28 – 2.06 (m, 4H), 1.90 (d, *J* = 7.5 Hz, 4H). ^{13}C NMR (101 MHz, $CDCl_3$) δ 161.82 (d, *J* = 245.2 Hz), 146.60, 138.13 (d, *J* = 3.1 Hz), 129.09 (q, *J* = 32.3 Hz), 126.73 (d, *J* = 8.0 Hz), 125.30, 125.03 (q, *J* = 3.7 Hz), 124.07 (q, *J* = 271.9 Hz), 114.90 (d, *J* = 21.3 Hz), 87.00, 86.85, 38.46,38.46. ^{19}F NMR (376 MHz, $CDCl_3$) δ -62.38, -115.50, -115.66 (m). FT-IR cm^{-1} 2949, 1510, 1324, 1119 GC/MS (m/z, relative intensity) 336 (M^+, 20) 173 (20), 123 (100), 95 (50). Melting point 65-68^{o}C.

1a (1-(4-methoxyphenyl)-4-(4-(trifluoromethyl)phenyl)-7-oxabicyclo[2.2.1]heptane)-Starting material

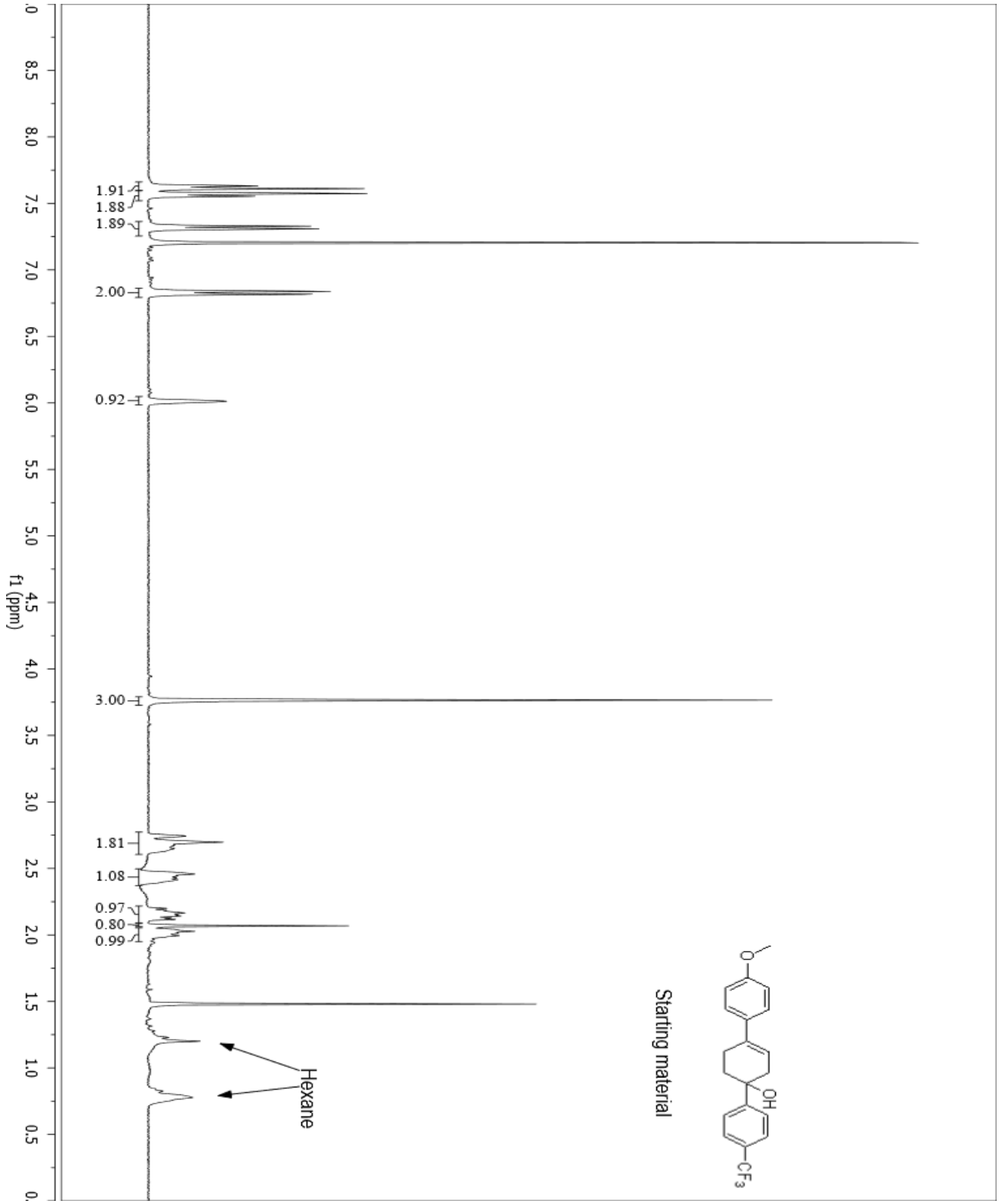

1a (1-(4-methoxyphenyl)-4-(4-(trifluoromethyl)phenyl)-7-oxabicyclo[2.2.1]heptane)-Proton

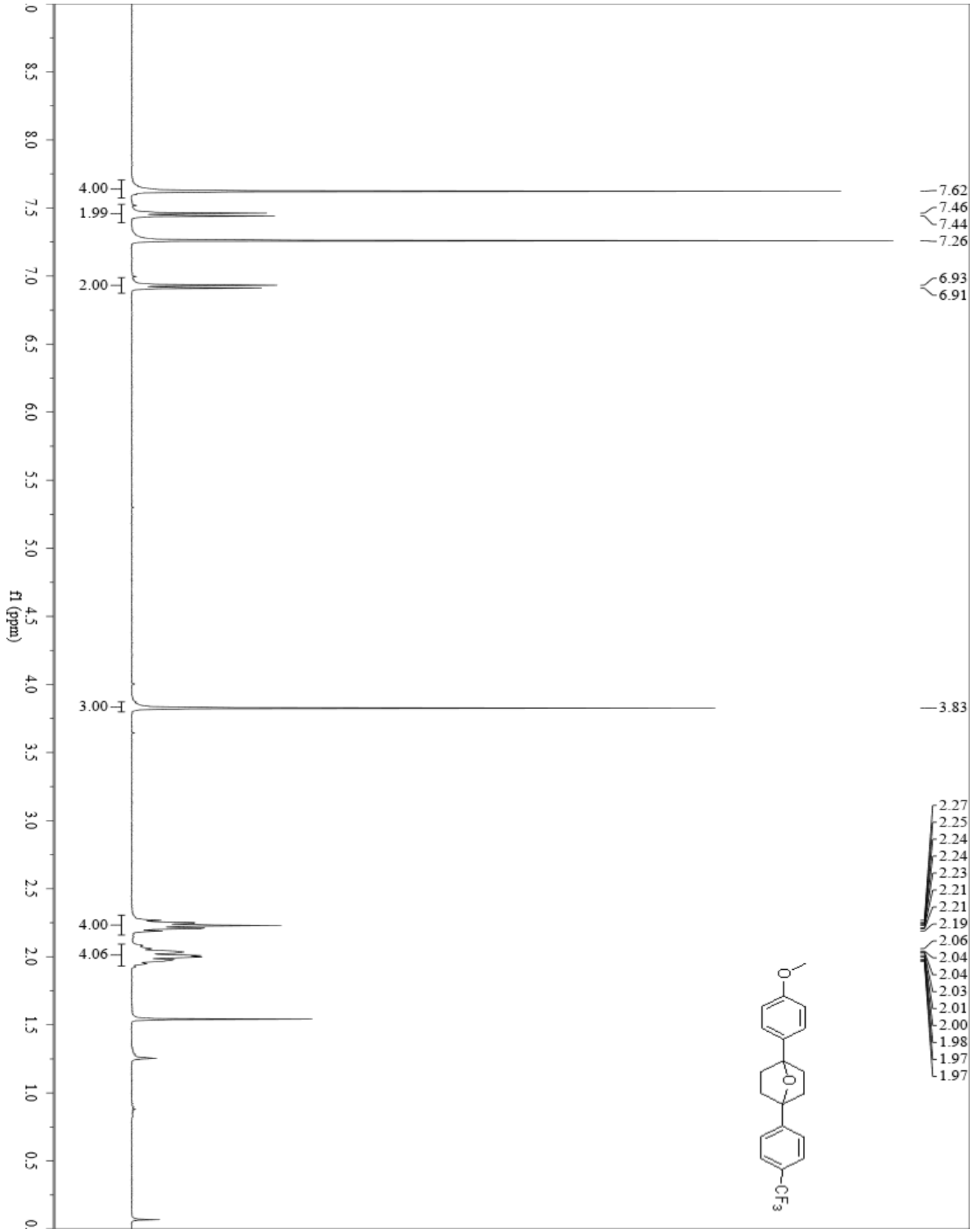

1a-(1-(4-methoxyphenyl)-4-(4-(trifluoromethyl)phenyl)-7-oxabicyclo[2.2.1]heptane)-Carbon

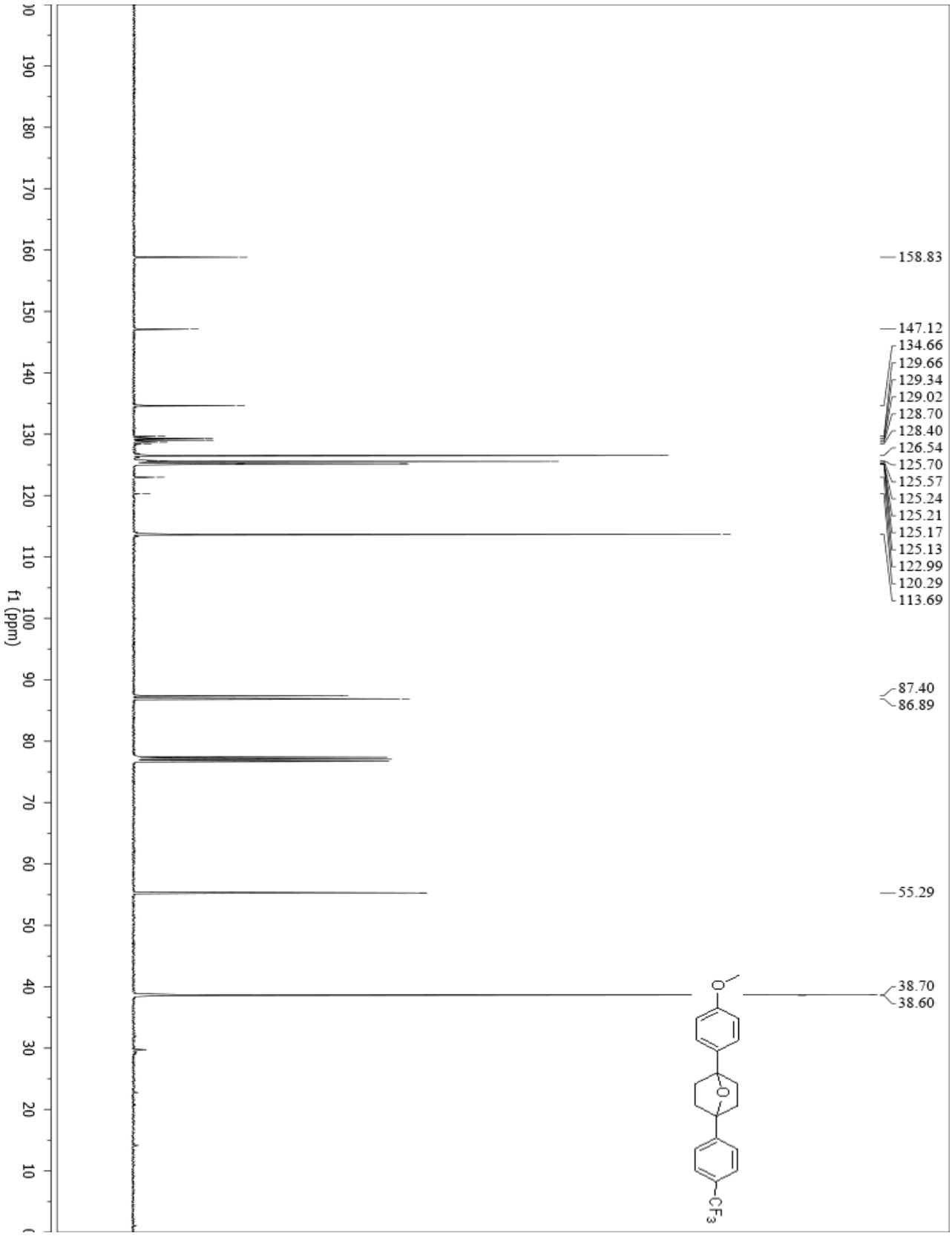

1a-(1-(4-methoxyphenyl)-4-(4-(trifluoromethyl)phenyl)-7-oxabicyclo[2.2.1]heptane)-Fluorine

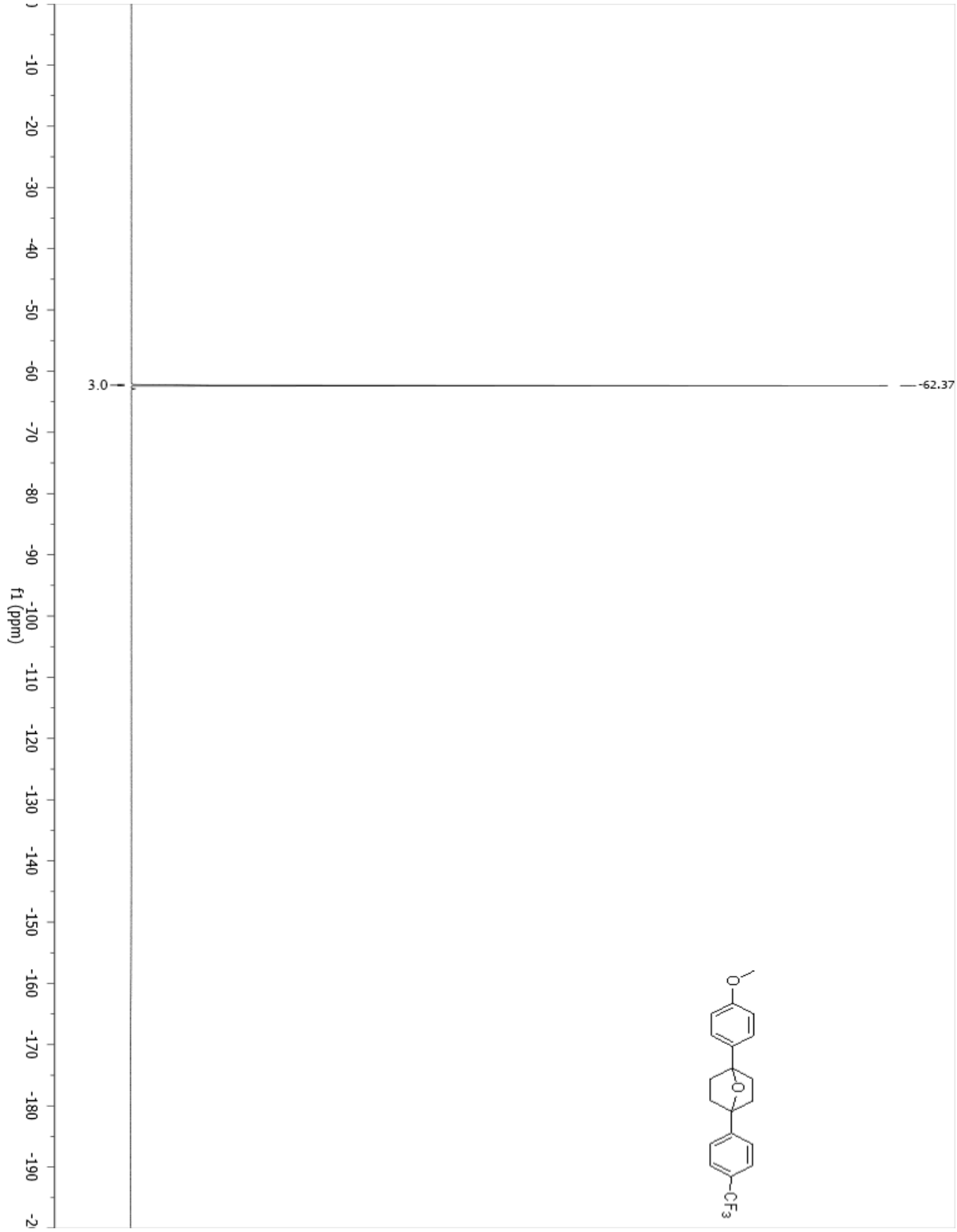

1b-1-(4-methoxyphenyl)-4-(4-(trifluoromethyl)phenyl)-7-oxabicyclo[2.2.1]heptane-2-d-

Proton

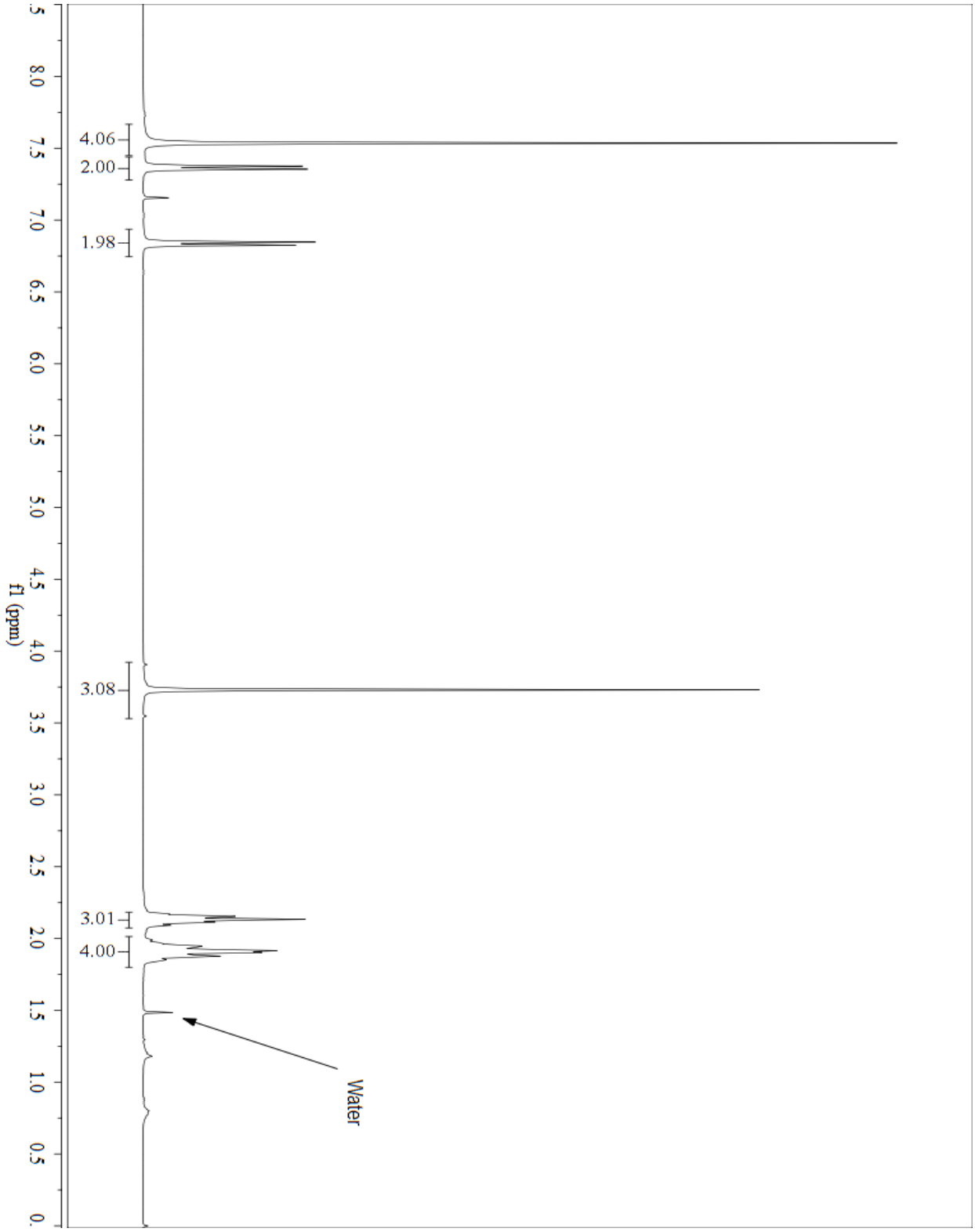

1b-1-(4-methoxyphenyl)-4-(4-(trifluoromethyl)phenyl)-7-oxabicyclo[2.2.1]heptane-2-d-Fluorine

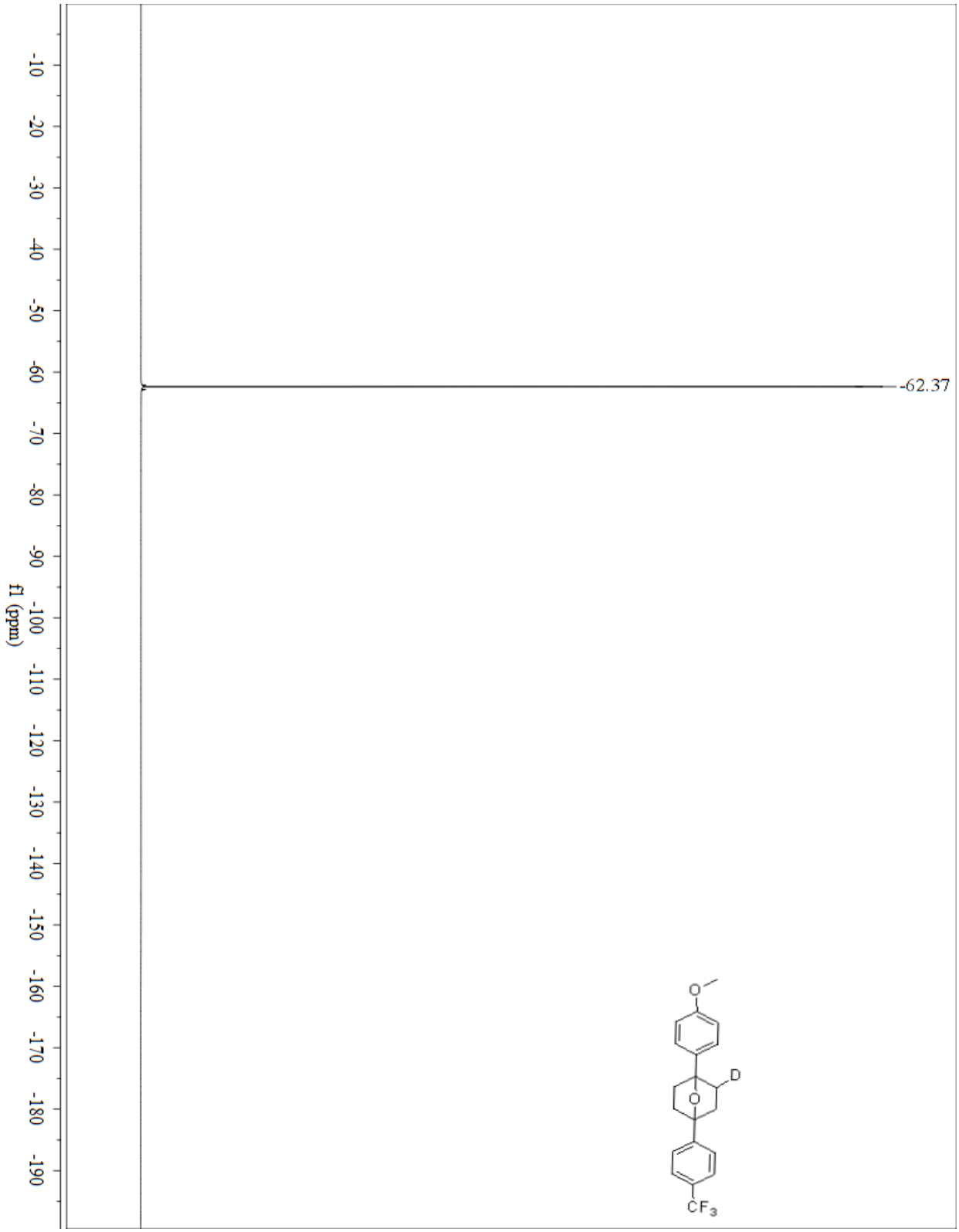

1b-1-(4-methoxyphenyl)-4-(4-(trifluoromethyl)phenyl)-7-oxabicyclo[2.2.1]heptane-2-d-Carbon

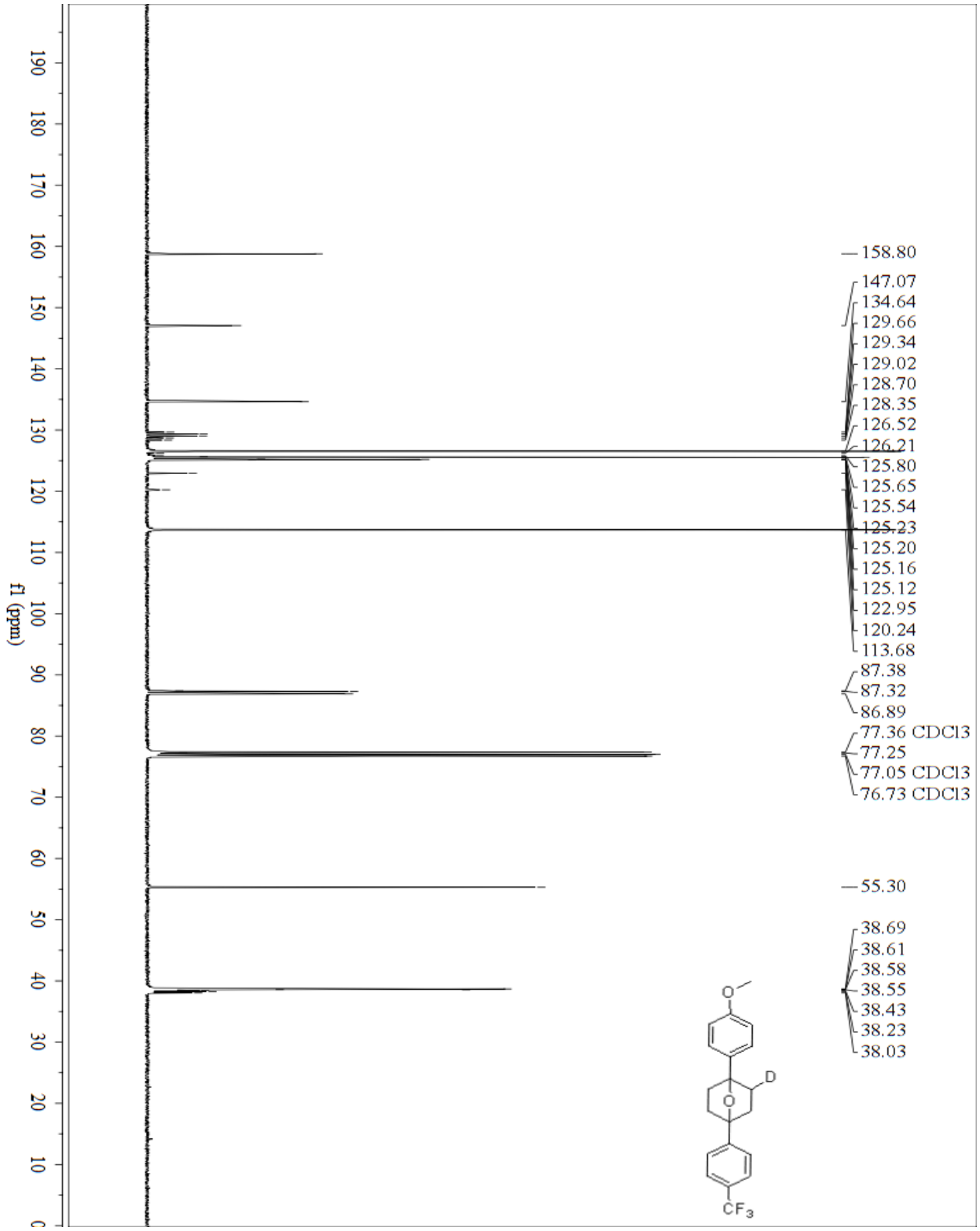

2a-(1-(4-chlorophenyl)-4-(4-methoxyphenyl)-7-oxabicyclo[2.2.1]heptane)-Starting Material

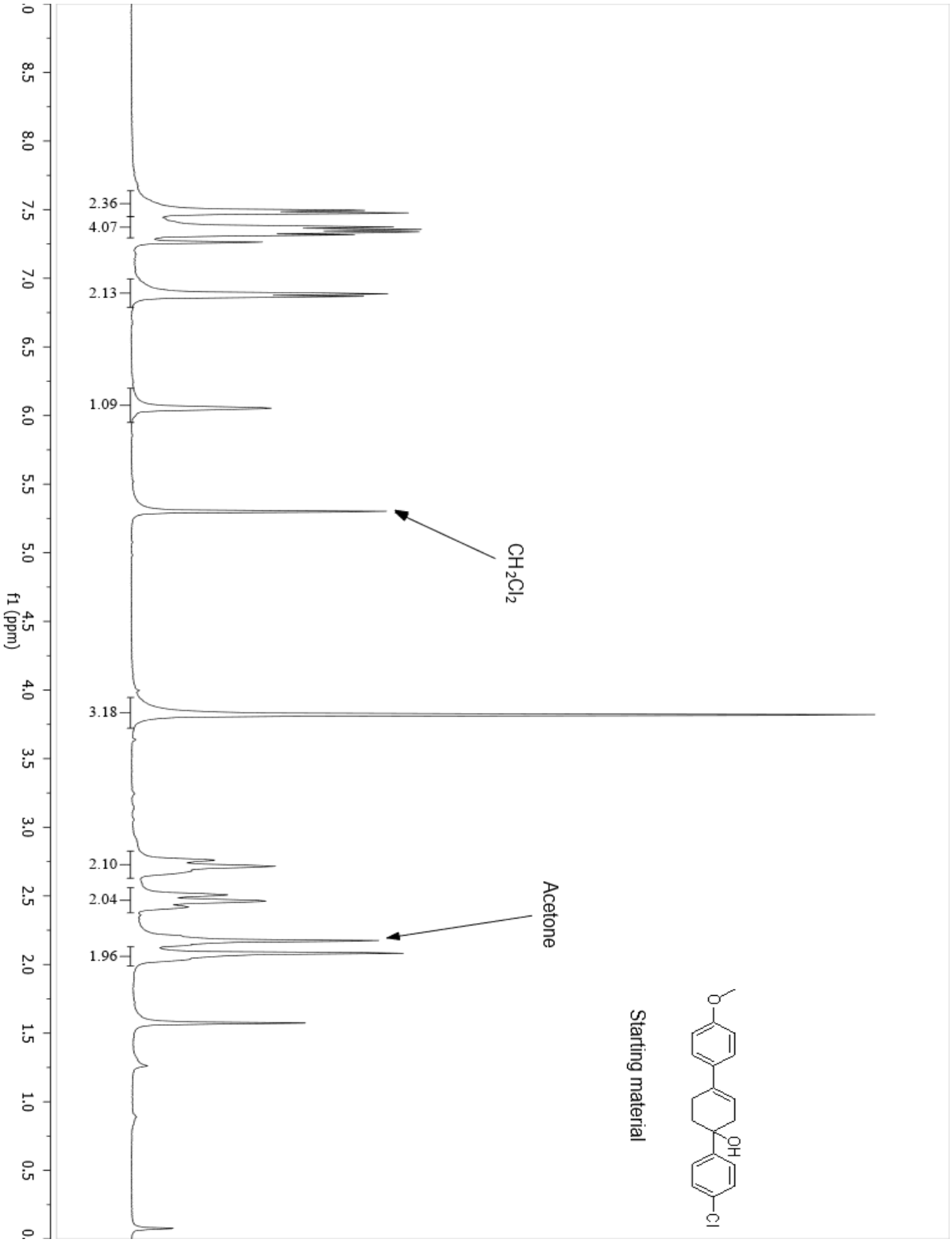

2a (1-(4-chlorophenyl)-4-(4-methoxyphenyl)-7-oxabicyclo[2.2.1]heptane)- Proton

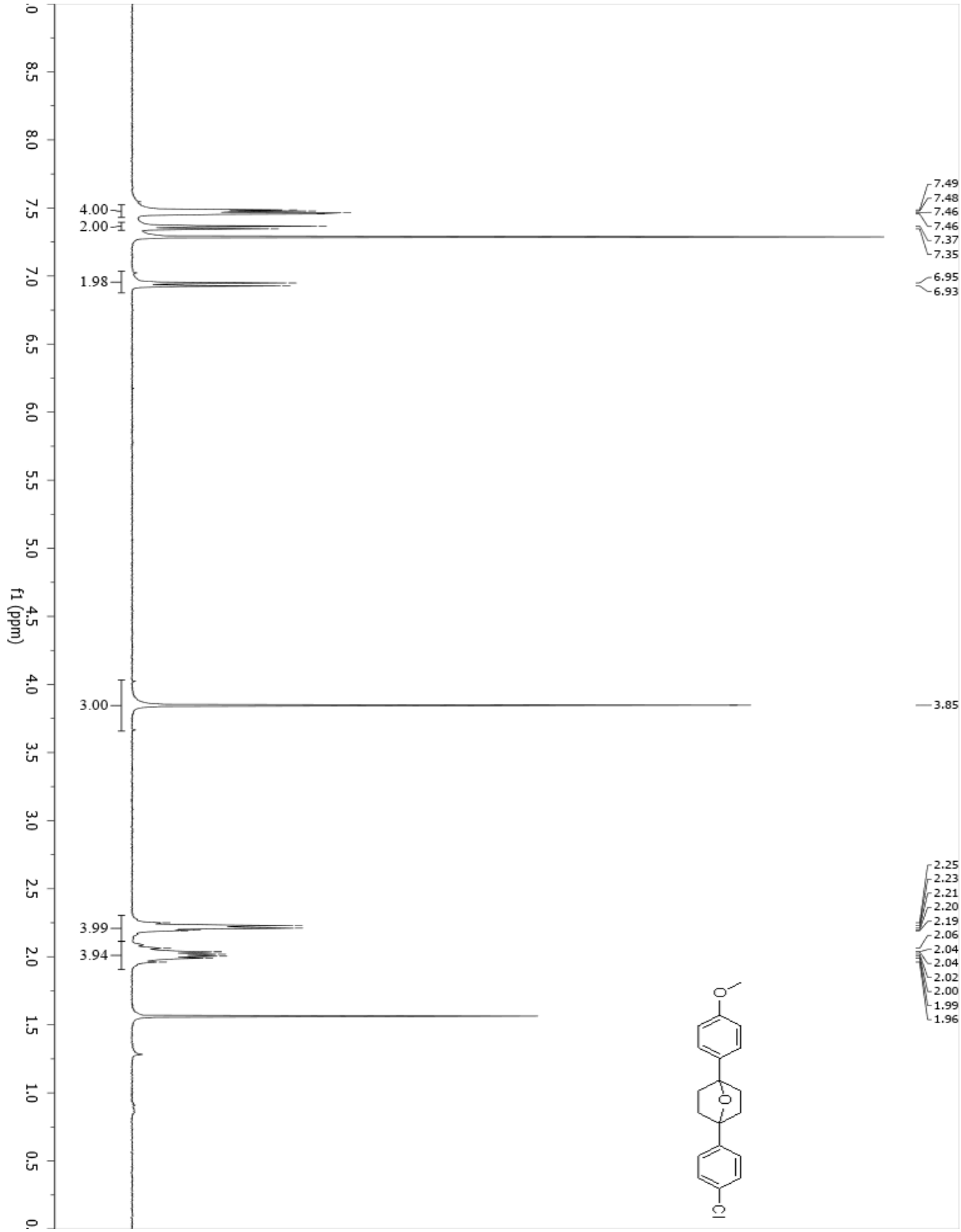

2a (1-(4-chlorophenyl)-4-(4-methoxyphenyl)-7-oxabicyclo[2.2.1]heptane)- Carbon

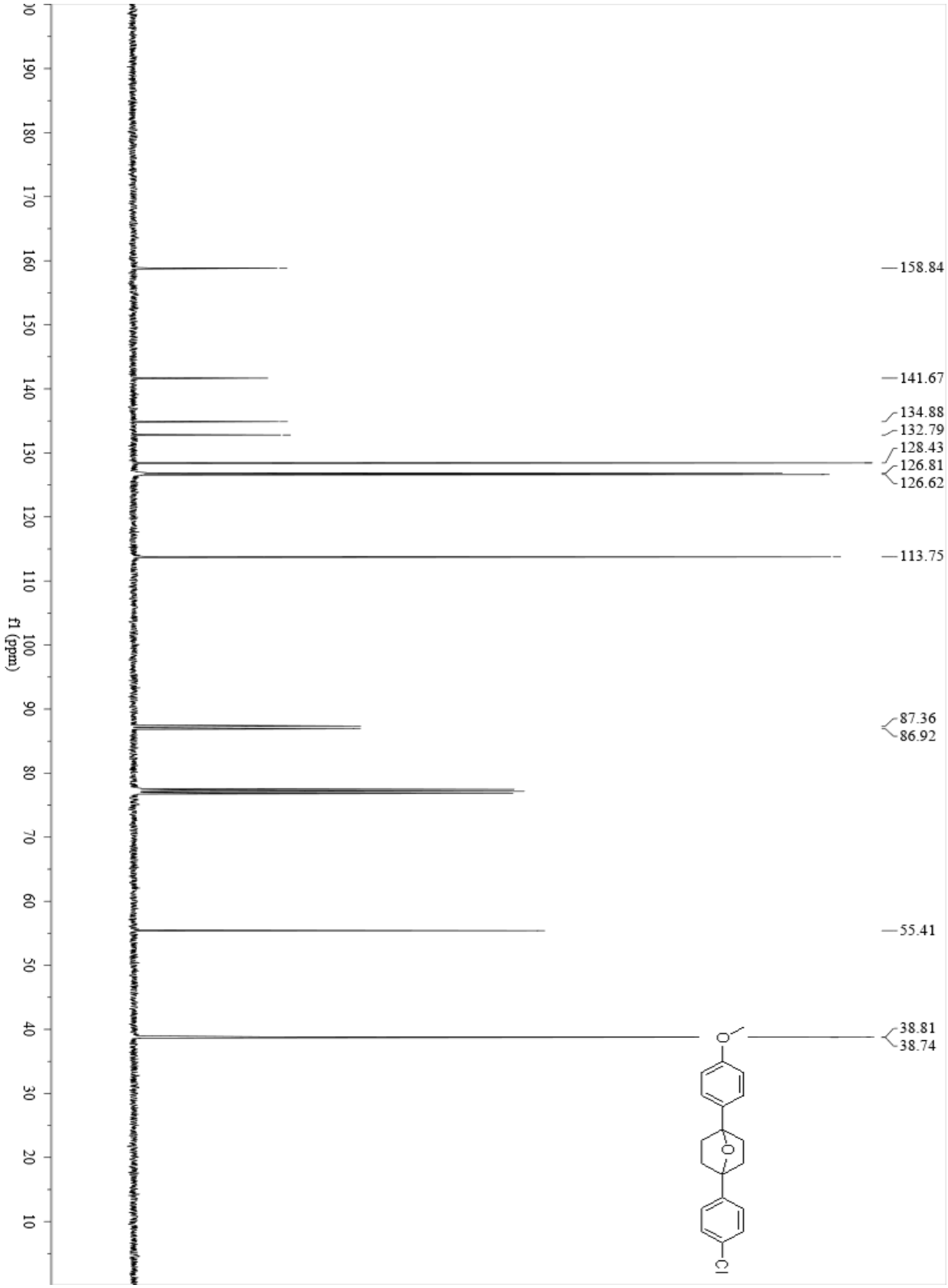

3a (1-(4-fluorophenyl)-4-(4-methoxyphenyl)-7-oxabicyclo[2.2.1]heptanes)- Starting material

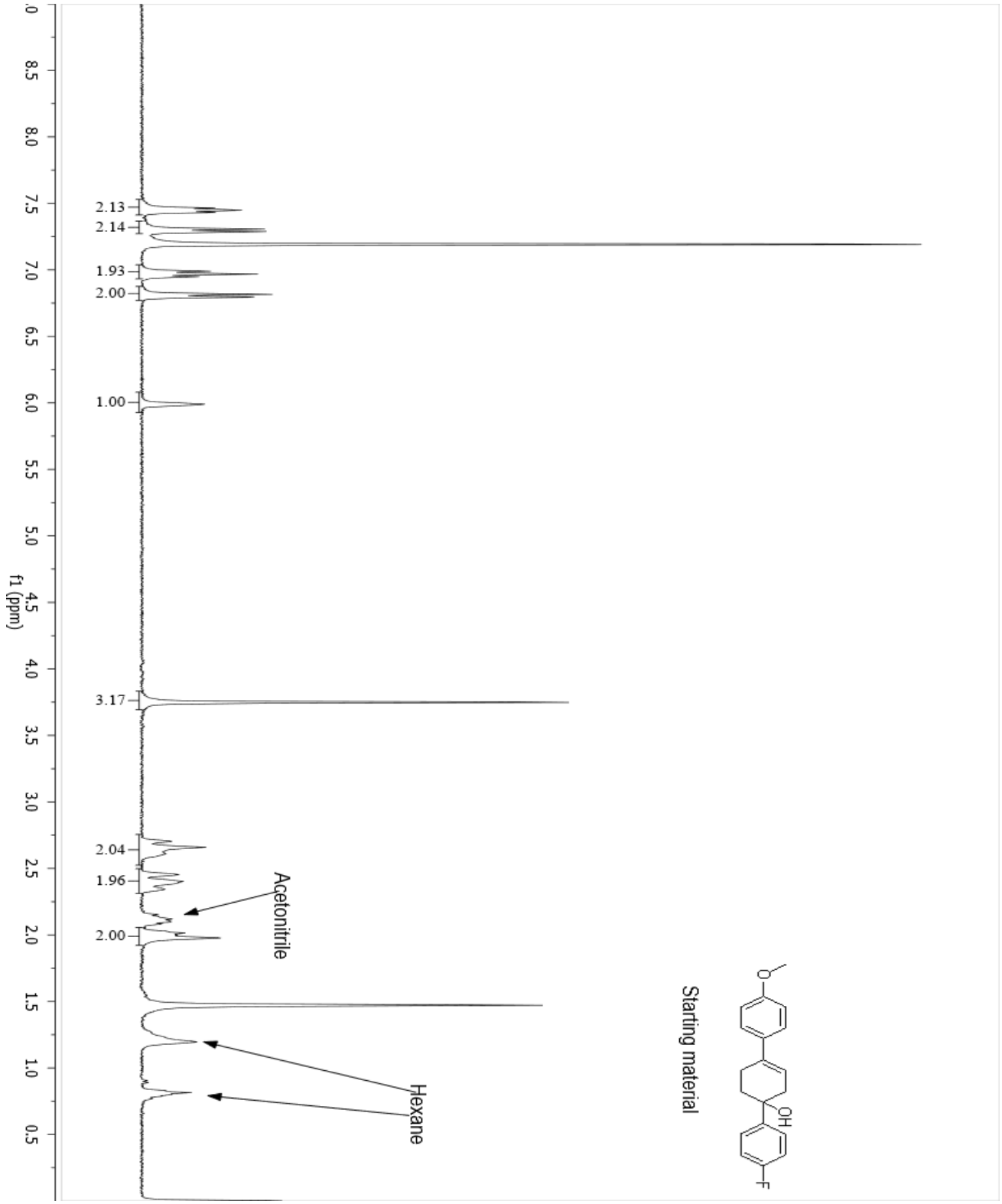

3a (1-(4-fluorophenyl)-4-(4-methoxyphenyl)-7-oxabicyclo[2.2.1]heptanes)- Proton

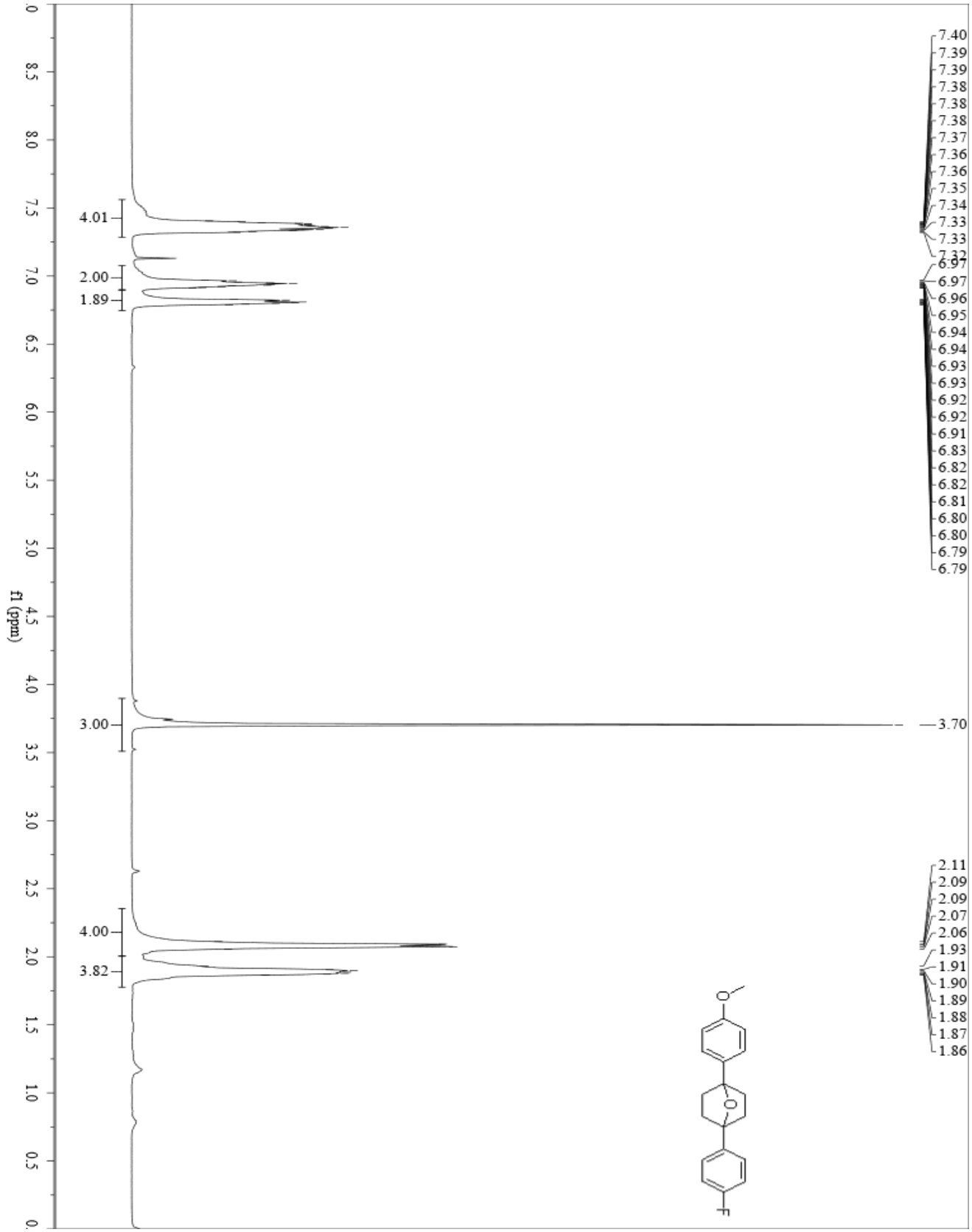

3a (1-(4-fluorophenyl)-4-(4-methoxyphenyl)-7-oxabicyclo[2.2.1]heptanes)- Carbon

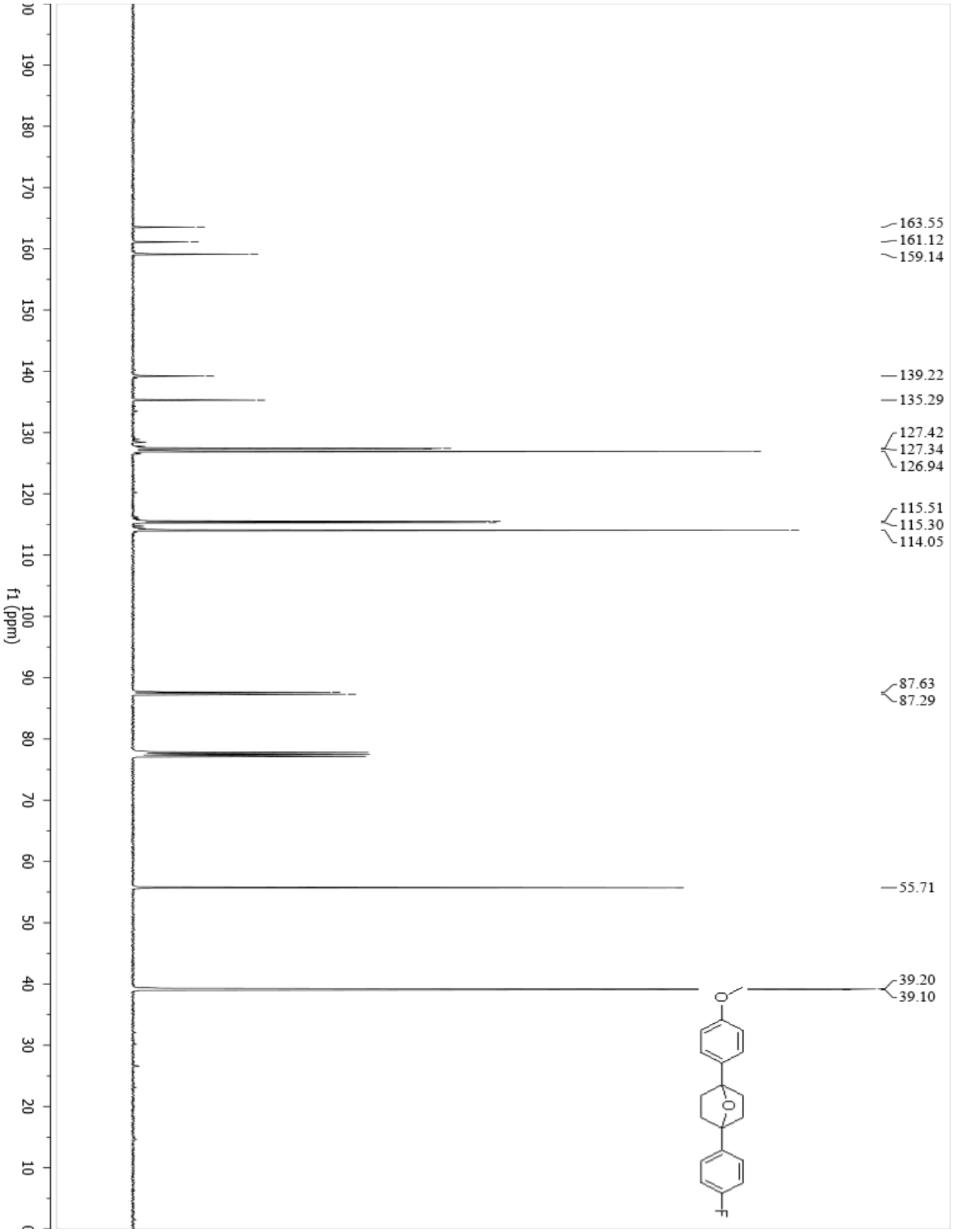

4a(1-(4-methoxyphenyl)-4-(perfluorophenyl)-7-oxabicyclo[2.2.1]heptanes)-Starting material

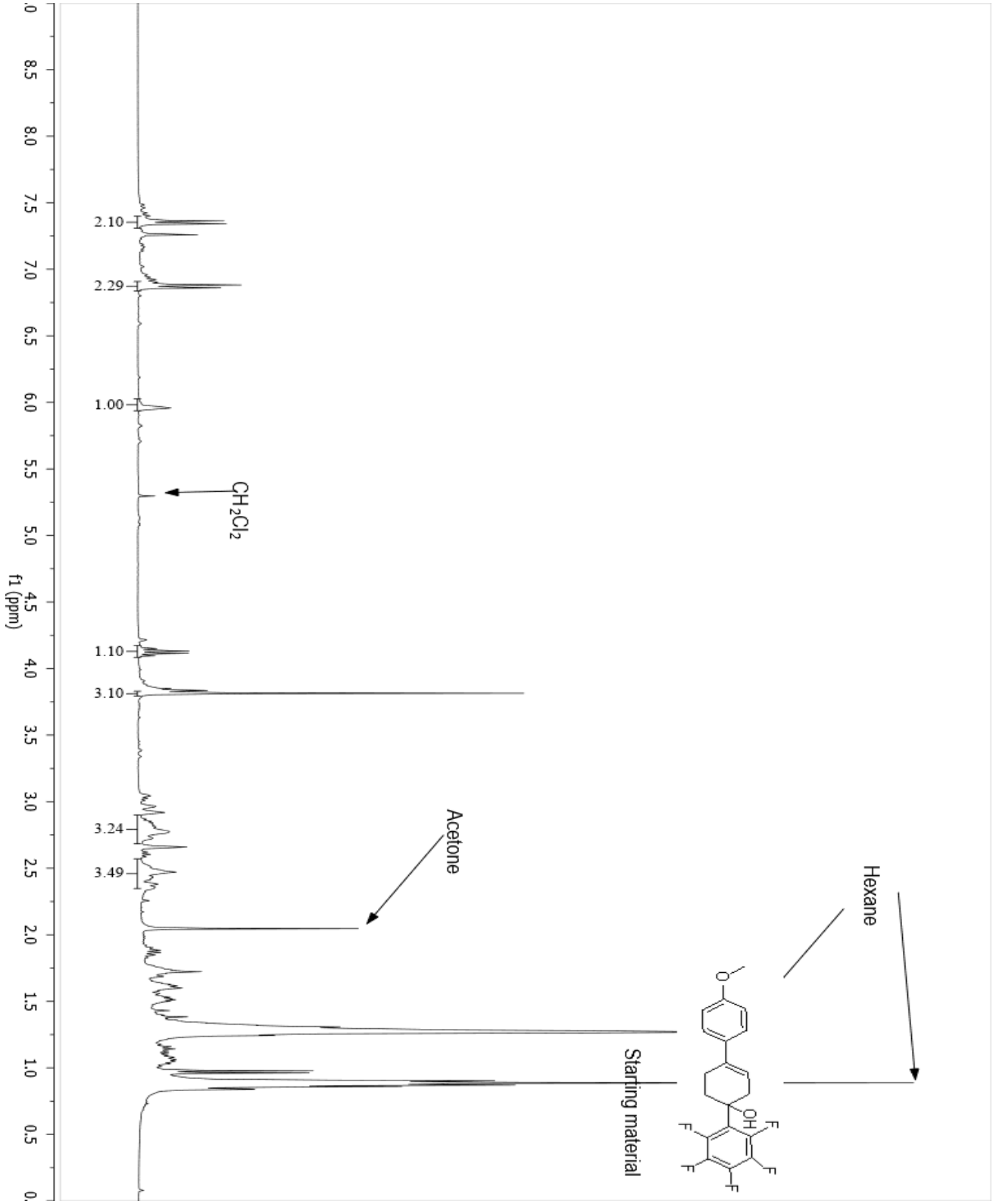

4a (1-(4-methoxyphenyl)-4-(perfluorophenyl)-7-oxabicyclo[2.2.1]heptanes)- Proton

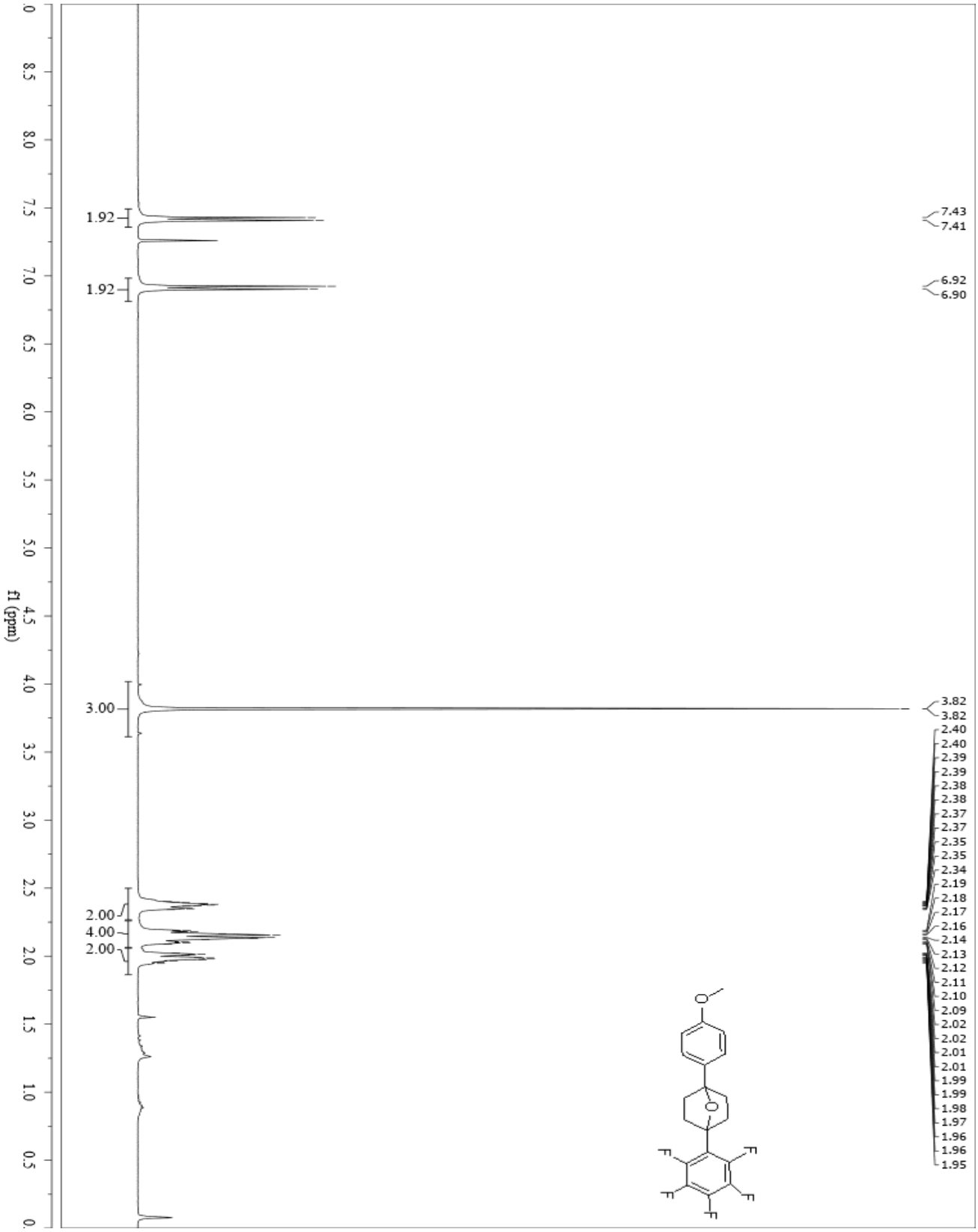

4a (1-(4-methoxyphenyl)-4-(perfluorophenyl)-7-oxabicyclo[2.2.1]heptanes)- Carbon

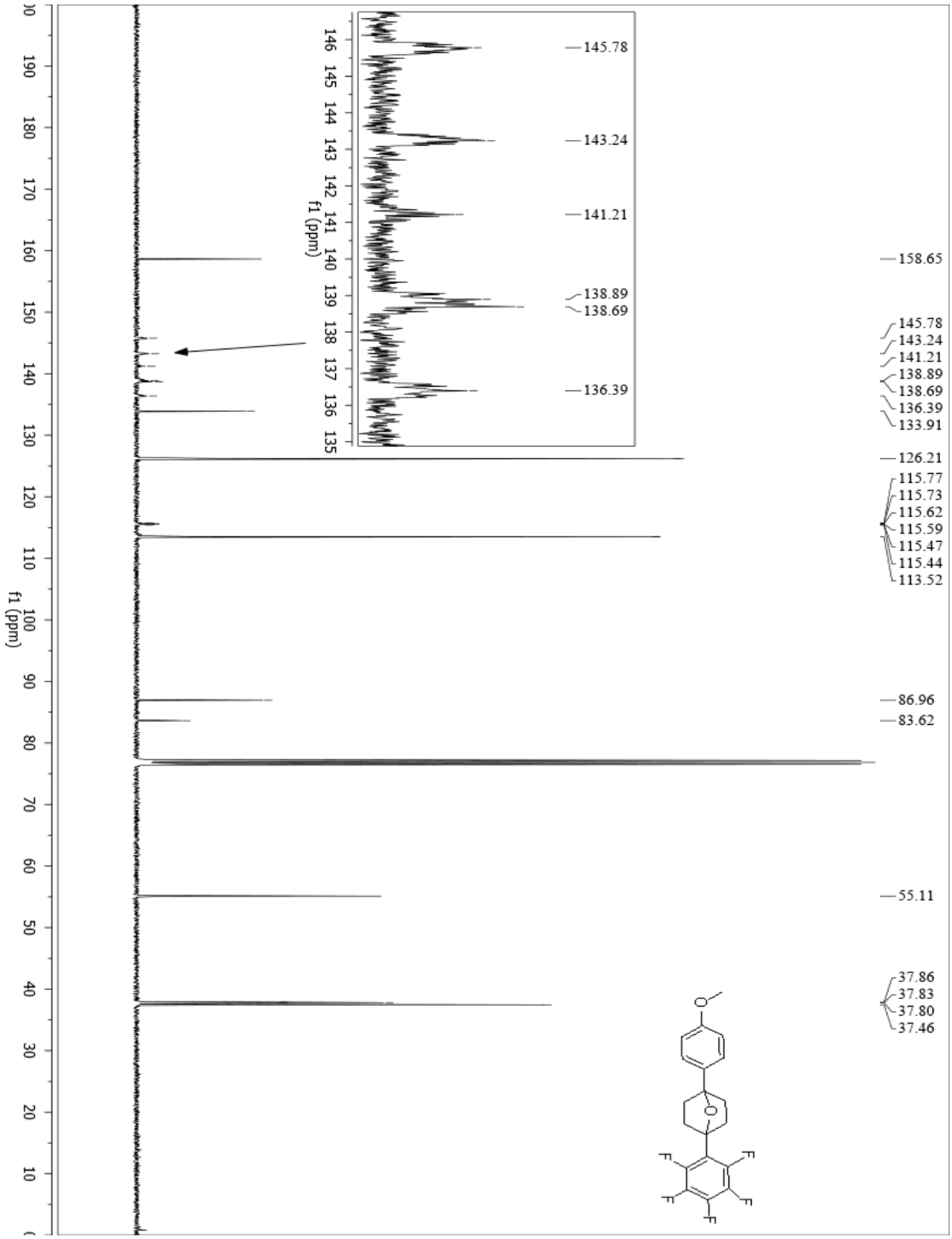

4a (1-(4-methoxyphenyl)-4-(perfluorophenyl)-7-oxabicyclo[2.2.1]heptanes)- Fluorine

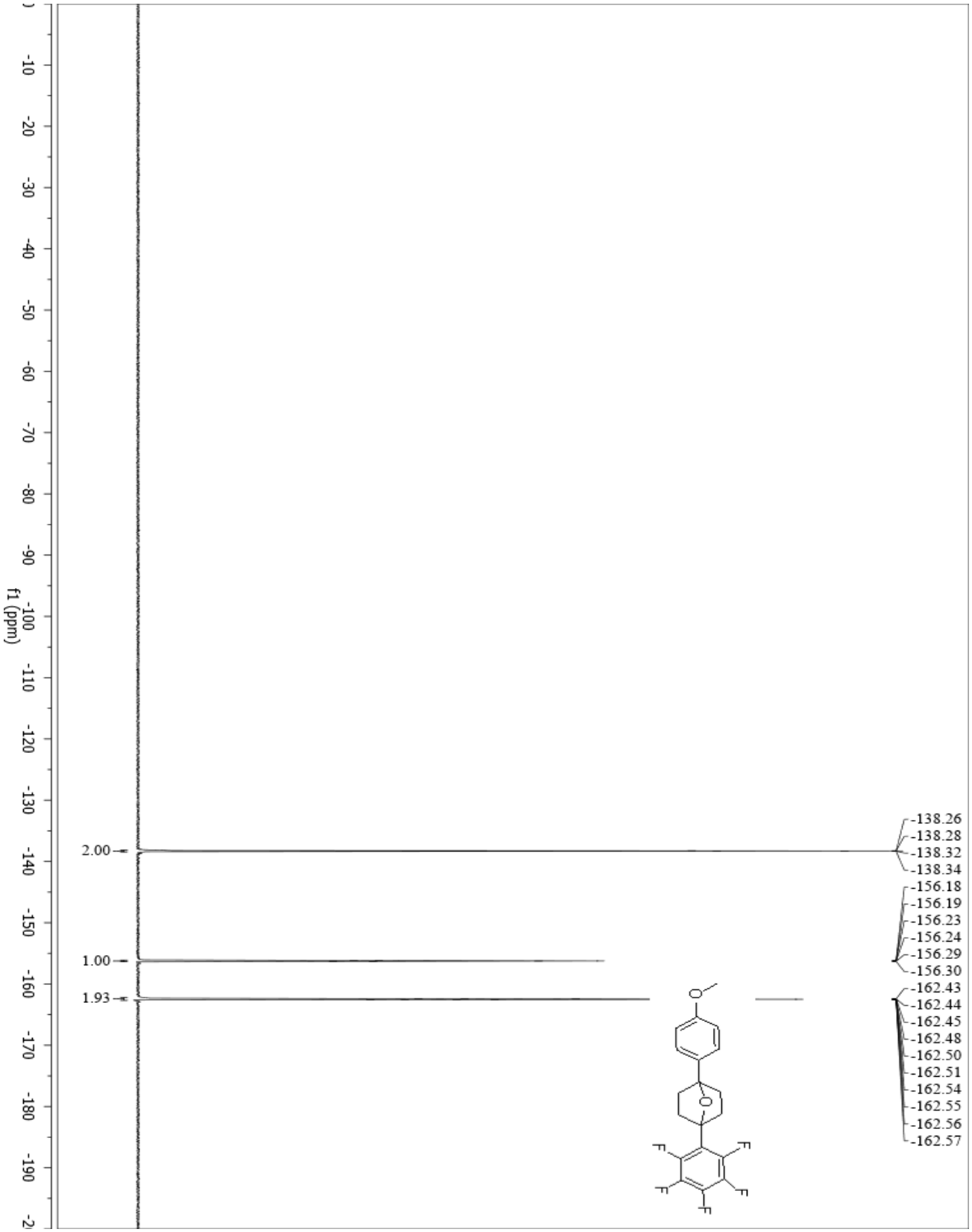

5a (1-(4-methoxyphenyl)-4-(p-tolyl)-7-oxabicyclo[2.2.1]heptane)- Starting material

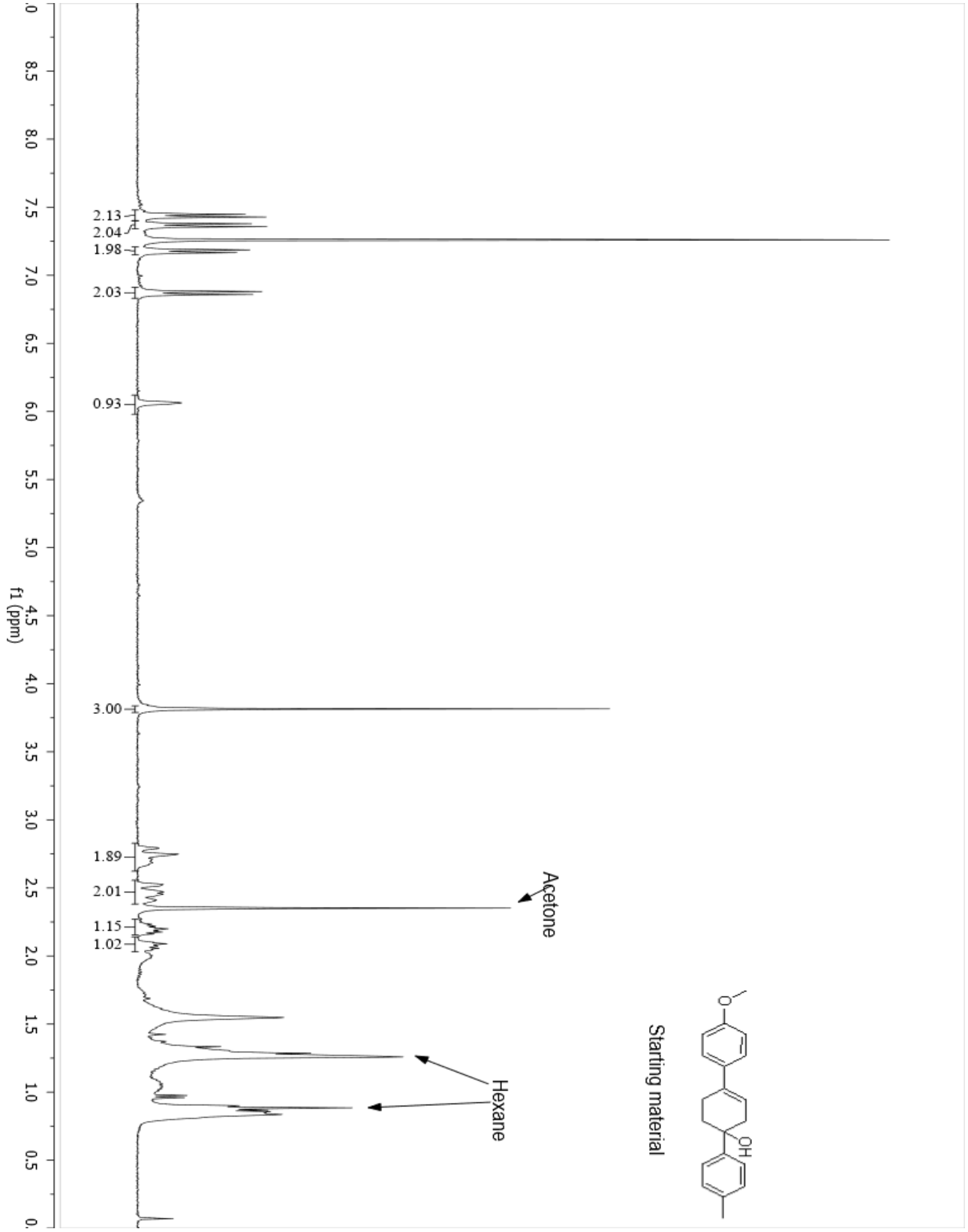

5a (1-(4-methoxyphenyl)-4-(p-tolyl)-7-oxabicyclo[2.2.1]heptane)- Proton

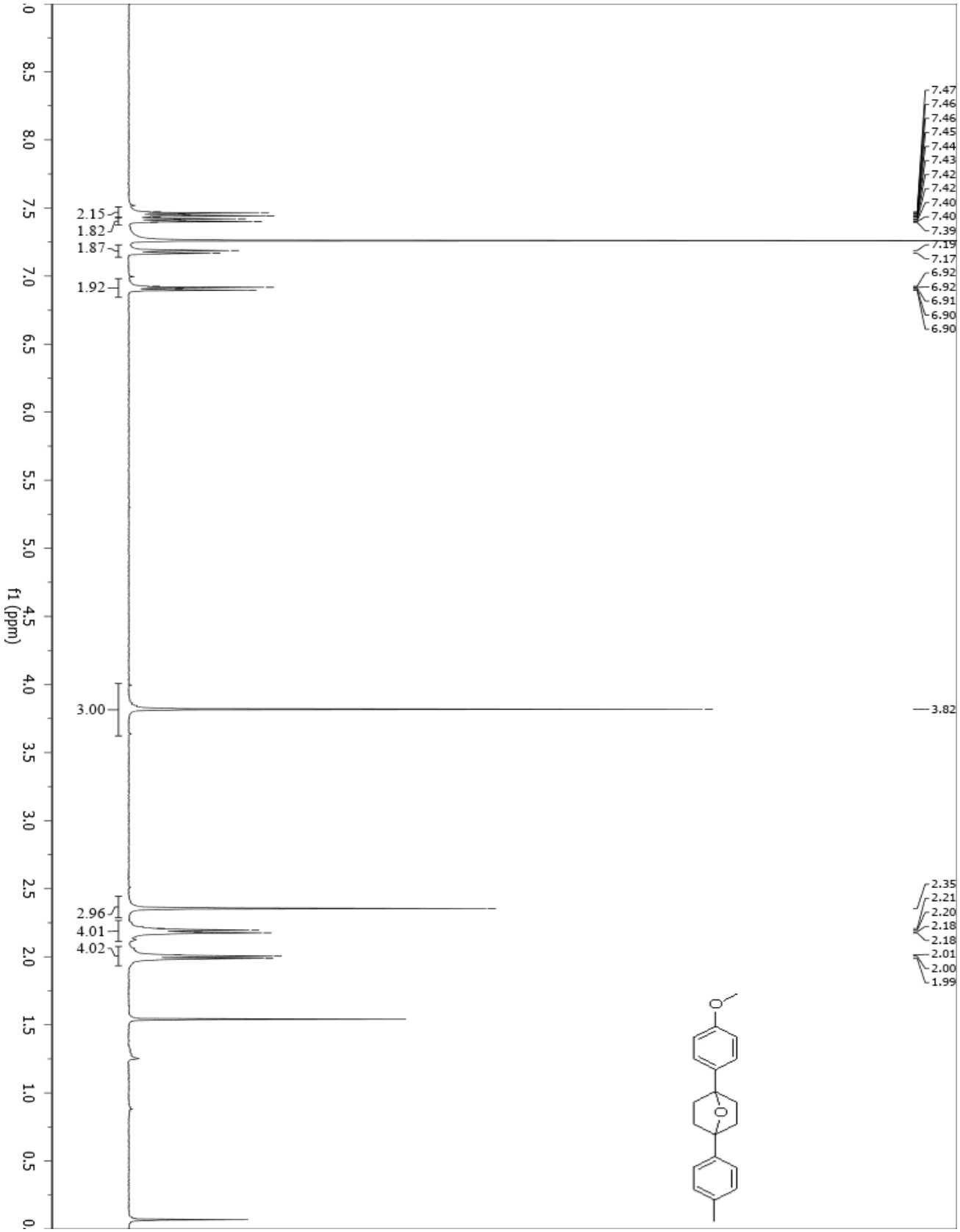

5a (1-(4-methoxyphenyl)-4-(p-tolyl)-7-oxabicyclo[2.2.1]heptane)- Carbon

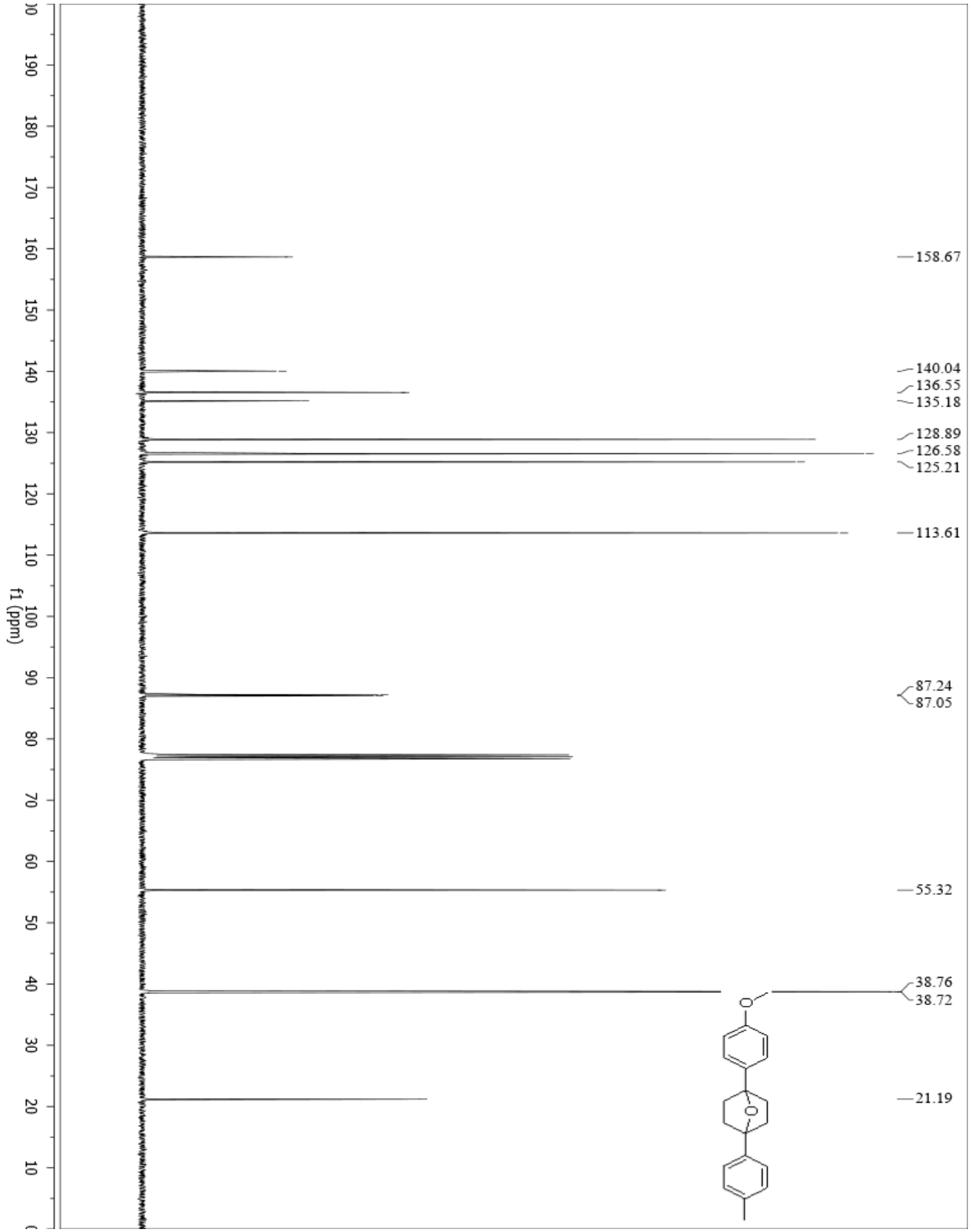

6a (1-(4-methoxyphenyl)-4-phenyl-7-oxabicyclo[2.2.1]heptane)- Starting material

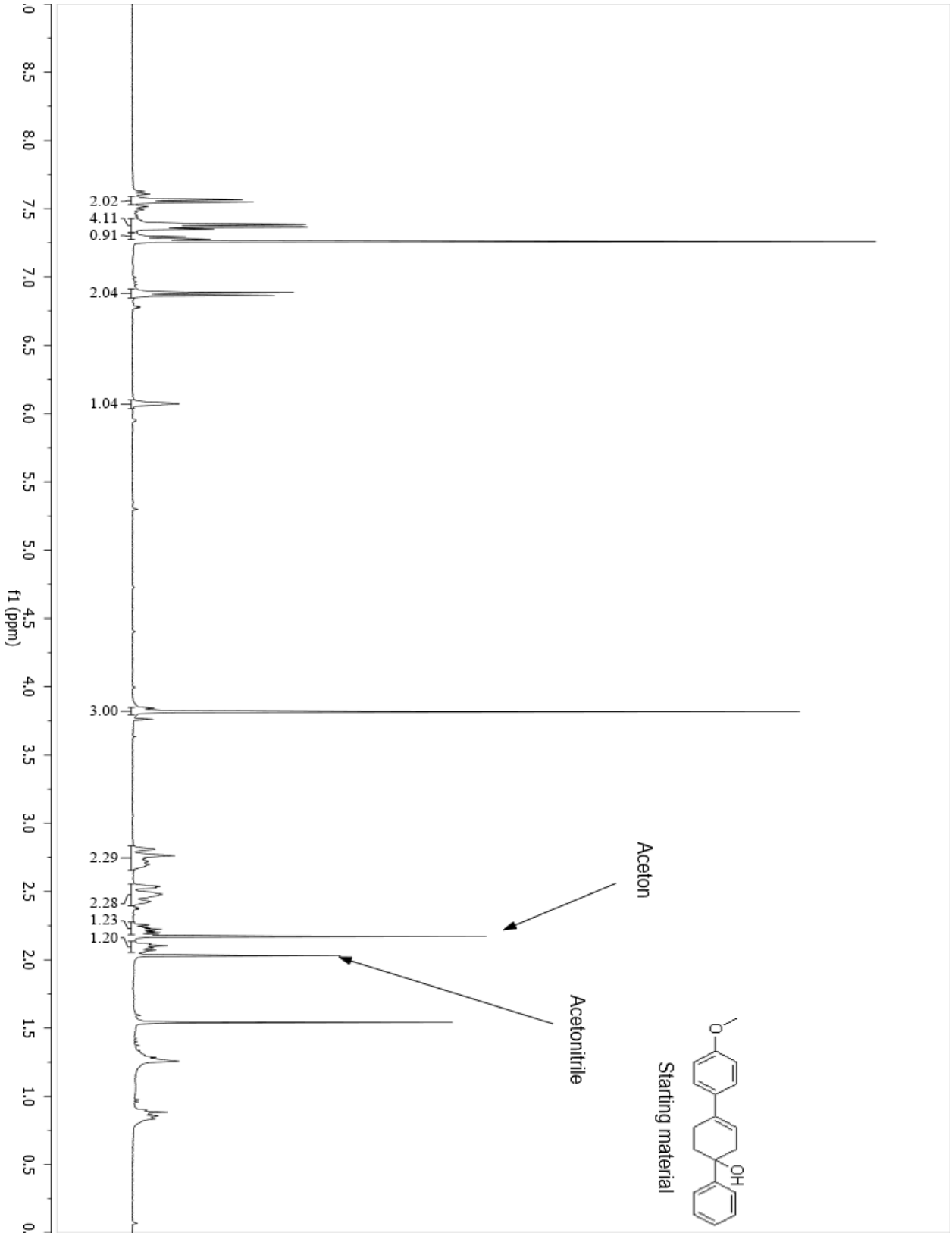

6a (1-(4-methoxyphenyl)-4-phenyl-7-oxabicyclo[2.2.1]heptane)- Proton

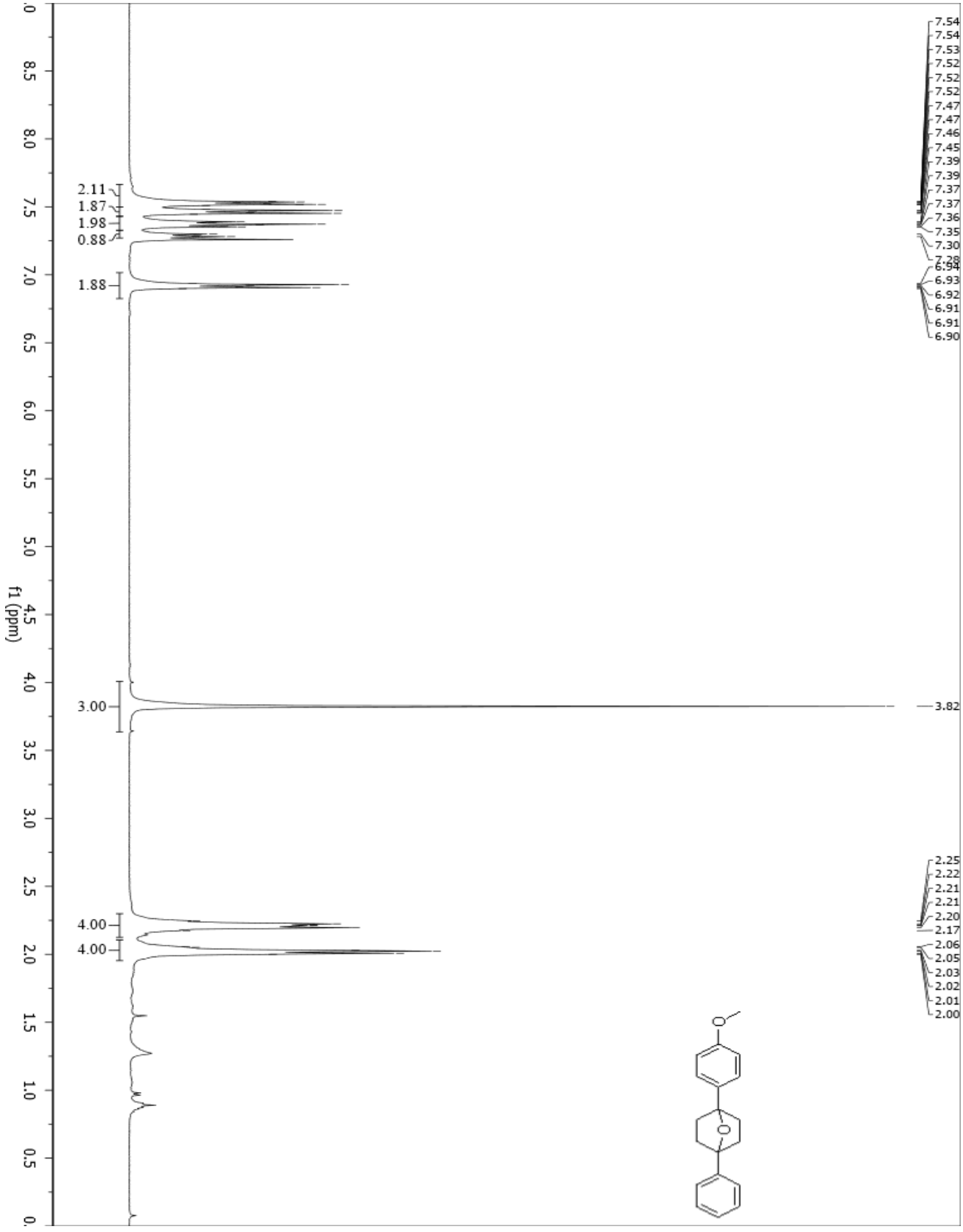

6a (1-(4-methoxyphenyl)-4-phenyl-7-oxabicyclo[2.2.1]heptane)- Carbon

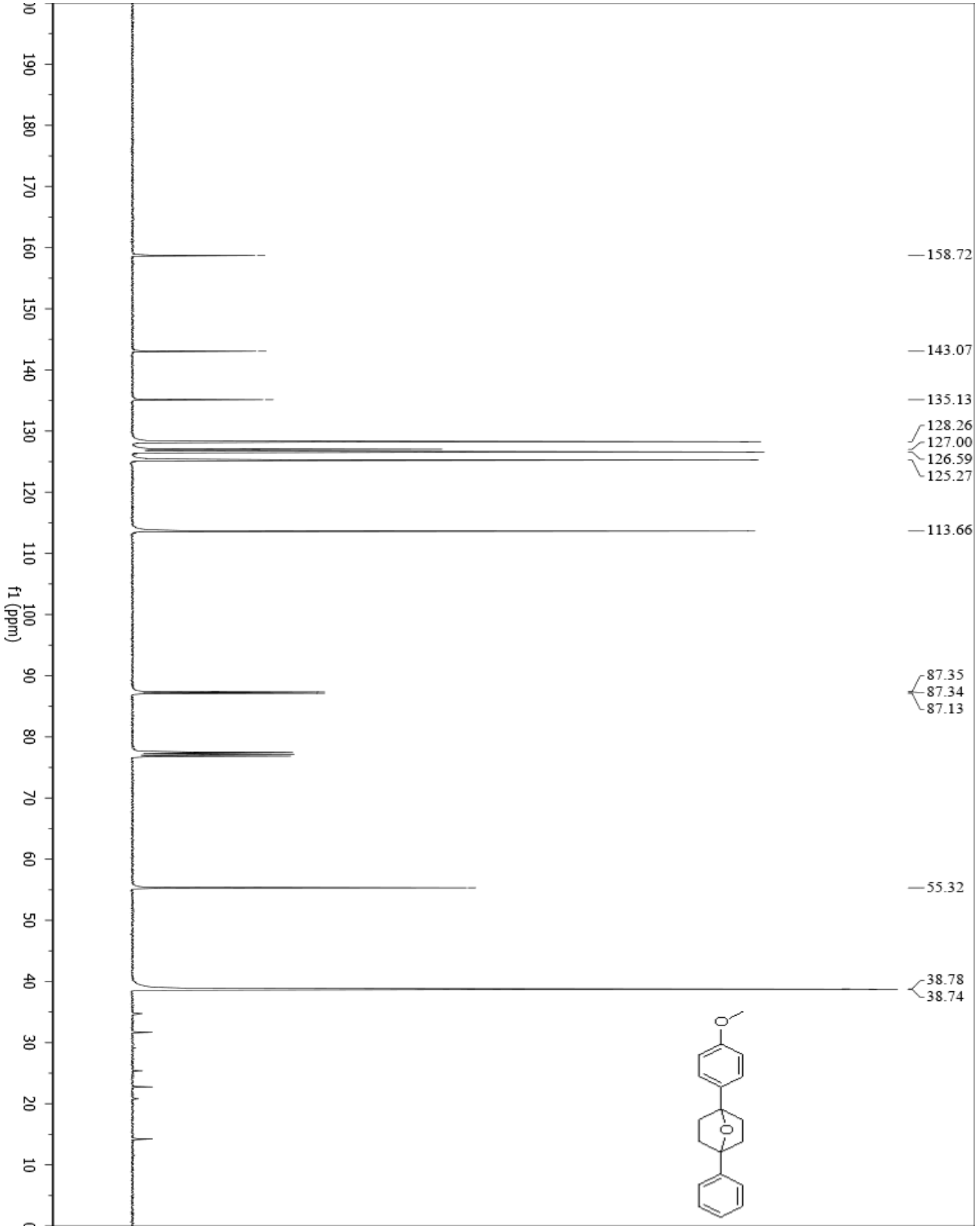

7a (1-ethynyl-4-(4-methoxyphenyl)-7-oxabicyclo[2.2.1]heptane)- Starting material

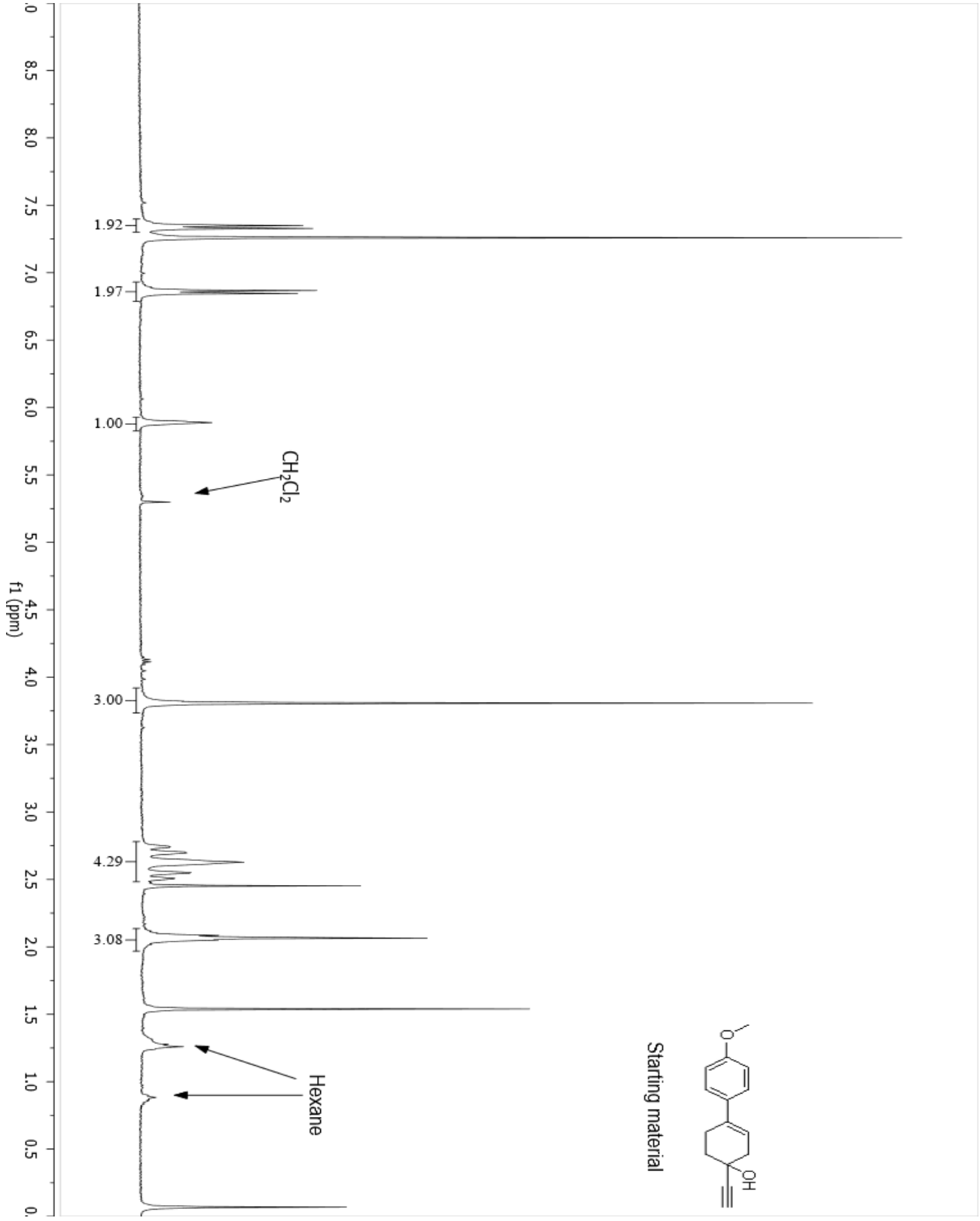

7a (1-ethynyl-4-(4-methoxyphenyl)-7-oxabicyclo[2.2.1]heptane)- Proton

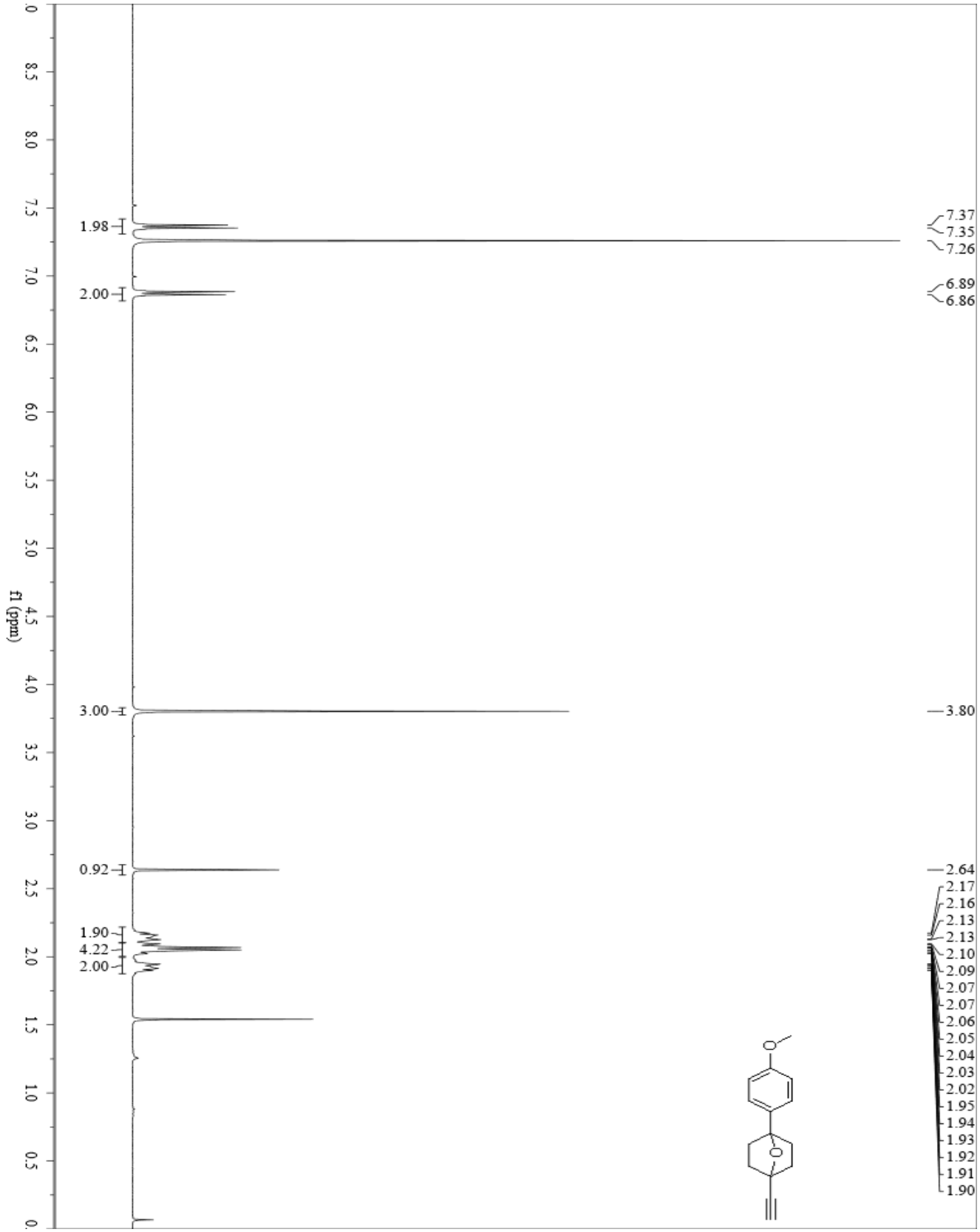

7a (1-ethynyl-4-(4-methoxyphenyl)-7-oxabicyclo[2.2.1]heptane)- Carbon

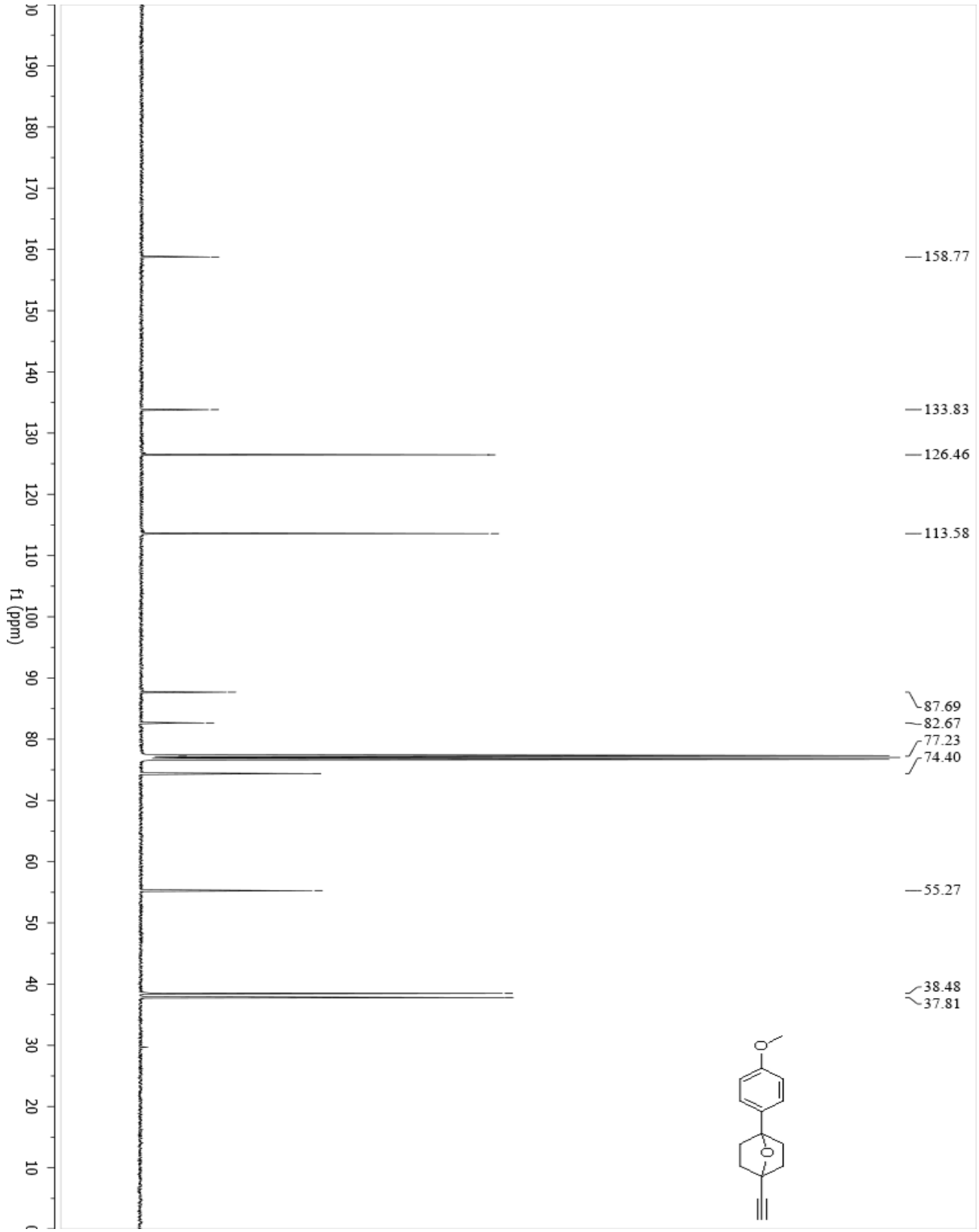

8a (1-ethyl-4-(4-methoxyphenyl)-7-oxabicyclo[2.2.1]heptane)- Starting material

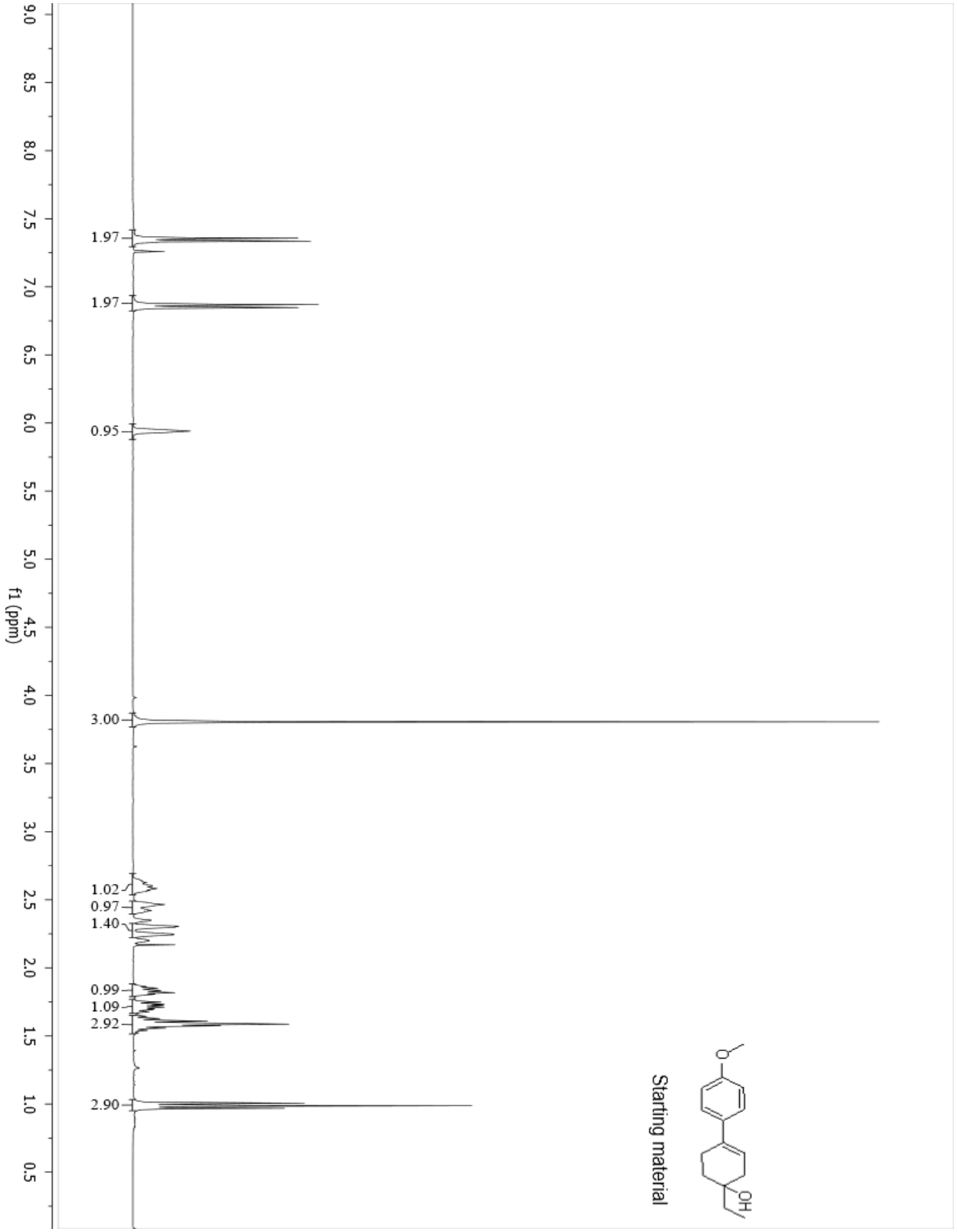

8a (1-ethyl-4-(4-methoxyphenyl)-7-oxabicyclo[2.2.1]heptane)- Proton

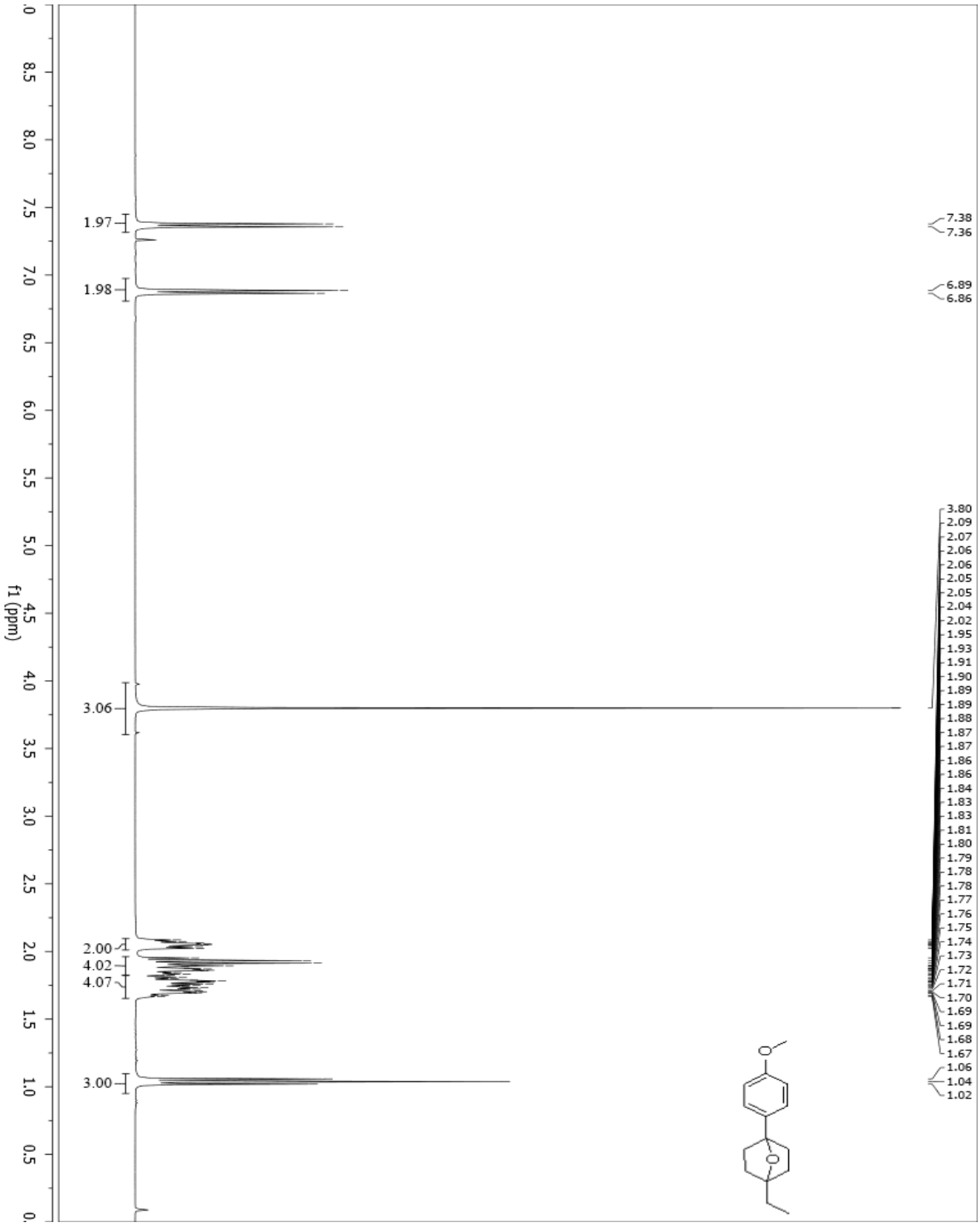

8a (1-ethyl-4-(4-methoxyphenyl)-7-oxabicyclo[2.2.1]heptane)- Carbon

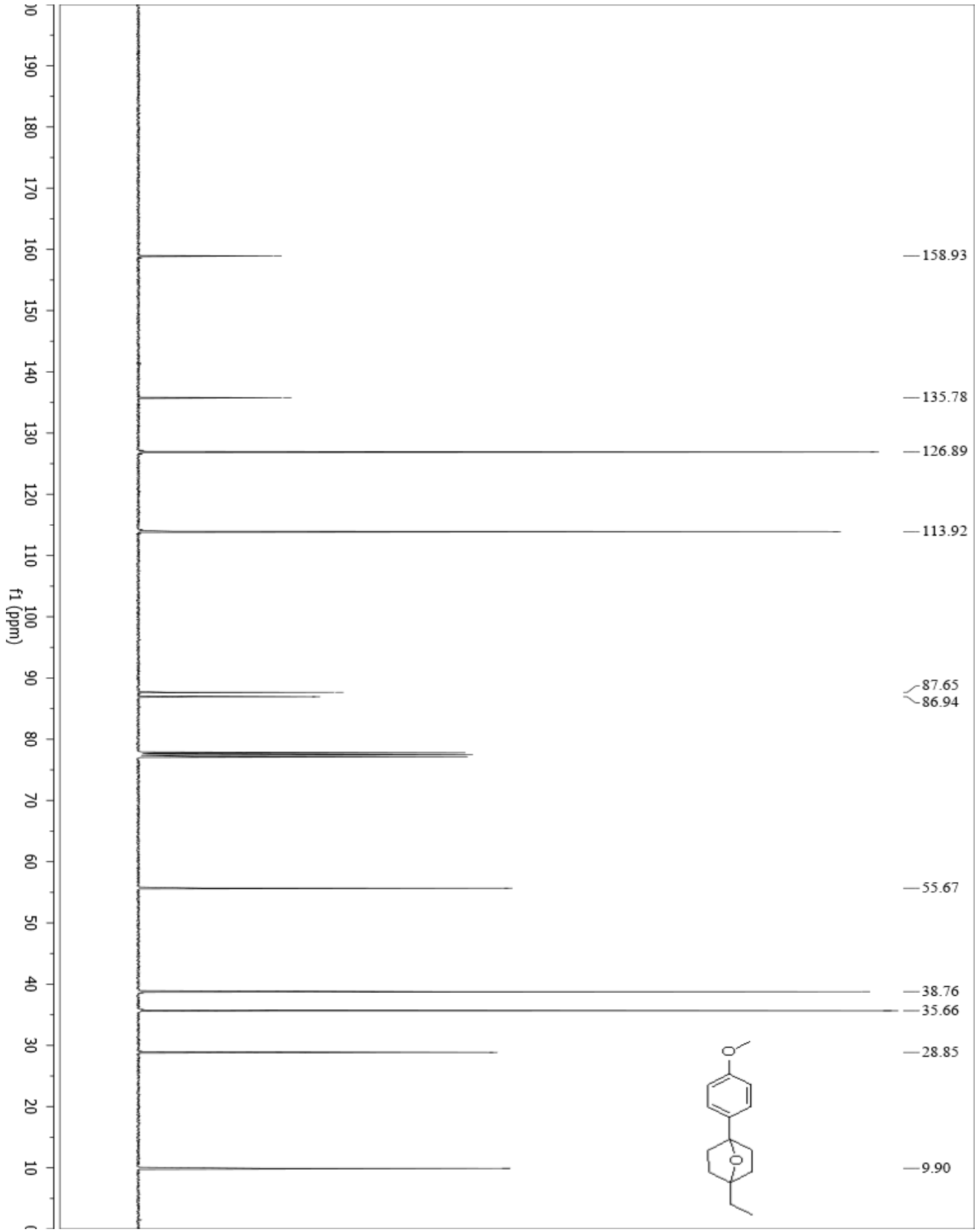

9a (1-(4-methoxyphenyl)-7-oxabicyclo[2.2.1]heptane)- Starting material

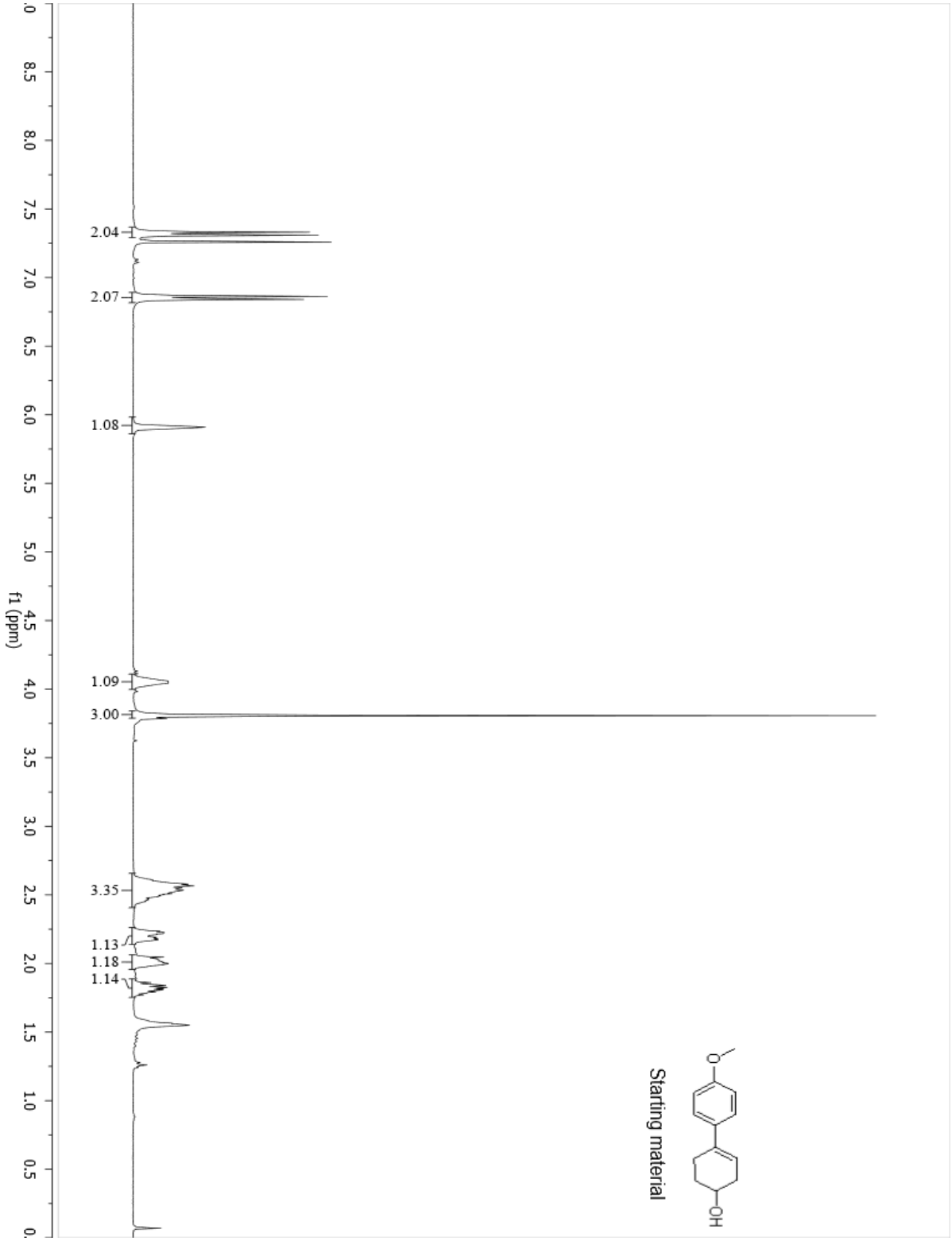

9a (1-(4-methoxyphenyl)-7-oxabicyclo[2.2.1]heptane)- Proton

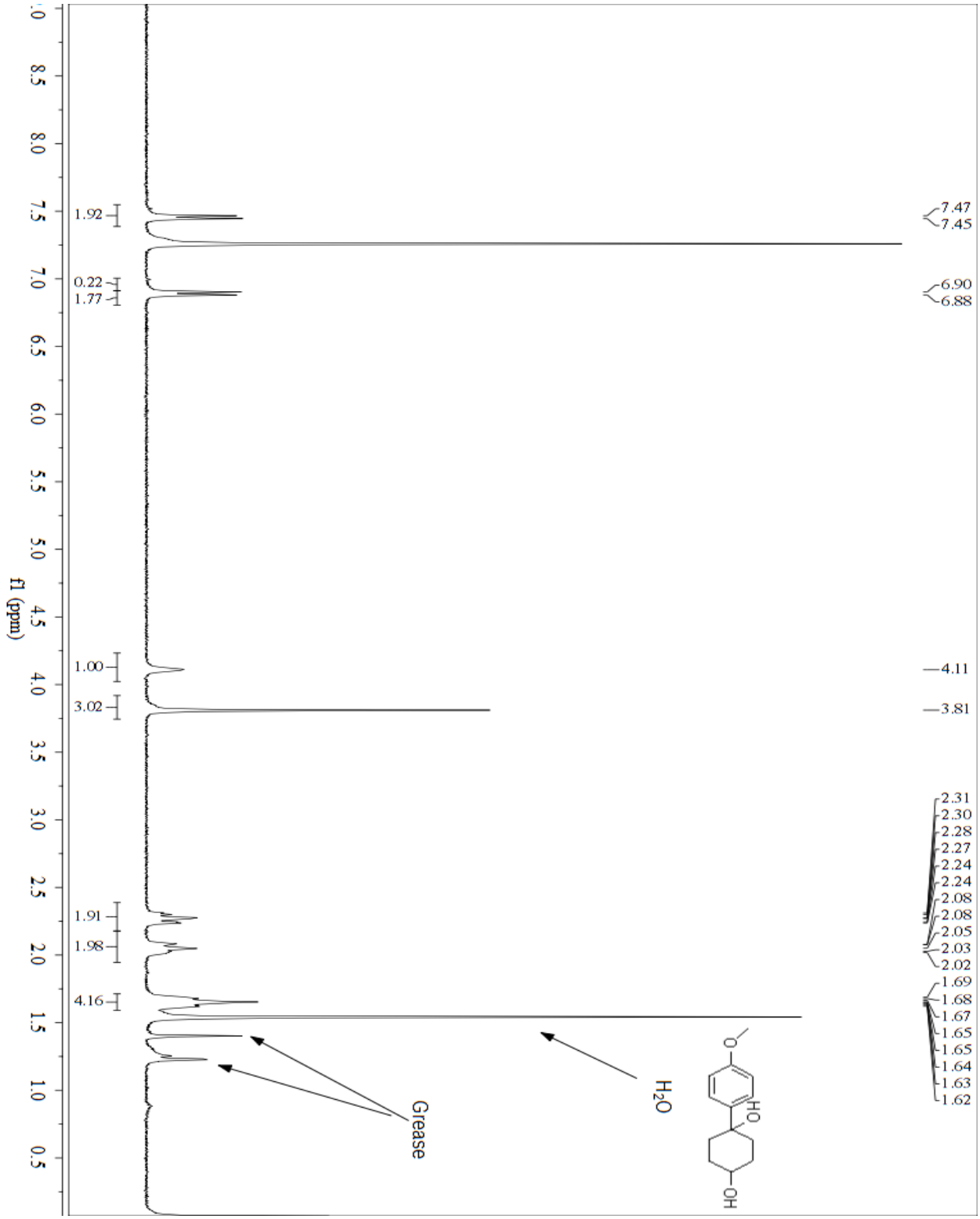

9a (1-(4-methoxyphenyl)-7-oxabicyclo[2.2.1]heptane)- Carbon

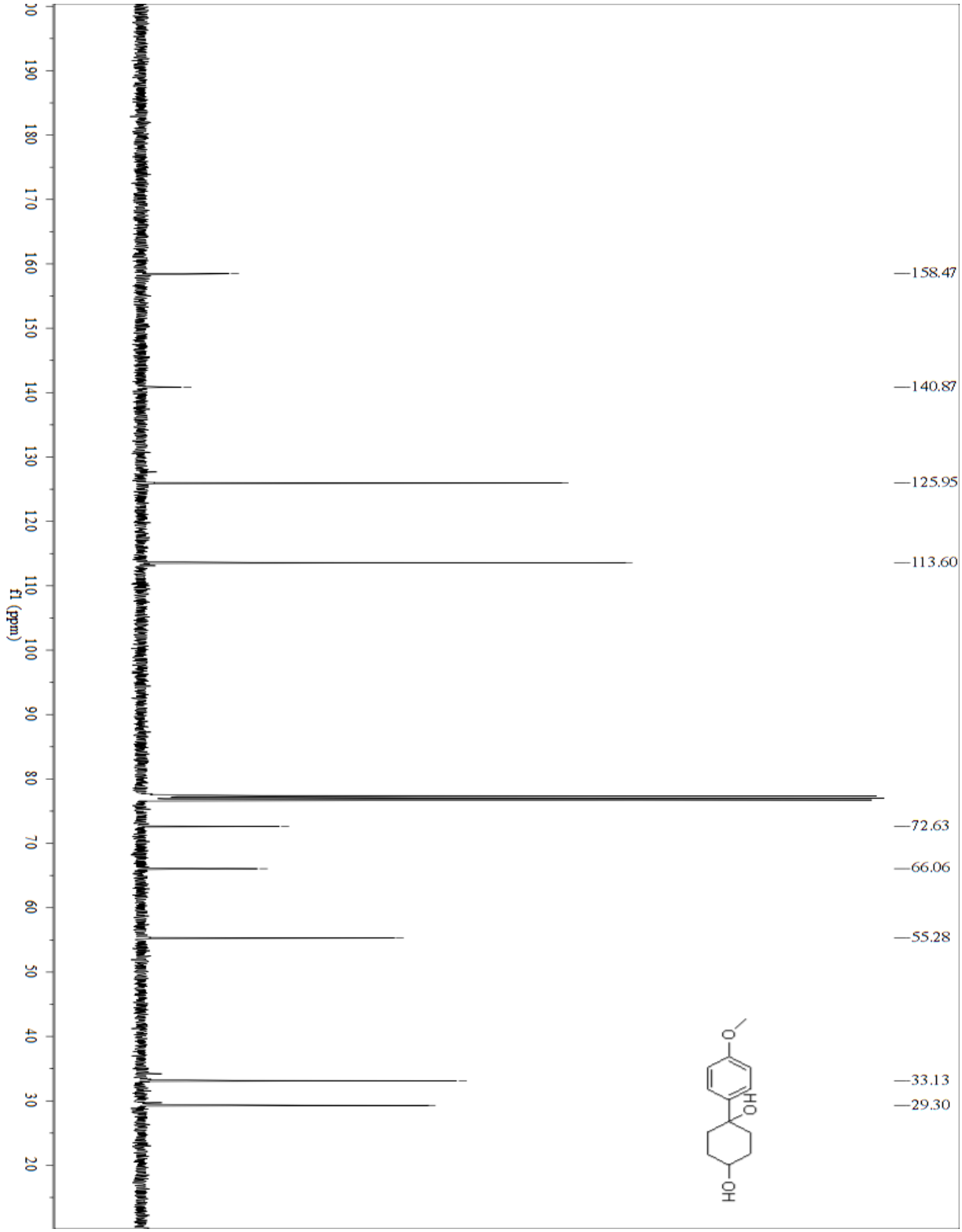

10a (1-phenyl-4-(4-(trifluoromethyl)phenyl)-7-oxabicyclo[2.2.1]heptane)- Starting material

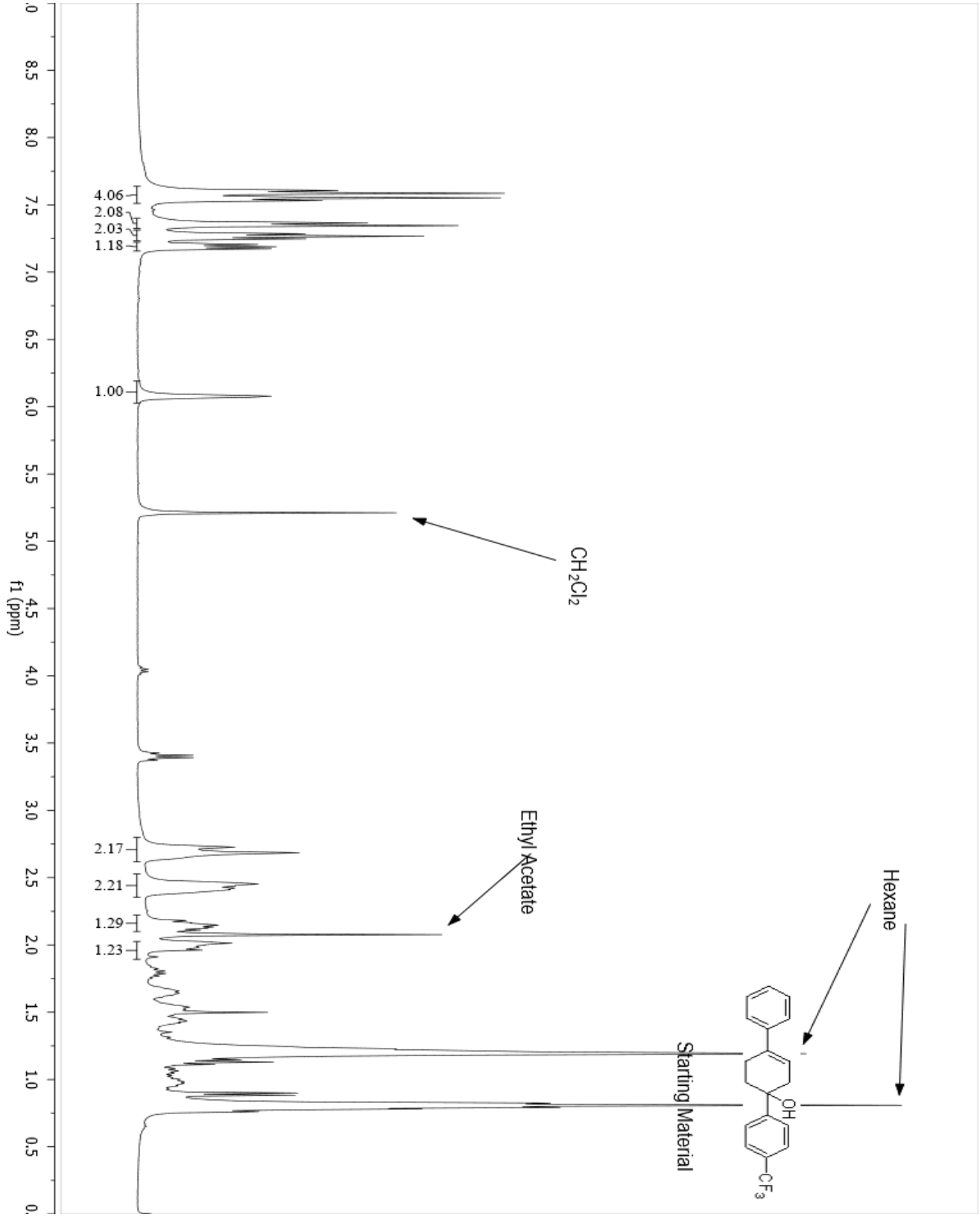

10a (1-phenyl-4-(4-(trifluoromethyl)phenyl)-7-oxabicyclo[2.2.1]heptane)- Proton

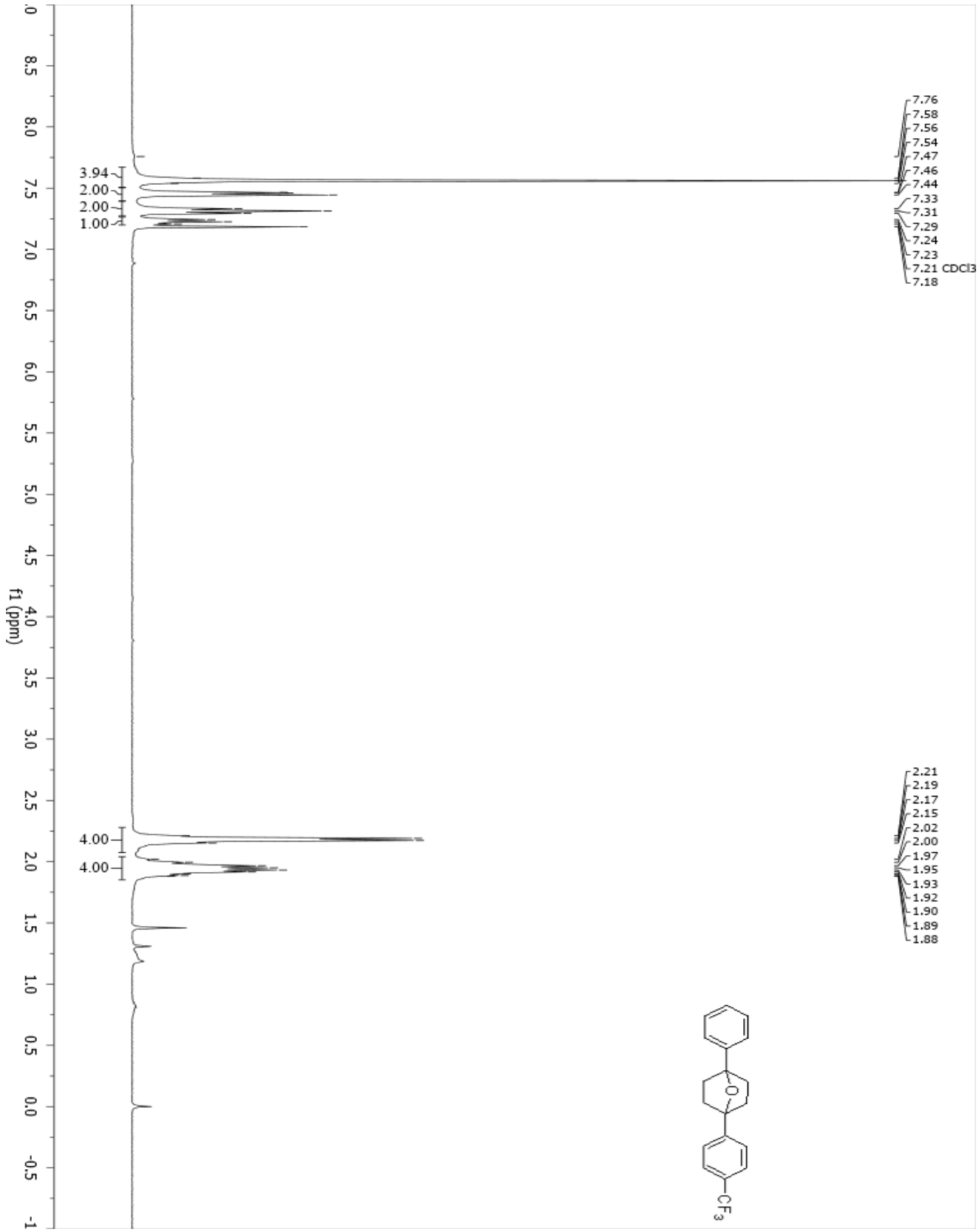

10a (1-phenyl-4-(4-(trifluoromethyl)phenyl)-7-oxabicyclo[2.2.1]heptane)- Carbon

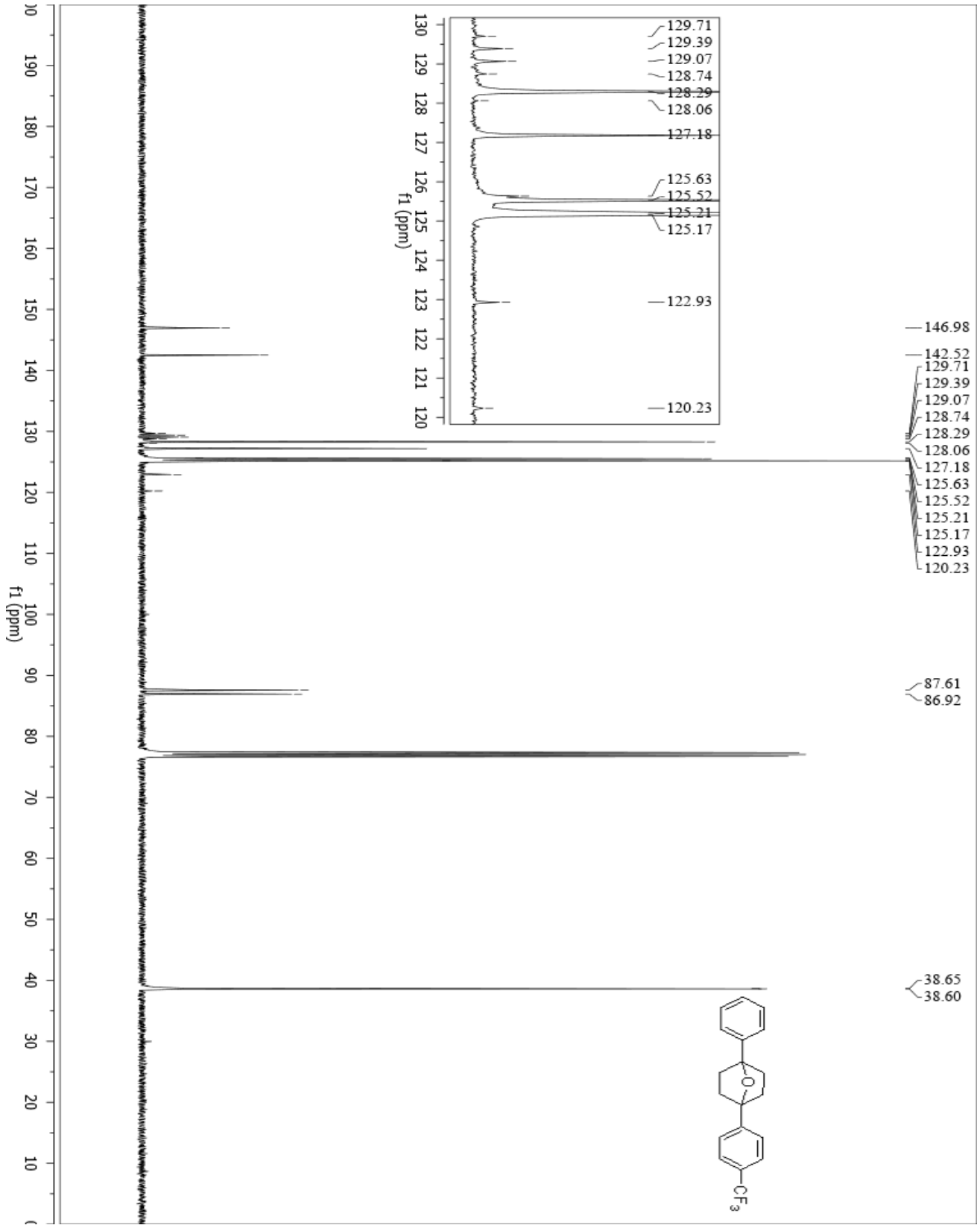

10a (1-phenyl-4-(4-(trifluoromethyl)phenyl)-7-oxabicyclo[2.2.1]heptane)- Fluorine

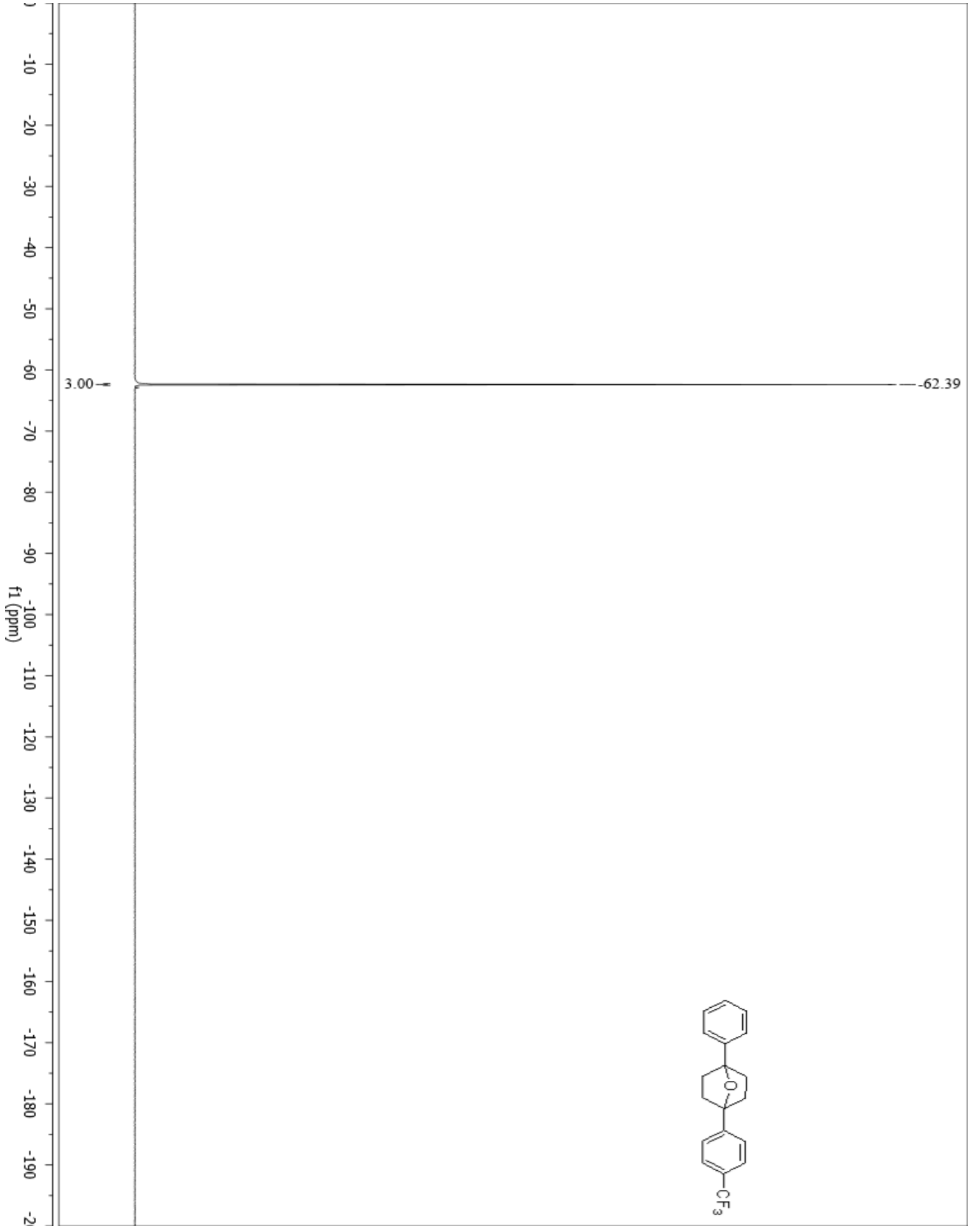

11a (1-(4-chlorophenyl)-4-(4-(trifluoromethyl)phenyl)-7-oxabicyclo[2.2.1]heptane)- Starting Material

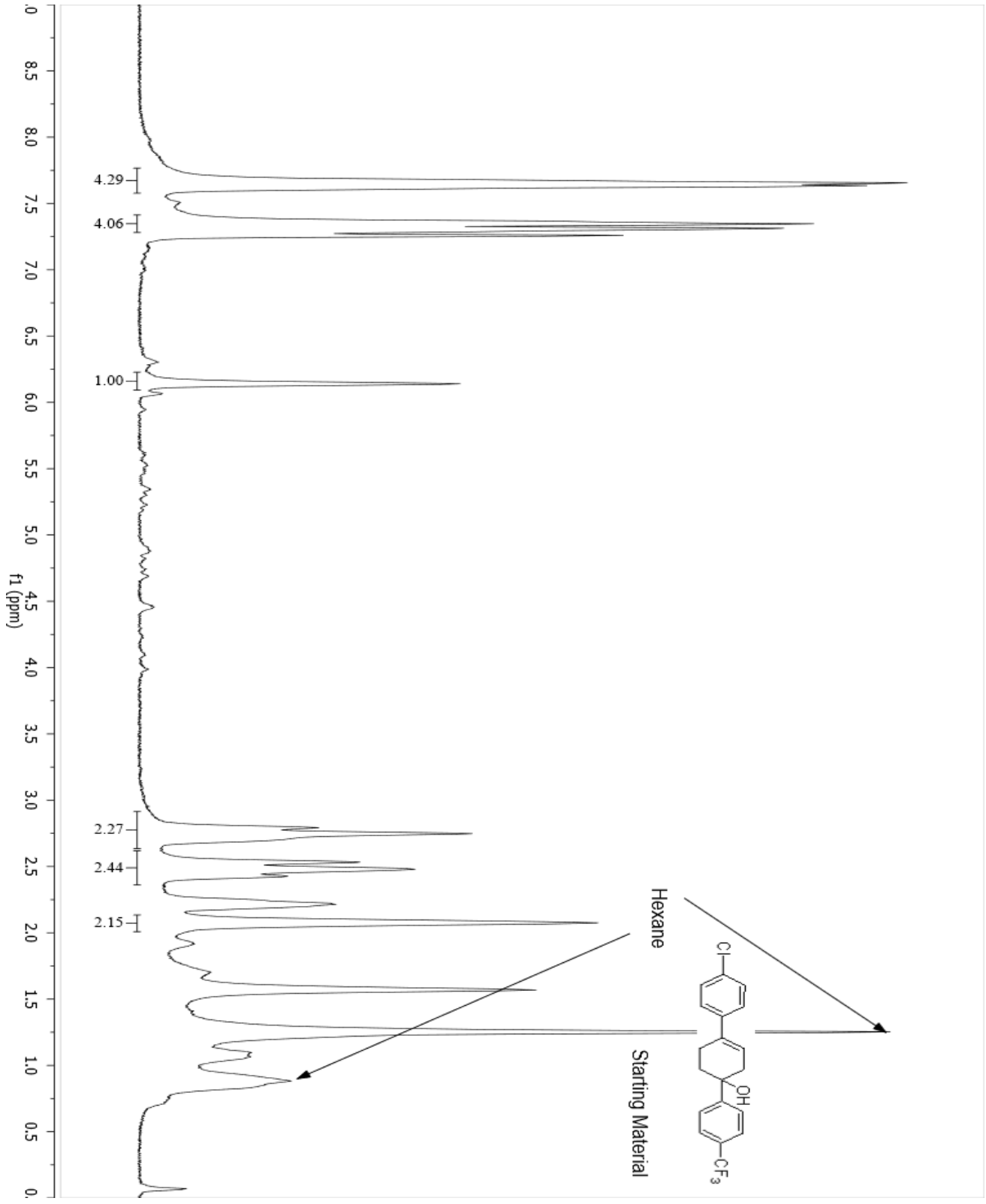

11a (1-(4-chlorophenyl)-4-(4-(trifluoromethyl)phenyl)-7-oxabicyclo[2.2.1]heptane)- Proton

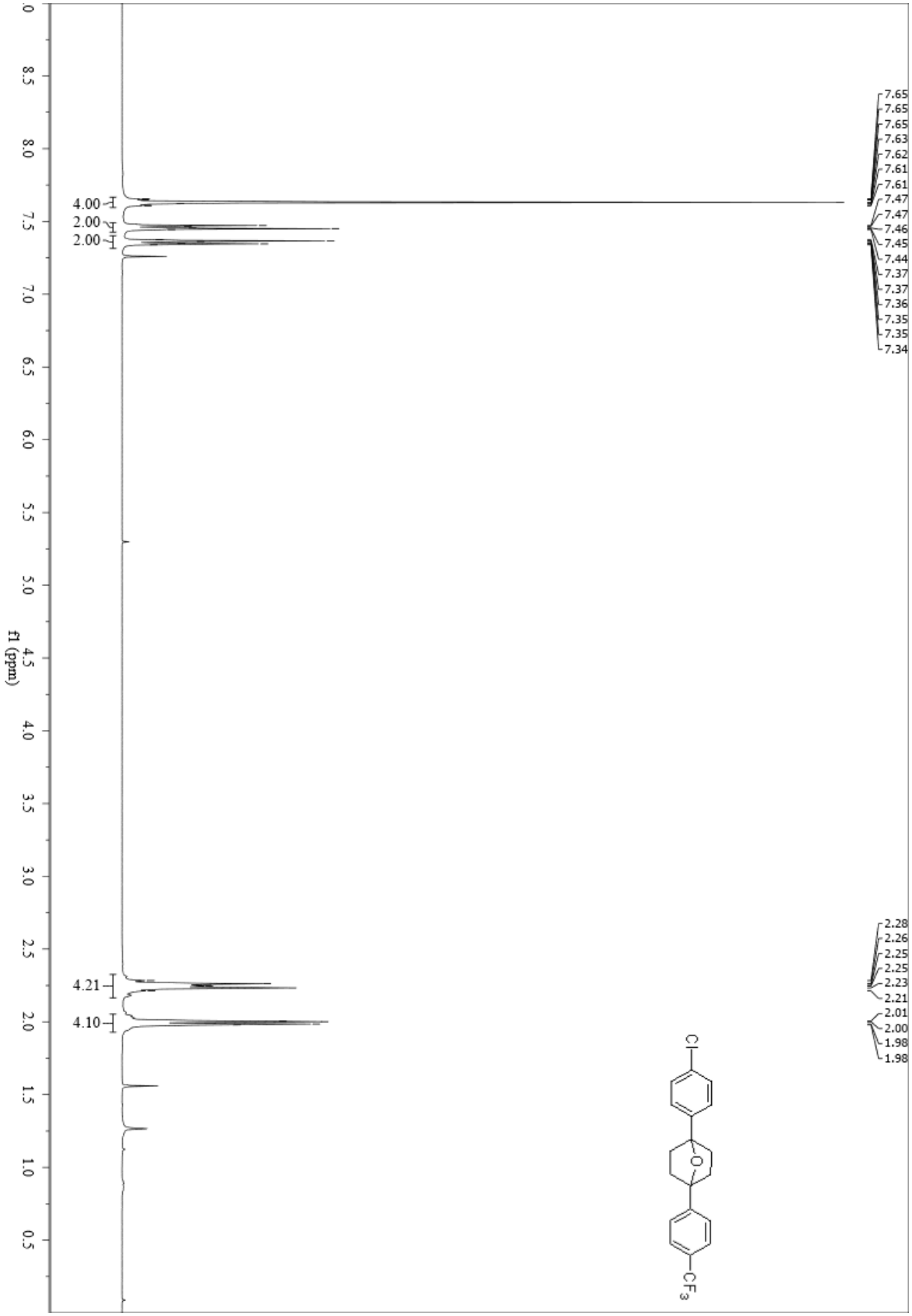

11a (1-(4-chlorophenyl)-4-(4-(trifluoromethyl)phenyl)-7-oxabicyclo[2.2.1]heptane)- Carbon

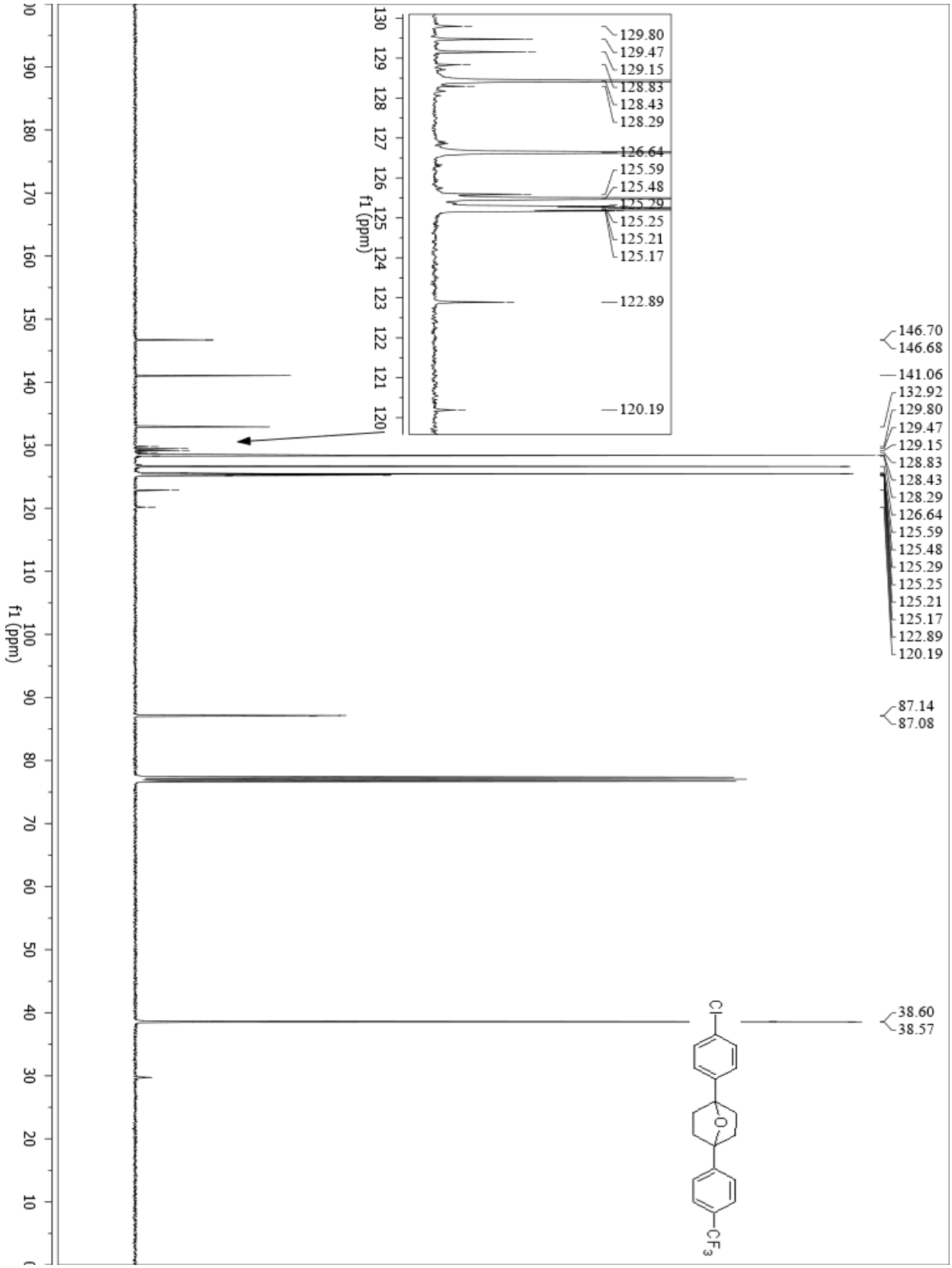

11a(1-(4-chlorophenyl)-4-(4-(trifluoromethyl)phenyl)-7-oxabicyclo[2.2.1]heptane)- Flourine

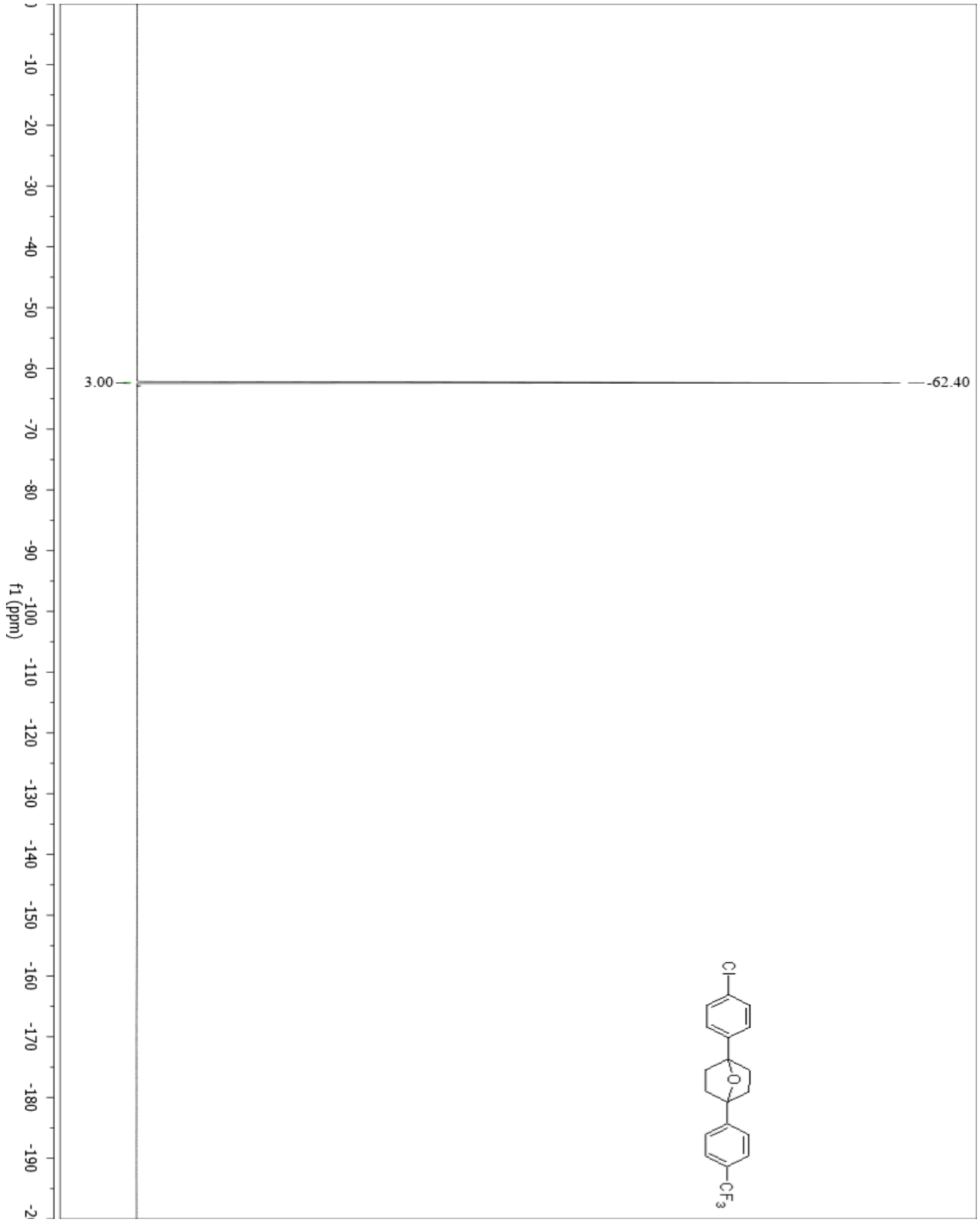

12a (1-(4-fluorophenyl)-4-(4-(trifluoromethyl)phenyl)-7-oxabicyclo[2.2.1]heptane)- Starting Material

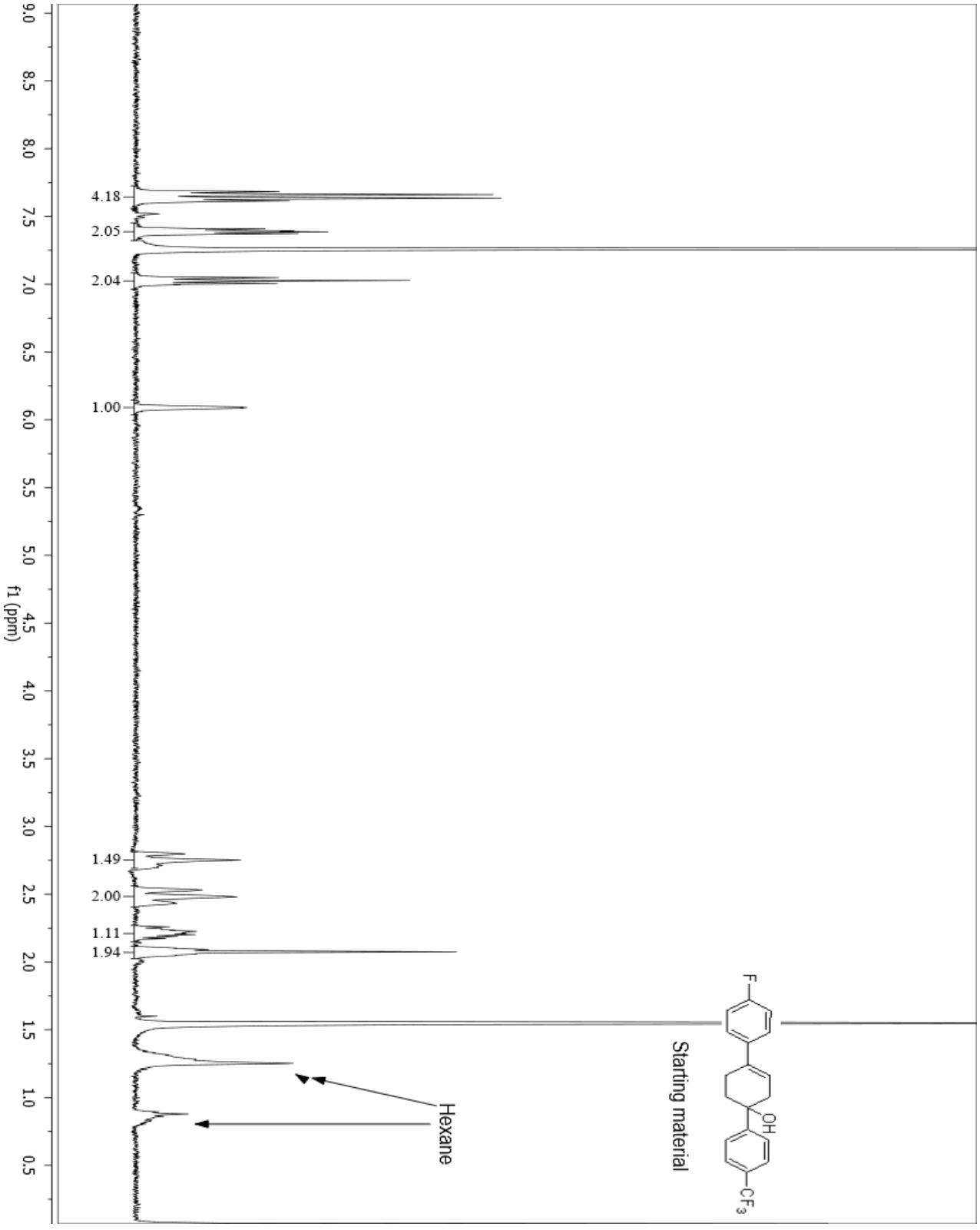

12a (1-(4-fluorophenyl)-4-(4-(trifluoromethyl)phenyl)-7-oxabicyclo[2.2.1]heptane)- Proton

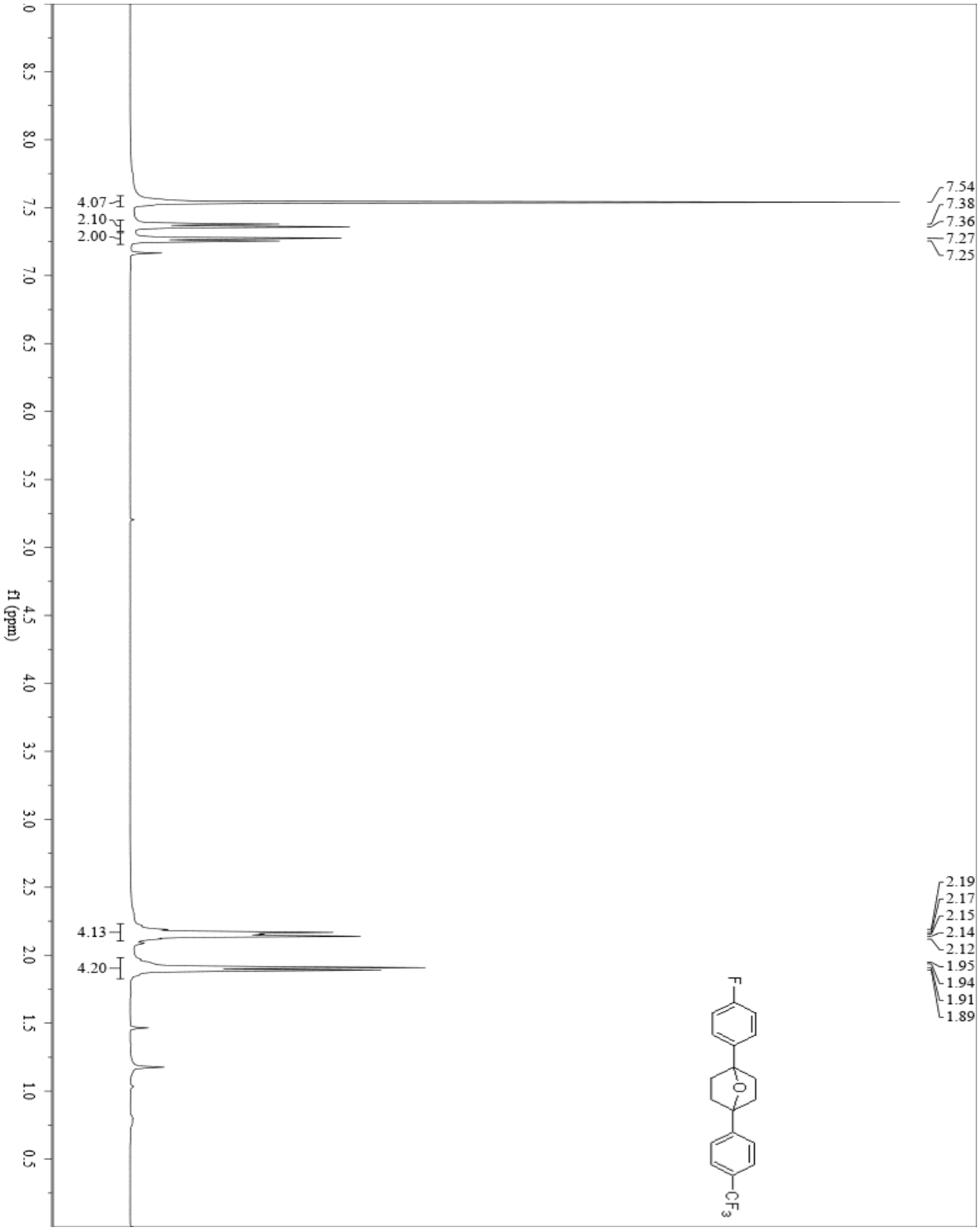

12a (1-(4-fluorophenyl)-4-(4-(trifluoromethyl)phenyl)-7-oxabicyclo[2.2.1]heptane)- Carbon

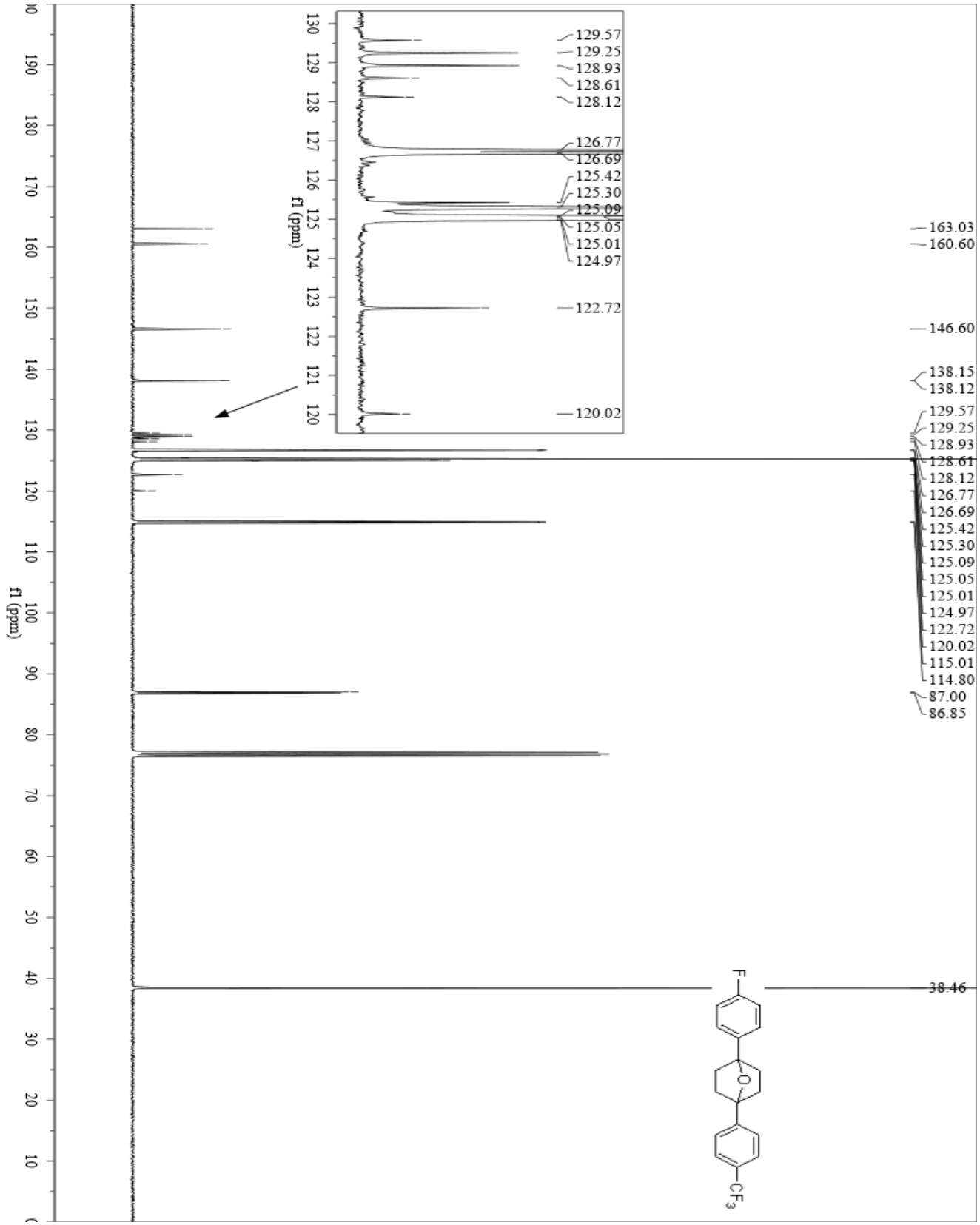

12a (1-(4-fluorophenyl)-4-(4-(trifluoromethyl)phenyl)-7-oxabicyclo[2.2.1]heptane)- Fluorine

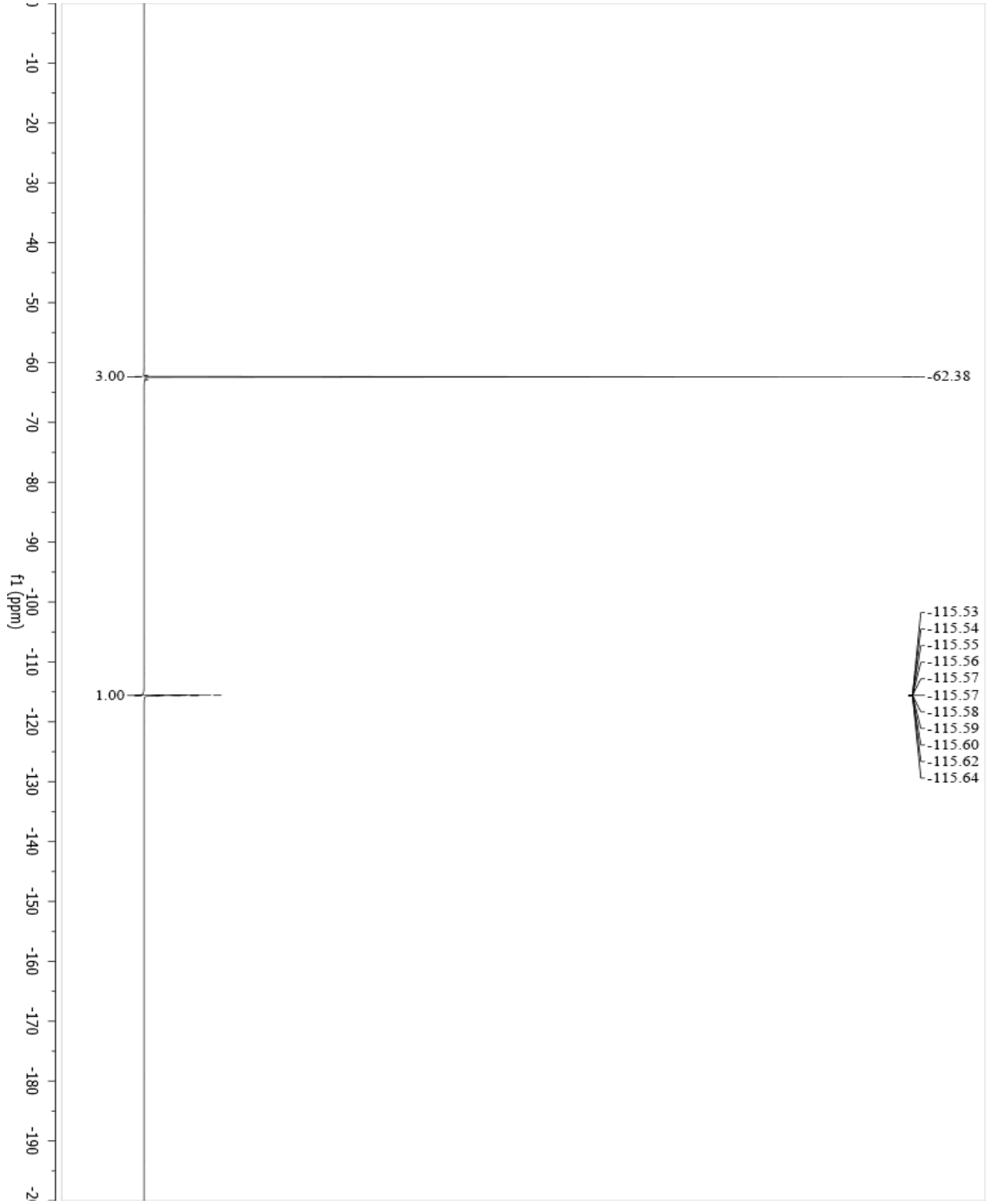

1a (1-(4-methoxyphenyl)-4-(4-(trifluoromethyl)phenyl)-7-oxabicyclo[2.2.1]heptane)-GCMS

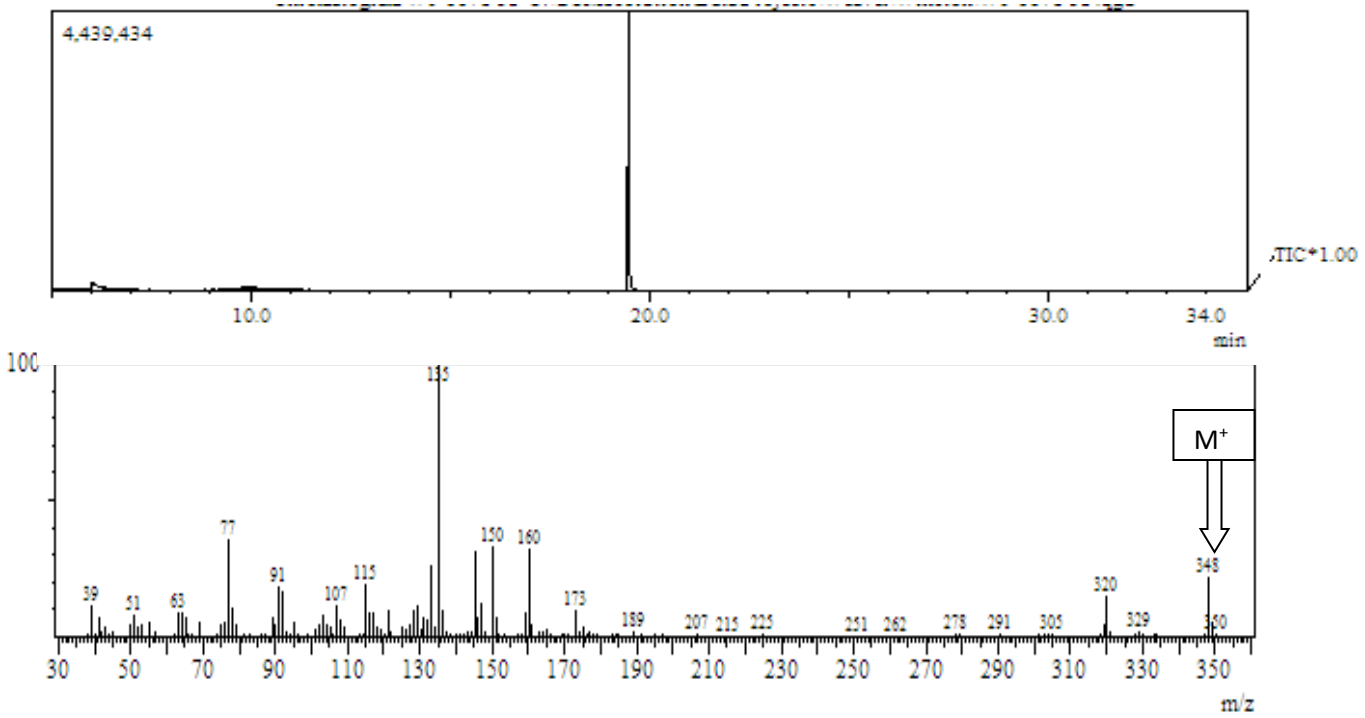

2a (1-(4-chlorophenyl)-4-(4-methoxyphenyl)-7-oxabicyclo[2.2.1]heptane)- GC-MS

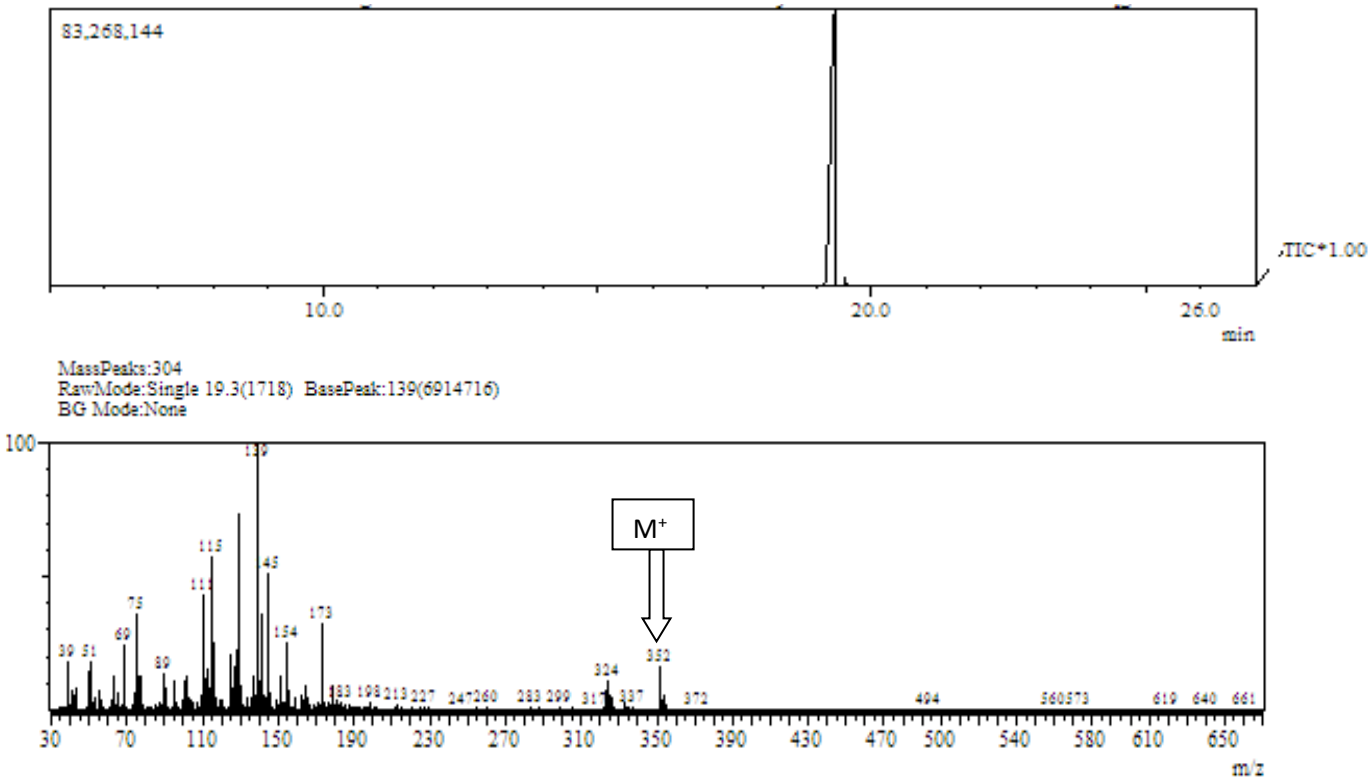

3a (1-(4-fluorophenyl)-4-(4-methoxyphenyl)-7-oxabicyclo[2.2.1]heptanes)- GC-MS

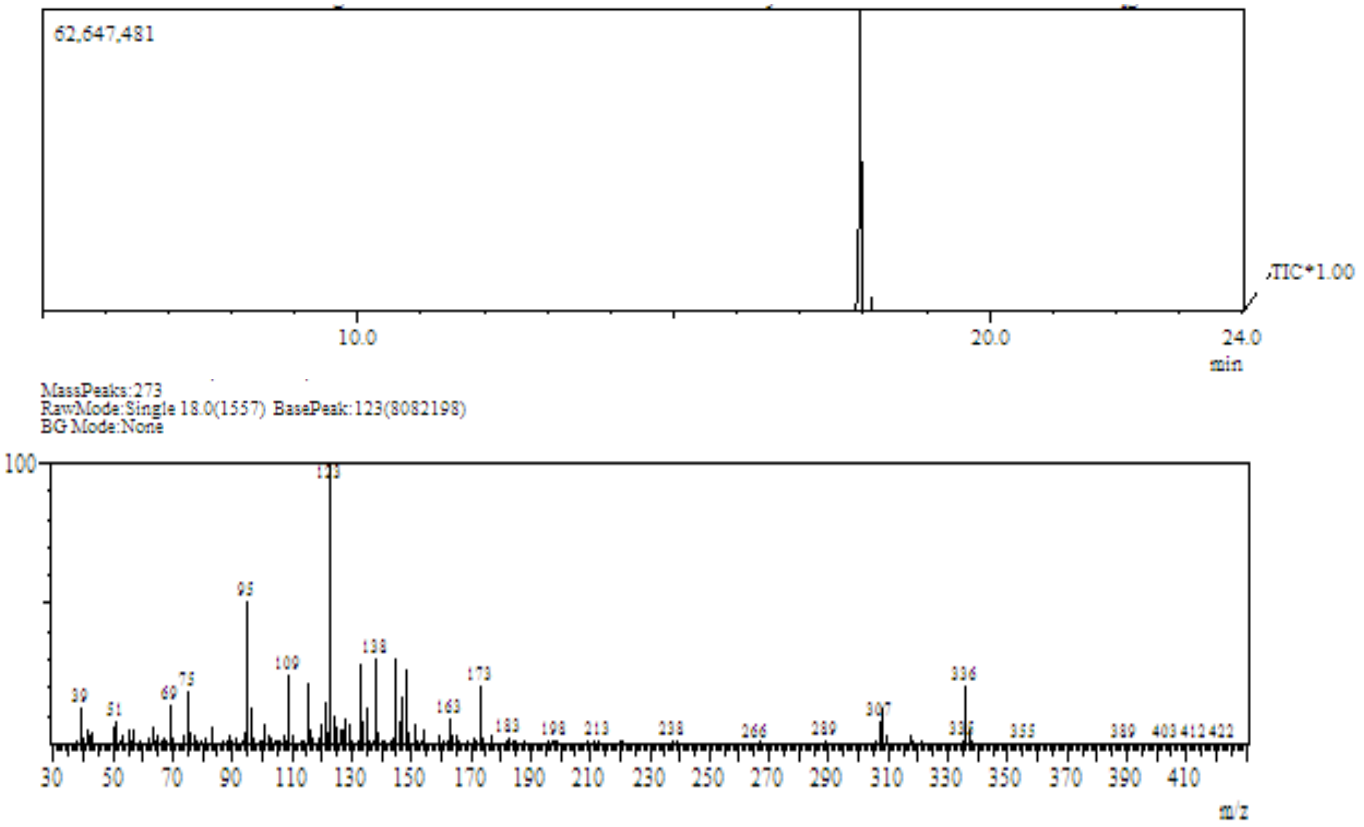

4a (1-(4-methoxyphenyl)-4-(perfluorophenyl)-7-oxabicyclo[2.2.1]heptanes)

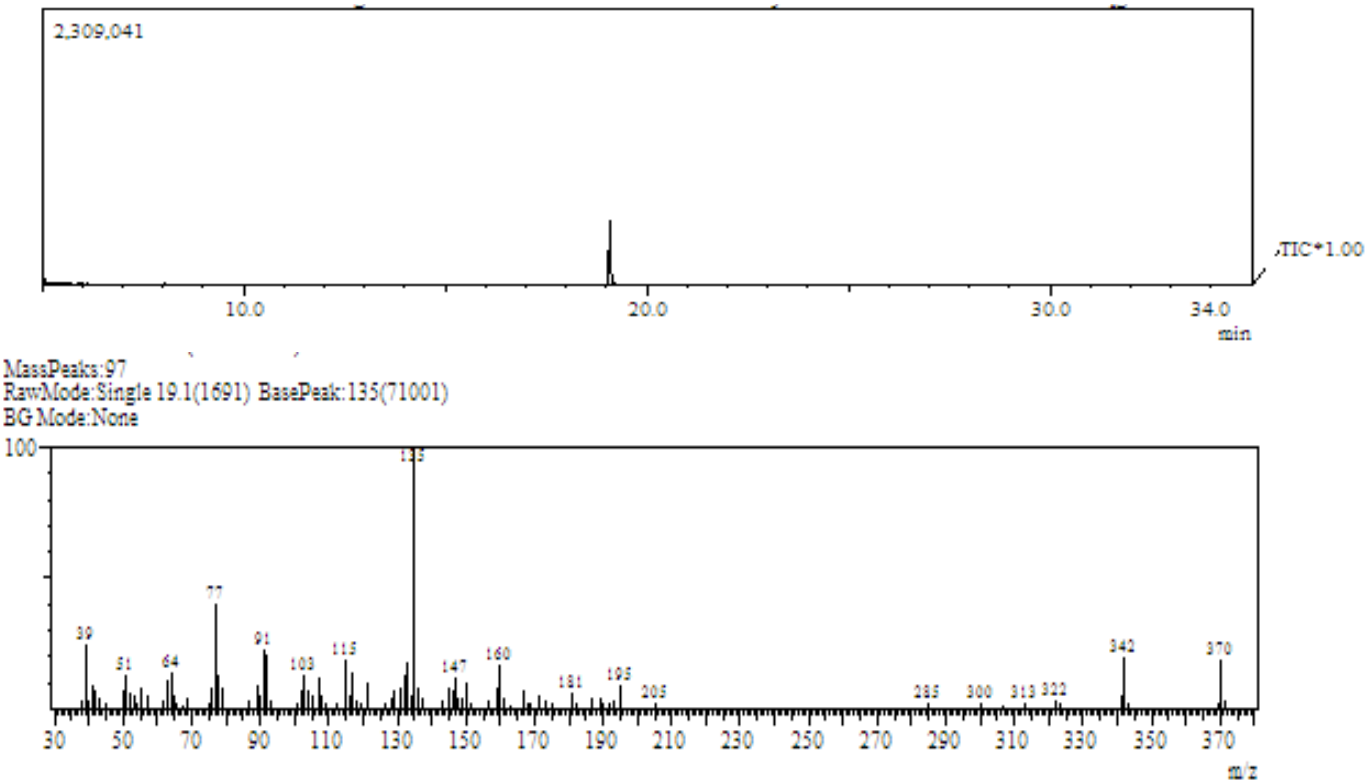

5a (1-(4-methoxyphenyl)-4-(p-tolyl)-7-oxabicyclo[2.2.1]heptane)

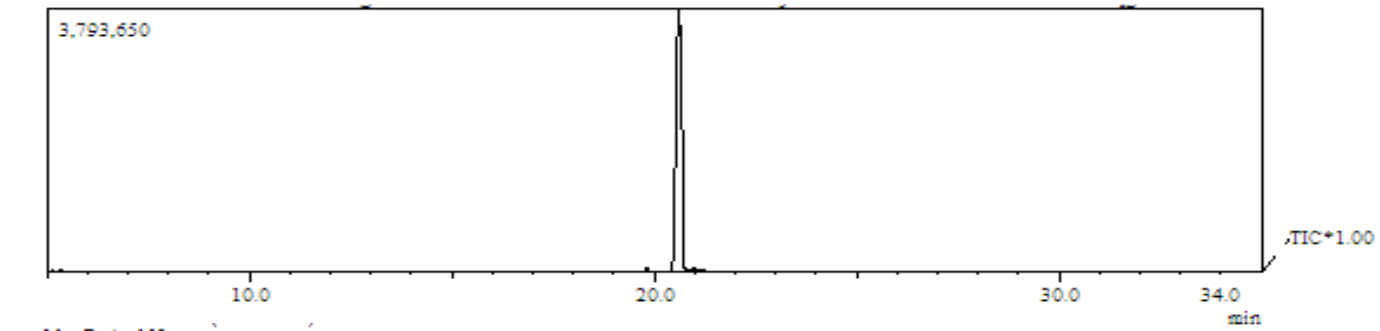

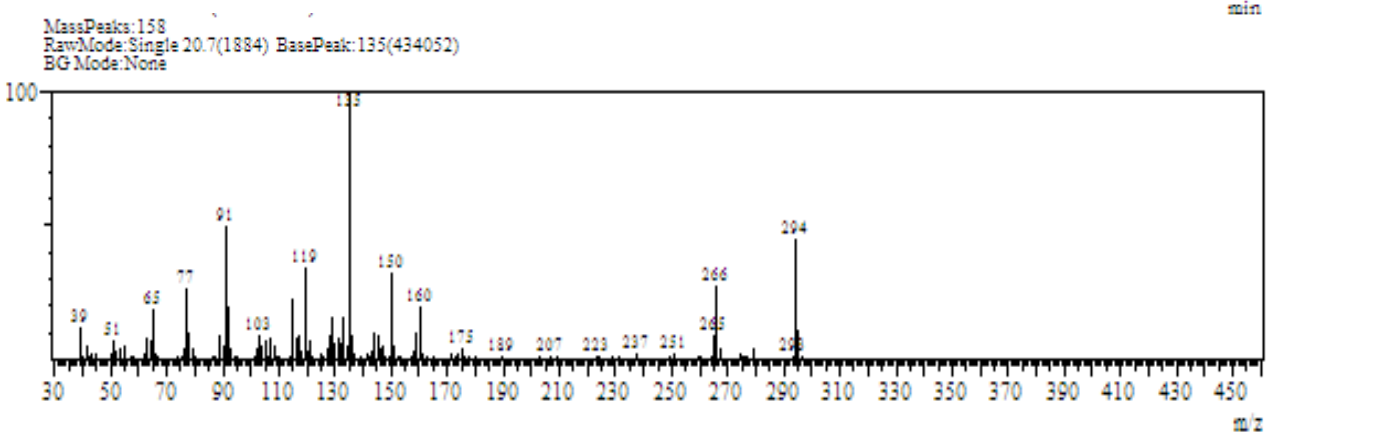

6a (1-(4-methoxyphenyl)-4-phenyl-7-oxabicyclo[2.2.1]heptane)

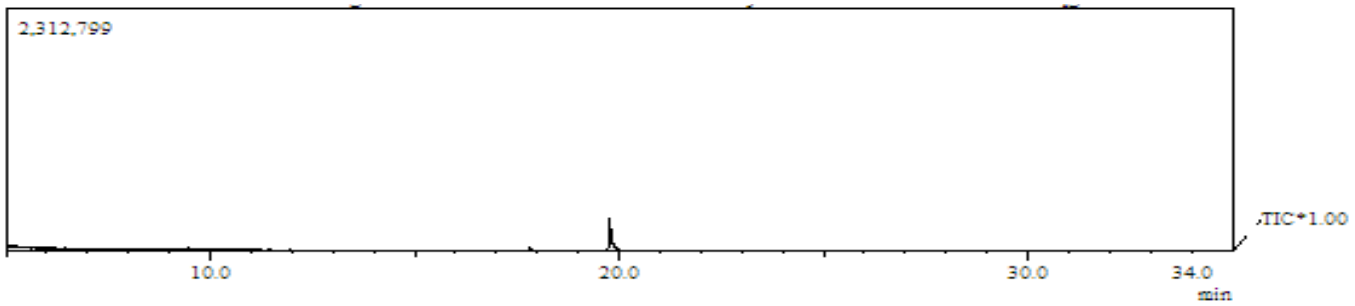

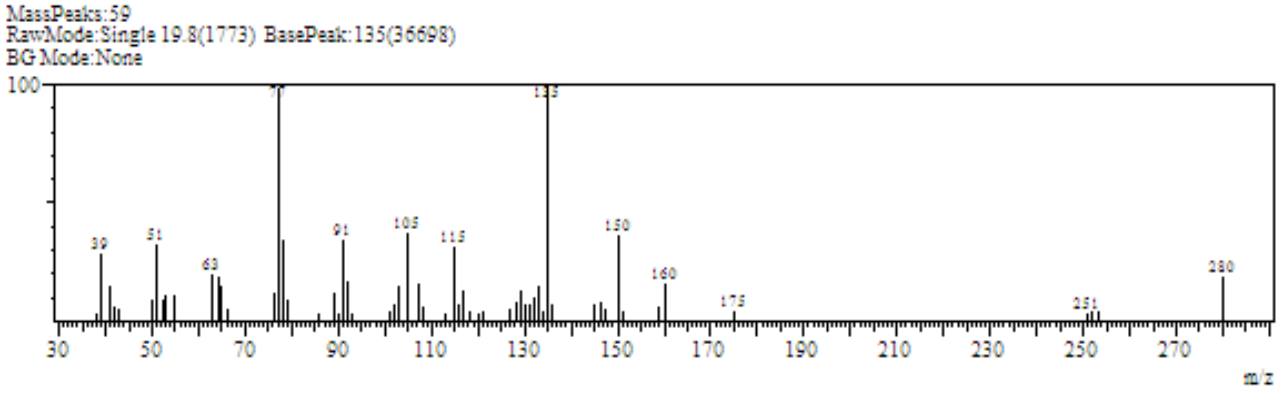

7a (1-ethynyl-4-(4-methoxyphenyl)-7-oxabicyclo[2.2.1]heptane)

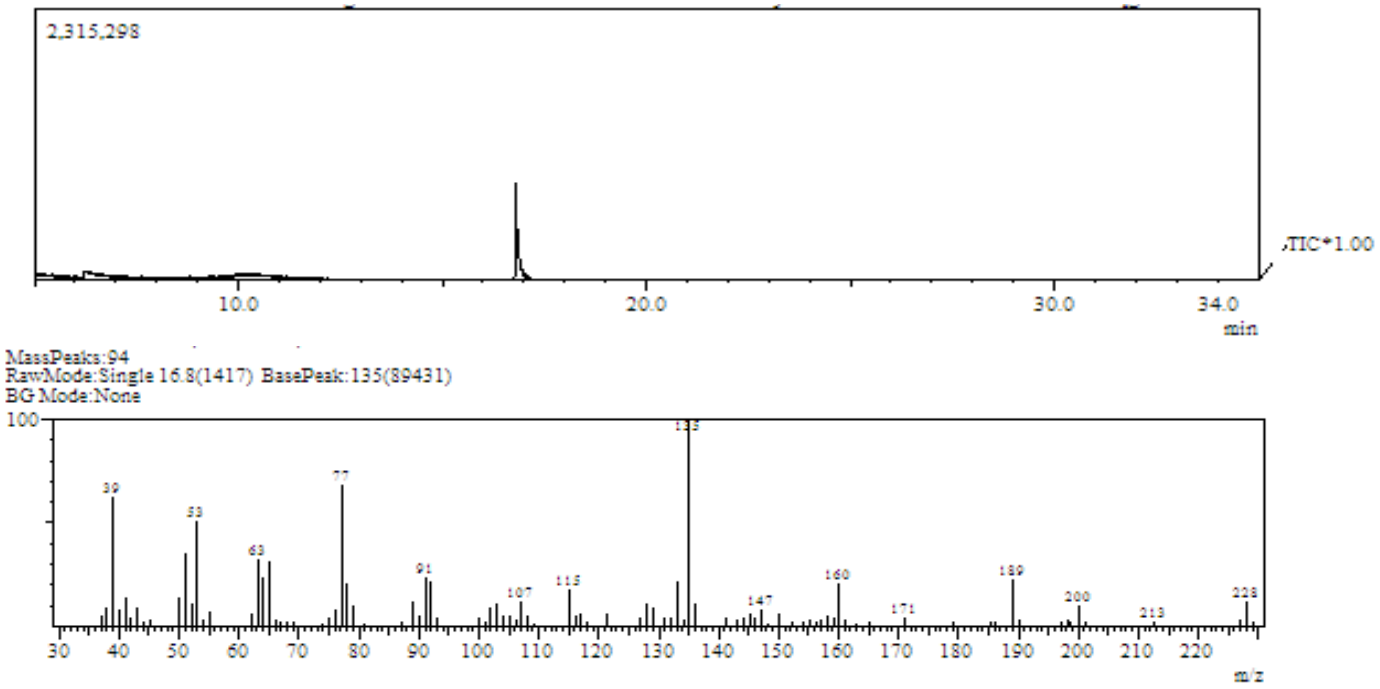

8a (1-ethyl-4-(4-methoxyphenyl)-7-oxabicyclo[2.2.1]heptane)

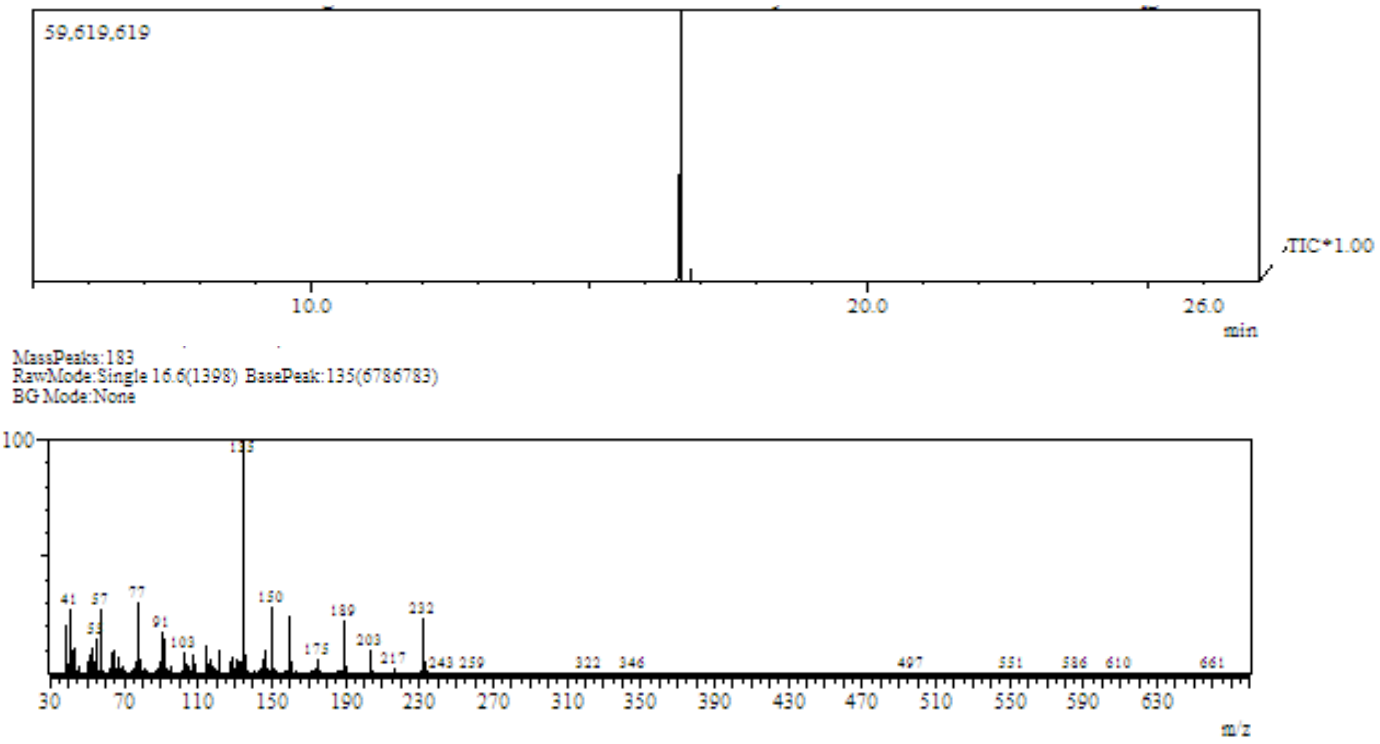

10a (1-phenyl-4-(4-(trifluoromethyl)phenyl)-7-oxabicyclo[2.2.1]heptane)-GC-MS

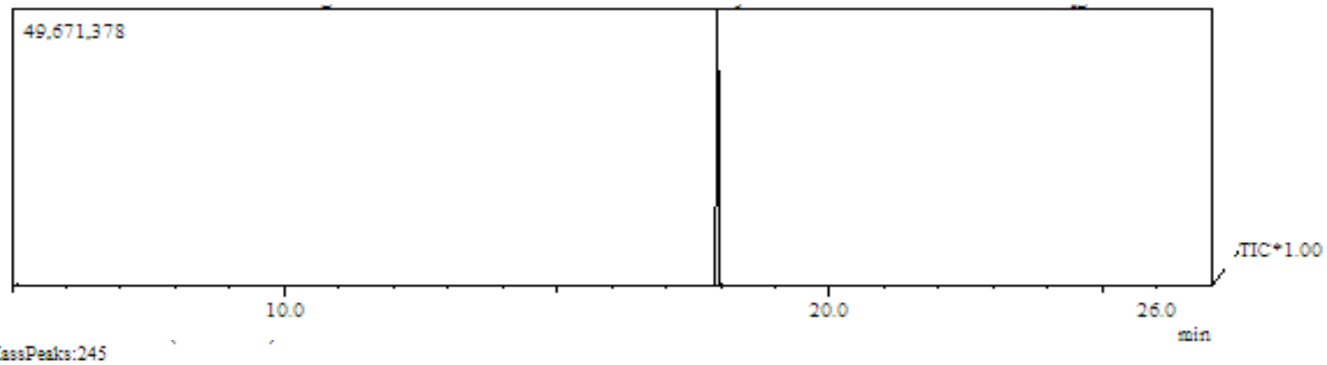

MassPeaks:245
RawMode:Single 17.9(1555) BasePeak:105(6056865)
BG Mode:None

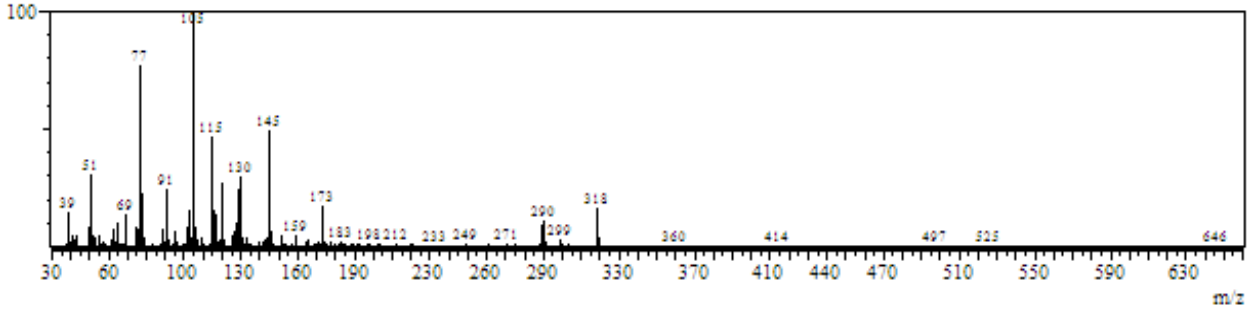

11a (1-(4-chlorophenyl)-4-(4-(trifluoromethyl)phenyl)-7-oxabicyclo[2.2.1]heptane)- GC-MS

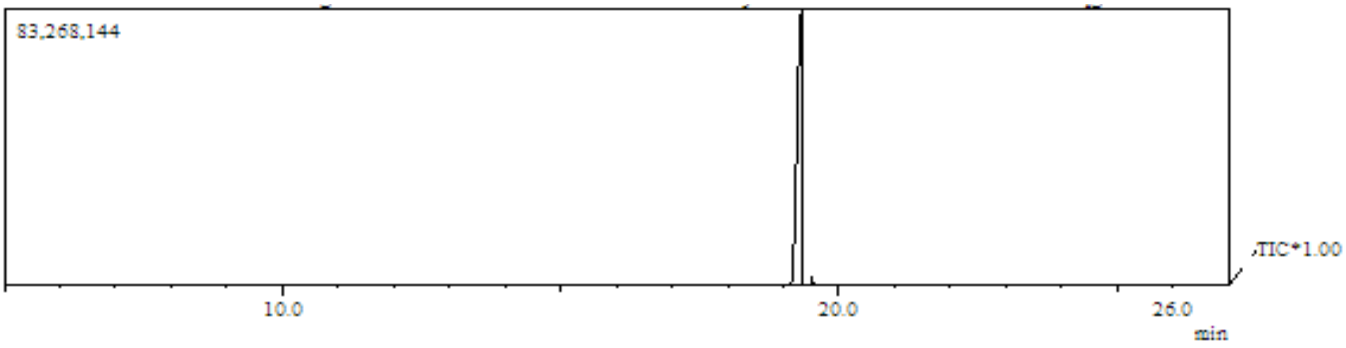

MassPeaks:304
RawMode:Single 19.3(1718) BasePeak:139(6914716)
BG Mode:None

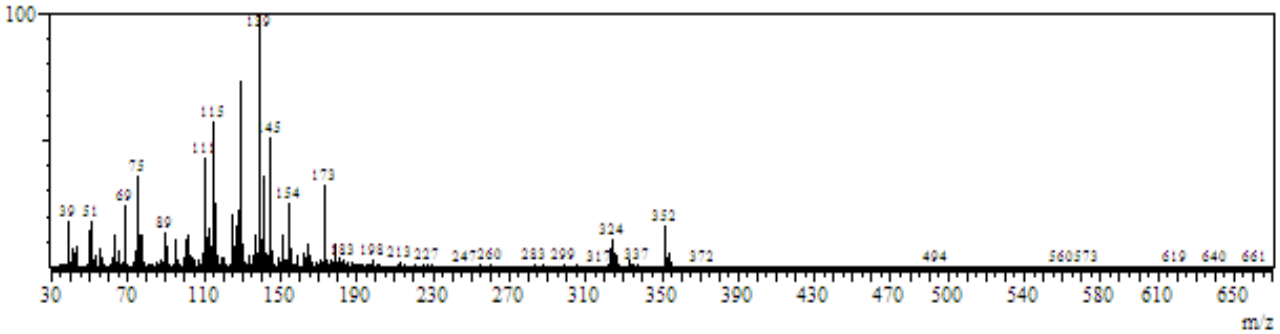

12a (1-(4-fluorophenyl)-4-(4-(trifluoromethyl)phenyl)-7-oxabicyclo[2.2.1]heptane)-GC-MS

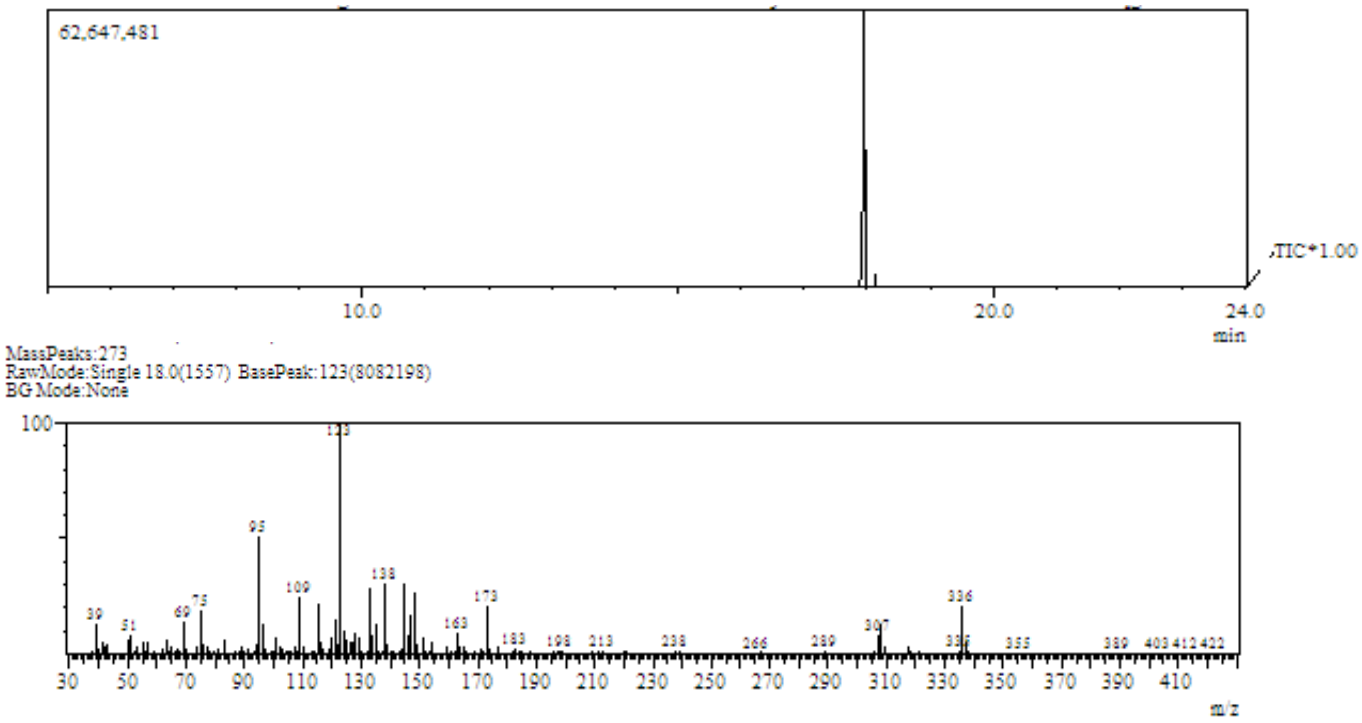

Section 2: The Cartesian coordination, energy minimization, ^{1}H NMR chemical shift data.

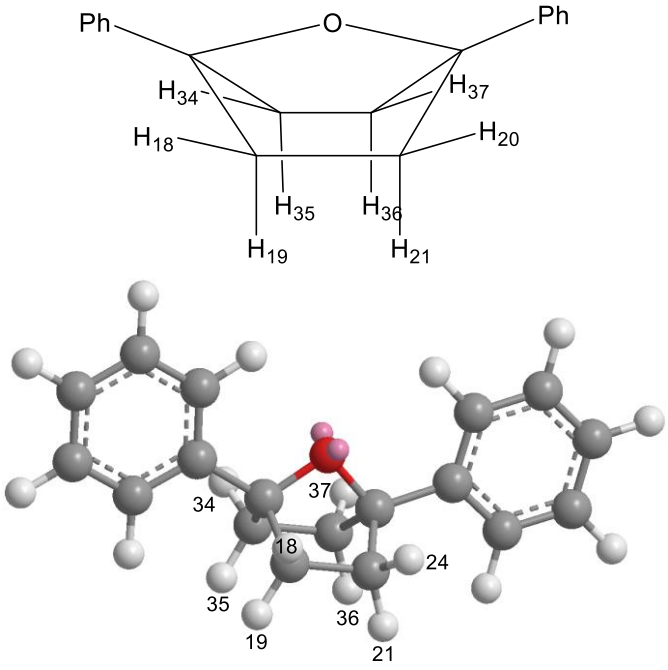

The Cartesian data

Calling FoFJK, ICntrl= 2127 FMM=F ISym2X=0 I1Cent= 0 IOpClX= 0 NMat=1 NMatS=1 NMatT=0.

***** Axes restored to original set *****

Center Number	Atomic NumberX	Forces (Hartrees/Bohr) Y	Z
1	6	0.003450179	-0.002403503	-0.006634031
2	6	-0.001395833	0.000803962	0.005725736
3	6	0.001318950	-0.000239749	0.002792625
4	6	-0.001011058	0.000022608	-0.000146204
5	6	-0.000015718	0.000198781	-0.001469234
6	6	0.001318866	-0.000026481	-0.000005965
7	6	-0.001471401	0.000010069	0.003110009
8	1	0.000205971	0.000252912	-0.000188283
9	1	-0.000314832	-0.000018220	0.000157870
10	1	-0.000013349	-0.000123868	0.000452270
11	1	0.000296772	-0.000073377	0.000263742
12	1	-0.000410858	0.000295521	-0.000140834
13	6	-0.002114879	0.000022882	-0.002682784
14	6	0.000483725	-0.000766873	0.003299160
15	6	0.006761220	-0.003694246	0.001452011

16	6	0.001120140	0.000720816	0.004014301
17	6	-0.002152336	0.001768020	-0.003178252
18	1	0.000177723	-0.000021696	-0.000045947
19	1	0.001004694	-0.000599185	-0.000237763
20	1	0.000115551	0.000073099	-0.000096123
21	1	0.000788224	-0.000503393	-0.000647042
22	8	-0.001783852	0.000723832	0.000811617
23	6	-0.005034305	0.001948846	-0.002540242
24	6	-0.001114449	0.000576355	-0.002900969
25	6	-0.000514388	-0.000119009	0.000781065
26	6	0.000897923	-0.000150520	0.001117702
27	6	0.001008360	0.000102236	-0.000946232
28	6	-0.003254142	0.000596389	-0.001023561
29	1	0.000310278	0.000232265	-0.000016403
30	1	-0.000361695	-0.000012851	0.000105310
31	1	-0.000305217	-0.000027007	-0.000316425
32	1	0.000020356	0.000031107	-0.000396322
33	1	-0.000156280	0.000199007	0.000444367
34	1	0.000082095	0.000230397	-0.000048558
35	1	0.000902373	-0.000088518	-0.000579322
36	1	0.001036795	-0.000120870	-0.000303890
37	1	0.000124397	0.000180259	0.000016604

Cartesian Forces: Max 0.006761220 RMS 0.001692526

The ^{1}H NMR chemical shift.

Atom	Symbol	Isotropic	Anisotropy
1	C*	88.9501	76.7934
2	C*	135.184	176.6439
3	C*	118.3845	153.5249
4	C*	121.1197	161.9149
5	C*	119.9542	160.8596
6	C*	122.3489	163.0528
7	C*	118.4074	159.9481
8	H*	8.0459	11.1968
9	H*	7.4128	5.1587
10	H*	7.2482	3.8188
11	H*	7.3331	4.9806
12	H*	7.1779	9.9282
13	C*	44.4436	35.2242
14	C*	44.4316	35.2037
15	C*	88.9499	76.7933
16	C*	44.4398	35.2209
17	C*	44.4279	35.2005
18	H*	2.5318	6.5548
19	H*	2.6774	7.9435
20	H*	2.5313	6.5523
21	H*	2.6763	7.9397
22	O	195.3128	96.4485
23	C*	135.1841	176.6440
24	C*	118.3844	153.5250

25	C*	121.1196	161.9148
26	C*	119.9542	160.8596
27	C*	122.3488	163.0528
28	C*	118.4075	159.9482
29	H*	8.0459	11.1968
30	H*	7.4128	5.1587
31	H*	7.2482	3.8188
32	H*	7.3331	4.9806
33	H*	7.1779	9.9282
34	H*	2.5318	6.5541
35	H*	2.677	7.9427
36	H*	2.6759	7.9388
37	H*	2.5312	6.5516

Chapter 2

ON THE EXISTENCE OF TRANS-CYCLOHEPTENE AND ITS USE SYNTHESIS OF DIMER-CYCOHEPTANOL

I. INTRODUCTION

Building off our work with phenylcyclohexene, we anticipated that we should be able to generate *trans*-cycloheptene in a similar manner. As shown in Figure 1, the amount of strain contained in *trans*-cycloheptene is 35 kcal/mol which is ~10 kcal/mol less than the corresponding *trans*-cyclohexene (45 kcal/mol). Correspondingly, the barrier for reversion increases from 10-15 kcal/mol to 20-25 kcal/mol. Consequently, *trans*-cycloheptene is expected to have a longer life-time.[1] While we have not found any intermolecular reaction feasible with *trans*-cyclohexene except the photocatalytic hydration of 1-(4-methoxyphenyl)cyclohexane-1,4-diol (**9b**, Scheme 10, Chapter 1). Given the longer lifetime, it is conceivable that intermolecular reactions should be feasible with the *trans*-cycloheptene species.

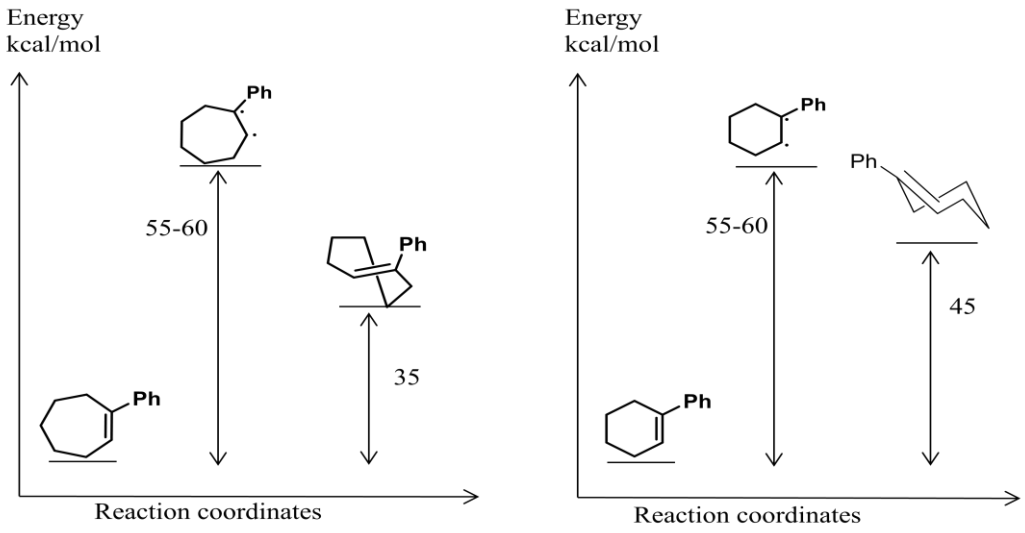

Figure 1: Energy vs. Reaction coordinates of 1-phenyl cycloheptene (left) of 1-phenyl cyclohexene (right)

When substrate 2-(4-fluorophenyl)cyclohept-2-en-1-ol was irradiated using visible light in the presence of catalytic amounts of *fac*-Ir(4'-F-ppy)$_3$ (**2b**) we observed the formation of a [2+2] dimerization product (1R,5aS,5bS,10R,10aS,10bS)-10a,10b-bis(4fluorophenyl)tetradecahydrocyclobuta[1,2:3,4]di[7]annulene-1,10-diol (**1a**) (Scheme 1). The diastereoselectivity was very high and the structure was confirmed via an X-ray crystallographic analysis (Figure 2) (Table 1 is a summary of crystallographic and refinement data for compound 1a). The X-ray structure revealed the relative stereochemistry of the major product. The product is a head-to-head dimer in which the cyclobutane ring is *trans*-fused to both 7-membered rings. The relative orientation of the two ring fusions is such that **1a** possess C2-symmetry rather than the *meso*-symmetry.

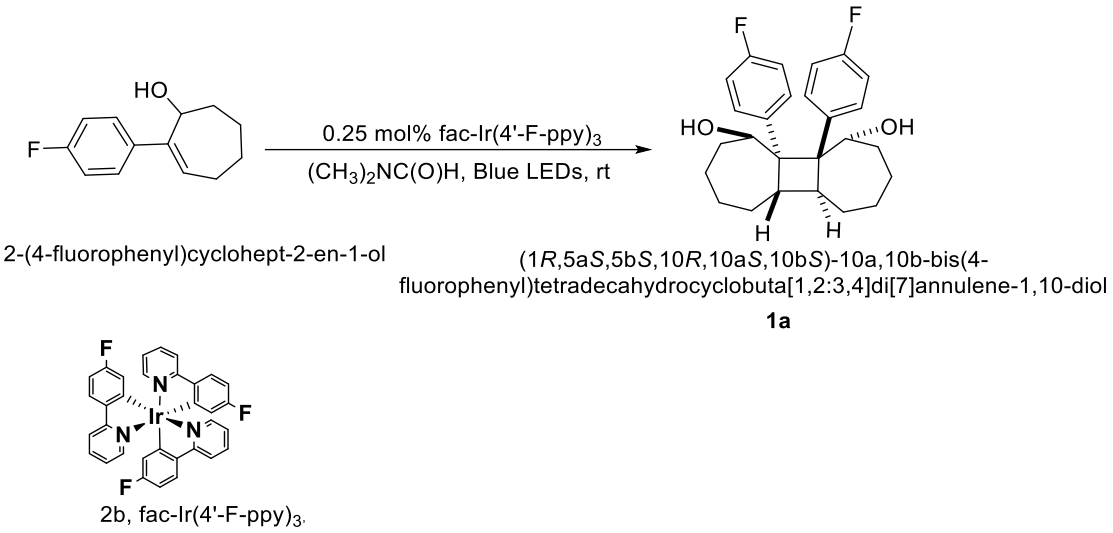

Scheme 1: The reaction of 2-(4-fluorophenyl)cyclohept-2-en-1-ol (**1a**) to make dimer product (1b)

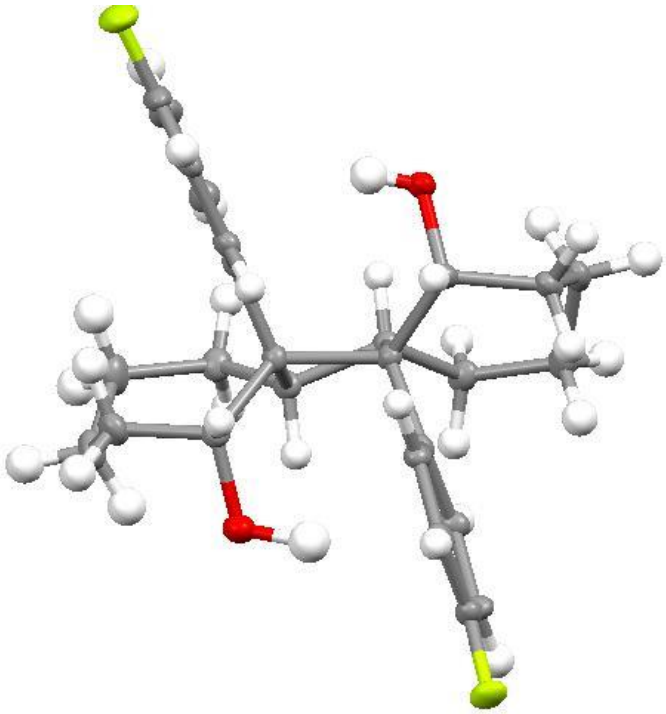

Figure 2: Two views of **1a** determined by X-ray crystallographic analysis.

Table 1: Summary of Crystallographic and Refinement Data for Compound.

Formula	$C_{26}H_{30}F_2O_2$
Formula weight	412.50
Temp, K	100
Crystal system	triclinic
Space group	2
Hall symbol	-P 1
No.	122
a, Å	8.719(2)
b, Å	9.572(2)
c, Å	12.839(3)
α, degree	73.103(3)
β, degree	81.352(3)
γ, degree	77.937(3)
Z	2
Cell vol, $Å^3$	998.0(4)
Density (diffrn) g cm^{-3}	1.373
Absorb coeff, mm^{-1}	0.097
F(000)	440
Data range ($\theta_{min} - \theta_{max}$), deg	
Measdreflns	19956
Max/min trans	1.011/-0.326
Restraints/ params	1.032/277
GOF	1.032
R [$F_2 > 2\sigma(F_2)$]	0.0526
R_w (F_2)	0.1389

One particularly attractive feature of this reaction is the good level of stereoinduction that the single stereocenterin the alcohol of the starting material imposes on the product. Recall, that the number of potential stereoisomers increases as a function of number of stereocenters within a molecule, 2^n in which n is the number of stereocenters. Thus, 64 stereoisomers are possible and if the head-to-tail regioisomer is included (64) the total increases to 128 possible isomers. However, we observed a single diastereomer and regioisomer, in most cases. The high level of stereoinduction and the C2 symmetric nature of the product with two alcohol groups is

reminiscent of the chiral Taddol motif, which have been used extensively in asymmetric chemistry.[2,6]

II. RESULT AND DISCUSSION

Often, solvent plays a substantial role in the reaction, thus, we started our study by performing the reaction in several solvents (Table 1). While the reaction took place smoothly in most of the solvents, the greatest conversion was achieved using DMF, which completed in less than 28 hours.

Table 1: Optimization with different solvents.

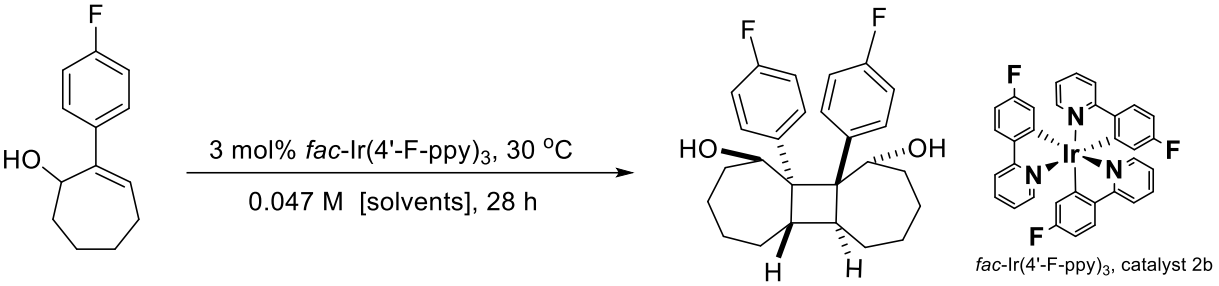

Solvent	Conversion
Acetonitrile	80 %
Methylene chloride	72 %
Dimethyl formamide	100 %
Toluene	97 %
Tetrahydrofuran	83 %
Ether	47 %

The conversion was determined by ^{19}FNMR at 28 h.

Next, we examined the role of the catalyst on the reaction. The catalyst loading, 0.08 mol% was substantially lower than the initial solvent screen (3 mol%) which was expected to both reduce the amount of catalyst used as well as slow the rate of the reaction, such that it was easier to discern the effect of catalyst structure on the rate. We examined the dimerization of 2-phenylcyclohept-2-en-1-ol as a function of different photocatalysts. We expected that the catalyst structure would play an important role since, it was known that catalyst volume plays a significant role in the isomerization of styrene derivatives, and to a lesser extent so does the emissive energy.[5] In Table 2, catalyst **2b** gave higher percent conversion compare to **2a**, **3c**, and **3a**. We used catalyst **2b** as the final optimization.

Table 2: Optimization of the reaction with photocatalysts

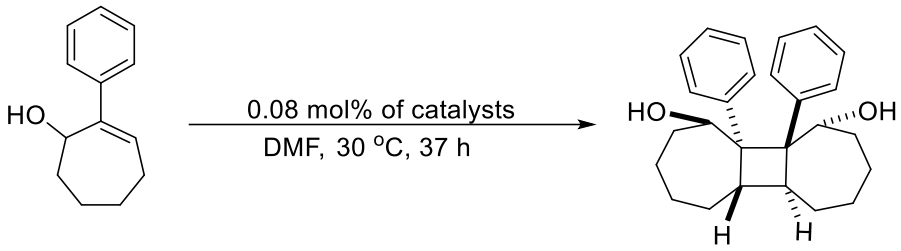

Entry	Catalyst	Conversion
1.	2a	48 %
2.	2b	55 %
3.	3c	36 %
4.	3a	23 %

The conversion was determined by NMR at 37 h.

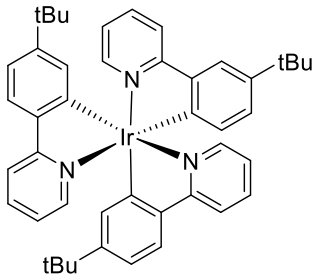

2a

Emission: 54.5 kcal/mol
Radius: 5.00 Å

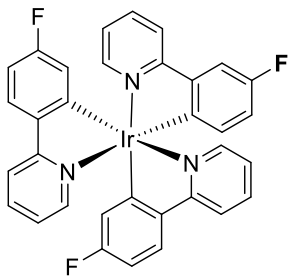

2b

Emission: 58.6 kcal/mol
Radius: 4.57 Å

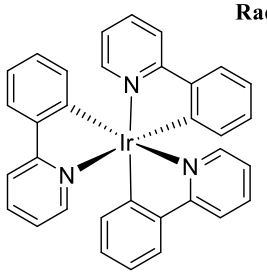

2c

Emission: 55.2 kcal/mol
Radius: 4.40 Å

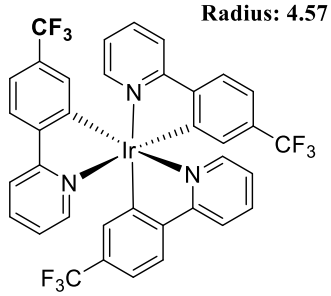

2d

Emission: 56.4 kcal/mol
Radius: 4.80 Å

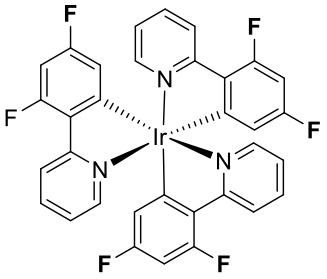

2e

Emission: 60.1 kcal/mol
Radius: 4.62 Å

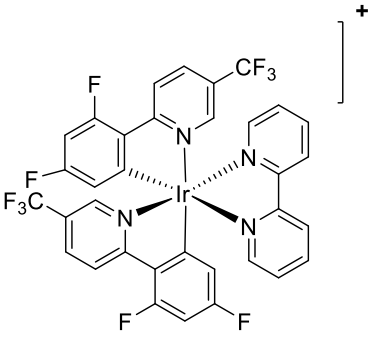

3a

Emission: 60.4 kcal/mol
Radius: n/a Å

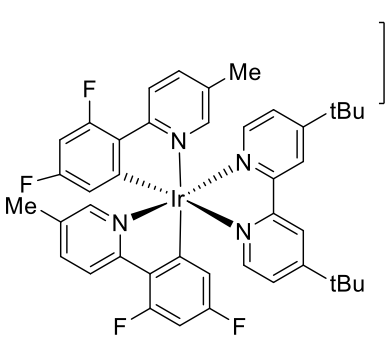

3b

Emission: 60.2 kcal/mol
Radius: n/a Å

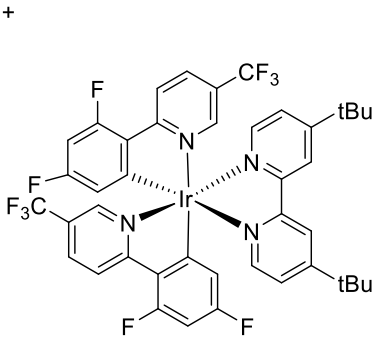

3c

Emission: 60.1 kcal/mol
Radius: 5.02 Å

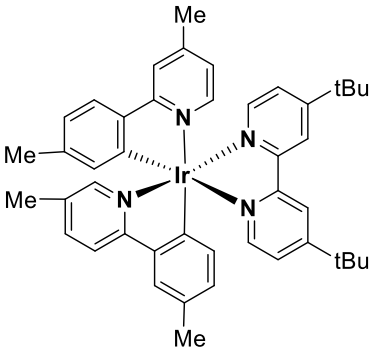

3d

Emission: 47.89 kcal/mol
Radius: n/a Å

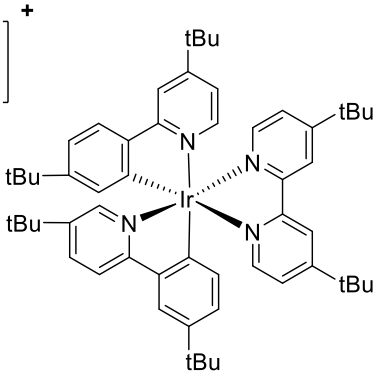

3e

Emission: 49.04 kcal/mol
Radius: n/a Å

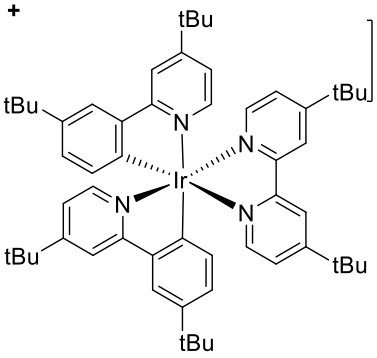

3f

Emission: 46.56 kcal/mol
Radius: n/a Å

The amount of catalyst loading also effects to the rate of the reaction. Table 3 shows the consequences of varying the catalyst loading. The reaction proceeded to the highest conversion, within 22 h, using 0.125 mol% of catalyst **2b**.

Table 3: Catalyst loading optimization.

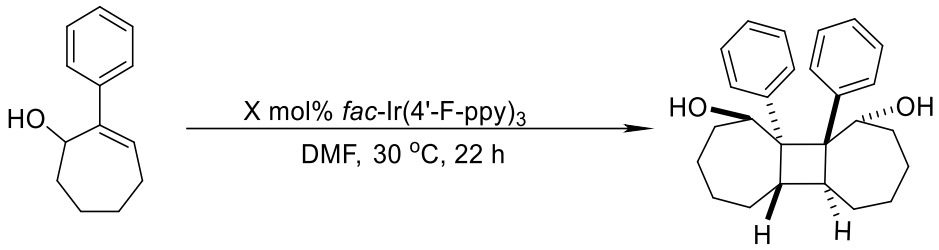

Entry	Mol%	Conversion
1.	0.125	95 %
2.	0.0625	88 %
3.	0.0315	50 %

The conversion was determined by ^{1}H NMR. The reaction run with 0.5 M concentration in 22 h.

Because the reaction is intermolecular in nature, we expected that the reaction will be accelerated at higher concentration. Increasing the concentration, increases the frequency of collisions that have the appropriate trajectory and energy to undergo bond formation. Table 4 shows the results of the dimerization reaction at several concentrations. The reaction goes faster at 0.5 M compared to 1 M and 0.25 M concentration.

Table 4: Reaction concentration optimization

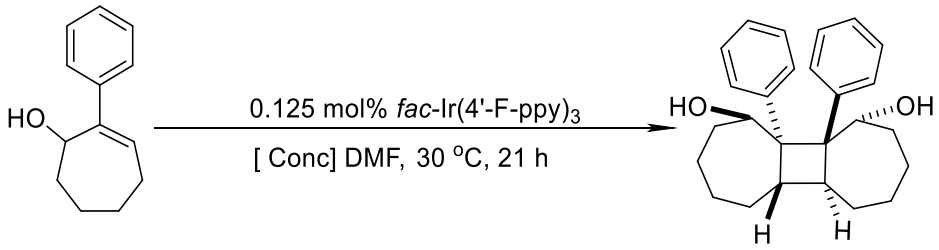

Entry	Reaction concentration (M)	Conversion	Volume	Moles of Pdt
1.	1	40 %	0.3 mL	0.12
2.	0.5	50 %	0.6 mL	0.15
3.	0.25	40.3 %	1.2 mL	0.12

The conversion was determined by NMR at 21 h.

In our previous work with cyclohexene, we observed that the reaction temperature had a significant effect on the rate. We ran the reaction at different temperatures and observed its effect on the conversion, (Table 5).The temperature profile was more muted in this case than in the 6-membered ring case. On either side of 30 °C, we observed a slight retardation of the reaction rate.

Table 5: Optimization with different temperatures

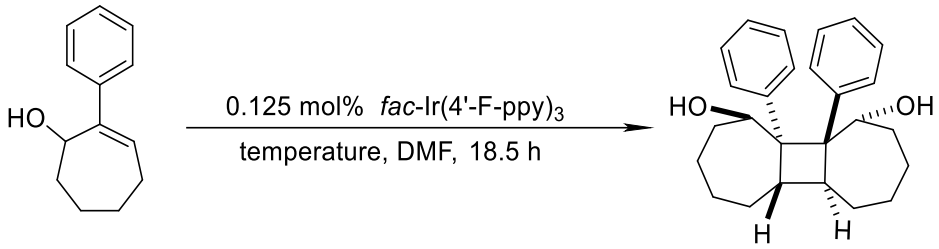

Entry	Temperature (°C)	Conversion
1.	-30	80 %
2.	0	79 %
3.	15	76 %
4.	30	96 %
5.	37.5	92 %
6.	45	72 %
7.	90	70 %

The conversion was determined by ^{1}H NMR. The reaction run with 0.5 M concentration at 18.5 h.

The final optimized conditions are 0.125 mol% of *fac*-Ir(4'-F-ppy)$_3$, 0.5 M DMF, 30 °C, blue LEDs, and degassed with argon. In Table 6, the substrate with C_6F_5 (**8a**) did not react. To try to elucidate the reason the reaction failed to produce **8a**, we ran a reaction with an ortho-chloro on

the phenyl functional group (**7a**). However, again this failed to react. While the chlorine is still an electron withdrawing group, it is significantly less electron negative than the cumulative effect of the five fluorines. These results suggest the reaction fails to produce dimer when there are substituents at the ortho position. This is confirmed by the fact that other strong electron withdrawing groups located at other positions (**2a** and**3a**) gave good yields, from 69% to 85%. The substrates with weak electron withdrawing groups (**1a** and **4a**) were isolated in good yields 74 % and 82 %. The substrate with a neutral functional group (**5a**) gave 68% yield. The lower yield, in this case, may have been due to a competitive decomposition pathway of the starting material. The electron donating functional group (**6a**) gave zero percent yield of the desired product, this due to the effect of strong electron donating functional group, which made the starting material more prone to decomposition. The di-ester (**9a**) gave very high percent yield 84 % and indicates that the alcohol proton is not needed for the high diastereo-induction. Furthermore, the incorporation of a *N*-tosyl group into the ring shows that the seven membered ring may be comprised of more than just methylenes(**10a**,71 % yield).

Table 6: Final product and yield

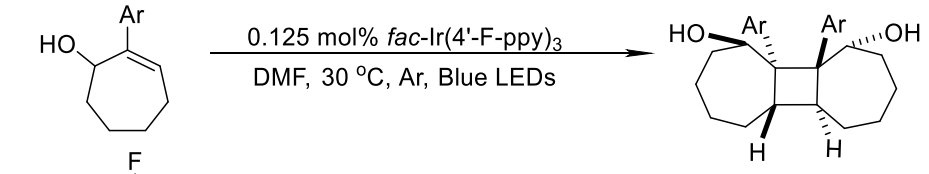

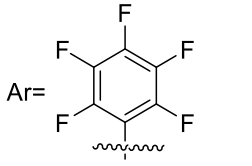

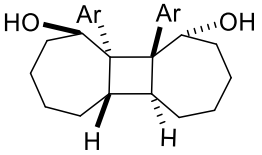

N/R
8a WT-2191

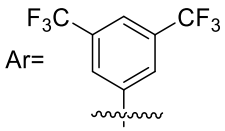

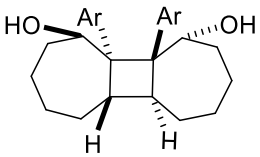

69 %
2a WT-2196

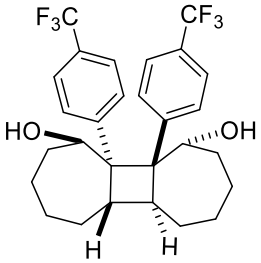

57 %
3a WT-2199

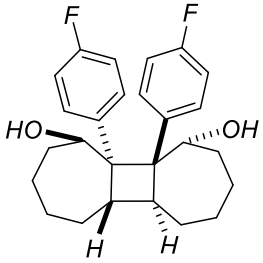

55 %
1a WT-2192
None Racemic
58%

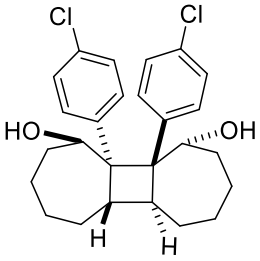

74 %
4a WT-2197

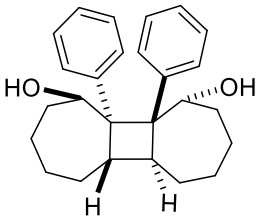

68 %
5a WT-2193

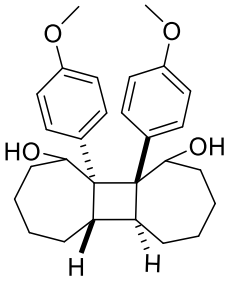

0%
6a WT-2198

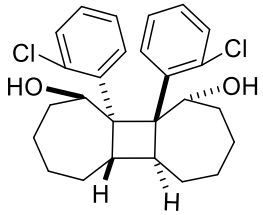

N/R
7a WT-2217

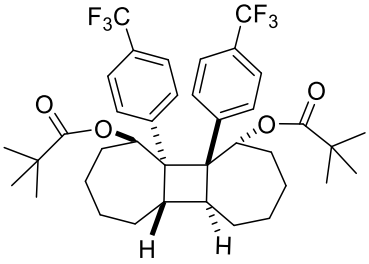

84 %
9a KS

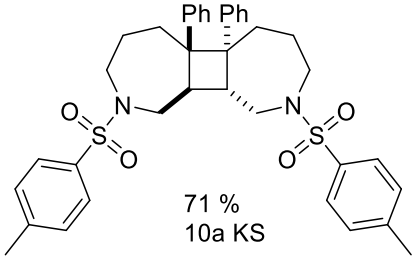

71 %
10a KS

III. CONCLUSION

We developed a new method to generate *trans*-cyclohexene utilizing blue LEDs, which provides access to novel cyclohexenol dimers, which could be used to develop a new type of chiral ligand. This shows the usefulness of the photocatalysisin the synthesis of strained alkenes like cyclohexene or cycloheptene whose strain can then be used to facilitate subsequent reactions.

IV. REFERENCE:

(1) Inoue, Y; Ueoka, T; Kuroda, T; Hakushi, T. J. Chem. Soc. Perkin Trans, 2 1983, 983 and references cited therein.

(2) Al-Majid, A. M. ;Barakat, A; Mabkhot, Y. N; Islam, M. S. . I. J. Mol. Scien. 2012,*13*(3), 2727–2743.

(3) Singh, A.; Teegardin, K.; Kelly, M.; Prasad, K. S.; Krishnan, S.; Weaver, J. D. J. Org. Chem. 2015, 776, 51.

(4) Friese, A.; Hell-Momeni, K.; Zündorf, I.; Winckler, T.; Dingermann, T.; Dannhardt, G. J. Med. Chem. 2002, 45, 1535.

(5) Singh, A; Fennell, C. J; Weaver, J. D. Chem. Sci. 2016

(6) Arnaud. V; Andres. C. Adv. Synth. Catal. 2006, 348, 2363-2370

V. SUPPORTIVE INFORMATION

Section 1: General Experimental

All reagents were obtained from commercial suppliers (Aldrich, Oakwood chemicals, and VWR) and used without further purification unless otherwise noted. Acetonitrile (CH_3CN) was dried using molecular sieves. Photocatalyst 2b was synthesized by using our previous method.[16] Reactions were monitored by thin layer chromatography (TLC), obtained from sorbent technology Silica XHL TLC Plates, w/UV254, glass backed, 250 μm, and were visualized with ultraviolet light, potassium permanganate stain. Reaction progress was occasionally monitored GC-MS (QP 2010S, Shimadzu equipped with auto sampler).

Photo catalytic reactions were set up in a light bath which is described below. Strips of blue LEDs,(18 LED's/ft) were purchased from Solid Apollo and were wrapped around on the walls of glass crystallization dish and secured with masking tape and then wrapped with aluminum foil. A lid which rest on the top was fashioned from cardboard and holes were made such that reaction tubes (12 X 75 mm cultural borosilicate tube) were held firmly in the cardboard lid which was placed on the top of bath. Water was added to the bath such that the tubes were submerged in the water which was maintained at 30 ^oC with the aid of a sand bath connected to a thermostat.

Flash chromatography was carried out with Merck 60 Å, mesh 230-400 silica gel. NMR spectra were obtained on 400 MHz Bruker Avance III spectrometer. ^{1}H and ^{13}C NMR chemical shifts are reported in ppm relative to the residual protio solvent peak (^{1}H, ^{13}C). IR spectra were recorded on Perkin Elmer 2000 FT-IR..Melting points were determined on Mel-Temp apparatus and reported uncorrected. Molecular weight of the molecules was carried out by Agilent 6850 Series GC-MS system.

Section 2: Synthesize substrates

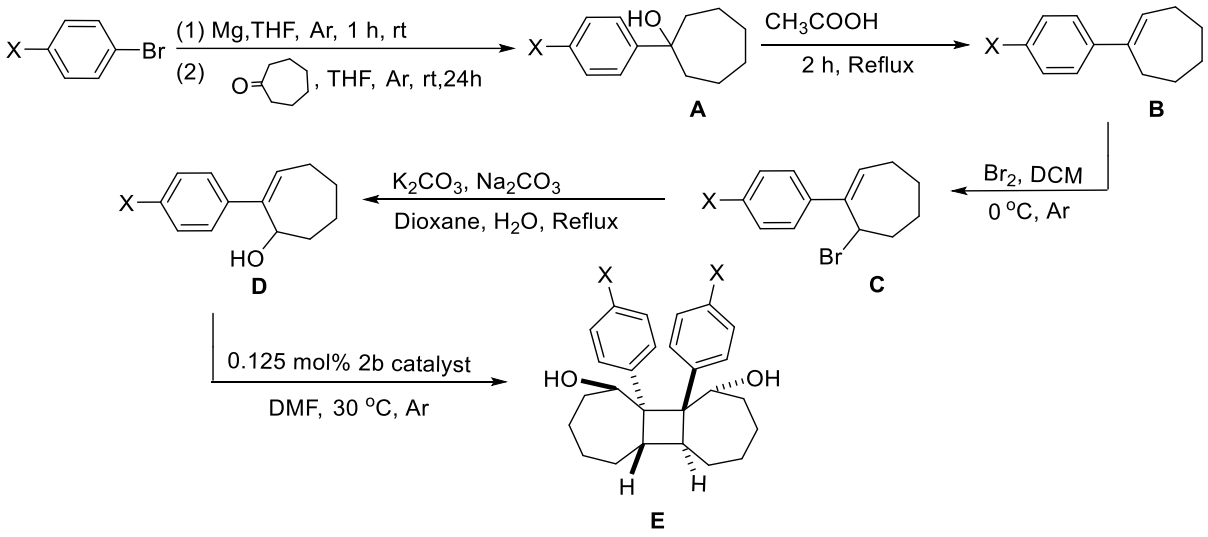

Table 1: Summary of various substrates A with percent yields.

S.No	X	% Yield of A	% Yield of B	% Yield of C	% Yield of D
1	Methoxy	70	92	100	17
2	Hydrogen	88	89	82	44
3	Fluoride	37	93	100	21
4	Chloride	77	79	83	62
5	Trifluoromethyl	94	63	98	53

General Procedure A[3].

To an oven dried round bottom flash equipped with magnetic stir bar was added magnesium metal (107.14mmol, 1.2equiv), a pinch of I_2, THF (10equiv) then 1-bromo-4-methoxybenzene (98.21 mmol, 1.1equiv) was added portion-wise. The mixture was stirred at room temperature for 1 hour. After the complete consumption of 1-bromo-4-methoxybenzene, the reaction mixture was cooled to 0^{o}C, and cyclohexanone(89.29mmol, 1 equiv) was added drop-wise to the mixture. The reaction mixture heated at 55 ^{o}C until goes to completion in 5 h. After the completion, the mixture was quenched by NH_4Cl (50 mL) and extracted with EtOAc (3x50 mL). The combined organic layer was washed with 0.1 M NaOH (40 mL). The organic layer was separated and dried with $MgSO_4$, and concentrated to obtain the crude product.

General Procedure B[4].

To an oven dried round bottom flash equipped with magnetic stir bar was added A (1 equiv), CH_3CCOH (10equiv). The mixture was heated to 118^{o}C. The mixture was stirred at room temperature for 12 hours. After the completion, the mixture was quenched by saturated $NaHCO_3$ (1 mL) and extract with DCM (2x10 mL). The combined organic layer was washed with distilled water (10 mL). The organic layer was separated and dried with $MgSO_4$, and concentrated to obtain the crude product that was purified by normal phase chromatography. Normal phase chromatography was performed using Hexane: Ethyl acetate over 0-70 volume columns using flow rated from 35-80 mL/min on Redisep column of 40-80 g with product detection at 254 and 288 nm. The product is dilute in 100 % hexane.

General Procedure C

To an oven dried round bottom flash equipped with magnetic stir bar was added compound B (1 g, 1 equiv), Dichloromethane (5 ml). The mixture was stirred at 0 ^{o}C, then added Br_2 (1 equiv) portion-wise. After the completion, the mixture was dried with $MgSO_4$, and concentrated to obtain the brown liquid product.

General procedure D

To a 500ml round bottom flash equipped with magnetic stir bar was added compound C (1 equiv), K_2CO_3 (1.1 equiv), Na_2CO_3 (2.5 equiv), Dioxane (100 ml), water (100 ml). The mixture was reflux overnight at 108^{o}C. After the completion, the mixture was cooled to room temperature and extracted with ethyl acetate (2x10 mL). The organic layer was separated and dried with $MgSO_4$, and concentrated to obtain the crude product that was purified by normal phase chromatography. Normal phase chromatography was performed using Hexane: Ethyl acetate over 0-70 volume columns using flow rated from 35-80 mL/min on Redisep column of 40 g with product detection at 254 and 288 nm. The product is dilute in 5-10 % ethyl acetate.

General procedure D

A 20 mL disposable scintillation vial was charged with compound D (1 equiv), 0.125 mol% of stock solution of 2b catalyst, *fac*-Ir(4'-F-ppy)$_3$(2 mg, 0.0028 mmol 2b catalyst, 2.26 mL dimethylformamide).The mixture was added into NMR tubes. A sealed glass capillary containing C_6D_6 was added to each NMR tube. The NMR tube was capped with a septum (Ace glass, part no. 9096-25) and secured with parafilm. The reaction was degassed via Ar bubbling for 10 min at room temperature, then placed in the light bath (*vide supra*) such that the filled portion of the tube was submerged under water. The reaction was monitored periodically by ^{1}H NMR. After the

complete consumption of starting material, the reaction was worked up with water and extracted with hexane (4x10 ml). The organic layer was separated and dried with $MgSO_4$, and concentrated to obtain the crude product that was purified by normal phase chromatography. Normal phase chromatography was performed using Hexane: Ethyl acetate over 0-70 volume columns using flow rated from 35-80 mL/min on Redisep column of 4 g with product detection at 254 and 288 nm. The product is dilute in 1-5 % ethyl acetate.

1a (1R,5aS,5bS,10R,10aS,10bS)-10a,10b-bis(4-fluorophenyl)tetradecahydrocyclobuta[1,2:3,4]di[7]annulene-1,10-diol

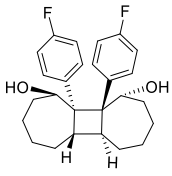

General procedure **1a** was followed using 2-(4-fluorophenyl)cyclohept-2-en-1-ol(100.00 mg, 0.48 mmol, 1.0 equiv), 0.48 mL of stock solution of 2b catalyst, *fac*-Ir(4'-F-ppy)$_3$ (2 mg, 0.0028 mmol 2b catalyst, 2.26 mL DMF), and the reaction concentration at 0.5 M was used to afford **1a** in 82% yield (82 mg) as white solid. ^{1}H NMR (400 MHz, $CDCl_3$) δ 7.86 – 7.75 (m, 1H), 7.50 – 7.37 (m, 1H), 7.22 – 7.07 (m, 2H), 4.07 (s, 1H), 3.58 – 0.24 (m, 2H), 2.13 – 1.91 (m, 2H), 1.88 – 1.74 (m, 1H), 1.69 – 1.21 (m, 5H). ^{19}F NMR (376 MHz, Chloroform-*d*) δ -114.95 (hept, *J* = 8.5, 4.3 Hz). ^{13}C NMR (101 MHz, $CDCl_3$) δ 162.30, 159.84, 140.35 (d, *J* = 3.9 Hz), 130.02 (d, *J* = 7.0 Hz), 128.34 (d, *J* = 7.3 Hz), 116.10 (dd, *J* = 82.6, 20.6 Hz), 74.17, 61.39, 36.33, 34.36, 28.05, 26.73, 20.28.FT-IR cm^{-1}3604, 2934, 1230, 845. Melting point 185-190^{o}C.

2a (1R,5aS,5bS,10R,10aS,10bS)-10a,10b-bis(3,5-bis(trifluoromethyl)phenyl)tetradecahydrocyclobuta[1,2:3,4]di[7]annulene-1,10-diol

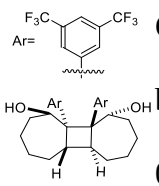

General procedure **2a** was followed using 2-(3,5-bis(trifluoromethyl)phenyl)cyclohept-2-en-1-ol (100.00 mg, 0.31mmol, 1.0 equiv), 0.174 mL of stock solution of 2b catalyst,*fac*-Ir(4'-F-ppy)$_3$ (2 mg, 0.0028 mmol 2b

catalyst, 2.26 mL DMF), and the reaction concentration at 0.5 M was used to afford **2a** in 69% yield (69mg) as white solid. The crude material was purified by flash chromatography using hexane: ethyl acetate on a 4 g silica column with product eluting at 5%.^{1}H NMR (400 MHz, $CDCl_3$) δ 8.25 (s, 1H), 7.76 (d, *J* = 10.0 Hz, 2H), 4.06 (s, 1H), 3.52 (q, *J* = 13.0, 9.9 Hz, 1H), 2.10 (d, *J* = 9.1 Hz, 2H), 1.94 – 1.82 (m, 1H), 1.69 – 1.47 (m, 2H), 1.41 – 1.23 (m, 3H).^{19}F NMR (376 MHz, $CDCl_3$) δ -62.72, -62.86.^{13}C NMR (101 MHz, $CDCl_3$) δ 147.67, 131.78 – 131.15 (m), 132.26 – 128.51 (m), 129.30, 126.23, 124.78 (d, *J* = 10.7 Hz), 122.07 (d, *J* = 10.6 Hz), 120.50 – 119.37 (m), 72.69, 61.76, 36.27, 35.54, 27.85, 26.40, 19.96.FT-IR cm^{-1} 3475, 2931, 1127, 891. Melting point 220-225^{o}C.

3a (1R,5aS,5bS,10R,10aS,10bS)-10a,10b-bis(4-(trifluoromethyl)phenyl)tetradecahydrocyclobuta[1,2:3,4]di[7]annulene-1,10-diol

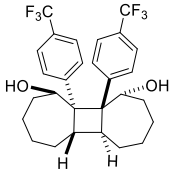

General procedure **3a** was followed using 2-(4-(trifluoromethyl)phenyl)cyclohept-2-en-1-ol(100.00 mg, 0.39 mmol, 1.0 equiv), 0.357 mL of stock solution of 2b catalyst, fac-Ir(4'-F-ppy)$_3$(2 mg, 0.0028 mmol 2b catalyst, 2.26 mL DMF), and the reaction concentration at 0.5 M was used to afford **3a** in 85% yield (85 mg) as white solid^{1}H NMR (400 MHz, $CDCl_3$) δ 7.99 (d, *J* = 8.2 Hz, 1H), 7.69 (t, 2H), 7.59 (d, *J* = 8.3 Hz, 1H), 4.13 (s, 1H), 3.54 (t, *J* = 6.3 Hz, 1H), 2.13 – 1.99 (m, 2H), 1.88 – 1.78 (m, 1H), 1.68 – 1.48 (m, 2H), 1.46 – 1.36 (m, 2H), 1.36 – 1.28 (m, 1H). ^{19}F NMR (376 MHz, $CDCl_3$) δ -62.57.^{13}C NMR (101 MHz, $CDCl_3$) δ 149.18, 129.10, 128.77 (q, *J* = 33.0 Hz), 127.04, 125.93 (q, *J* = 3.7 Hz), 125.72 (q, *J* = 3.7 Hz), 123.86 (q, *J* = 272.0 Hz), 73.74, 62.75, 36.42, 34.64, 28.02, 26.70, 20.12.FT-IR cm^{-1} 3604, 2934, 1230, 845. Melting point 190-195^{o}C.

4a (1R,5aS,5bS,10R,10aS,10bS)-10a,10b-bis(4-chlorophenyl)tetradecahydrocyclobuta[1,2:3,4]di[7]annulene-1,10-diol

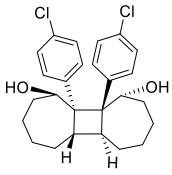

General procedure **4a** was followed using2-(4-chlorophenyl)cyclohept-2-en-1-ol(100.00 mg, 0.45 mmol, 1.0 equiv), 0.45 mL of stock solution of 2b catalyst,*fac*-Ir(4'-F-ppy)$_3$(2 mg, 0.0028 mmol 2b catalyst, 2.26 mL DMF), and the reaction concentration at 0.5 M was used to afford **4a** in 74% yield (74 mg) as white solid. ^{1}H NMR (400 MHz, $CDCl_3$) δ 7.77 (dd, *J* = 8.5, 2.2 Hz, 1H), 7.47 – 7.34 (m, 3H), 4.06 (p, *J* = 2.2 Hz, 1H), 3.48 (p, *J* = 6.4, 3.2 Hz, 1H), 2.17 – 1.89 (m, 2H), 1.94 – 1.68 (m, 1H), 1.68 – 1.13 (m, 5H).^{13}C NMR (101 MHz, $CDCl_3$) δ 143.21, 132.46, 129.96, 129.50, 128.99, 128.16, 73.92, 61.85, 36.33, 34.50, 28.03, 26.72, 20.24.FT-IR cm^{-1} 3399, 2920, 1098, 749. Melting point 190-195ºC.

5a (1R,5aS,5bS,10R,10aS,10bS)-10a,10b-diphenyltetradecahydrocyclobuta[1,2:3,4]di[7]annulene-1,10-diol

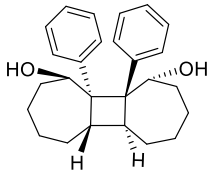

General procedure **1f** was followed using 2-phenylcyclohept-2-en-1-ol (100.00 mg, 0.53 mmol, 1.0 equiv), 0.53 mL of stock solution of 2b catalyst, fac-Ir(4'-F-ppy)$_3$(2 mg, 0.0028 mmol 2b catalyst, 2.26 mL DMF), and the reaction concentration at 0.5 M was used to afford **1f** in 68% yield (68 mg) as white solid. ^{1}H NMR (400 MHz, $CDCl_3$) δ 7.85 (d, *J* = 7.9 Hz, 1H), 7.62 – 7.37 (m, 3H), 7.31 (t, *J* = 7.3 Hz, 1H), 4.13 (s, 1H), 3.50 (p, *J* = 6.2 Hz, 1H), 2.16 – 1.94 (m, 3H), 1.79 (dt, *J* = 14.7, 7.3 Hz, 1H), 1.69 – 1.43 (m, 3H), 1.29 (dt, *J* = 12.4, 6.1 Hz, 2H). ^{13}C NMR (101 MHz, $CDCl_3$) δ 144.74, 129.37, 128.90, 128.46, 127.02, 126.52, 74.30, 62.13, 36.32, 34.38, 28.21, 26.82, 20.38.FT-IR cm^{-1} 3419, 2922, 1028, 710. Melting point 191-194ºC.

2a (1R,5aS,5bS,10R,10aS,10bS)-10a,10b-bis(3,5-bis(trifluoromethyl)phenyl)tetradecahydrocyclobuta[1,2:3,4]di[7]annulene-1,10-diol- Proton

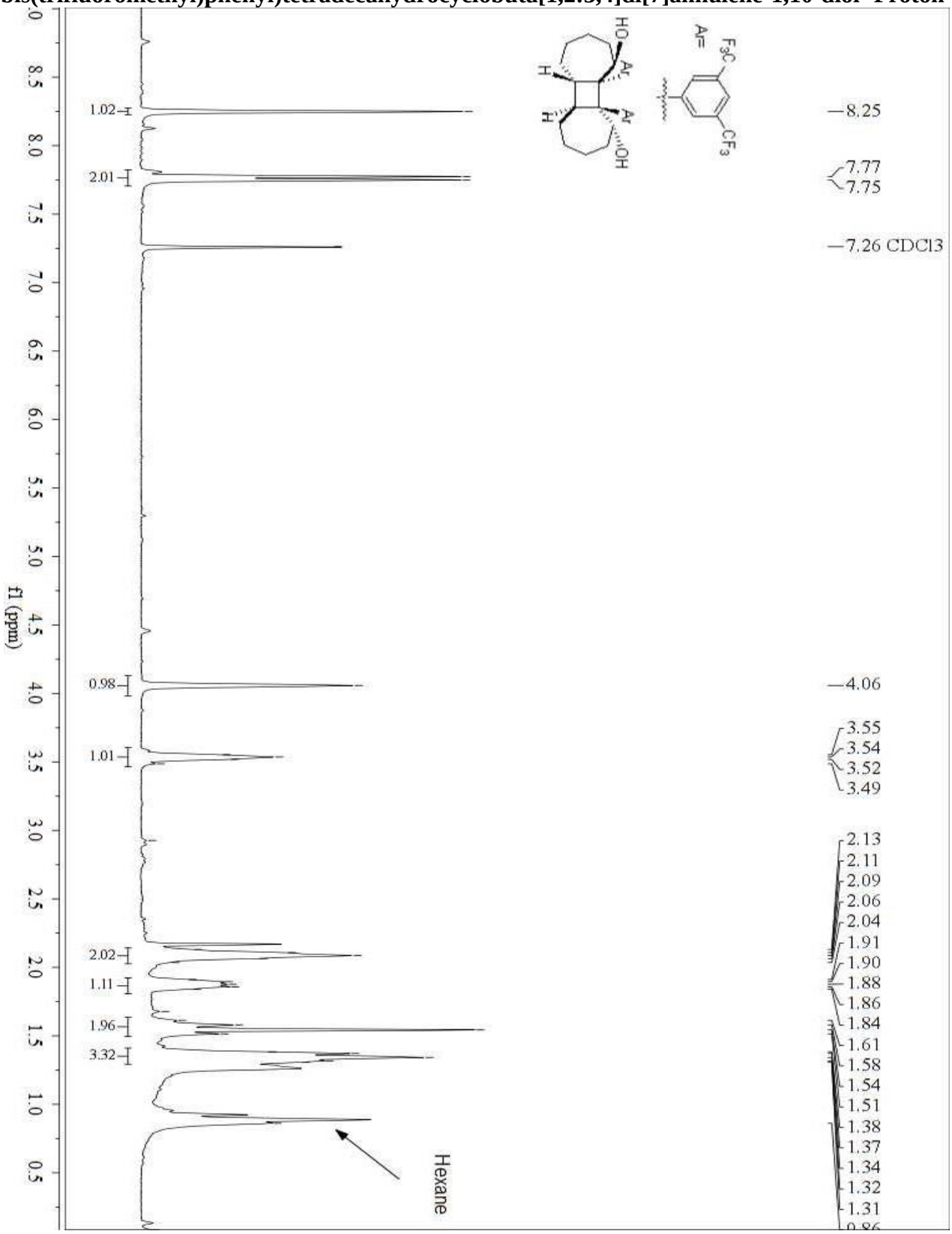

2a (1R,5aS,5bS,10R,10aS,10bS)-10a,10b-bis(3,5-bis(trifluoromethyl)phenyl)tetradecahydrocyclobuta[1,2:3,4]di[7]annulene-1,10-diol-^{19}F

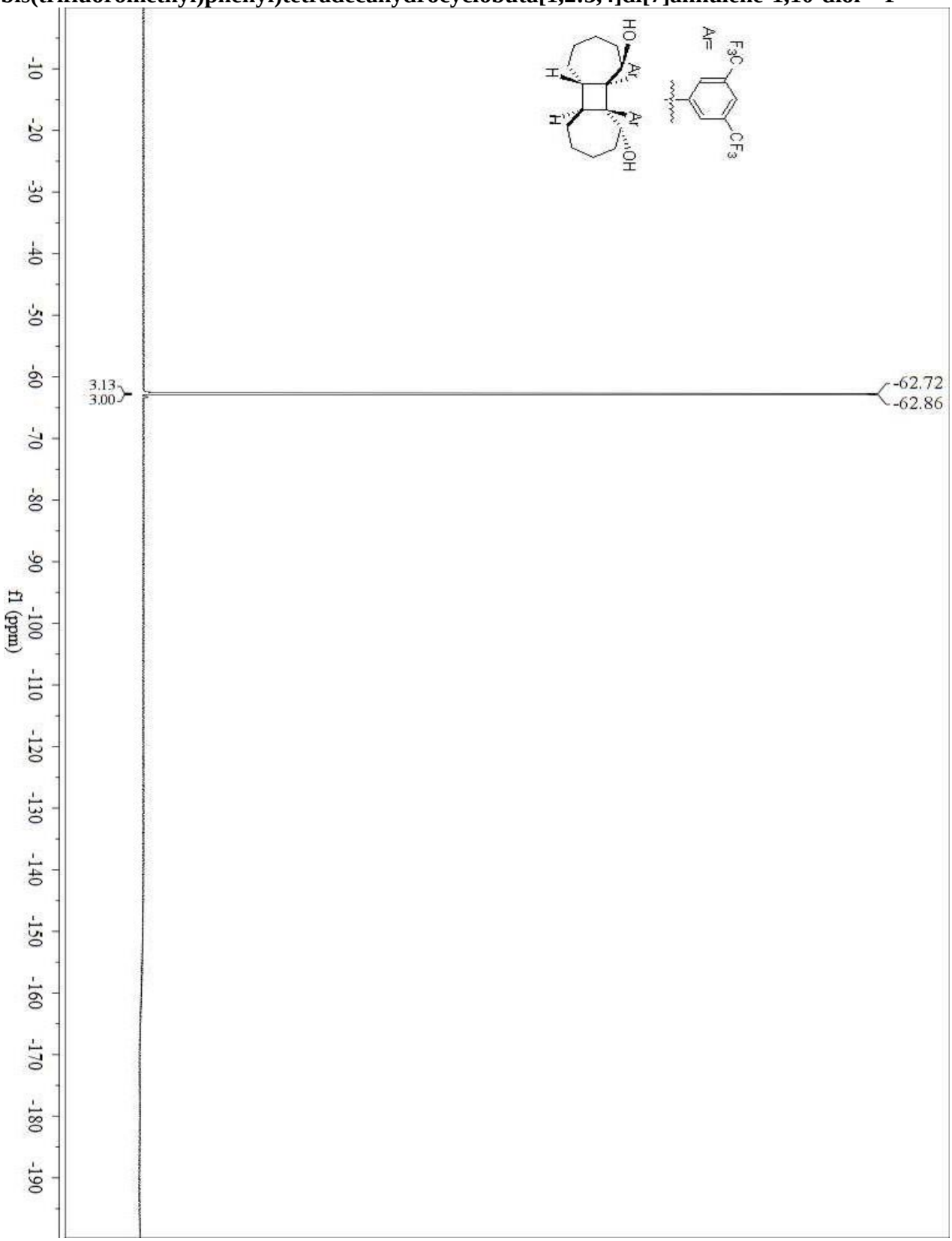

2a (1R,5aS,5bS,10R,10aS,10bS)-10a,10b-bis(3,5-bis(trifluoromethyl)phenyl)tetradecahydrocyclobuta[1,2:3,4]di[7]annulene-1,10-diol-^{13}C

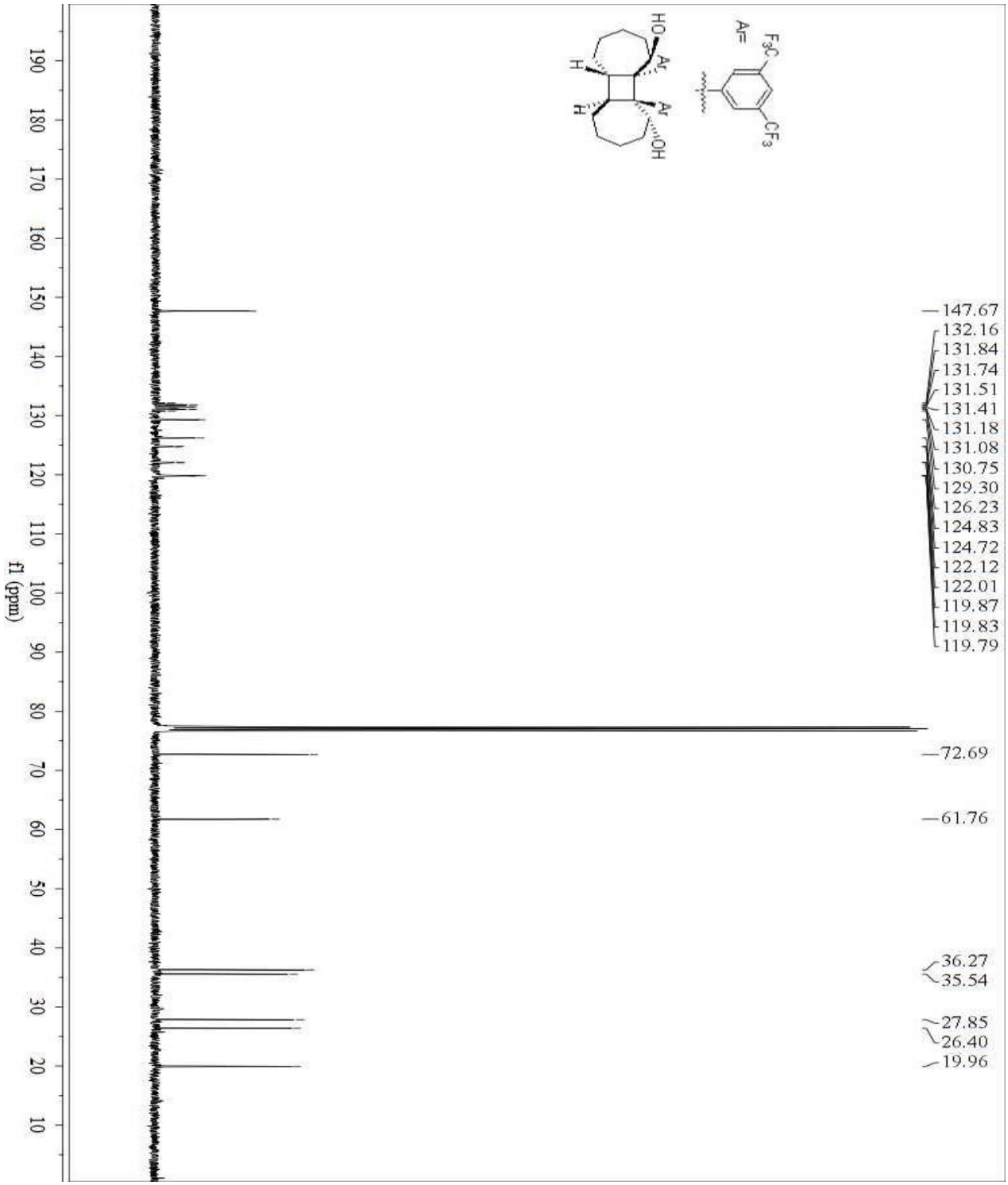

2a (1R,5aS,5bS,10R,10aS,10bS)-10a,10b-bis(3,5-bis(trifluoromethyl)phenyl)tetradecahydrocyclobuta[1,2:3,4]di[7]annulene-1,10-diol-Starting material

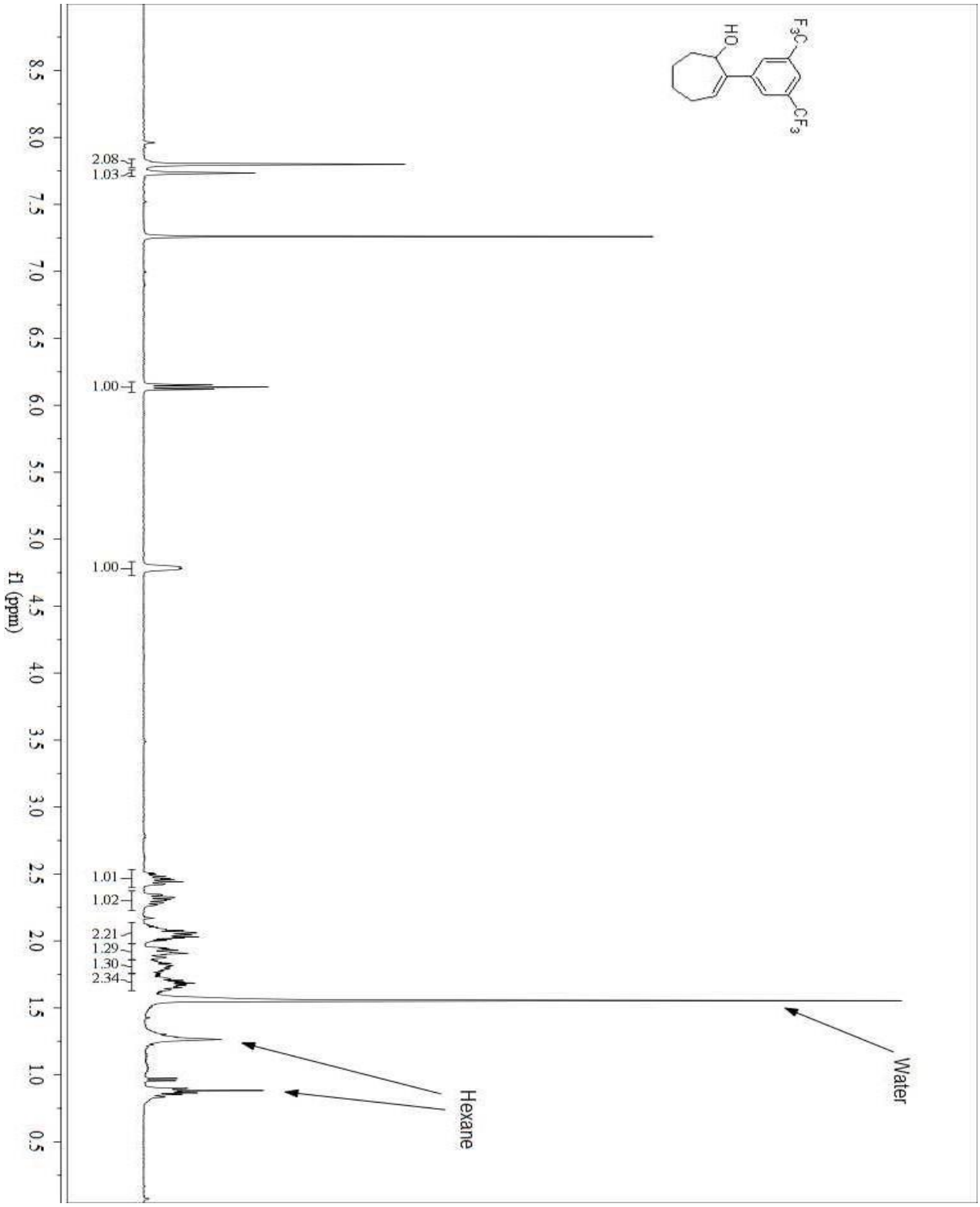

3a (1R,5aS,5bS,10R,10aS,10bS)-10a,10b-bis(4-(trifluoromethyl)phenyl)tetradecahydrocyclobuta[1,2:3,4]di[7]annulene-1,10-diol-Proton

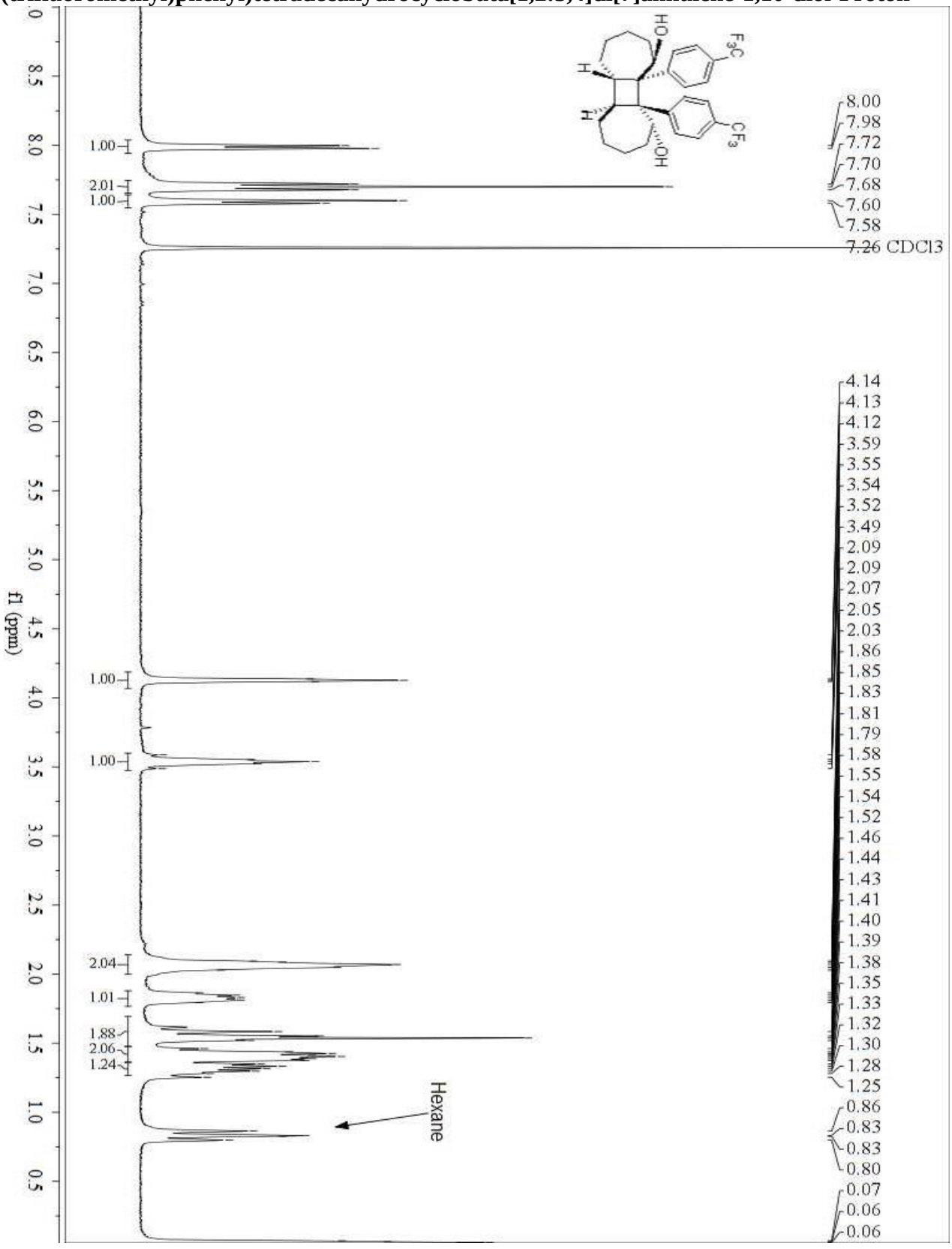

3a (1R,5aS,5bS,10R,10aS,10bS)-10a,10b-bis(4-(trifluoromethyl)phenyl)tetradecahydrocyclobuta[1,2:3,4]di[7]annulene-1,10-diol-^{19}F

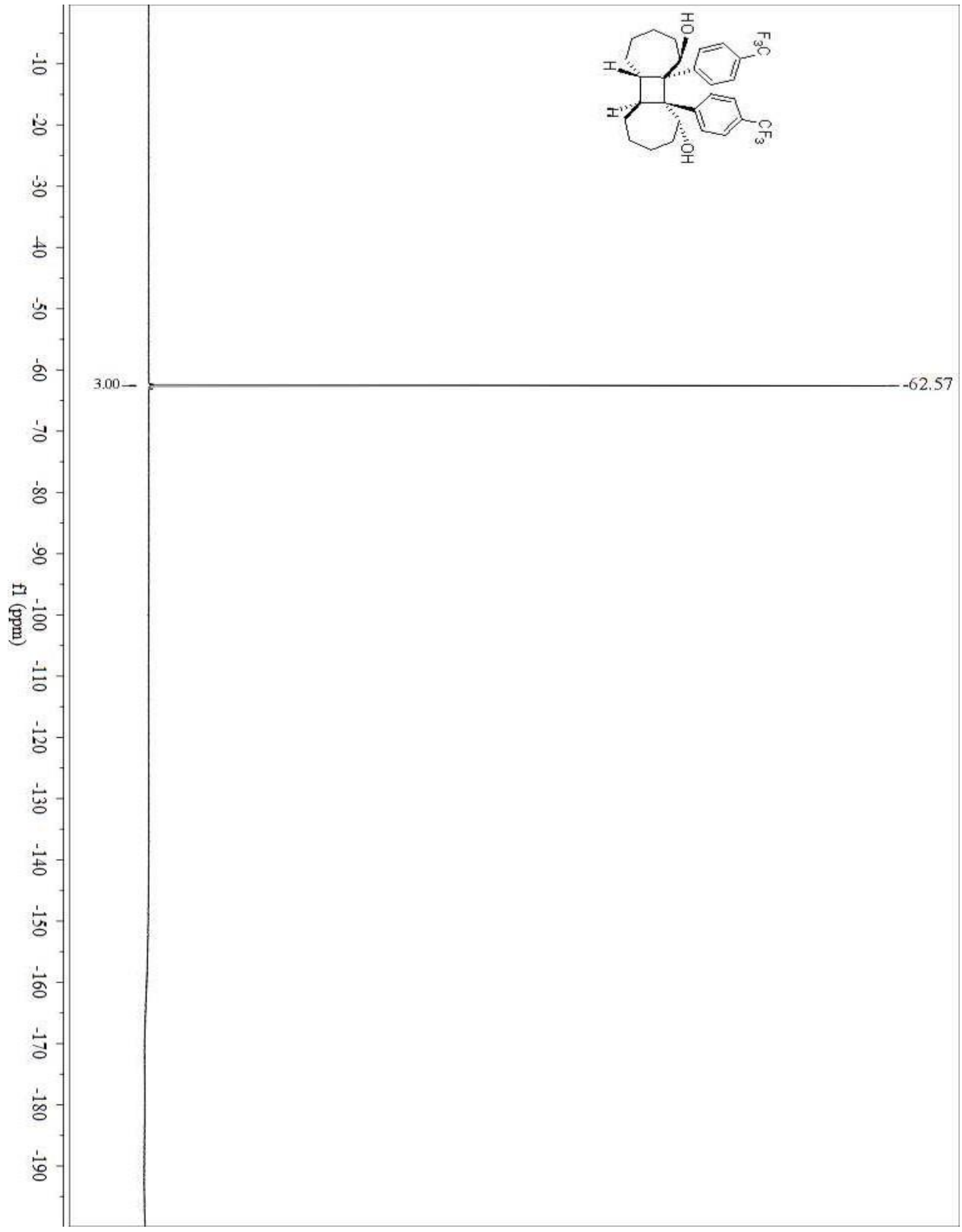

3a (1R,5aS,5bS,10R,10aS,10bS)-10a,10b-bis(4-(trifluoromethyl)phenyl)tetradecahydrocyclobuta[1,2:3,4]di[7]annulene-1,10-diol-^{13}C

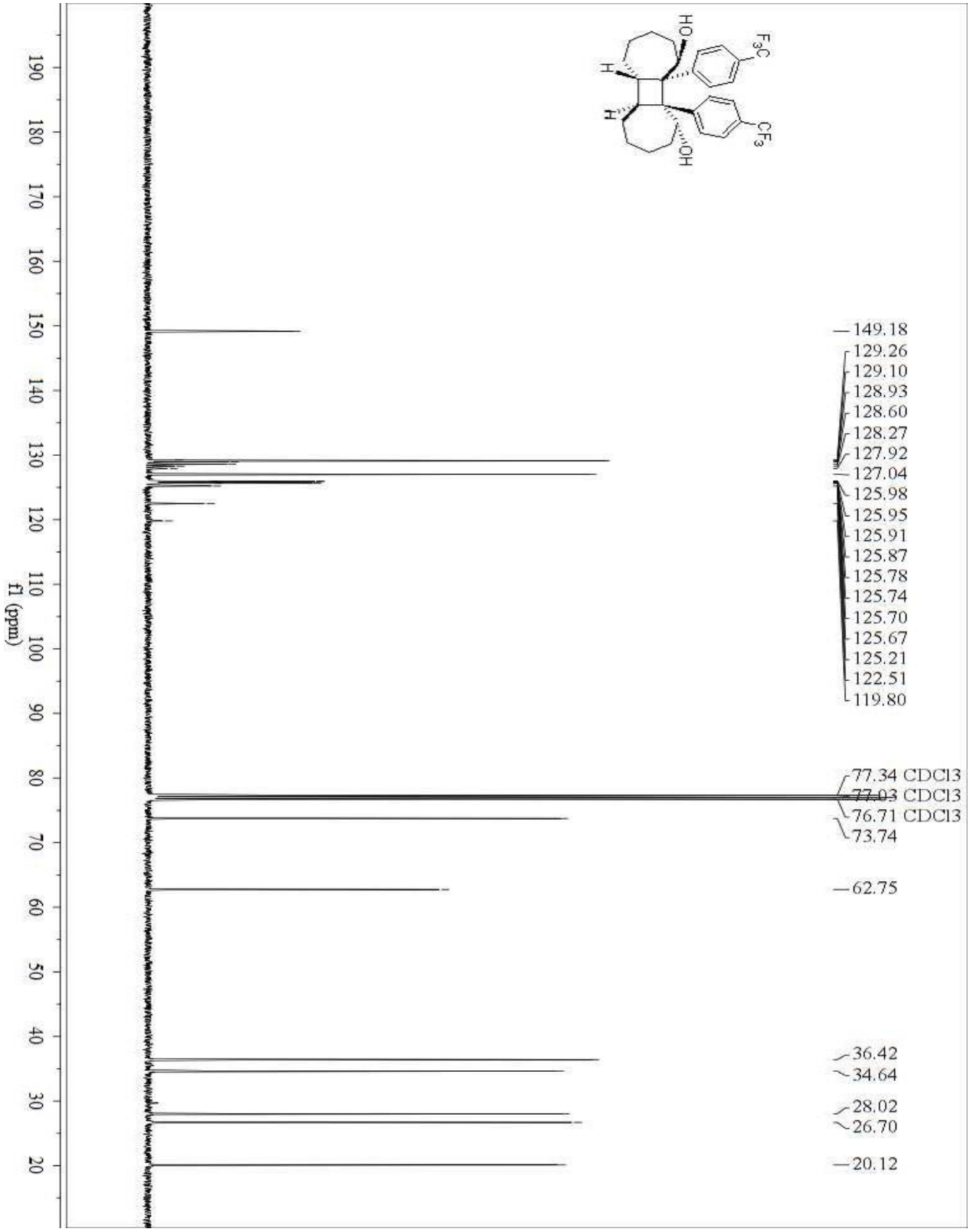

3a (1R,5aS,5bS,10R,10aS,10bS)-10a,10b-bis(4-(trifluoromethyl)phenyl)tetradecahydrocyclobuta[1,2:3,4]di[7]annulene-1,10-diol-Starting material

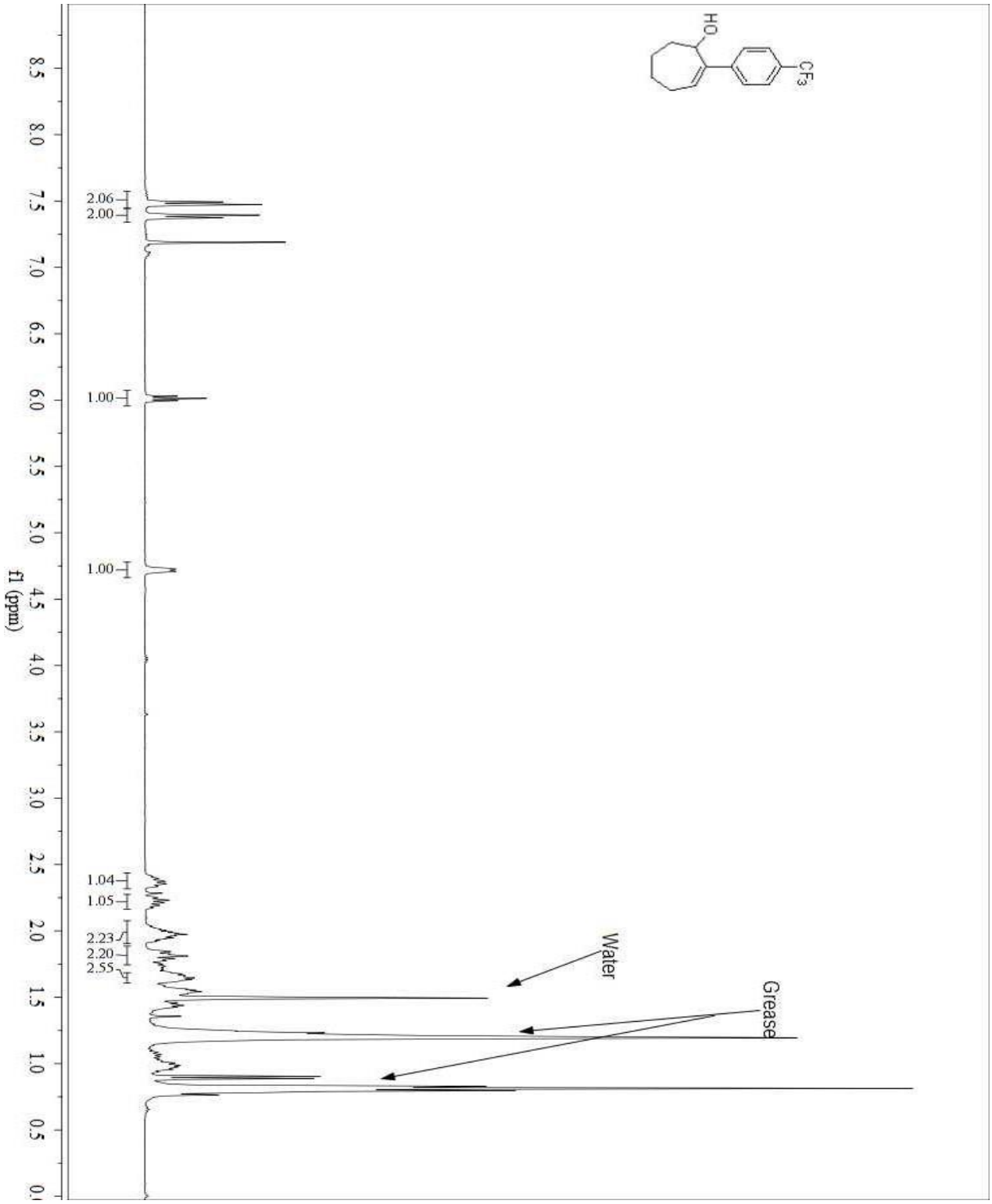

1a(1R,5aS,5bS,10R,10aS,10bS)-10a,10b-bis(4-fluorophenyl)tetradecahydrocyclobuta[1,2:3,4]di[7]annulene-1,10-diol-Proton

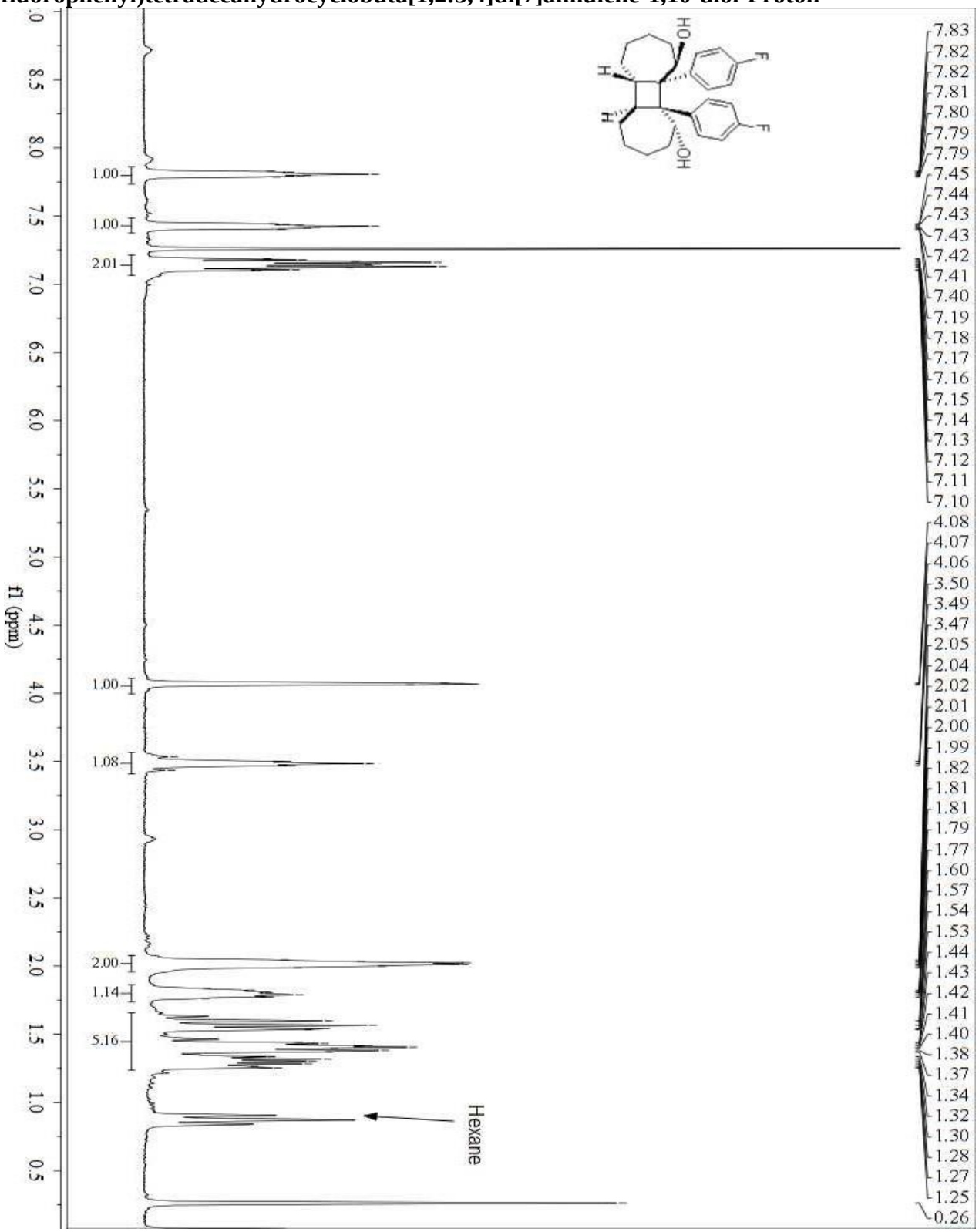

1a (1R,5aS,5bS,10R,10aS,10bS)-10a,10b-bis(4-fluorophenyl)tetradecahydrocyclobuta[1,2:3,4]di[7]annulene-1,10-diol-^{19}F

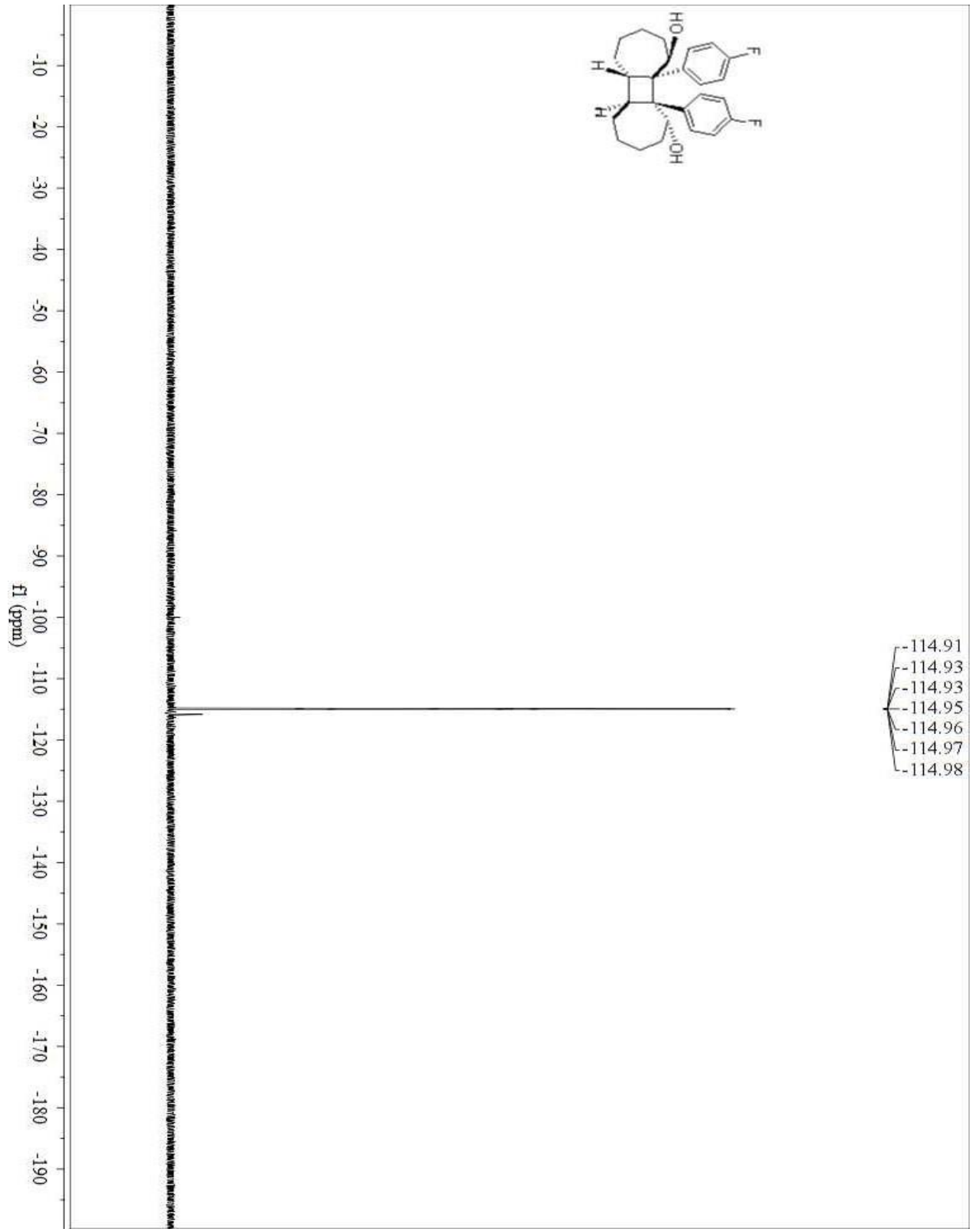

1a (1R,5aS,5bS,10R,10aS,10bS)-10a,10b-bis(4-fluorophenyl)tetradecahydrocyclobuta[1,2:3,4]di[7]annulene-1,10-diol-^{13}C

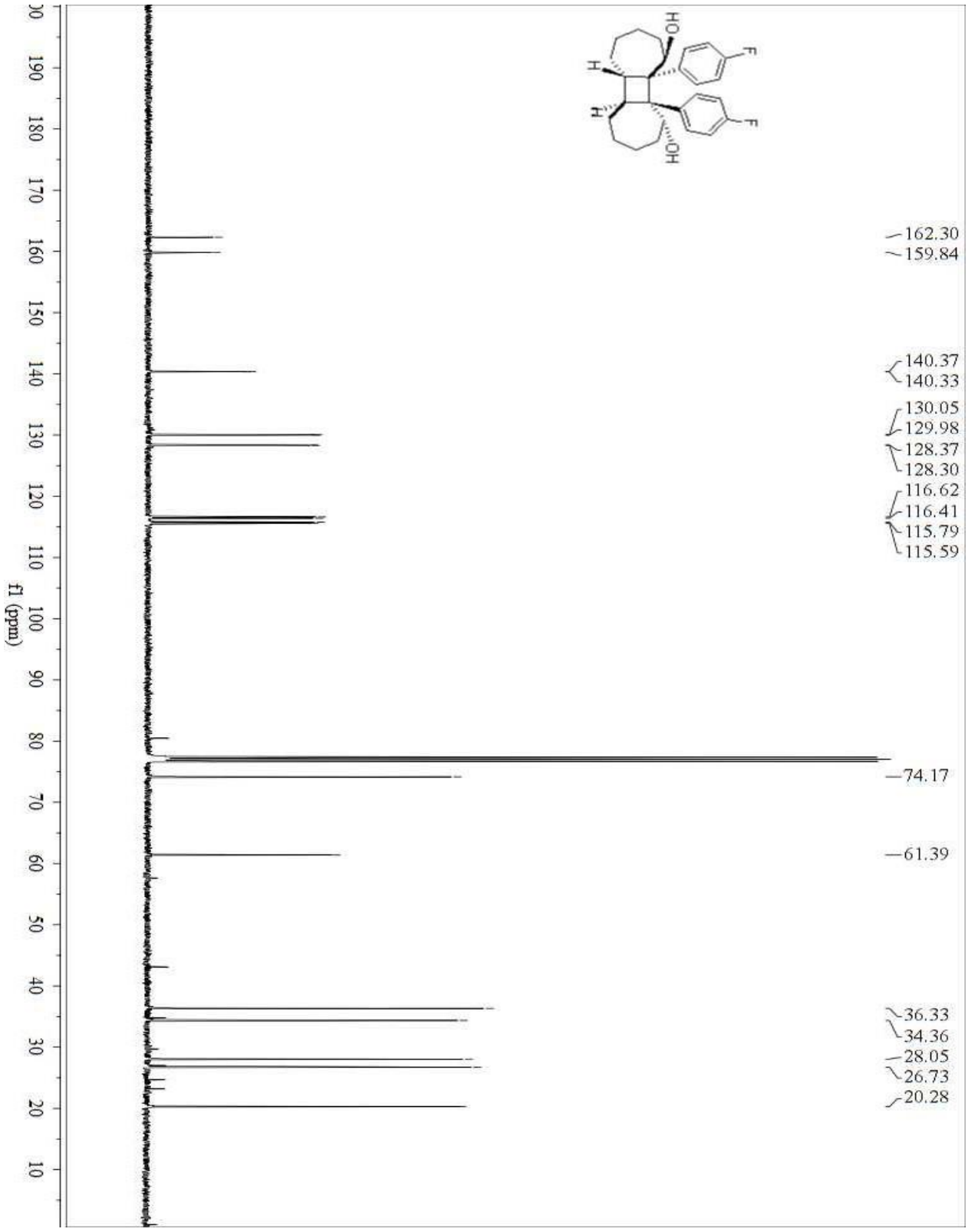

1a (1R,5aS,5bS,10R,10aS,10bS)-10a,10b-bis(4-fluorophenyl)tetradecahydrocyclobuta[1,2:3,4]di[7]annulene-1,10-diol-Starting material

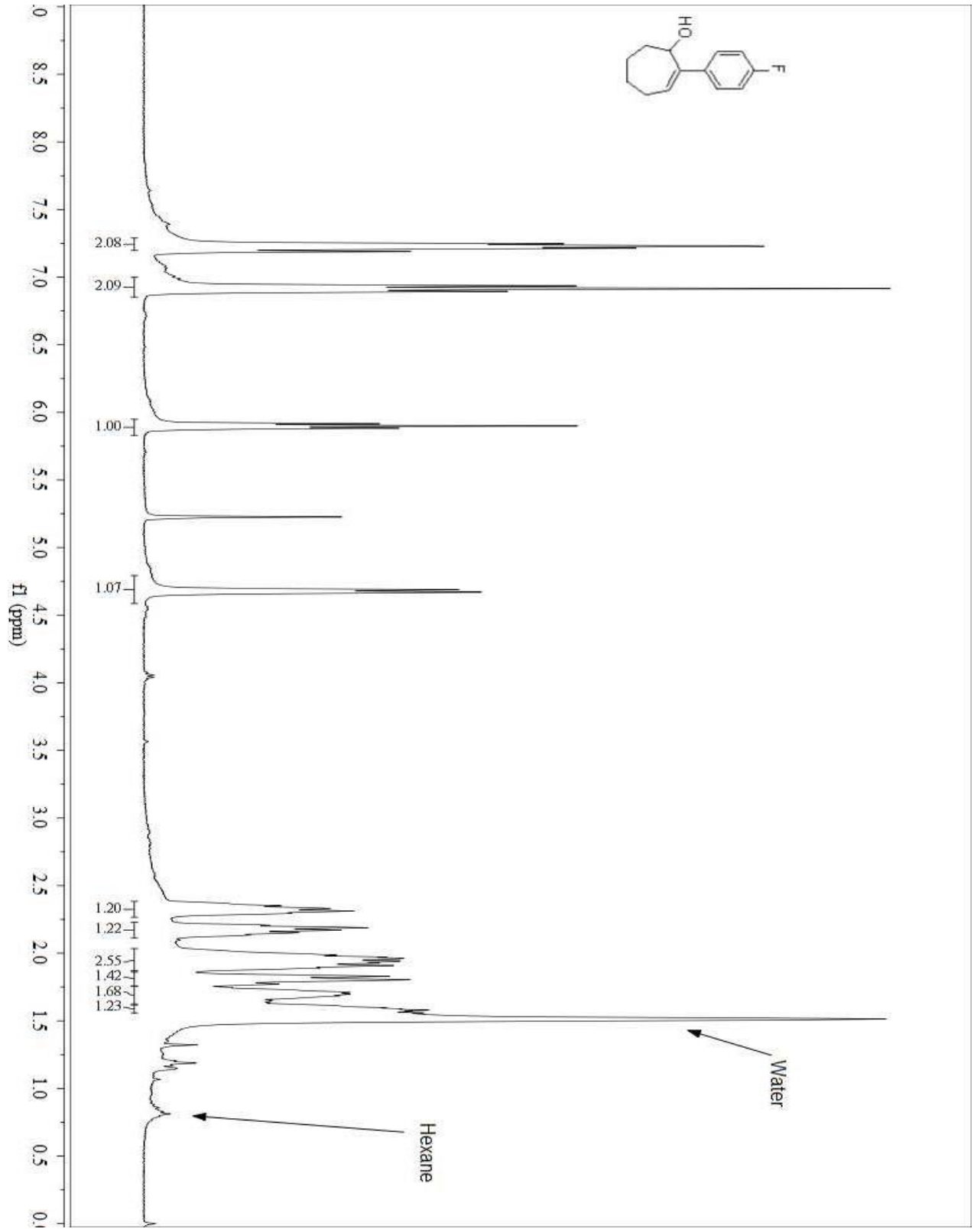

4a (1R,5aS,5bS,10R,10aS,10bS)-10a,10b-bis(4-chlorophenyl)tetradecahydrocyclobuta[1,2:3,4]di[7]annulene-1,10-diol-Proton

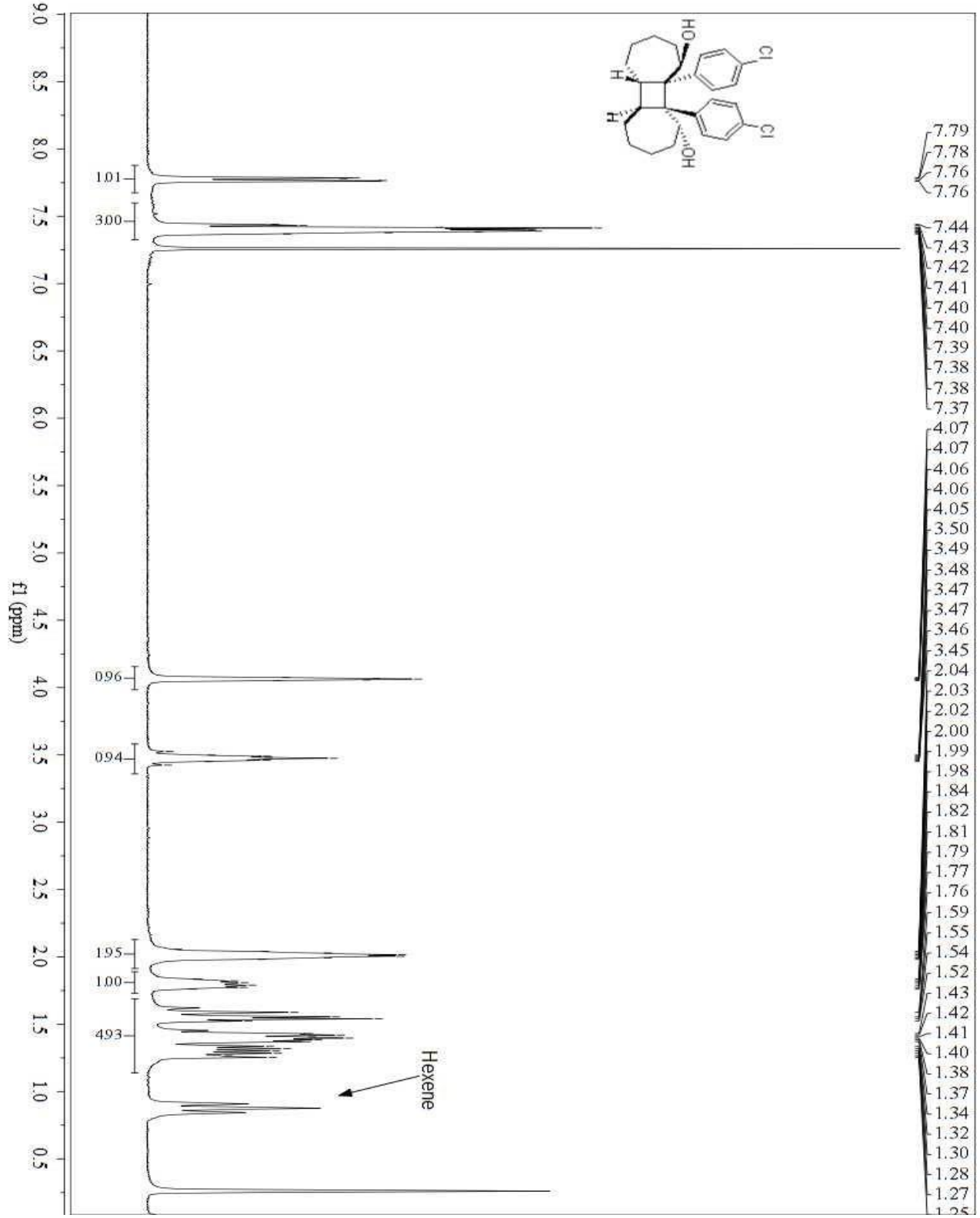

4a (1R,5aS,5bS,10R,10aS,10bS)-10a,10b-bis(4-chlorophenyl)tetradecahydrocyclobuta[1,2:3,4]di[7]annulene-1,10-diol-^{13}C

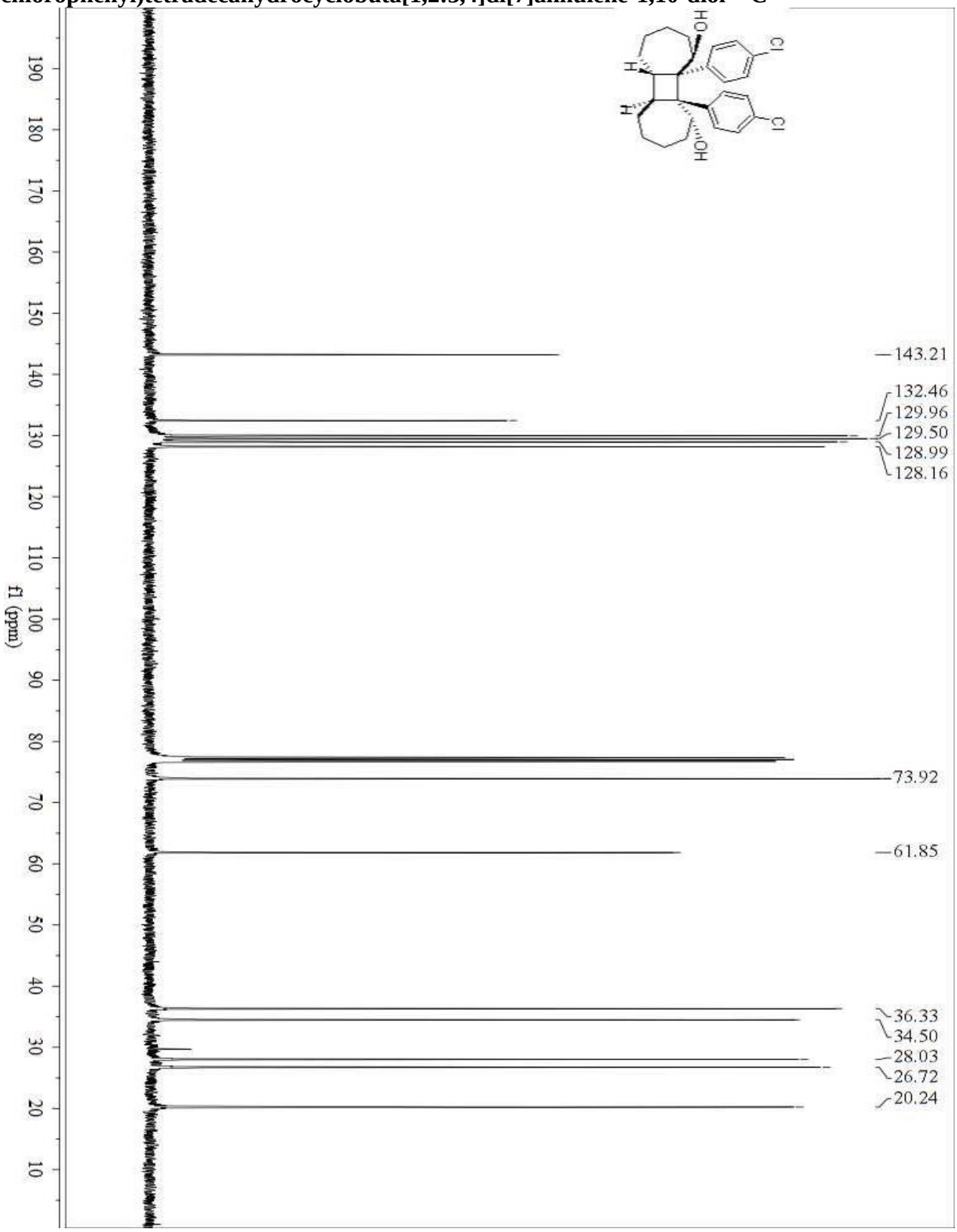

5a(1R,5aS,5bS,10R,10aS,10bS)-10a,10b-

diphenyltetradecahydrocyclobuta[1,2:3,4]di[7]annulene-1,10-diol-Proton

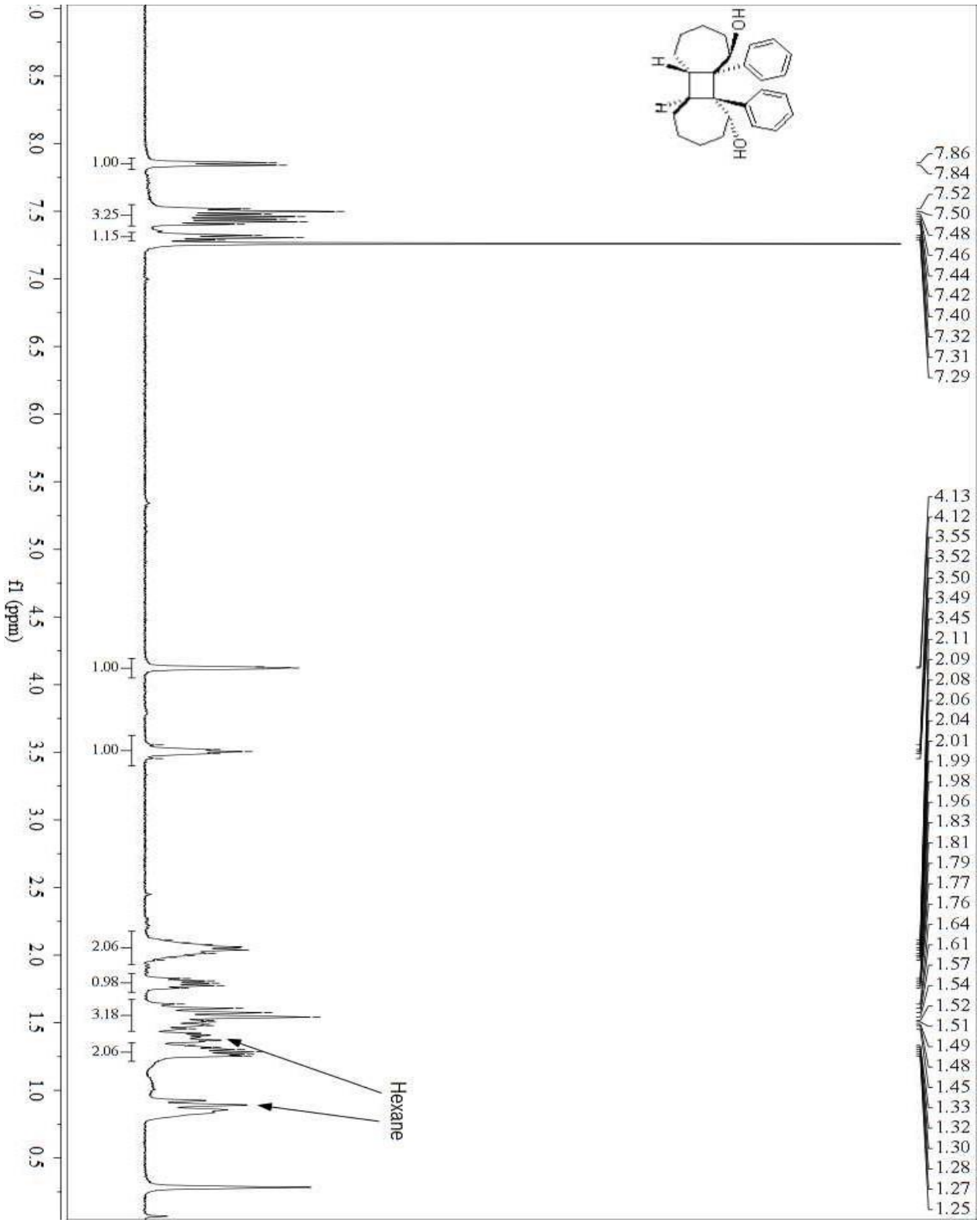

5a(1R,5aS,5bS,10R,10aS,10bS)-10a,10b-diphenyltetradecahydrocyclobuta[1,2:3,4]di[7]annulene-1,10-diol-^{13}C

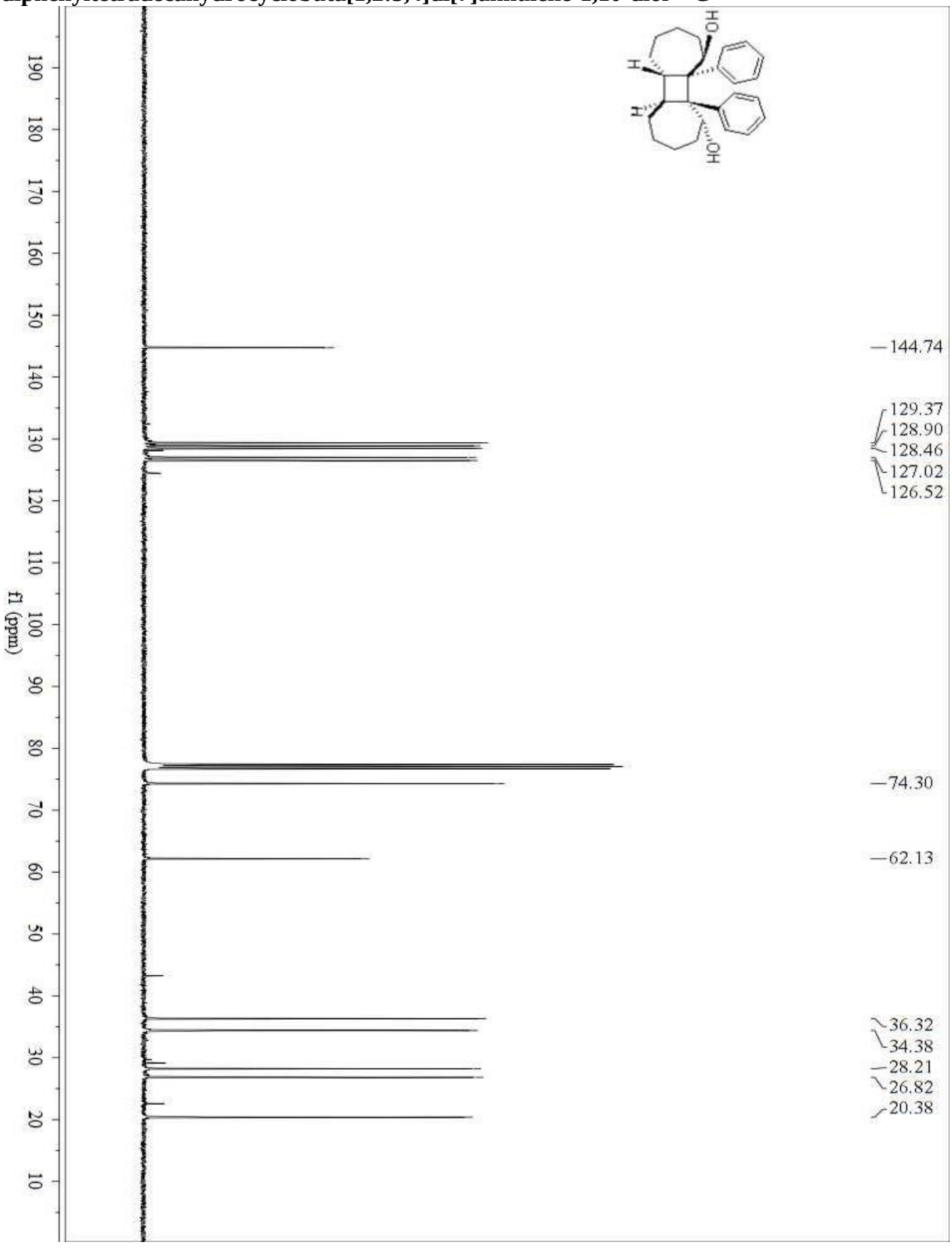

5a (1R,5aS,5bS,10R,10aS,10bS)-10a,10b-bis(4-chlorophenyl)tetradecahydrocyclobuta[1,2:3,4]di[7]annulene-1,10-diol-Starting material

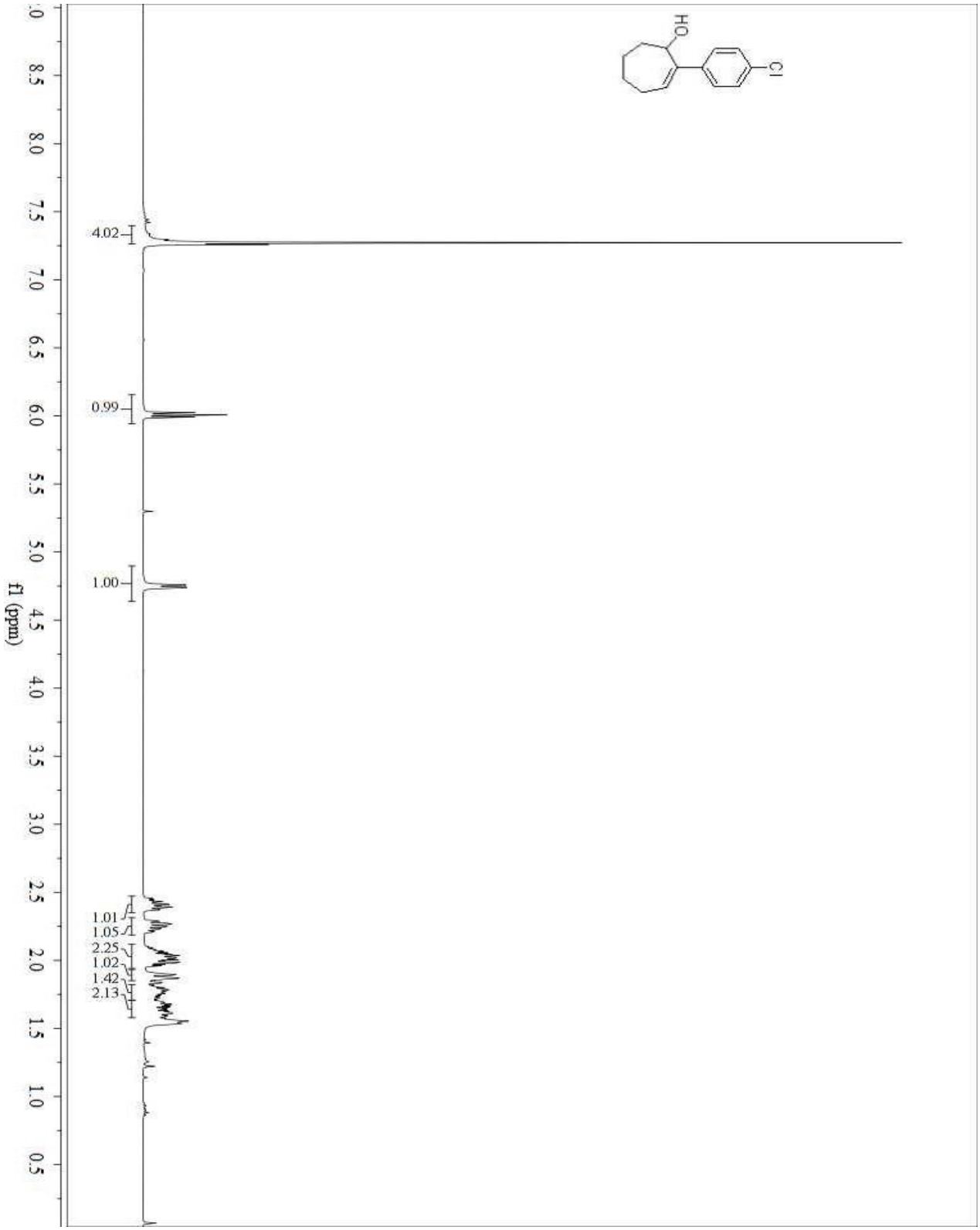

Section 2: Data and calculation of 1a crystal structure**.**

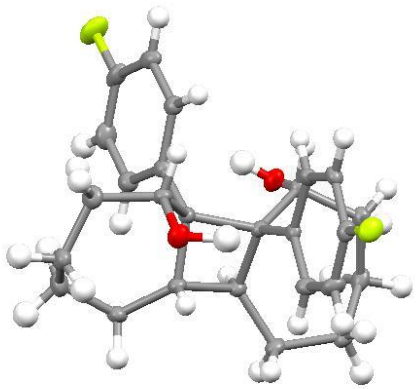

data_bisphen_fi_abs

_audit_creation_date 2016-05-11

_audit_creation_method

;

Olex2 1.2

(compiled 2015.01.26 svn.r3150 for OlexSys, GUI svn.r4998)

;

_publ_contact_author_address ?

_publ_contact_author_email ?

_publ_contact_author_name ''

_publ_contact_author_phone ?

_publ_section_references

;

Dolomanov, O.V., Bourhis, L.J., Gildea, R.J, Howard, J.A.K. &Puschmann, H.

(2009), J. Appl. Cryst. 42, 339-341.

Sheldrick, G.M. (2008). ActaCryst. A64, 112-122.

;

_chemical_name_common ?

_chemical_name_systematic

;

?

;

_chemical_formula_moiety 'C26 H30 F2 O2'

_chemical_formula_sum 'C26 H30 F2 O2'

_chemical_formula_weight 412.50

_chemical_melting_point ?

loop_

_atom_type_symbol

_atom_type_description

_atom_type_scat_dispersion_real

_atom_type_scat_dispersion_imag

_atom_type_scat_source

'C' 'C' 0.0033 0.0016 'International Tables Vol C Tables 4.2.6.8 and 6.1.1.4'

'H' 'H' 0.0000 0.0000 'International Tables Vol C Tables 4.2.6.8 and 6.1.1.4'

'F' 'F' 0.0171 0.0103 'International Tables Vol C Tables 4.2.6.8 and 6.1.1.4'

'O' 'O' 0.0106 0.0060 'International Tables Vol C Tables 4.2.6.8 and 6.1.1.4'

_space_group_crystal_system 'triclinic'

_space_group_IT_number 2

_space_group_name_H-M_alt 'P -1'

_space_group_name_Hall '-P 1'

loop_

_space_group_symop_id

_space_group_symop_operation_xyz

1 'x, y, z'

2 '-x, -y, -z'

_cell_length_a 8.719(2)

_cell_length_b 9.572(2)

_cell_length_c 12.839(3)

_cell_angle_alpha 73.103(3)

_cell_angle_beta 81.352(3)

_cell_angle_gamma 77.937(3)

_cell_volume 998.0(4)

_cell_formula_units_Z 2

_cell_measurement_reflns_used 9114

_cell_measurement_temperature 100

_cell_measurement_theta_max 30.66

_cell_measurement_theta_min 2.26

_exptl_absorpt_coefficient_mu 0.097

_exptl_absorpt_correction_T_max 0.7461

_exptl_absorpt_correction_T_min 0.5632

_exptl_absorpt_correction_type multi-scan

_exptl_absorpt_process_details

;

SADABS-2014/5 (Bruker,2014/5) was used for absorption correction.

wR2(int) was 0.1386 before and 0.0765 after correction.

The Ratio of minimum to maximum transmission is 0.7549.

The \l/2 correction factor is 0.00150.

;

_exptl_crystal_colour 'clear light colourless'

_exptl_crystal_colour_lustre clear

_exptl_crystal_colour_modifier light

_exptl_crystal_colour_primarycolourless

_exptl_crystal_density_diffrn 1.373

_exptl_crystal_density_meas ?

_exptl_crystal_density_method 'not measured'

_exptl_crystal_description 'Rectangle'

_exptl_crystal_F_000 440

_exptl_crystal_size_max 0.103

_exptl_crystal_size_mid 0.087

_exptl_crystal_size_min 0.05

_exptl_special_details

;

?

;

_diffrn_reflns_av_R_equivalents 0.0746

_diffrn_reflns_av_unetI/netI 0.0517

_diffrn_reflns_limit_h_max 10

_diffrn_reflns_limit_h_min -10

_diffrn_reflns_limit_k_max 11

_diffrn_reflns_limit_k_min -11

_diffrn_reflns_limit_l_max 15

_diffrn_reflns_limit_l_min -15

_diffrn_reflns_number 19956

_diffrn_reflns_theta_full 26.02

_diffrn_reflns_theta_max 26.02

_diffrn_reflns_theta_min 1.67

_diffrn_ambient_temperature 100

_diffrn_detector_area_resol_mean ?

_diffrn_measured_fraction_theta_full 0.960

_diffrn_measured_fraction_theta_max 0.960

_diffrn_measurement_device_type 'Bruker APEX-II CCD'

_diffrn_measurement_method '\f and \w scans'

_diffrn_radiation_monochromator graphite

_diffrn_radiation_typeMoK\a

_diffrn_radiation_wavelength 0.71073

_diffrn_source 'fine-focus sealed tube'

_diffrn_standards_number 0

_reflns_number_gt 2923

_reflns_number_total 3773

_reflns_threshold_expression>2sigma(I)

_computing_cell_refinement 'Bruker SAINT'

_computing_data_collection 'Bruker APEX2'

_computing_data_reduction 'Bruker SAINT'

_computing_molecular_graphics 'Bruker SHELXTL'

_computing_publication_material 'Bruker SHELXTL'

_computing_structure_refinement 'SHELXL-2014 (Sheldrick 2014)'

_computing_structure_solution 'SHELXS-97 (Sheldrick 2008)'

_refine_diff_density_max 1.011

_refine_diff_density_min -0.326

_refine_diff_density_rms 0.061

_refine_ls_extinction_coef ?

_refine_ls_extinction_method none

_refine_ls_goodness_of_fit_ref 1.032

_refine_ls_hydrogen_treatment mixed

_refine_ls_matrix_type full

_refine_ls_number_parameters 277

_refine_ls_number_reflns 3773

_refine_ls_number_restraints 0

_refine_ls_R_factor_all 0.0720

_refine_ls_R_factor_gt 0.0526

_refine_ls_restrained_S_all 1.032

_refine_ls_shift/su_max 0.000

_refine_ls_shift/su_mean 0.000

_refine_ls_structure_factor_coefFsqd

_refine_ls_weighting_details

'calc w=1/[\s^2^(Fo^2^)+(0.0620P)^2^+0.8394P] where P=(Fo^2^+2Fc^2^)/3'

_refine_ls_weighting_schemecalc

_refine_ls_wR_factor_gt 0.1284

_refine_ls_wR_factor_ref 0.1389

_refine_special_details

;

Refinement of F^2^ against ALL reflections. The weighted R-factor wR and goodness of fit S are based on F^2^, conventional R-factors R are based on F, with F set to zero for negative F^2^. The threshold expression of F^2^ >2sigma(F^2^) is used only for calculating R-factors(gt) etc. and is not relevant to the choice of reflections for refinement. R-factors based on F^2^ are statistically about twice as large as those based on F, and R-factors based on ALL data will be even larger.

;

_olex2_refinement_description

;

1. Fixed Uiso

At 1.2 times of:

All C(H) groups, All C(H,H) groups

At 1.5 times of:

All O(H) groups

2.a Ternary CH refined with riding coordinates:

C10(H10), C8(H8), C3(H3), C1(H1A)

2.b Secondary CH2 refined with riding coordinates:

C11(H11A,H11B), C12(H12A,H12B), C13(H13A,H13B), C14(H14A,H14B), C4(H4A,H4B), C5(H5A,H5B), C6(H6A,H6B), C7(H7A,H7B)

2.c Aromatic/amide H refined with riding coordinates:

C19(H19), C20(H20), C26(H26), C25(H25), C22(H22), C23(H23), C16(H16), C17(H17)

;

_atom_sites_solution_hydrogensgeom

_atom_sites_solution_primary direct

_atom_sites_solution_secondarydifmap

loop_

_atom_site_label

_atom_site_type_symbol

_atom_site_fract_x

_atom_site_fract_y

_atom_site_fract_z

_atom_site_U_iso_or_equiv

_atom_site_adp_type

_atom_site_occupancy

_atom_site_calc_flag

_atom_site_disorder_assembly

_atom_site_disorder_group

_atom_site_refinement_flags_posn

F1 F 0.34128(16) 0.31275(17) -0.06017(12) 0.0366(4) Uani 1 d . . .

F2 F 1.40870(14) -0.45018(15) 0.26734(11) 0.0266(3) Uani 1 d . . .

O1 O 0.52784(17) -0.08936(18) 0.28593(13) 0.0214(4) Uani 1 d . . .

H1 H 0.525(3) -0.021(3) 0.234(2) 0.032 Uiso 1 d . . R

O2 O 1.13249(18) 0.05197(19) 0.18436(14) 0.0258(4) Uani 1 d . . .

H2 H 1.147(3) -0.063(3) 0.223(2) 0.039 Uiso 1 d . . R

C18 C 0.4569(3) 0.2555(3) 0.00819(19) 0.0248(5) Uani 1 d . . .

C19 C 0.5773(3) 0.1490(3) -0.01605(18) 0.0217(5) Uani 1 d . . .

H19 H 0.5800 0.1153 -0.0791 0.026 Uiso 1 calc . . R

C20 C 0.6945(2) 0.0920(2) 0.05393(17) 0.0179(5) Uani 1 d . . .

H20 H 0.7774 0.0164 0.0390 0.021 Uiso 1 calc . . R

C15 C 0.6956(2) 0.1418(2) 0.14655(17) 0.0158(4) Uani 1 d . . .

C2 C 0.8340(2) 0.0761(2) 0.21573(17) 0.0159(4) Uani 1 d . . .

C9 C 0.8127(2) -0.0864(2) 0.29814(17) 0.0151(4) Uani 1 d . . .

C21 C 0.9696(2) -0.1912(2) 0.29851(17) 0.0154(4) Uani 1 d . . .

C26 C 1.0758(3) -0.2227(3) 0.37674(18) 0.0203(5) Uani 1 d . . .

H26 H 1.0464 -0.1829 0.4380 0.024 Uiso 1 calc . . R

C25 C 1.2232(3) -0.3102(3) 0.36788(19) 0.0231(5) Uani 1 d . . .

H25 H 1.2942 -0.3298 0.4218 0.028 Uiso 1 calc . . R

C24 C 1.2635(2) -0.3675(2) 0.27935(18) 0.0191(5) Uani 1 d . . .

C22 C 1.0172(2) -0.2543(2) 0.21060(18) 0.0171(5) Uani 1 d . . .

H22 H 0.9468 -0.2366 0.1566 0.020 Uiso 1 calc . . R

C23 C 1.1638(3) -0.3417(2) 0.20014(18) 0.0192(5) Uani 1 d . . .

H23 H 1.1945 -0.3828 0.1396 0.023 Uiso 1 calc . . R

C10 C 0.6845(2) -0.1715(2) 0.28714(18) 0.0174(5) Uani 1 d . . .

H10 H 0.7129 -0.2057 0.2191 0.021 Uiso 1 calc . . R

C11 C 0.6741(3) -0.3065(2) 0.38606(18) 0.0200(5) Uani 1 d . . .

H11A H 0.7792 -0.3707 0.3908 0.024 Uiso 1 calc . . R

H11B H 0.6005 -0.3640 0.3726 0.024 Uiso 1 calc . . R

C12 C 0.6198(3) -0.2730(3) 0.49712(19) 0.0226(5) Uani 1 d . . .

H12A H 0.5309 -0.1884 0.4871 0.027 Uiso 1 calc . . R

H12B H 0.5792 -0.3600 0.5477 0.027 Uiso 1 calc . . R

C13 C 0.7454(3) -0.2361(3) 0.55173(19) 0.0239(5) Uani 1 d . . .

H13A H 0.8462 -0.3026 0.5403 0.029 Uiso 1 calc . . R

H13B H 0.7144 -0.2586 0.6314 0.029 Uiso 1 calc . . R

C14 C 0.7739(3) -0.0750(2) 0.51111(17) 0.0200(5) Uani 1 d . . .

H14A H 0.6982 -0.0147 0.5535 0.024 Uiso 1 calc . . R

H14B H 0.8813 -0.0725 0.5261 0.024 Uiso 1 calc . . R

C8 C 0.7574(3) -0.0039(2) 0.38924(17) 0.0166(5) Uani 1 d . . .

H8 H 0.6424 0.0351 0.3833 0.020 Uiso 1 calc . . R

C3 C 0.8423(3) 0.1231(2) 0.32127(17) 0.0171(5) Uani 1 d . . .

H3 H 0.9547 0.0908 0.3381 0.021 Uiso 1 calc . . R

C4 C 0.7957(3) 0.2819(2) 0.33167(18) 0.0211(5) Uani 1 d . . .

H4A H 0.8466 0.2897 0.3932 0.025 Uiso 1 calc . . R

H4B H 0.6802 0.3029 0.3499 0.025 Uiso 1 calc . . R

C5 C 0.8409(3) 0.4006(3) 0.2281(2) 0.0291(6) Uani 1 d . . .

H5A H 0.7534 0.4294 0.1809 0.035 Uiso 1 calc . . R

H5B H 0.8489 0.4894 0.2504 0.035 Uiso 1 calc . . R

C6 C 0.9919(3) 0.3602(3) 0.1597(2) 0.0278(6) Uani 1 d . . .

H6A H 1.0737 0.3068 0.2099 0.033 Uiso 1 calc . . R

H6B H 1.0266 0.4534 0.1149 0.033 Uiso 1 calc . . R

C7 C 0.9866(3) 0.2659(3) 0.08348(19) 0.0247(5) Uani 1 d . . .

H7A H 0.8912 0.3081 0.0440 0.030 Uiso 1 calc . . R

H7B H 1.0790 0.2754 0.0283 0.030 Uiso 1 calc . . R

C1 C 0.9855(2) 0.1016(2) 0.13584(17) 0.0175(5) Uani 1 d . . .

H1A H 0.9888 0.0517 0.0769 0.021 Uiso 1 calc . . R

C16 C 0.5685(3) 0.2477(3) 0.16843(19) 0.0224(5) Uani 1 d . . .

H16 H 0.5638 0.2818 0.2315 0.027 Uiso 1 calc . . R

C17 C 0.4486(3) 0.3045(3) 0.0998(2) 0.0270(5) Uani 1 d . . .

H17 H 0.3620 0.3761 0.1159 0.032 Uiso 1 calc . . R

loop_

_atom_site_aniso_label

_atom_site_aniso_U_11

_atom_site_aniso_U_22

_atom_site_aniso_U_33

_atom_site_aniso_U_23

_atom_site_aniso_U_13

_atom_site_aniso_U_12

F1 0.0235(8) 0.0459(9) 0.0335(8) 0.0036(7) -0.0137(6) -0.0035(7)

F2 0.0160(7) 0.0309(8) 0.0273(7) -0.0067(6) 0.0000(5) 0.0055(6)

O1 0.0148(8) 0.0235(9) 0.0217(9) 0.0000(7) -0.0008(6) -0.0036(7)

O2 0.0184(8) 0.0277(9) 0.0294(9) -0.0039(7) -0.0035(7) -0.0046(7)

C18 0.0176(11) 0.0271(13) 0.0249(12) 0.0049(10) -0.0080(10) -0.0065(10)

C19 0.0205(11) 0.0294(13) 0.0164(11) -0.0032(10) -0.0001(9) -0.0125(10)

C20 0.0152(11) 0.0210(11) 0.0168(11) -0.0038(9) 0.0016(9) -0.0054(9)

C15 0.0148(10) 0.0178(11) 0.0138(10) -0.0020(9) 0.0018(8) -0.0062(8)

C2 0.0182(11) 0.0162(11) 0.0137(10) -0.0041(9) -0.0002(8) -0.0043(9)

C9 0.0145(10) 0.0172(11) 0.0124(10) -0.0029(8) -0.0008(8) -0.0021(8)

C21 0.0151(10) 0.0150(10) 0.0149(10) -0.0018(8) 0.0012(8) -0.0053(8)

C26 0.0170(11) 0.0279(12) 0.0169(11) -0.0087(10) 0.0006(9) -0.0035(9)

C25 0.0166(11) 0.0329(13) 0.0189(11) -0.0053(10) -0.0055(9) -0.0019(10)

C24 0.0140(10) 0.0190(11) 0.0208(11) -0.0024(9) 0.0018(9) -0.0016(9)

C22 0.0151(10) 0.0187(11) 0.0184(11) -0.0050(9) -0.0032(9) -0.0040(9)

C23 0.0216(11) 0.0167(11) 0.0205(11) -0.0077(9) 0.0023(9) -0.0051(9)

C10 0.0141(10) 0.0192(11) 0.0188(11) -0.0052(9) -0.0004(8) -0.0031(9)

C11 0.0151(10) 0.0189(11) 0.0249(12) -0.0047(9) 0.0012(9) -0.0048(9)

C12 0.0191(11) 0.0214(12) 0.0221(12) 0.0000(10) 0.0032(9) -0.0039(9)

C13 0.0231(12) 0.0258(13) 0.0172(11) -0.0014(10) 0.0034(9) -0.0019(10)

C14 0.0218(12) 0.0222(12) 0.0134(11) -0.0046(9) 0.0005(9) -0.0001(9)

C8 0.0174(11) 0.0172(11) 0.0146(11) -0.0052(9) -0.0005(8) -0.0016(9)

C3 0.0185(11) 0.0204(11) 0.0126(10) -0.0049(9) -0.0009(8) -0.0034(9)

C4 0.0274(12) 0.0205(12) 0.0172(11) -0.0068(9) -0.0030(9) -0.0047(10)

C5 0.0367(14) 0.0188(12) 0.0301(14) -0.0054(10) 0.0011(11) -0.0061(11)

C6 0.0379(14) 0.0233(12) 0.0229(12) -0.0028(10) -0.0022(11) -0.0123(11)

C7 0.0228(12) 0.0264(13) 0.0234(12) -0.0043(10) 0.0043(10) -0.0087(10)

C1 0.0182(11) 0.0219(11) 0.0137(10) -0.0053(9) -0.0023(8) -0.0055(9)

C16 0.0226(12) 0.0231(12) 0.0208(12) -0.0062(10) 0.0001(9) -0.0035(10)

C17 0.0180(11) 0.0224(12) 0.0356(14) -0.0048(11) -0.0008(10) 0.0017(9)

_geom_special_details

;

All esds (except the esd in the dihedral angle between two l.s. planes)
are estimated using the full covariance matrix. The cell esds are taken
into account individually in the estimation of esds in distances, angles
and torsion angles; correlations between esds in cell parameters are only
used when they are defined by crystal symmetry. An approximate (isotropic)
treatment of cell esds is used for estimating esds involving l.s. planes.

;

loop_

_geom_bond_atom_site_label_1

_geom_bond_atom_site_label_2

_geom_bond_distance

_geom_bond_site_symmetry_2

_geom_bond_publ_flag

F1 C18 1.358(3) . ?

F2 C24 1.359(2) . ?

O1 H1 0.79(3) . ?

O1 C10 1.426(3) . ?

O2 H2 1.06(3) . ?

O2 C1 1.439(3) . ?

C18 C19 1.370(3) . ?

C18 C17 1.374(4) . ?

C19 H19 0.9500 . ?

C19 C20 1.381(3) . ?

C20 H20 0.9500 . ?

C20 C15 1.406(3) . ?

C15 C2 1.523(3) . ?

C15 C16 1.392(3) . ?

C2 C9 1.637(3) . ?

C2 C3 1.562(3) . ?

C2 C1 1.561(3) . ?

C9 C21 1.518(3) . ?

C9 C10 1.558(3) . ?

C9 C8 1.559(3) . ?

C21 C26 1.395(3) . ?

C21 C22 1.400(3) . ?

C26 H26 0.9500 . ?

C26 C25 1.388(3) . ?

C25 H25 0.9500 . ?

C25 C24 1.370(3) . ?

C24 C23 1.372(3) . ?

C22 H22 0.9500 . ?

C22 C23 1.385(3) . ?

C23 H23 0.9500 . ?

C10 H10 1.0000 . ?

C10 C11 1.534(3) . ?

C11 H11A 0.9900 . ?

C11 H11B 0.9900 . ?

C11 C12 1.536(3) . ?

C12 H12A 0.9900 . ?

C12 H12B 0.9900 . ?

C12 C13 1.533(3) . ?

C13 H13A 0.9900 . ?

C13 H13B 0.9900 . ?

C13 C14 1.538(3) . ?

C14 H14A 0.9900 . ?

C14 H14B 0.9900 . ?

C14 C8 1.530(3) . ?

C8 H8 1.0000 . ?

C8 C3 1.534(3) . ?

C3 H3 1.0000 . ?

C3 C4 1.529(3) . ?

C4 H4A 0.9900 . ?

C4 H4B 0.9900 . ?

C4 C5 1.538(3) . ?

C5 H5A 0.9900 . ?

C5 H5B 0.9900 . ?

C5 C6 1.514(4) . ?

C6 H6A 0.9900 . ?

C6 H6B 0.9900 . ?

C6 C7 1.523(3) . ?

C7 H7A 0.9900 . ?

C7 H7B 0.9900 . ?

C7 C1 1.522(3) . ?

C1 H1A 1.0000 . ?

C16 H16 0.9500 . ?

C16 C17 1.388(3) . ?

C17 H17 0.9500 . ?

loop_

_geom_angle_atom_site_label_1

_geom_angle_atom_site_label_2

_geom_angle_atom_site_label_3

_geom_angle

_geom_angle_site_symmetry_1

_geom_angle_site_symmetry_3

_geom_angle_publ_flag

C10 O1 H1 108(2) . . ?

C1 O2 H2 109.9(15) . . ?

F1 C18 C19 118.6(2) . . ?

F1 C18 C17 119.2(2) . . ?

C19 C18 C17 122.2(2) . . ?

C18 C19 H19 121.0 . . ?

C18 C19 C20 118.0(2) . . ?

C20 C19 H19 121.0 . . ?

C19 C20 H20 118.8 . . ?

C19 C20 C15 122.3(2) . . ?

C15 C20 H20 118.8 . . ?

C20 C15 C2 118.11(19) . . ?

C16 C15 C20 117.1(2) . . ?

C16 C15 C2 124.8(2) . . ?

C15 C2 C9 111.11(16) . . ?

C15 C2 C3 121.29(18) . . ?

C15 C2 C1 106.05(17) . . ?

C3 C2 C9 85.97(15) . . ?

C1 C2 C9 122.46(17) . . ?

C1 C2 C3 110.09(17) . . ?

C21 C9 C2 109.10(16) . . ?

C21 C9 C10 107.22(17) . . ?

C21 C9 C8 121.01(17) . . ?

C10 C9 C2 122.23(17) . . ?

C10 C9 C8 110.92(16) . . ?

C8 C9 C2 86.18(15) . . ?

C26 C21 C9 124.78(19) . . ?

C26 C21 C22 116.88(19) . . ?

C22 C21 C9 118.21(18) . . ?

C21 C26 H26 119.0 . . ?

C25 C26 C21 122.1(2) . . ?

C25 C26 H26 119.0 . . ?

C26 C25 H25 120.9 . . ?

C24 C25 C26 118.3(2) . . ?

C24 C25 H25 120.9 . . ?

F2 C24 C25 119.4(2) . . ?

F2 C24 C23 118.19(19) . . ?

C25 C24 C23 122.4(2) . . ?

C21 C22 H22 119.0 . . ?

C23 C22 C21 121.9(2) . . ?

C23 C22 H22 119.0 . . ?

C24 C23 C22 118.4(2) . . ?

C24 C23 H23 120.8 . . ?

C22 C23 H23 120.8 . . ?

O1 C10 C9 115.05(17) . . ?

O1 C10 H10 109.1 . . ?

O1 C10 C11 103.80(17) . . ?

C9 C10 H10 109.1 . . ?

C11 C10 C9 110.43(17) . . ?

C11 C10 H10 109.1 . . ?

C10 C11 H11A 108.3 . . ?

C10 C11 H11B 108.3 . . ?

C10 C11 C12 116.00(18) . . ?

H11A C11 H11B 107.4 . . ?

C12 C11 H11A 108.3 . . ?

C12 C11 H11B 108.3 . . ?

C11 C12 H12A 108.3 . . ?

C11 C12 H12B 108.3 . . ?

H12A C12 H12B 107.4 . . ?

C13 C12 C11 115.94(18) . . ?

C13 C12 H12A 108.3 . . ?

C13 C12 H12B 108.3 . . ?

C12 C13 H13A 108.4 . . ?

C12 C13 H13B 108.4 . . ?

C12 C13 C14 115.70(19) . . ?

H13A C13 H13B 107.4 . . ?

C14 C13 H13A 108.4 . . ?

C14 C13 H13B 108.4 . . ?

C13 C14 H14A 108.7 . . ?

C13 C14 H14B 108.7 . . ?

H14A C14 H14B 107.6 . . ?

C8 C14 C13 114.27(18) . . ?

C8 C14 H14A 108.7 . . ?

C8 C14 H14B 108.7 . . ?

C9 C8 H8 105.8 . . ?

C14 C8 C9 124.61(18) . . ?

C14 C8 H8 105.8 . . ?

C14 C8 C3 122.89(18) . . ?

C3 C8 C9 89.71(15) . . ?

C3 C8 H8 105.8 . . ?

C2 C3 H3 105.6 . . ?

C8 C3 C2 89.73(15) . . ?

C8 C3 H3 105.6 . . ?

C4 C3 C2 124.53(18) . . ?

C4 C3 C8 123.43(18) . . ?

C4 C3 H3 105.6 . . ?

C3 C4 H4A 108.7 . . ?

C3 C4 H4B 108.7 . . ?

C3 C4 C5 114.20(19) . . ?

H4A C4 H4B 107.6 . . ?

C5 C4 H4A 108.7 . . ?

C5 C4 H4B 108.7 . . ?

C4 C5 H5A 107.9 . . ?

C4 C5 H5B 107.9 . . ?

H5A C5 H5B 107.2 . . ?

C6 C5 C4 117.4(2) . . ?

C6 C5 H5A 107.9 . . ?

C6 C5 H5B 107.9 . . ?

C5 C6 H6A 108.0 . . ?

C5 C6 H6B 108.0 . . ?

C5 C6 C7 117.3(2) . . ?

H6A C6 H6B 107.2 . . ?

C7 C6 H6A 108.0 . . ?

C7 C6 H6B 108.0 . . ?

C6 C7 H7A 108.1 . . ?

C6 C7 H7B 108.1 . . ?

H7A C7 H7B 107.3 . . ?

C1 C7 C6 116.86(19) . . ?

C1 C7 H7A 108.1 . . ?

C1 C7 H7B 108.1 . . ?

O2 C1 C2 115.97(17) . . ?

O2 C1 C7 102.76(17) . . ?

O2 C1 H1A 108.8 . . ?

C2 C1 H1A 108.8 . . ?

C7 C1 C2 111.46(18) . . ?

C7 C1 H1A 108.8 . . ?

C15 C16 H16 119.4 . . ?

C17 C16 C15 121.2(2) . . ?

C17 C16 H16 119.4 . . ?

C18 C17 C16 119.1(2) . . ?

C18 C17 H17 120.5 . . ?

C16 C17 H17 120.5 . . ?

loop_

_geom_torsion_atom_site_label_1

_geom_torsion_atom_site_label_2

_geom_torsion_atom_site_label_3

_geom_torsion_atom_site_label_4

_geom_torsion

_geom_torsion_site_symmetry_1

_geom_torsion_site_symmetry_2

_geom_torsion_site_symmetry_3

_geom_torsion_site_symmetry_4

_geom_torsion_publ_flag

F1 C18 C19 C20 179.79(19) . . . . ?

F1 C18 C17 C16 -178.8(2) . . . . ?

F2 C24 C23 C22 -178.38(18) . . . . ?

O1 C10 C11 C12 -59.6(2) . . . . ?

C18 C19 C20 C15 -1.4(3) . . . . ?

C19 C18 C17 C16 2.1(4) . . . . ?

C19 C20 C15 C2 -177.49(19) . . . . ?

C19 C20 C15 C16 2.9(3) . . . . ?

C20 C15 C2 C9 -80.2(2) . . . . ?

C20 C15 C2 C3 -178.67(18) . . . . ?

C20 C15 C2 C1 55.0(2) . . . . ?

C20 C15 C16 C17 -1.8(3) . . . . ?

C15 C2 C9 C21 137.56(18) . . . . ?

C15 C2 C9 C10 11.5(3) . . . . ?

C15 C2 C9 C8 -100.89(18) . . . . ?

C15 C2 C3 C8 90.8(2) . . . . ?

C15 C2 C3 C4 -40.9(3) . . . . ?

C15 C2 C1 O2 178.10(17) . . . . ?

C15 C2 C1 C7 61.0(2) . . . . ?

C15 C16 C17 C18 -0.5(3) . . . . ?

C2 C15 C16 C17 178.5(2) . . . . ?

C2 C9 C21 C26 97.0(2) . . . . ?

C2 C9 C21 C22 -78.6(2) . . . . ?

C2 C9 C10 O1 -53.4(3) . . . . ?

C2 C9 C10 C11 -170.47(17) . . . . ?

C2 C9 C8 C14 -152.6(2) . . . . ?

C2 C9 C8 C3 -21.53(15) . . . . ?

C2 C3 C4 C5 -37.8(3) . . . . ?

C9 C2 C3 C8 -21.50(15) . . . . ?

C9 C2 C3 C4 -153.2(2) . . . . ?

C9 C2 C1 O2 -53.1(3) . . . . ?

C9 C2 C1 C7 -170.15(18) . . . . ?

C9 C21 C26 C25 -174.6(2) . . . . ?

C9 C21 C22 C23 174.83(19) . . . . ?

C9 C10 C11 C12 64.2(2) . . . . ?

C9 C8 C3 C2 22.56(16) . . . . ?

C9 C8 C3 C4 155.1(2) . . . . ?

C21 C9 C10 O1 179.70(17) . . . . ?

C21 C9 C10 C11 62.6(2) . . . . ?

C21 C9 C8 C14 -42.5(3) . . . . ?

C21 C9 C8 C3 88.5(2) . . . . ?

C21 C26 C25 C24 -0.4(3) . . . . ?

C21 C22 C23 C24 0.6(3) . . . . ?

C26 C21 C22 C23 -1.1(3) . . . . ?

C26 C25 C24 F2 178.25(19) . . . . ?

C26 C25 C24 C23 -0.2(3) . . . . ?

C25 C24 C23 C22 0.1(3) . . . . ?

C22 C21 C26 C25 1.0(3) . . . . ?

C10 C9 C21 C26 -128.7(2) . . . . ?

C10 C9 C21 C22 55.7(2) . . . . ?

C10 C9 C8 C14 84.3(2) . . . . ?

C10 C9 C8 C3 -144.66(17) . . . . ?

C10 C11 C12 C13 -79.3(2) . . . . ?

C11 C12 C13 C14 81.9(2) . . . . ?

C12 C13 C14 C8 -34.8(3) . . . . ?

C13 C14 C8 C9 -37.9(3) . . . . ?

C13 C14 C8 C3 -153.96(19) . . . . ?

C14 C8 C3 C2 154.9(2) . . . . ?

C14 C8 C3 C4 -72.6(3) . . . . ?

C8 C9 C21 C26 -0.2(3) . . . . ?

C8 C9 C21 C22 -175.85(18) . . . . ?

C8 C9 C10 O1 45.6(2) . . . . ?

C8 C9 C10 C11 -71.5(2) . . . . ?

C8 C3 C4 C5 -154.4(2) . . . . ?

C3 C2 C9 C21 -100.38(17) . . . . ?

C3 C2 C9 C10 133.56(19) . . . . ?

C3 C2 C9 C8 21.17(15) . . . . ?

C3 C2 C1 O2 45.2(2) . . . . ?

C3 C2 C1 C7 -71.9(2) . . . . ?

C3 C4 C5 C6 -34.2(3) . . . . ?

C4 C5 C6 C7 79.2(3) . . . . ?

C5 C6 C7 C1 -75.9(3) . . . . ?

C6 C7 C1 O2 -61.2(2) . . . . ?

C6 C7 C1 C2 63.6(3) . . . . ?

C1 C2 C9 C21 10.9(3) . . . . ?

C1 C2 C9 C10 -115.1(2) . . . . ?

C1 C2 C9 C8 132.47(19) . . . . ?

C1 C2 C3 C8 -144.67(17) . . . . ?

C1 C2 C3 C4 83.6(2) . . . . ?

C16 C15 C2 C9 99.4(2) . . . . ?

C16 C15 C2 C3 0.9(3) . . . . ?

C16 C15 C2 C1 -125.4(2) . . . . ?

C17 C18 C19 C20 -1.1(3) . . . . ?

_olex2_submission_special_instructions 'No special instructions were received'

VITA

Winston (Cường) Vi Trinh

Candidate for the Degree of

Master of Science in Chemistry

Thesis: ON THE EXISTENCE OF TRANS-CYCLOHEXENE AND TRANS-CYCLOHEPTENE

Major Field: Chemistry

Biographical:

Education:

Completed the requirements for the Master of ScienceinChemistry at Oklahoma State University, Stillwater, Oklahoma in December, 2016.

Completed the requirements for the Bachelor of Science in Chemistryat the University of Texas at Austin, Austin, Texas in 2013.